



**Characterization of Apoptotic Parasites for
the Identification of Novel Target Molecules
in the Treatment of Leishmaniasis**

Dissertation

zur Erlangung des Grades
Doktor der Naturwissenschaften

vorgelegt beim Fachbereich
Biologie und Chemie (FB 08)
der Justus-Liebig-Universität Gießen

Michaela Bergmann

Frankfurt am Main, 2021

Eidesstattliche Erklärung

Ich erkläre: Ich habe die vorgelegte Dissertation selbstständig und ohne unerlaubte fremde Hilfe und nur mit den Hilfen angefertigt, die ich in der Dissertation angegeben habe. Alle Textstellen, die wörtlich oder sinngemäß aus veröffentlichten Schriften entnommen sind, und alle Angaben, die auf mündlichen Auskünften beruhen, sind als solche kenntlich gemacht. Ich stimme einer evtl. Überprüfung meiner Dissertation durch eine Antiplagiat-Software zu. Bei den von mir durchgeführten und in der Dissertation erwähnten Untersuchungen habe ich die Grundsätze guter wissenschaftlicher Praxis, wie sie in der „Satzung der Justus-Liebig-Universität Gießen zur Sicherung guter wissenschaftlicher Praxis“ niedergelegt sind, eingehalten.

Gießen, den _____

Michaela Bergmann

Table of Contents

Table of Contents	I
Abbreviations	IV
Zusammenfassung.....	VII
Summary	VIII
1. Introduction	- 1 -
1.1. Leishmaniasis	- 1 -
1.1.1. Drugs against Leishmaniasis.....	- 2 -
1.1.2. Vaccination against Leishmaniasis	- 3 -
1.2. <i>Leishmania spp.</i>	- 4 -
1.2.1. The Role of Apoptosis in Infection	- 5 -
1.2.2. Genetics in <i>Leishmania</i>	- 6 -
1.2.3. CRISPR/Cas9 Toolkit	- 7 -
1.3. Apoptosis.....	- 9 -
1.4. Apoptosis in <i>Leishmania</i>	- 11 -
1.4.1. Endonuclease G.....	- 12 -
1.4.2. Metacaspase	- 13 -
1.5. Hypothesis and Aims.....	- 13 -
2. Materials and Methods.....	- 17 -
2.1. Materials	- 17 -
2.1.1. Reagents.....	- 17 -
2.1.2. Buffers	- 18 -
2.1.3. Media	- 20 -
2.1.4. Primers	- 21 -
2.1.5. Plasmids.....	- 23 -
2.1.6. Antibodies and Dyes.....	- 24 -
2.1.7. Kits.....	- 24 -
2.1.8. Compounds and Inhibitors.....	- 25 -
2.1.9. Antibiotics.....	- 25 -
2.1.10. Enzymes.....	- 26 -
2.1.11. <i>Leishmania</i> Strains.....	- 26 -
2.1.12. Human Primary Cells	- 27 -
2.1.13. Bacterial Strains.....	- 27 -

TABLE OF CONTENTS

2.2.	Methods	- 27 -
2.2.1.	Cell Biological Methods	- 27 -
2.2.1.1.	Preparation of Blood Agar Plates	- 27 -
2.2.1.2.	Cultivation of Leishmania Promastigotes	- 28 -
2.2.1.3.	Isolation and Cultivation of Leishmania Amastigotes	- 28 -
2.2.1.4.	Isolation of Human Peripheral Blood Mononuclear Cells (PBMCs).....	- 28 -
2.2.1.5.	Generation of Human Monocyte-Derived Macrophages (hMDMs).....	- 29 -
2.2.1.6.	Infection of hMDM with Leishmania	- 29 -
2.2.1.7.	Assessment of Intracellular Parasite Proliferation	- 30 -
2.2.1.8.	Isolation of Exosomes	- 30 -
2.2.2.	Cell Death Assays	- 30 -
2.2.2.1.	Cell Proliferation via MTT Assay	- 30 -
2.2.2.2.	Phosphatidylserine Externalization via Annexin Binding Assay	- 30 -
2.2.2.3.	DNA Fragmentation via Cell Cycle Assay	- 31 -
2.2.2.4.	DNA Fragmentation via TUNEL Assay	- 32 -
2.2.2.5.	ROS Detection.....	- 33 -
2.2.3.	Molecular Genetic Methods.....	- 33 -
2.2.3.1.	Preparation of Chemically Competent Bacterial Cells.....	- 33 -
2.2.3.2.	Transformation	- 33 -
2.2.3.3.	Restriction Cloning.....	- 33 -
2.2.3.4.	Gibson Assembly.....	- 35 -
2.2.3.5.	Stable Integration of Cas9/T7 in Leishmania	- 35 -
2.2.3.6.	Stable Integration of eGFP and DiCre in Leishmania.....	- 35 -
2.2.3.7.	Generation of Knock-outs.....	- 36 -
2.2.3.8.	Generation of inducible Knock-outs.....	- 38 -
2.2.3.9.	Confirmation of Knock-outs.....	- 39 -
2.2.3.10.	qRT-PCR	- 40 -
2.2.4.	Biochemical Methods	- 40 -
2.2.4.1.	Western Blot.....	- 40 -
2.2.4.2.	Preparation of Mass Spectrometry Samples for Proteomic Analysis.....	- 41 -
2.2.4.3.	Preparation of Mass Spectrometry Samples for Lipidomic Analysis	- 41 -
2.2.4.4.	Enzyme-linked immunosorbent assay (ELISA).....	- 42 -
2.2.5.	Microscopy	- 42 -
2.2.6.	Statistical Analysis	- 42 -
3.	Results	- 43 -

3.1.	Apoptosis Induction through different Compounds	- 43 -
3.2.	Mass Spectrometry Analysis of <i>Leishmania major</i>	- 48 -
3.2.1.	Assessment of Time Points of Apoptosis Induction for Mass Spectrometry	- 48 -
3.2.2.	Analysis of Mass Spectrometry Data.....	- 51 -
3.2.2.1.	Differential Expression Analysis of Promastigotes.....	- 55 -
3.2.2.2.	Differential Expression Analysis of Amastigotes	- 58 -
3.3.	Knock-outs of Mass Spectrometry Targets	- 63 -
3.4.	Endonuclease G and Metacaspase.....	- 69 -
3.5.	Pentose Phosphate Pathway as Drug Target	- 78 -
3.6.	Establishment of an Inducible Knock-out System	- 82 -
3.7.	The Role of <i>Leishmania</i> PS on the Human Immune System	- 87 -
4.	Discussion.....	- 90 -
4.1.	Induction of Apoptosis in <i>Leishmania</i>	- 92 -
4.2.	Search for New Proteins Involved in <i>Leishmania</i> Apoptosis.....	- 94 -
4.3.	Endonuclease G and Metacaspase.....	- 102 -
4.4.	Pentose Phosphate Pathway as Drug Target	- 105 -
4.5.	Establishment of an Inducible Knock-out System	- 108 -
4.6.	The Role of <i>Leishmania</i> PS on the Human Immune System	- 109 -
4.7.	Conclusion and Outlook	- 111 -
5.	References.....	- 113 -
6.	Supplement	- 132 -

Abbreviations

AAM	Alex Amastigotes Medium
BSA	Bovine Serum Albumin
Cas9	CRISPR-associated gene 9
cDNA	Complementary DNA
CDS	Coding sequence
CFSE	Carboxyfluorescein diacetate N-succinimidyl ester
CIP	Calf intestinal alkaline phosphatase
CL	Cutaneous leishmaniasis
CRISPR	Clustered regularly interspaced short palindromic repeats
Ct	Cycle threshold
Da	Dalton
DMSO	Dimethyl sulfoxide
DNA	Deoxyribonucleic acid
EDTA	Ethylenediaminetetraacetic acid
EtOH	Ethanol
FACS	Fluorescence activated cell sorting
FCS	Fetal calf serum
GOI	Gene of Interest
hMDM	Human Monocyte Derived Macrophages
HR	Homologous Region
KO	Knock-out
Ld	Leishmania donovani
Lm	Leishmania major
LPS	Lipopolysaccharide
LSM	Lymphocyte Separation Medium
MACS	Magnetic-Activated Cell Sorting
ML	Mucocutaneous leishmaniasis
mRNA	Messenger RNA
MTT	3-[4,5-dimethylthiazole-2-yl]-2,5-diphenyltetrazolium bromide

MOI	Multiplicity of Infection
UTR	Untranslated region
PAGE	Polyacrylamide gel electrophoresis
PBMC	Peripheral Blood Mononuclear Cell
PBS	Phosphate buffered saline
PCR	Polymerase chain reaction
PKDL	Post-kala-azar dermal leishmaniasis
PMN	Polymorphonuclear neutrophil granulocytes
PS	Phosphatidylserine
RNA	Ribonucleic acid
RT	Room temperature
ROS	Reactive Oxygen Species
SDS	Sodium dodecyl sulfate
sgRNA	Single Guide RNA
TEMED	N,N,N',N'-Tetramethylethylenediamin
Tris	Tris(hydroxymethyl)aminomethane
TSAP	Thermosensitive Alkaline Phosphatase
TUNEL	Terminal deoxynucleotidyl transferase dUTP Nick End Labeling
TWEEN 20	Polyoxyethylene (20) sorbitan monolaurate
VL	Visceral leishmaniasis
WHO	World Health Organization

Nucleobases are abbreviated using the common single letter code.

Zusammenfassung

Durch den Biss einer infizierten Sandmücke kann es zur Übertragung des parasitären Erregers *Leishmania* kommen, der verantwortlich ist für die vernachlässigte Tropenkrankheit Leishmaniose. Da es bisher weder zufriedenstellende Medikamente gibt, noch eine Impfung, ist die Suche nach neuen Möglichkeiten zur Eindämmung der Krankheit von äußerster Wichtigkeit. In früheren Untersuchungen konnte gezeigt werden, dass Leishmanien einen programmierten Zelltod (Apoptose), mit den gleichen Charakteristika wie Säugerzellen, durchlaufen können. Jedoch konnte keins der Apoptose-regulierenden Gene aus Säugerzellen im parasitären Genom gefunden werden. Zudem konnte nachgewiesen werden, dass apoptotische Leishmanien entscheidend für die Krankheitsentwicklung sind, vermutlich spielt das auf toten Parasiten präsentierte Phosphatidylserin (PS) hier eine Rolle. Folglich habe ich die Hypothese, dass die Identifizierung neuer Apoptose-involvierter Proteine mögliche Medikamenten- oder Impfstoff-Zielmoleküle offenbaren könnte. Zu diesem Zweck habe ich die Effizienz der verschiedenen Substanzen Staurosporin, Miltefosin, Harmonin und Compound 10 Apoptose in den verschiedenen Leishmanien Stadien Promastigoten und Amastigoten zu induzieren, untersucht. Dabei konnte ich deutliche Unterschiede der Substanzen auf die beiden Stadien ausmachen. Die Substanzen habe ich des Weiteren benutzt um Apoptose zu induzieren und mittels markierungsfreier, quantitativer Massenspektrometrie (MS) Proteine, die während dieses Vorgangs unterschiedlich reguliert sind, zu identifizieren. Ich konnte 55% des *L. major* Proteoms identifizieren und 4416 Proteine in Promastigoten und 2376 in Amastigoten quantifizieren. In Apoptose-induzierten Bedingungen, konnte ich 15 hoch- und 189 herunterregulierte Proteine in Promastigoten und 455 hoch- und 633 herunterregulierte Protein in Amastigoten finden. In diesen unterschiedlich regulierten Proteinen vermute ich potentielle Ziele zum weiteren Verständnis des Apoptosemechanismus sowie beeinhalteten diese vielversprechende Medikamentenziele. Proteine, die in allen Apoptosebedingungen hochreguliert waren, sind: EF1 α , p1/s1 Nuklease, Polyubiquitin und 40S ribosomales Protein S2. Um die Vermutung zu bestätigen, dass diese Proteine in der Apoptose involviert sind, habe ich mittels CRISPR/Cas9 knock-outs (KO) der Ziele durchgeführt und diese auf ihre Apoptosecharakteristika untersucht. Von keinem der genannten konnte ein vollständiger KO erzielt werden, was auf eine wichtige Rolle im Überleben des Parasiten hindeuten kann. Zudem wurden auch Proteine untersucht, deren Rolle in der Leishmanien Apoptose in der Literatur gezeigt wurde. Unsere Daten zeigen eine neue Rolle für ABCG2 in der Verteidigung gegen reaktive Sauerstoffspezies. Zudem konnte die Bedeutung von EndoG in der DNA Fragmentierung bestätigt werden. Ferner wurde nachgewiesen, dass EndoG und MCA eine Rolle im intrazellulären Überleben in den Wirtszellen hat. Mit Fokus auf das anti-inflammatorische Potenzial von PS konnten wir mittels MS das Vorhandensein spezifischer PS Spezies auf toten Leishmanien nachweisen. Vorläufige Daten mit Exosomen deuten darauf hin, dass PS von apoptotischen Parasiten tatsächlich eine anti-inflammatorische Immunantwort induzieren kann. Insgesamt liefert diese Arbeit einen sehr wertvollen MS-Datensatz und neue CRISPR/Cas9-Instrumente, die unser Wissen über Apoptosemechanismen in Leishmanien erweitern. Es hat das Potenzial, neue Wirkstoffkandidaten aufzudecken, die mit dem Zelltod des Parasiten in Verbindung gebracht werden, sowie die Entwicklung eines Impfstoffstamms zu ermöglichen.

Summary

Through the bite of an infected sand fly, the parasitic infectious agent *Leishmania* is transmitted to its mammalian host where it causes the neglected tropical disease leishmaniasis. Since up to date, there is neither a satisfying drug to treat the disease nor a protective vaccination available against the parasite, new options for disease containment are urgently needed. In former studies, it could be shown that *Leishmania* undergo programmed cell death (apoptosis) while showing the same phenotypic characteristics as mammalian cells. However, none of the genes that regulate apoptosis in mammals can be found in the parasite's genome. Moreover, it was demonstrated that apoptotic *Leishmania* are crucial for disease development and that this is probably due to phosphatidylserine (PS) moieties, which are presented on the cell surface of dead parasites. Correspondingly, I hypothesize that the identification of novel apoptosis-involved proteins reveals potential new targets for drug or vaccine development. For this purpose, I investigated the efficiency of the selected compounds staurosporine, miltefosine, harmonine and 1o to induce apoptosis in the *Leishmania* promastigote and amastigote life stage. Here, I could see clear differences of the substances in both stages. Further, I used the compounds to induce apoptosis and to subsequently identify and quantify differently regulated proteins during this process by label-free quantitative mass spectrometry (MS). I was able to identify 55% of the *L. major* promastigote proteome, quantifying 4416 proteins in promastigotes and 2376 in amastigotes. Focusing on apoptosis-inducing conditions, I found 15 up- and 189 downregulated proteins in promastigotes and 455 up- and 633 downregulated proteins in amastigotes. Within these differently regulated proteins, I expect potential targets for the further understanding of apoptosis mechanisms and it might contain promising drug targets. The proteins elongation factor 1 α , p1/s1 nuclease, polyubiquitin and 40S ribosomal protein S2 were upregulated in all apoptosis-inducing conditions tested. To prove my assumption that these proteins are involved in apoptosis, I used CRISPR/Cas9 technology to generate the respective gene knockouts of the identified targets and assessed their apoptosis characteristics. For none of these four targets, a full knockout could be achieved, suggesting an important role of these proteins for parasite survival. Apart from that, I also expanded the range of putative apoptosis-regulating targets to those described in already published research data. My results indicate a new role of the ATP-binding cassette transporter, ABCG2, in the defense against reactive oxygen species. In addition, the importance of the endonuclease EndoG in DNA fragmentation was shown. Moreover, EndoG and the metacaspase MCA have substantial function in the survival of the parasite inside the mammalian host cell. Focussing on the anti-inflammatory potential of PS by MS, we could demonstrate the presence of specific PS species only on apoptotic promastigotes, preliminary data using exosomes suggests that apoptotic parasites derived PS might indeed induce an anti-inflammatory immune response. Altogether, this work provides a very valuable MS dataset and new CRISPR/Cas9 tools increasing our knowledge on apoptosis mechanisms in *Leishmania*. It has the potential to reveal new drug target candidates, which are linked to cell death in the parasite as well as enabling the development of a vaccine strain.

1. Introduction

1.1. Leishmaniasis

The neglected, tropical disease leishmaniasis is caused by the protozoan parasite *Leishmania* that is transmitted through the bite of the female sand fly *Phlebotomus* or *Lutzomyia*. According to world health organization (WHO) classification, the disease can occur in three different manifestations: visceral, cutaneous and mucocutaneous leishmaniasis¹.



Figure 1. Leishmaniasis can occur in different forms: visceral (A), post-kala-azar dermal leishmaniasis (B), cutaneous (C) and mucocutaneous (D) leishmaniasis. Visceral leishmaniasis (VL) causes the enlargement of spleen and liver and is therefore fatal if untreated. After a recovered VL the post-kala-azar dermal leishmaniasis (PKDL) can occur, which leads to rash. The cutaneous form is the most common one, leading to lesions on exposed parts of the body. The destruction of the nose can be seen in the lower right picture of a patient with mucocutaneous leishmaniasis (ML). Pictures A – C are adapted from WHO Leishmaniasis Photo Gallery², D is adapted from Gomes et al (2014)³.

Visceral leishmaniasis (VL) is the most serious form of the disease, also known as kala-azar. This form is fatal in over 95% of cases, if untreated. The symptoms reach from fever, anemia, weight loss to an enlargement of spleen and liver¹ (see **Figure 1A**). It is endemic in 83 countries or territories, the estimated number of new VL cases per year are 50,000 – 90,000 with most cases in India, Sudan and Brazil (2019)¹. About 5 – 10% of patients who have recovered from VL are developing a post-kala-azar dermal leishmaniasis (PKDL). It occurs as a rash on face, upper arms, trunks and other parts of the body¹ (**Figure 1B**).

The most common form of disease is the cutaneous form. It leads to lesions, which often cure on its own but leave permanent scars and therefore a severe stigma⁴ (**Figure 1C**). In 2018, the disease was endemic in 92 countries or territories and there were between 600,000 and 1 million new cases reported with the highest numbers in Syria, Afghanistan and Pakistan¹.

The last and most disabling type of disease is called mucocutaneous leishmaniasis (ML). It causes a destruction of mucous membranes of nose, mouth and throat¹ (**Figure 1D**). Most of the cases of this disease are recorded in Bolivia, Brazil, Ethiopia and Peru¹.

The manifestation of the disease depends on the strain that infects the human. Typical strains, which lead to visceral leishmaniasis are *Leishmania donovani* (*L. donovani*) and *L. infantum*. Common strains causing cutaneous leishmaniasis are *L. major* or *L. aethiopica*. *L. braziliensis* causes the mucocutaneous form^{5,6}.

Many *Leishmania* infected persons do not develop any symptoms and therefore the disease remains unrecognized⁴. The co-infection with HIV is a big problem since patients are developing the whole clinical disease as well as high relapse and mortality rates¹. The highest co-infection rates of *Leishmania* and HIV are found in Brazil, Ethiopia and India¹.

1.1.1. Drugs against Leishmaniasis

Leishmaniasis is a poverty-related disease. The socioeconomic conditions that are associated with poverty, like bad sanitary conditions, malnutrition or migration, enhance the chance of *Leishmania* infections¹. While there is a broad range of drugs available against leishmaniasis, none of them is working without some disadvantages, as described in the following.

Pentavalent antimony (Sb^{5+}) is widely used against CL and VL, however resistant strains became evident in Bihar, India, where an increasing number of patients are unresponsive to pentavalent antimonial compounds^{7,8}. The high costs of the drug, which is correlated with a poor compliance and therefore disjointed treatments favor these unresponsiveness⁷. The proposed working mechanism of the drug includes the inhibition of trypanothione reductase in *Leishmania*, which leads to disrupted redox equilibrium and therefore the parasite is not able to react on oxidative stress⁹.

An alternative to Sb^{5+} is amphotericin B. This drug is very effective but needs to be administered as infusion in a hospital setting and shows also very severe side effects that can range from fever to death¹⁰. These side effects could be diminished through the use of a lipid formulation of amphotericin B, however this led to high costs of the treatment¹¹. The drug leads to a defect in the parasite membrane structure, which could be detected by the release of small molecules from the parasites. This increased permeability of the membrane causes the cell death of the parasite¹².

Developed in the 1990s, the phospholipid miltefosine showed a massive reduction of parasite burden in mice¹³. Where the oral route of administration is an advantage of this drug, its potential to cause birth defects is a disadvantage and therefore the drug cannot be used in pregnant women¹⁴. It is used for the treatment of CL and VL, it is cheap but also shows side effects like vomiting and diarrhea¹⁴ and emerging resistances were shown for *L. infantum* in Brazil¹⁵. In *Leishmania*, miltefosine inhibits the synthesis of phosphatidylcholine, disrupts the mitochondrial function by inhibition of cytochrome c oxidase¹⁶ and it destroys the calcium homeostasis by activation of calcium channels and acidocalcisomes to increase the intracellular calcium concentration massively¹⁷. Showing that miltefosin has a complex mode of action but the exact leishmanial target structure for miltefosin and the mechanism by which *Leishmania* parasites are killed is still unknown.

Treatment is possible but a satisfying drug against the different forms of leishmaniasis is not found until now. Problems include the upcoming resistance to the drugs currently in use, the toxicity/side effects and high costs of the treatment¹⁸. This highlights the need of developing new drugs.

1.1.2. Vaccination against Leishmaniasis

A very old method to immunize people against *Leishmania* is called leishmanization. In this method, parasites are collected from a patient's CL lesion, and are inoculated in a covered part of the body of a child. This leads mostly to a lesion of cutaneous leishmaniasis but after self-healing also to a life-long protection against a further infection¹⁹. After the development of *in vitro* *Leishmania* culture, the artificial leishmanization from harvested parasites was performed and thousands of people in the former Soviet Union as well as in Iran were immunized during the 1950s and 1960s^{20,21}. The WHO supported a leishmanization study in which *L. major* was produced under good manufacturing practice (GMP) conditions and 11/11 patients achieved full protection²². However, because of the usage of a viable and infective agent, general safety and ethical reasons resulted in this method not being pursued any further²³.

Other trials attempted the use of whole killed *L. amazonensis* (called Leishvaccine) or different strains of autoclaved *Leishmania*, all showed a high safety profile but a low efficiency²⁴. The use of *Leishmania* antigens as vaccines was very successful in canine leishmaniasis and resulted in two veterinary licensed vaccines. Leishmune[®] uses the fucose-mannose ligand (FML) and CaniLeish[®] uses extracted secreted proteins from *L. infantum*, while the latter is the only licensed vaccine in Europe²⁵. A next generation of vaccines are comprised of recombinant proteins, one of them (Leish-Tec[®]) is already licensed in Brazil for the use in dogs and contains the A2 antigen from *L. infantum*²⁶. A very promising new approach are DNA-based vaccines, ChAd63-KH has already accomplished clinical trial phase II, where it showed a high safety and induction of immune system. The vaccine encodes the two genes KMP-11 and HASPB from *L. donovani*²⁷. The development of CRISPR/Cas9 techniques in

Leishmania could also enable life-attenuated strains that are as effective as leishmanization but safer^{28–30}. This can be achieved by the deletion of a distinct gene, which leads to reduced virulence, as shown for cysteine protease from *L. mexicana*³⁰. Using this strategy, the parasites were shown to cause less disease in a mouse model and induced a protective T helper 1 response.

1.2. *Leishmania* spp.

In 1903, Major W. B. Leishman published the observation of distinct “bodies” in the spleen of a British soldier who was stationed in India³¹. He suggested that those “bodies” are related to trypanosoma. In the same year Major C. Donovan published the fact that he made the same observation³². Following to this, Major Ross suggested³² that this is a novel organism and these “bodies” were named *Leishmania donovani*³³.

The life cycle of *Leishmania* is diphasic, which means the parasites alternate between the flagellated promastigotes in the sand fly and the aflagellated amastigotes within the mammalian phagocytes. Common mammalian hosts are humans, dogs, rodents and monkeys³⁴.

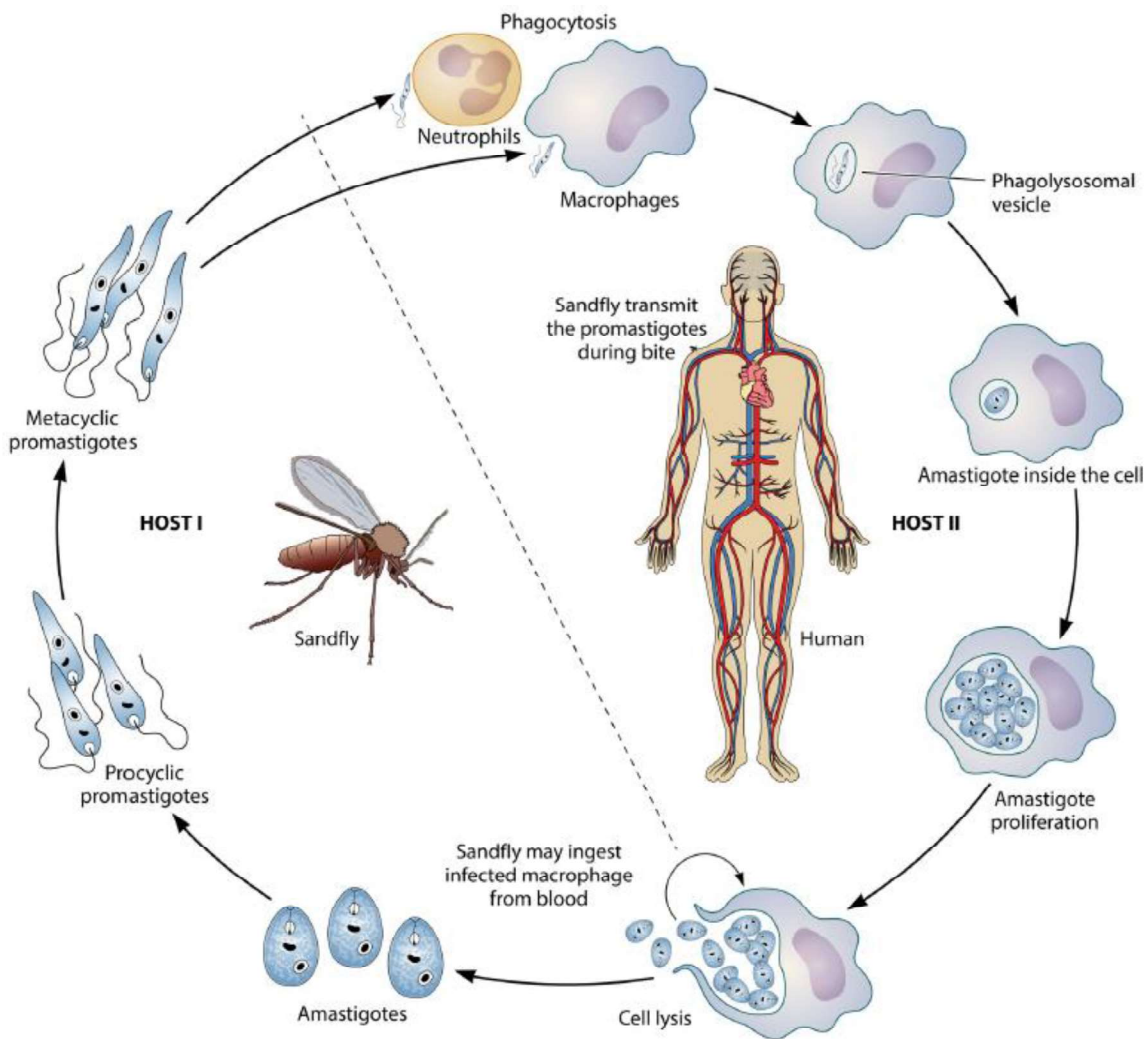


Figure 2. Lifecycle of the protozoan parasite *Leishmania* depicting the development in HOST I (female sand fly) and HOST II (human). Metacyclic promastigotes are transferred through the bite of the sand fly and infect in the human first neutrophils

and later the final host macrophages. The promastigotes reside in the phagolysosomal vesicle and transform there to its amastigote form. Amastigotes start proliferating and infect further cells during cell lysis. When the sand fly bites the human again the lifecycle is closed, since here the transformation from amastigote to promastigote takes place. As promastigote they transform from the procyclic to the infective metacyclic form. Figure is adapted from Prasanna et al (2021)³⁵.

Following the bite of an infected sand fly, the promastigote form of *Leishmania* parasites infiltrates the skin of the mammalian host and an inflammatory reaction is initiated. This involves the recruitment of polymorphonuclear neutrophil granulocytes (PMN) within the first hours after infection³⁶. They produce IL-8 when sensing the parasites, which has a chemotactic activity on additional PMNs and enhances phagocytosis of the parasite³⁷. Through delaying spontaneous apoptosis of PMNs, *Leishmania* survive within this initial host cell about two to three days³⁸. Hereupon, infected PMNs produce chemokines (MIP-1 α and MIP-1 β) that attract the second wave of phagocytes, this time mainly macrophages³⁹. The parasites can enter the macrophages directly or through phagocytosis of the infected apoptotic PMNs⁴⁰. Macrophages are the ultimate host cells for *Leishmania* in which they start differentiate to amastigotes and multiply. Therefore, this is also the time point at which disease symptoms become evident in the host³⁹. Through another blood meal, infected cells and amastigotes are taken up again by the sand fly. They reside in the sand fly's midgut and transform back to their promastigote form. Apart from viable promastigotes the inoculum consists also of apoptotic promastigotes⁴¹. The metacyclic infective parasites migrate to the pharyngeal valve and the lifecycle is closed⁴².

1.2.1. The Role of Apoptosis in Infection

It could be shown that the presence of apoptotic parasites is crucial for the infectivity of *Leishmania*⁴¹. In a susceptible murine model, separated apoptotic *Leishmania* were not able to cause a severe footpad swelling and exclusively viable ones did not either. However, the mixture of both led to a severe footpad swelling with an earlier onset of necrosis⁴¹. Separation of apoptotic parasites can be achieved by their ability to bind to annexin V via their surface-exposed phosphatidylserine (PS)⁴¹. However, for *Leishmania*, it is still controversial, which phospholipid is responsible for their annexin V binding⁴³. Apart from infectivity, apoptotic parasites play an important role for the survival of viable *Leishmania* in the host cell. Apoptotic promastigotes induce the production of anti-inflammatory TGF- β and suppress pro-inflammatory TNF α , leading to the silencing of effector functions in PMNs, which in turn favors the intracellular survival of viable parasites⁴¹.

The exact mechanism how apoptotic parasites can increase the infectivity remains elusive. However, it could be shown that apoptotic and viable *L. major* are targeted differently by the host cell's autophagy machinery⁴⁴. Further, the presence of apoptotic parasites decreased the release of pro-inflammatory cytokines and the consequential T-cell activation which results in a diminished immune

response against the pathogen. Taken together, the activation of the host's autophagy-machinery by apoptotic *Leishmania* contributes to overall parasite survival⁴⁴.

1.2.2. Genetics in *Leishmania*

Parasites of the genus *Leishmania* show very special genetic features that do not occur in organisms apart from the kinetoplasts. The size of the haploid *Leishmania* genome is about 35 Mb, organized in 36 chromosomes for the Old World species and, caused by chromosomal rearrangements, only 34 and 35 chromosomes for the New World species *L. mexicana* and *L. braziliensis*⁴⁵⁻⁴⁷. While the baseline somy in *Leishmania* is haploid, aneuploidy could be detected in all species⁴⁸. In *L. donovani* it could be shown that aneuploid chromosomes adapt to different environments in the sand fly and host macrophage⁴⁸. The only chromosomes that occur in the same configuration in all *Leishmania* species are chromosome 31 and chromosome 25, which are tetrasomic or disomic, respectively⁴⁹.

DNA synthesis in *Leishmania* is quite unusual, because during early S-phase, a single origin in each chromosome serves as start point, while in all cell cycle phases subtelomeric DNA synthesis can occur⁵⁰. In chromosome 1 of the *Leishmania major* Friedlin strain, the first 29 genes are situated on the same DNA strand, while the other 50 genes are located on the other DNA strand. This arrangement is called 'head-to-head'. Another organization, which can be found on chromosome 3 is 'tail-to-tail'⁵¹. Apart from this, *Leishmania* lacks the pathway of non-homologous end joining (NHEJ) but possesses a very efficient homologous recombination pathway, which was used for many years in order to perform genetic modifications in the parasite⁵². This becomes even more important when considering that *Leishmania* lack activity of the genetic tool RNA interference (RNAi). Only in the subgenus *Vianna* the necessary genes Dicer and Argonaute are found and show activity⁵³.

In theory, there are 8412 protein-coding genes found in *L. major*⁴⁹. A lot of genes in the genome are arranged as tandem repeats. These proteins can be assigned as important for cell survival, for example for replication, transcription or translation⁵¹. Several tandem duplications are ancient ones that are related on protein-sequence level but without significant DNA sequence similarity⁵¹. The genes found in *Leishmania* do not cluster in operons with similar function⁵¹.

In the parasite's protein-coding genes, there are no introns found, suggesting another splicing mechanism than the common cis-splicing^{46,51}. The process that takes place here, is called trans-splicing and was first discovered in *Trypanosoma brucei*⁵⁴. Here, the existence of a 35 nucleotides long mini-exon (later also called: spliced leader⁵⁵) at the 5' end of mRNAs was detected⁵⁶. Before splicing, the protein-coding genes are transcribed into polycistronic mRNAs and a spliced leader is trans-spliced

onto each mRNA. Therefore, a monocistronic capped transcript is generated, which is also polyadenylated in this step^{57,58}.

Until now, there are no promoter elements found for RNA polymerase II⁵⁹. Only one specific 3'-UTR element leads to a higher expression in amastigotes⁶⁰. Therefore, gene expression regulation must occur mainly on posttranscriptional level by trans-splicing, polyadenylation, mRNA stability, translation and protein stability⁵¹. Another suggested gene regulation method is the dosage of genes. As already mentioned, the *Leishmania* chromosomes are highly aneuploid, depending on the parasite's environment. Through the adaption of chromosome numbers, it is possible to provide a higher expression of specific genes⁴⁸. The genomic plasticity of *Leishmania* can also be seen by the possibility of generating parasite hybrids *in vitro*. The co-culture of a GFP-Neo *L. tropica* strain with a RFP-Hyg *L. tropica* leads to a hybrid strain combining both fluorescent proteins and drug-resistance markers⁶¹. This sexual cycle of *Leishmania* can therefore enhance the genetic exchange between different parasites.

1.2.3. CRISPR/Cas9 Toolkit

In 2017, Beneke et al. published a toolkit for rapid gene modification in kinetoplastids like *Leishmania* through the use of clustered regularly interspaced short palindromic repeats (CRISPR) and the CRISPR-associated gene 9 (Cas9)⁵². This toolkit enables very rapid and efficient knock-out and tagging of genes. The method requires a stable expression of the Cas9 endonuclease and the T7 RNA polymerase in *Leishmania*. Therefore, an *in vivo* transcription of the single guide RNA (sgRNA) template using the T7 RNA polymerase is possible. **Figure 3** shows the procedure of sgRNA *in vivo* transcription. An oligonucleotide is designed, which consists of the T7 promotor, a target site specific for the gene of interest (GOI) and a part of the sgRNA scaffold. For the design of the target-specific sequences, the online source LeishGEdit.net is used. A common PCR of the gene-specific oligonucleotide and the sgRNA scaffold leads to a PCR product that can be transfected to T7 polymerase-expressing *Leishmania*, achieving a sgRNA transcription *in vivo*. The complex formation of sgRNA with the Cas9 endonuclease and their binding to the genomic target site activates Cas9 and leads to the induction of DNA double strand breaks.

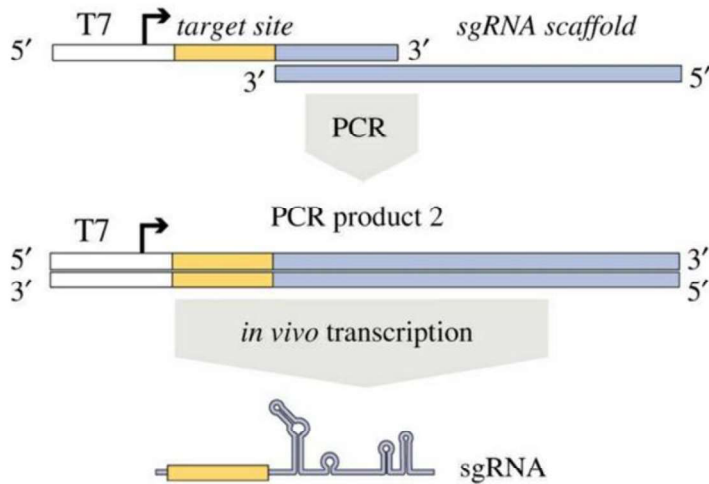


Figure 3. *In vivo* transcription of single guide RNA (sgRNA) within the CRISPR/Cas9 toolkit. By PCR, the T7 promoter is connected with the gene-specific target site and the scaffold for sgRNA. When the product is transfected to Cas9/T7 expressing cells, the *in vivo* transcription is carried out, leading to a gene-specific sgRNA. Figure is adopted from Beneke et al. (2017)⁵².

Gene tagging or knock-out can be promoted if a repair cassette is provided. The plasmids pT and pPLOT are serving as repair cassette for knockout or tagging, respectively. By PCR with primers specific for the UTRs of the GOI (also designed on LeishGEdit.net), a repair cassette with 5' and 3' UTR flanking a drug resistance, is prepared (**Figure 4**). Simultaneous transfection of the Cas9/T7-expressing parasites with the sgRNA template and the repair DNA fragment allows replacement of the GOI by the antibiotic resistance gene through homologous recombination. Culturing the transfected parasites in medium containing the selective antibiotics leads to a population of genetically manipulated parasites within a very short time period⁵².

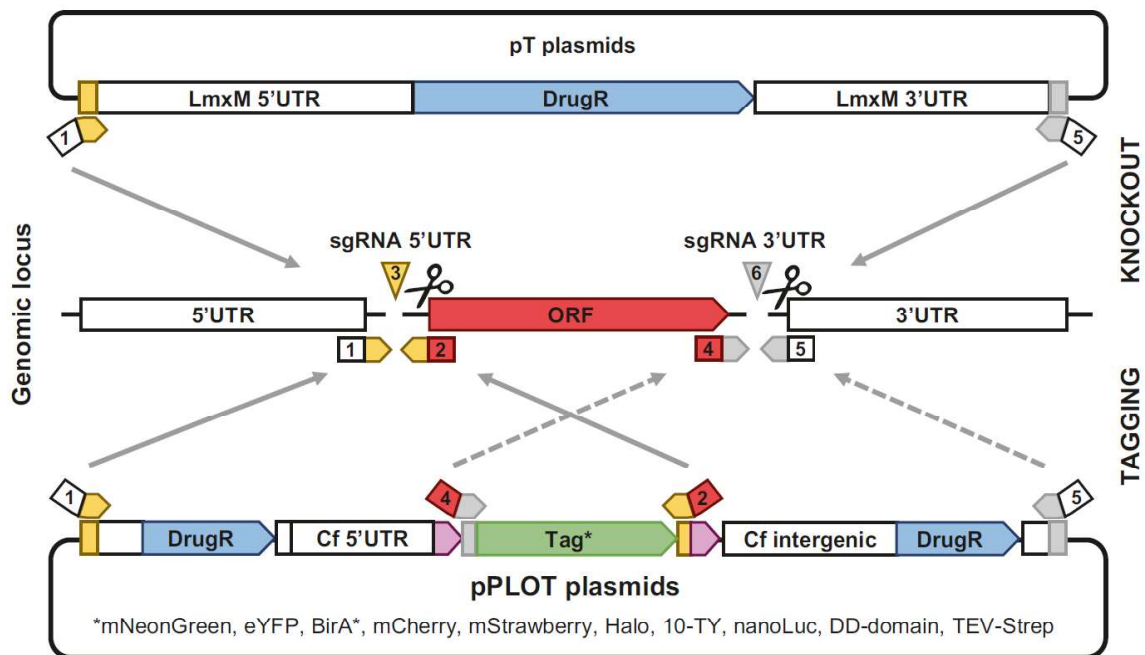


Figure 4. Plasmid system for genetic manipulation via CRISPR/Cas9 in *Leishmania*. The plasmid pT is used for knock-out, the plasmid pPLOT for tagging of the GOI in *Leishmania*. A set of only four primers (1-2, 4-5) is needed for both systems. The sgRNA cuts in the UTRs up- and downstream of the GOI (3, 6) Figure was adapted from Beneke et al (2019)⁶².

1.3. Apoptosis

The term apoptosis was first proposed by Kerr, Wyllie and Currie in 1972. They described it as the mechanism of controlled cell deletion, which can be caused by different stimuli⁶³. The importance of a programmed cell death was further studied in the model organism *Caenorhabditis elegans*. In this nematode, the development process is highly dependent on the apoptosis of distinct somatic cells at particular time points during development⁶⁴. The apoptosis triggers can derive from a broad variety of stimuli, for example cell damaging through drugs or irradiation⁶⁵, but also the binding of cytokines to so called death receptors like Fas⁶⁶ or TNF receptor⁶⁷. Already in 1972, the morphological changes that are induced by apoptosis were described very well. These include the shrinkage of the cell, chromatin condensation (also called pyknosis) as well as the formation of apoptotic bodies⁶³.

When apoptosis is induced, (either through intrinsic or extrinsic stimuli) a proteolytic cascade is started, which involves the cleavage of different pro-caspases to their active caspase form. Caspase stand for cysteinyl-aspartate specific protease and these enzymes can be grouped into initiator caspases (2, 8, 9, 10) and effector caspases (3, 6, 7)⁶⁸.

Intrinsic pathways of apoptosis always include the depolarization of the mitochondrial membrane, which leads to the release of pro-apoptotic proteins like cytochrome c, AIF or EndoG⁶⁹⁻⁷¹. Subsequently, cytochrome c binds APAF1 and form the apoptosome, which allows the activation of the initiator caspase-9 and further activation of the effector caspases 3, 6 and 7⁷².

On the contrary, the extrinsic pathway is initiated through ligands binding death receptors (**Figure 5**). After ligand binding, FADD and caspase 8 are recruited to the receptor, forming the so-called death-inducing signaling complex (DISC)⁷³. The following activation of caspase 8 leads to the cleavage of the effector caspases. However, a clear discrimination of pathways can be difficult, since also the interplay of extrinsic and intrinsic routes could be shown⁷⁴. Further, effector caspase 3 leads to the typical apoptosis characteristics, like extensive fragmentation of DNA by endonucleases to segments of 180 – 200 bp length⁷⁵.

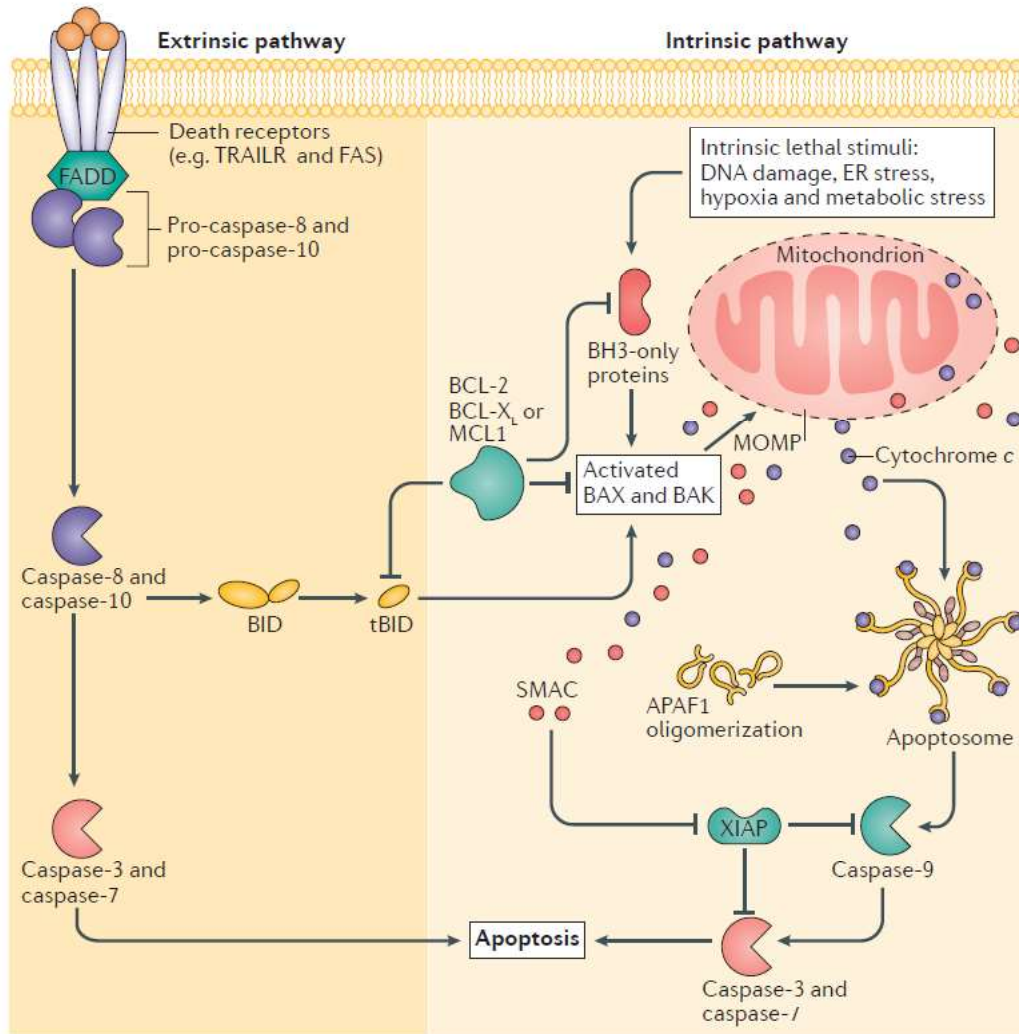


Figure 5. Extrinsic and intrinsic pathways of apoptosis in mammalian cells. Extrinsic stimuli are recognized via death receptors and lead to the cleavage and following activation of pro-caspase-8/10. That in turn leads to the activation of caspase-3 and 7. Intrinsic apoptosis stimuli favor the mitochondrial outer membrane permeabilization (MOMP), leading to the release of pro-apoptotic proteins like cytochrome c, the formation of the apoptosome and the activation of caspase-9. Consecutively, caspase-3 and 7 are activated and lead to apoptosis. Figure was adopted from Ichim et al⁷⁶.

Additionally, a restructuring of the cell membrane takes place during apoptosis. Phosphatidylserine (PS), which locates to the inner cell membrane under normal conditions, is exposed to the outside of the lipid bilayer in an apoptotic cell⁷⁷. This is executed through two main proteins: ATP11 and XKR8. Both are cleaved by caspase-3, while ATP11 is inactivated through the cleavage, XKR8 is activated. ATP11 is a flippase, which constantly traps phosphatidylserine in the inner leaflet of the membrane, through the inactivation, phosphatidylserine is not flipped back from the outside⁷⁸. On the other hand, XKR8 is a scramblase, which mediates the transfer of phospholipids between inner and outer leaflet⁷⁹.

Phosphatidylserine acts as eat-me signal for the silent uptake of apoptotic cells, since they are subsequently engulfed by phagocytic cells like macrophages⁸⁰. There is a relatively broad range of receptors present on phagocytes, which can recognize phosphatidylserine on apoptotic cells. These are: TIM1, TIM4, BAI1, RAGE, CD300 family, stabilins, MerTK (with the adaptors Gas6 and protein S), and $\alpha\beta 5$ integrin (with adaptor MFGE-8)⁸¹. This silent uptake involves also that there are no

inflammatory signals released during apoptosis, which is a feature that distinguishes apoptosis from other cell death processes like necrosis⁸².

A tight regulation of apoptosis is of great importance, since the dysregulation can lead to cancer. This becomes evident when looking at the pro-apoptotic protein p53, which is mutated in approximately 50% of human cancer⁸³. Therefore, the pathway of apoptosis is a target for potential drugs against cancer but also several other diseases like neurodegenerative, cardiovascular and infectious diseases⁸⁴. Within the pathway there are different approaches, ranging from targeting of the death receptors, caspases, anti- and pro-apoptotic proteins (e.g., p53)⁸⁵. The strategy for anti-cancer drugs is to promote apoptosis of the cancerous cell, while the opposite is strived for in neurodegenerative and cardiovascular diseases, where a prolonged survival of the cells is the main aim⁸⁴. One example of a drug that induces apoptosis and is approved against cancer is imatinib. The drug kills gastric cancer cells via the inhibition of tyrosine kinases, which in turn leads to ROS production and apoptosis⁸⁶. On the opposite, a drug that inhibits apoptosis is edaravone. It is used against amyotrophic lateral sclerosis (ALS) and for stroke recovery by reducing oxidative stress⁸⁷.

1.4. Apoptosis in *Leishmania*

Leishmania parasites can enter a programmed cell death, which shows all the characteristics of apoptosis: depolarization of mitochondrial potential, induction of reactive oxygen species (ROS), externalization of phosphatidylserine, DNA fragmentation, and shrinkage of the body^{41,44,88,89}. Until now, very little is known about proteins that are involved in apoptosis in *Leishmania*⁹⁰. The proteins that have an important function in mammalian apoptosis, like caspases, death receptors and pro- and anti-apoptotic proteins, are not encoded in the *Leishmania* genome⁹¹.

Some proteins have been suggested to play a role in leishmanial apoptosis but are not fully characterized as such yet. One is methionine aminopeptidase 2 (MAP2). Chemical inhibition of MAP2 in *Leishmania* prevented most apoptosis characteristics induced by miltefosine⁹². However, PS externalization and cell death could not be prevented through the inhibition of MAP2 in apoptotic parasites. Consequently, it was suggested that the protein is an effector molecule for the induction of apoptosis, but it is dispensable for leishmanial cell death. Another class of proteins are suggested because they carry a distinct domain that is unique for pro- and anti-apoptotic proteins (e.g., BH3 domain). Li-BH3AQP was found to harbor a BH3 domain and it could be shown that the overexpression of this protein in *Leishmania* leads to reduced parasite survival when apoptosis is induced through staurosporine⁹³. Another suggested effector protein is the cysteine proteinase C (CPC), which binds to the pan-caspase inhibitor Z-VAD-FMK and might therefore fulfill a similar role as caspases in

Leishmania. The KO of the *cpc* gene leads to enhanced survival after leishmanial apoptosis induction through hydrogen peroxide⁹⁴.

1.4.1. Endonuclease G

A well-characterized cell-death-related protein is Endonuclease G (EndoG). It was first described as a caspase-independent nuclease involved in the cell death in mice⁷¹. This nuclease has also homologs in *C. elegans* and humans with about 30% sequence identity and conserved amino acids for nuclease activity (S206, H209, E249)⁹⁵. A difference between mammalian EndoG (33 kDa) and leishmanial EndoG (54 kDa) is the size of the protein⁹⁶, which is correlated with its nuclease activity. In *Neurospora*, yeast and *Leishmania*, EndoG possesses full endo/exonuclease activities⁹⁷. In contrast, in mammals, EndoG is restricted to endonuclease activity, while a second protein, EXOG, exerts the 5' exonuclease activity⁹⁷. EndoG is located in the mitochondria, which was first suggested by the mitochondrial targeting signal, but could then also be confirmed by co-localization experiments⁹⁵. Upon apoptotic stimulus, EndoG is released from the mitochondria and moves to the nucleus^{95,96,98}. The mitochondrial localization of EndoG seems to be important for cell survival, since an ectopic expression of EndoG in the cytosol leads to cell death in HeLa cells⁹⁹. However, protein modelling of *L. infantum* EndoG reveals a pH-dependent domain, which leads to inactivation of the protein upon higher pH values, as it is found in the mitochondrial matrix. Lower pH values as in the cytosol, lead to the activation of EndoG¹⁰⁰.

The overexpression of EndoG in *L. donovani* has no effect on growth behavior in the promastigote stage. However, it leads to a significant reduction of the growth of axenic amastigotes, which is correlated with an increased DNA fragmentation. Oxidative stress in EndoG-overexpressing amastigotes increases DNA fragmentation significantly⁹⁵. Regarding the effect on the host cell macrophages, the overexpression of EndoG does not lead to an altered infection rate, but to a killing of the intracellular amastigotes within 96 hours⁹⁵. An EndoG knockdown in *T. brucei* had no effect on growth but cells were less susceptible to the toxic effects of H₂O₂, which could be seen by decreased DNA fragmentation measured by TdT-mediated dUTP-biotin nick end labeling (TUNEL) staining⁹⁵.

Immunoprecipitation experiments show an interaction of EndoG, FEN-1 and TatD-like nuclease in *L. donovani*, which comprise the so called 'degradasome'. Since a downregulation of EndoG leads to reduced apoptosis characteristics like ROS formation and mitochondrial membrane permeabilization, a negative feedback loop through EndoG is suggested⁹⁸.

The antibiotic Tunicamycin, which leads to unfolded protein response (UPR) in the endoplasmic reticulum (ER), also leads to the release of EndoG through mitochondrial membrane depolarization as a result of elevated ROS and calcium levels¹⁰¹. Another drug that leads to EndoG release in *L. donovani* and to activation of metacaspase, is the topoisomerase IB inhibitor Betulin¹⁰².

The search for anti-leishmanial compounds also involved EndoG as a drug target. The inhibition of the endonuclease shows reduced viability in promastigotes and amastigotes of *L. infantum*¹⁰³. These results were further confirmed by Rico et al⁹⁷: they were able to create a partial EndoG KO, which grew at a lower rate, had increased mitochondrial potential and exhibited lower infection rate and lower parasite burden. An overexpression of recombinant EndoG from *L. infantum* leads to parasites that are more susceptible to edelfosine-induced cell death. It is speculated that this observation is caused by an increase in the pro-apoptotic machinery⁹⁷.

1.4.2. Metacaspase

Leishmania does not possess caspases, but a metacaspase was found in the parasite that was thought to fulfill a similar function, even though with different substrate specificity. The catalytic dyad is comprised of histidine and cysteine as known for caspases¹⁰⁴. In 2006, researchers showed the importance of the metacaspase in order to induce cell death in *L. major*. They depleted the metacaspase analog in yeast and overexpressed the metacaspase MCA5 from *L. major*. MCA5 could completely restore the function of the yeast protein after induction of cell death through hydrogen peroxide¹⁰⁴. In *Leishmania donovani*, two additional metacaspases were found: MC1 and MC2. These enzymes could be inhibited by antipain and N α -Tosyl-Lys-chloromethylketone (TLCK)¹⁰⁵, both inhibitors of trypsin and trypsin-like serine proteases.

In 2007, the group of Jeremy Mottram published data on an essential role of metacaspase in the cell cycle progression of *L. major*. They showed that metacaspase is a microtubule-associated protein (MAP), like the EF1 α , since it associates with the mitotic spindle during cell division. An overexpression of MCA led to impaired kinetoplast segregation, mitosis and also cytokinesis. They stated that a knock-out of the gene was not possible, suggesting its role as potential drug target¹⁰⁶. However, recent improvements in knock-out techniques enabled the establishment of a metacaspase KO⁹⁰. The MCA KO showed implications in cell death and autophagy. After a 24h incubation with miltefosine, the MCA KO still did not show any signs of cell death like DNA fragmentation, stop of movement and loss of mitochondrial membrane potential⁹⁰. Further, a better growth during starvation could be seen for the MCA KO and an upregulation of MCA during starvation in the wildtype could link MCA to autophagy⁹⁰.

1.5. Hypothesis and Aims

In order to induce cell death in pathogenic parasites and thus, to render them innocuous, the pathway of apoptosis is a promising target for the development of drugs. Since it is my ultimate goal to find a proper way to kill *Leishmania*, we need a deeper understanding of the regulation of the

apoptosis pathway in the parasite. Although *Leishmania* do not encode for any homologs of known mammal apoptosis-regulating proteins, they show apoptosis characteristics like cell shrinkage, externalization of annexin-binding lipids and DNA fragmentation⁸⁹. Therefore, I hypothesize that *Leishmania* induces and proceeds apoptosis through a specialized mechanism, and I seek to elucidate this mechanism by the identification and characterization of proteins involved in its regulation. Further, it is my hypothesis that the identified apoptosis-regulating proteins can then serve as target for drug development: an inhibition of anti-apoptotic proteins would induce apoptosis and kill the parasites. On the other hand, an inhibition of pro-apoptotic proteins could impair apoptosis characteristics like PS externalization. This would lead to a decrease of the anti-inflammatory response of the human immune system and an anti-leishmanial T cell response. This approach could then also serve as the basis for vaccine development: instead of inhibiting a pro-apoptotic protein, I could produce a knockout strain targeting the anti-inflammatory potential of PS, which should then result in a protective inflammatory immune response enabling a protection against a further challenge with wildtype *Leishmania*.

Based on this, I have the following aims (**Figure 6**):

1. Establishment of the CRISPR/Cas9 *Leishmania* system in our lab to investigate target genes potentially involved in leishmanial apoptosis (in cooperation with Prof. Jiménez Ruiz, University of Alcalá).
2. Inducing drug mediated parasite apoptosis to identify promastigote and amastigote specific proteins that are involved in the process of apoptosis by employing label free quantitative mass spectrometry (in cooperation with Prof. Tenzer, University Mainz).
3. Functional characterization of gene knockouts in *Leishmania* in order to confirm potential targets of pro- and anti-apoptotic proteins for drug development.
4. Identification and characterization of effects of knockout mutants on the human immune system aiming to find parasites lacking anti-inflammatory properties for future vaccine development.

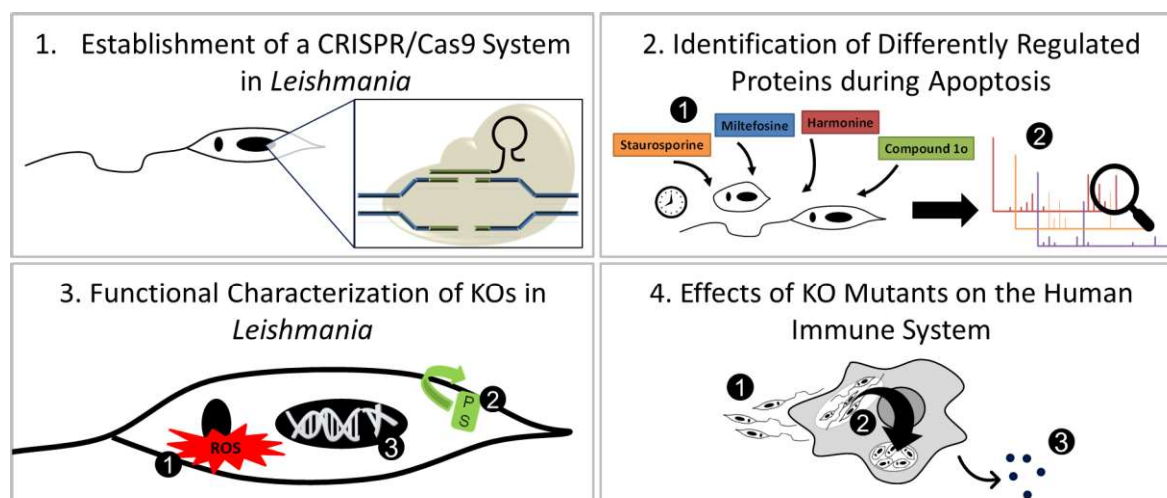


Figure 6. Aims that are strived for in this thesis. First of all, a CRISPR/Cas9 system is applied in *Leishmania* to achieve knock-out (KO) strains of specific genes, which might be involved in apoptosis mechanisms. Following, the induction of cell death in the parasites through different compounds are investigated in more detail (2.①) and are used to identify differently regulated proteins during apoptosis by label free quantitative LC-MS/MS (2.②). In the third step, KO strains of potential pro- or anti-apoptotic targets are characterized regarding their reactive oxygen species (ROS) production (3.①), phosphatidylserine (PS) externalization (3.②) and DNA fragmentation (3.③) during apoptosis with the aim to find possible drug targets. In a last step, the effects of the KO strains on the human immune system are investigated including the infection rate of human primary macrophages (4.①), the intracellular transformation and proliferation of *Leishmania* (4.②) and the pro- and anti-inflammatory response of macrophages by cytokine secretion (4.③).

2. Materials and Methods

2.1. Materials

2.1.1. Reagents

2-Mercaptoethanol	Sigma-Aldrich
2-Propanol	VWR
Acrylamide	Serva
Agarose, LE	Biozym Scientific
Ammonium persulfate	Serva
Aqua bidest.	Medienküche PEI
Biopterin	Sigma-Aldrich
Bovine Serum Albumin (BSA)	Sigma-Aldrich
Casyton	OMNI Life Science
Difco Brain Heart Infusion Agar	Becton Dickenson
Diff Quik Fixative, Solution I and II	Medion Diagnostics
Dimethyl sulfoxide (DMSO)	AppliChem
ECL plus western blotting substrate	Thermo Fisher
Ethylenediaminetetraacetic acid (EDTA)	Merck
Ethanol, absolute	VWR
FACS Clean	Medienküche PEI
FACS Flow	Medienküche PEI
FACS Rinse	Medienküche PEI
Fetal Calf Serum (FCS)	Sigma-Aldrich
Glycerol	Citifluor
Hemin	Sigma-Aldrich
HEPES	AppliChem
Histopaque®-1077	Sigma-Aldrich
Histopaque®-1119	Sigma-Aldrich
Human interferon- γ (IFN- γ)	Sigma-Aldrich
Human recombinant Granulocyte Macrophage Colony Stimulating Factor (GM-CSF)	Bayer
Human recombinant Macrophage Colony Stimulating	R&D Systems

MATERIALS AND METHODS

Factor (M-CSF)	
Human Serum Type AB	Lonza
Hydrochloric acid (HCl)	Merck
LB Agar	Merck
L-glutamine	Merck
Lipopolysaccharide (LPS)	Sigma-Aldrich
Medium 199	Gibco
Milk powder	TSI
Mowiol Mounting Medium	Sigma-Aldrich
Paraformaldehyde	Sigma-Aldrich
Penicillin/Streptomycin	Biochrom
Rabbit Blood, defibrinated	Elocin-Lab
RNase AWAY	VWR
Roswell Park Memorial Institute (RPMI) 1640 Medium	Sigma-Aldrich
Sodium bicarbonate	Sigma
Sodium dodecyl sulfate (SDS)	Merck
N, N, N',N'-tetramethylethylenediamine (TEMED)	Serva

2.1.2. Buffers

Buffer	Receipt
Ammoniumchloride solution	0.15 M Ammoniumchloride Aqua bidest.
Blocking solution	TBS-T 5% milk powder (w/v)
Blotting buffer	50 mM Tris 40 mM Glycin 0.0375% SDS (w/v) 2.5% Methanol (v/v) Aqua bidest.
PBS without Ca ²⁺ and Mg ²⁺ pH 7.1 (1x)	136.9 mM sodium chloride 2.68 mM potassium chloride 1.47 mM potassium dihydrogen orthophosphate 8.1 mM sodium dihydrogen phosphate Aqua bidest.
MACS buffer	0.5% BSA (w/v) 0.5 mM EDTA PBS pH 7.2
Ringer solution	147 mM NaCl 4 mM KCl

Running buffer (5x)	2.2 mM CaCl ₂ Aqua bidest. 125 mM Tris 1.25 M Glycine 0.5% SDS (w/v) Aqua bidest.
Separating gel buffer pH 8.8 (4x)	1.5 M Tris-HCl pH 8.8 0.4% SDS (w/v) Aqua bidest.
Stacking gel buffer pH 6.8 (4x)	0.5 M Tris-HCl pH 6.8 0.4% SDS (w/v) Aqua bidest.
TAE buffer (20x)	0.8 M Tris-HCl pH 8.0 20 mM EDTA 2.25% acetic acid Aqua bidest.
TBS buffer (10x)	50 mM Tris-HCl pH 7.4 150 mM NaCl Aqua bidest.
TBS/T solution	1 x TBS buffer 0.5% Tween 20 (v/v)
Washing-buffer	1x PBS without Ca ²⁺ and Mg ²⁺ pH 7.1 5% complete-medium (v/v)
Zimmerman buffer	132 mM NaCl 8 mM KCl 8 mM Na ₂ HPO ₄ 1.5 mM KH ₂ PO ₄ 0.5 mM MgAc ₂ 90 μM CaOAc ₂ Aqua bidest. pH 7 sterile filtered
TFB1	30 mM KAc 100 mM RbCl 10 mM CaCl ₂ x 2 H ₂ O 50 mM MnCl ₂ x 4 H ₂ O 15% Glycerol Aqua bidest. pH 5.8 sterile filtered
TFB2	10 mM MOPS 75 mM CaCl ₂ 10 mM RbCl 15% Glycerol Aqua bidest. pH 6.5

sterile filtered

2.1.3. Media

Medium	Receipt
Amastigote Medium (AAM)	RPMI-1640 10% FCS (v/v) 3 mM L-glutamine 100 U/mL Penicillin 100 µg/mL Streptomycin pH 5.5 sterile filtered
Liquid Medium	Medium 199 10% FCS (v/v) 100 U/mL Penicillin 100 µg/mL Streptomycin 20 mM HEPES buffer 100 µM Adenine 0.05% Hemin (w/v) 0.041% Biotin (w/v)
Leishmania Medium (LM)	RPMI 1640 5% FCS (v/v) 2 mM L-glutamine 100 U/mL Penicillin 100 µg/mL Streptomycin 10 mM HEPES buffer 50 µM β-Mercaptoethanol
Complete Medium (KM)	RPMI 1640 10% FCS (v/v) 2 mM L-glutamine 100 U/mL Penicillin 100 µg/mL Streptomycin 10 mM HEPES buffer 50 µM β-Mercaptoethanol
Blood agar medium (Novy-Nicolle-McNeal)	16% Rabbit blood defibrinated 16% PBS 66.2% Brain heart infusion agar 66.2 U/mL Penicillin 66.2 µg/mL Streptomycin
LB Medium	2.5% LB Bouillon (Miller) Aqua bidest.
Ampicillin Agar Plates	3.7% LB Agar 100 µg/mL Ampicillin Aqua bidest.
S.O.C. Medium	2.66% SOB-Medium

M199 Plates

20 mM D-Glucose
Aqua bidest.
16.06 g/l M199
0.35 g/l NaHCO ₃
5 mg/l Hemin
0.6 mg/l Biopterin
20% FCS
100 U/mL Penicillin
100 µg/mL Streptomycin
1.5% LB Agar
Aqua bidest.

2.1.4. Primers

All primers were obtained from Eurofins (HPSF-purified).

The following primers were used for qRT-PCR:

Target Gene	Forward (5' -> 3')	Reverse (5' -> 3')
KMP11-2	GCCTGGATGAGGAGTTCAACA	GTGCTCCTTCATCTCGGG
LmjF.36.6260 (Carboxypeptidase)	CTACGCGGAAATCAAGTCGC	AGCGCAATCTGCTTCTCCTT
TRYP4	CCTGCTGGAGGCTTTTCAGT	GTTGTGGTCGACCTTCATGC
LmjF.17.0082 (Elongation factor 1-alpha)	TTCGCGGAAATCGAGTCCAA	CTTGATCGCCTTGGGGTTCT
LmjF.18.1300 (Uncharacterized protein)	ATTGGCCGCATCTTCAAGGA	ACACCGGCAGAAGTAAGGTG
LmjF.30.1500 (p1/s1 nuclease)	TGTGCGTGACTGAGGTTCTC	CCATCGCGTCAAGCTTTTCC
LmjF.35.0030 (Pyruvate kinase)	ATCACACAAGGCGTGGAGAG	CATGAAAACCACGGCACCTG
LmjF.05.0960 (Dipeptidyl-peptidase III)	GGCCGCACCATTGCAATTTA	TCTGGCGAATGTCGTCGTAG
ABCG2	GCGCCTACAGAGGACACCTA	TGGGAGTCTACCTTGCCAGA
LmjF.10.0610 (EndoG)	CCGAGCCATCTGTTCAAGGT	CTGAAGCCCTGTGATACGCT
SMP-4	AGTTCACGTGAAGGTGACG	TGGATGAAGGGCTCCGTAGT
G6PD	GAGCAGTCTCATGCTGATCAGG	GTTGATGCGATCGCACGATTC
6PGD	GCGAATCTCGCCCTGAACAT	TTCAGGTTGGCGCAAATTTTC
MCA5	CAACGGGTTACCCAGTCCAC	CCAACCTGGACTCTGTGGTG

MATERIALS AND METHODS

The following primers were used for restriction cloning:

Target Gene	Sequence	Restriction Site
LmG6PD_fwd	CCG CTC GAG ATG TCG GAA GAG C	XhoI
LmG6PD_rev	GAA GAT CTT CAC AGC TTA TTC GAG GGA AG	BglII
LmPGD_fwd	GGGAATTCCATATGTCTGAACGACCTCGGCATTATC	NdeI
LmPGD_rev	GGA ATT CCA TAT G CT ACT GCA GTG CG	NdeI
LdG6PD_fwd	CCG CTC GAG ATG TCC GAA GAG C	XhoI
LdG6PD_rev	GGA ATT CCA TAT GTC ACA GCT TGT TCG ACG	Clal

The following primers were used for Gibson Assembly:

Plasmid	Primer Name	Sequence
pSSU_SAT	CPB_fwd	gggatcactctcggcatggacgagctgtacaagtgaccttCCTTCTAGATG CCCTTGTGTG
	CPB_rev	atcaccgaaatcttcatactCACTAGTCGCGGACGCGG
	SAT_fwd	gcccgcgtccgcgactagtAGTATGAAGATTTTCGGTGATCC
	SAT_rev	ggcatcgctgcaaccaccacacacgcacacaagggcatTCTAGAACTC TTTAGGCGTC
pSSU_SAT_EndoG	CPB_fwd	gggatcactctcggcatggacgagctgtacaagtgaccttCCTTCTAGATG CCCTTGTGTG
	CPB_rev	ccgagcagccggcgatcatCACTAGTCGCGGACGCGG
	EndoG_fwd	gcccgcgtccgcgactagtATGATCGCCCGGCTGCTC
	EndoG_rev	atcaccgaaatcttcatactTCAGCGTCGCTCTGCCTG
	SAT_fwd	accaggcagagcgacgctgaAGTATGAAGATTTTCGGTGATCC
	SAT_rev	ggcatcgctgcaaccaccacacacgcacacaagggcatTCTAGAACTC TTTAGGCGTC
pTNeo_eGFP_loxP	loxP_fwd	tcttctcactgacattccatATAACTTCGTATAGCATAACATTATACGA AGTTATAATTGCC
	loxP_rev	GGCTACGGTGGACGGCTC
	dsRed_CPB_fwd	TTGAGCCGTCCACCGTAG
	dsRed_CPB_rev	gaagggagggggagggtatGGAACAGAAGGAAGCAATGAAC

The following primers were used for PCR:

Primer	Sequence
Puromycin Resistance fwd	TATCCGCGGCTTACAACGCTTG
Puromycin Resistance rev	ACCGCAAAGAAAATGTGGGAATGTGG
Blasticidin Resistance fwd	GCCGCATCTTCACTGGTGTCAA
Blasticidin Resistance rev	TCGGCTGTCCATCACTGTCCT
Geneticin Resistance fwd	CCATTGAACAAGATGGATTGCACGC

Geneticin Resistance rev	CGGCCATTTTCCACCATGATATT
Nourseothricin Resistance fwd	GAAGATTTTCGGTGATCCCTGAGCAG
Nourseothricin Resistance rev	CATCCTGTGCTCCCGAGAACC

Further primers for CRISPR/Cas9-related cloning or for confirmation of genetic manipulations can be found in the **Supplement**.

2.1.5. Plasmids

Backbone	Insert	Resistance Gene	Source
pIRmcs3-/+	-	SAT	Antonio Jiménez Ruiz
	LmG6PD	SAT	This thesis
	LmPGD	SAT	This thesis
	LdG6PD	SAT	This thesis
pGL2339	-	Blasticidin	Jeziel Damasceno
pGL2314	-	Puromycin	Jeziel Damasceno
pTNeo	loxP/eGFP	Neo	This thesis
pSSU	eGFP	SAT	This thesis
	eGFP/EndoG	SAT	This thesis

Plasmids for CRISPR/Cas9 knock-outs were published in Beneke et al (2017)⁵² and obtained from Antonio Jiménez Ruiz.

Plasmid	Resistance Marker	Fusion Tag	Size
pTB007	Hygromycin	Flag::NLS::Cas9::NLS	15.4 kb
		NLS::T7 RNAP	
pTBlast	Blasticidin		1.7 kb
pTPuro	Puromycin		1.8 kb
pTNeo	Geneticin		1.75 kb

2.1.6. Antibodies and Dyes

Antibody	Dilution / Concentration	Company
FITC-Annexin A5	1:100	Miltenyi
Carboxyfluorescein diacetate N-succinimidyl ester (CFSE)	4 µM	Sigma
DHE	50 µM	Life Technologies
DHR123	3 µM	Life Technologies
Ethidium bromide solution	10 ng/ml	Merck
Goat anti-mouse IgG (H+L), HRP conjugated	160 ng/ml	Thermo Scientific
H ₂ DCFDA	1 µM	Sigma
3-[4,5-dimethylthiazole-2-yl]-2,5-diphenyltetrazolium bromide (MTT)	1.1 mM	Abcam
Monoclonal Anti-FLAG® M2 antibody (mouse)	160 ng/ml	Sigma-Aldrich
Propidiumiodide	1 µg/ml	Sigma Aldrich
Rabbit anti-Lm Serum	1:100	Prof. Uwe Ritter, Regensburg
Rhodamine 123	10 µg/ml	Thermo Fisher
TriTrack DNA Loading Dye 6x	1x	Thermo Fisher
OxyBURST	5 µg/ml	Thermo Fisher
DAPI	300 nM	Carl Roth
Chicken anti-rabbit Alexa647 antibody	2.5 µg/ml	Thermo Fisher

2.1.7. Kits

Kit	Company
DNeasy Blood & Tissue Kit	Qiagen
RNeasy Plus Mini Kit	Qiagen
Qiaprep Spin Miniprep Kit	Qiagen
NucleoBon Xtra Maxi Kit	Macherey-Nagel
MESA Blue qPCR MasterMix Plus	Eurogentec
PWO MasterMix	Roche
Rapid DNA Ligation Kit	Thermo Fisher
Im Prom-II Reverse Transkription System	Promega
CD14 MicroBead Kit, human	Miltenyi Biotec
illustra GFX PCR DNA and Gel Band Purification Kit	GE Healthcare Life Sciences
In Situ Cell Death Detection Kit	Sigma

NEBuilder® HiFi DNA Assembly Master Mix
 Human IL-10 DuoSet ELISA
 Human TNF α DuoSet ELISA
 Platinum™ SuperFi™ PCR Master Mix
 123count™ eBeads Counting Beads

New England Biolabs
R&D Systems
R&D Systems
Invitrogen
Thermo Fisher Scientific

2.1.8. Compounds and Inhibitors

Compound	Source	Stock Concentration	Final Concentration
Miltefosine	Calbiochem	1.96 mM	25 μ M
Staurosporine	AdipoGen / Biomol	10 mM	25 μ M
Harmonine	Prof. Andreas Vilcinskis, Gießen	14.725 mM	30 μ M
Compound 1o	Prof. Katja Becker, Gießen	10 mM	25 μ M
Aurintricarboxylic acid (ATA)	Sigma Aldrich	20 mM	50 μ M
Antipain	Carl Roth	75 mM	2 μ M

2.1.9. Antibiotics

Antibody	Concentration	Company
Hygromycin	30 μ g/ml	Invitrogen
Puromycin	20 μ g/ml (<i>L. donovani</i>) / 40 μ g/ml (<i>L. major</i>)	Invitrogen
Blasticidin	10 μ g/ml	Invitrogen
Nourseothricin	100 μ g/ml	Jena Bioscience
G418	40 μ g/ml	Invivogen
Ampicillin	100 μ g/ml	VWR
Kanamycin	30 μ g/ml	VWR

2.1.10. Enzymes

Enzyme	Company
BglII	Thermo Fisher
Clal	Thermo Fisher
KpnI (Fast Digest)	Thermo Fisher
NdeI	Thermo Fisher
PacI	New England Biolabs
PmeI	New England Biolabs
SmaI	Thermo Fisher
SpeI-HF	New England Biolabs
SwaI (Fast Digest)	Thermo Fisher
XbaI	New England Biolabs
XhoI	Thermo Fisher
Thermosensitive Alkaline Phosphatase	Promega
RNase	Thermo Fisher
T4 DNA Ligase	Promega
Quick CIP (calf intestinal alkaline phosphatase)	New England Biolabs

2.1.11. *Leishmania* Strains

- *Leishmania major* isolate MHOM/IL/81/FEBNI wildtype

The wildtype strain was isolated from a skin biopsy of an Israeli patient. It was kindly provided by Dr. Frank Ebert (Bernhard Nocht Institute for Tropical Medicine, Hamburg, Germany).

- *Leishmania major* dsRed

MHOM/IL/81/FEBNI strain with stable expression of dsRed fluorescent protein from *Discosoma* sp.

- *Leishmania major* Cas9/T7

MHOM/IL/81/FEBNI strain with stable expression of Cas9 endonuclease and T7 RNA polymerase for the generation of knock-out strains. The strain was produced by Celia López Gutiérrez in the laboratory of Antonio Jiménez Ruiz in Alcalá de Henares, Spain.

- *Leishmania donovani* Africa isolate MHOM/ET/67/HU3 Z18 wildtype

Strain isolate of *Leishmania donovani* MHOM/ET/67/HU3 Z18 obtained from the *Leishmania* collection of Montpellier, France (Patrick Bastien).

- *Leishmania donovani* Africa Cas9/T7

L. donovani Africa isolate with stable integration of Cas9 endonuclease and T7 RNA polymerase. It was created during this thesis.

- *Leishmania donovani* Africa Cas9/T7/DiCre

L. donovani Africa Cas9/T7 strain with stable integration of DiCre recombinase for the generation of inducible KOs. Integration into the ribosomal locus was performed using the pGL2339 plasmid obtained from Jaziel Damasceno, Glasgow. The strain was created during this thesis.

2.1.12. Human Primary Cells

Human peripheral blood mononuclear cells (PBMCs) were isolated out of anonymized buffy coats from DRK blood donation center Frankfurt am Main.

2.1.13. Bacterial Strains

Chemically competent *E. coli* TOP10 F Prime cells were used for transformations and obtained from Jörg Kirberg, Paul-Ehrlich-Institut.

2.2. Methods

2.2.1. Cell Biological Methods

All experiments were carried out under sterile conditions with autoclaved materials.

If not indicated otherwise, all centrifugation steps in tubes with parasites were carried out at 2400xg, and with human cells at 68xg for 8 min at room temperature. Centrifugation of 96-well plates were carried out at 440xg for 4 min at 4°C.

2.2.1.1. Preparation of Blood Agar Plates

20.8 g brain heart infusion agar was mixed with 400 ml water and autoclaved. Meanwhile, 100 ml PBS were preheated to 42°C in a sterile petri dish and defibrinated rabbit blood was preheated to 37°C. When agar was cooled down to about 55°C it was added to the PBS in the petri dish and after reaching about 45°C, 4 ml penicillin/streptomycin and 100 ml defibrinated rabbit blood were added. Using a multi-channel pipette, 60 µl blood agar was distributed to each well of a 96-well plate in a 45 angle. Plates were stored at 4°C.

2.2.1.2. *Cultivation of Leishmania Promastigotes*

Leishmania promastigotes were cultivated in biphasic 96-well plates with a solid phase (blood agar for *L. major* and M199 agar for *L. donovani*) and a liquid phase (Leishmania medium) at 27°C and 5% CO₂. For passaging, stationary phase promastigotes were seeded at a concentration of 1x10⁶/ml (living and dead) in agar plates until they reached again the stationary growth phase (6 – 10 days). After 8 serial passages another aliquot of parasites was thawed.

For transgenic parasites, the Leishmania medium was supplemented with the respective antibiotic.

2.2.1.3. *Isolation and Cultivation of Leishmania Amastigotes*

Logarithmic phase promastigotes were transferred to liquid medium and supplemented with 10% FCS for three days at 27°C. Medium was changed to AAM and washed three times with the first centrifugation step at 1400xg. Promastigotes were counted and seeded to a 24-well plate at a concentration of 20x10⁶/ml and incubated at 33°C for 7 – 14 days. To achieve a sufficient purity of amastigotes, the supernatant was removed and replaced by fresh AAM.

If the purity of amastigotes was below 90%, a density gradient centrifugation was carried out. For this, Histopaque1119 was diluted with AAM to achieve 50, 70, 80 and 90% solutions. 100% Histopaque1119 was given to the bottom of a tube and the 90%, 80% and 70% solutions were carefully layered on top of the 100% Histopaque1119. Amastigotes were centrifuged and resuspended in 50% solution, which was layered on the top of the density gradient. The gradient was centrifuged at 2400xg for 35 min without brake and the interphases between 70 – 80% and 80 – 90% were collected. After washing the interphases two times with AAM they were used for experiments or counted and adjusted to a concentration of 20x10⁶/ml and seeded to a 24-well plate.

2.2.1.4. *Isolation of Human Peripheral Blood Mononuclear Cells (PBMCs)*

Human peripheral blood mononuclear cells (PBMCs) were isolated from buffy coats. For this, the blood cell concentrate was diluted 1:5 in prewarmed PBS and layered carefully on top of 15 ml of Lymphocyte Separation Medium (LSM). Gradient was centrifuged at 545xg for 30 min with lowest acceleration and deceleration. The interphase between plasma at the top and LSM in the middle contained the PBMCs and was collected for further washing steps. The cells were filled up with washing buffer and centrifuged three times at decreasing speed (1084xg, 573xg and 143xg) for 8 min. Lysis of erythrocytes was further carried out by addition of 10 ml cold ammonium chloride for 10 min at room temperature. A further washing step at 143xg followed and cells were counted using a CASY Cell Counter.

2.2.1.5. *Generation of Human Monocyte-Derived Macrophages (hMDMs)*

Monocytes were either separated by plastic adherence or by CD14⁺ magnetic-activated cell sorting (MACS).

For plastic adherence, 40 – 50x10⁶ PBMCs were seeded in a T-25 flask in 5 ml of complete medium supplemented with 1% human serum and incubated for 1 h at 37°C. Supernatant containing all non-adherent cells were removed and further washed twice with washing buffer.

For CD14⁺ MACS, PBMCs were centrifuged and washed with 50 ml MACS buffer. 5 µl anti-CD14 microbeads and 95 µl MACS buffer was added to 100x10⁶ PBMCs and incubated for 15 min at 4°C. Cells were washed with 50 ml MACS buffer and pellet was resuspended in 5 ml MACS buffer. Meanwhile, a large separation column was placed in a magnetic field and equilibrated with 5 ml MACS buffer. The cell suspension was applied onto the column and three washing steps with 3 ml MACS buffer each followed. For elution of CD14⁺ cells, the column was removed from the magnetic field and 5 ml MACS buffer was applied onto the column. Eluted monocytes were counted by CASY cell counter and seeded in a 6-well plate with 3x10⁶ cells per well.

Differentiation to type 1 macrophages was achieved by adding 10 ng/ml GM-CSF, to type 2 by adding 30 ng/ml M-CSF to complete medium¹⁰⁷. After 5 – 7 days at 37°C macrophages were fully differentiated.

2.2.1.6. *Infection of hMDM with Leishmania*

Macrophages were detached from the culture plate surface by putting them on ice for 30 min and further mechanically with a cell scraper. The cells were harvested and flasks/plates were washed with cold PBS. Cells were sedimented by centrifugation, resuspended in complete medium and counted by CASY Cell Counter. Macrophages were adjusted to a concentration of 1x10⁶/ml in complete medium.

For infection experiments, stationary phase promastigotes were counted and adjusted to a concentration of 1x10⁶/µl in complete medium. Parasites were added to macrophages with a multiplicity of infection (MOI) of 10. Cells were incubated at 37°C for 3 h and extracellular parasites were washed away by centrifugation. Infected macrophages were incubated for 24 h or 96 h at 37°C and used for further experiments.

For determining the infection rate by flow cytometry, parasites lacking the expression of a fluorescent protein had to be stained with a fluorescent dye prior to infection. For this, parasites were incubated for 20 min in 4 µM CFSE at 27°C. Staining solution was washed away two times with PBS and infection was carried out.

If infection was further tracked by microscopy, CytoSpins and Diff-Quik were performed and analyzed with an inverse microscope at 400x magnification.

2.2.1.7. Assessment of Intracellular Parasite Proliferation

Fluorescent parasites (eGFP+) were used for infection of macrophages. Mean fluorescence intensity (MF) was measured via flow cytometry one day after infection and four days after infection. By dividing these two numbers, the increase of fluorescence and therefore the intracellular proliferation could be measured.

2.2.1.8. Isolation of Exosomes

Parasites from logarithmic and stationary growth phase were harvested and washed in LM without FCS. Afterwards, they were seeded at a density of 2×10^8 /ml in LM without FCS in T-25 flasks and incubated overnight at 27°C, 5% CO₂. All further steps were performed on ice or 4°C. Parasites were centrifuged and supernatant was transferred to new tubes and centrifuged at 10,000xg, 15 min using a JA-20 rotor. Supernatant was again moved to fresh tubes and centrifugation was repeated. A sterile filtration of the supernatant with a 0.22 µm filter followed and it was subjected to ultracentrifugation at 100,000xg, 90 min. The supernatant was discarded and pellet was resuspended in 35 mL HBSS. Another ultracentrifugation at 100,000xg for 90 min followed and supernatant was discarded. The pellet was resuspended in 1 mL HBSS and checked for quality and quantity via Nanoparticle Tracking Analysis (NTA).

2.2.2. Cell Death Assays

2.2.2.1. Cell Proliferation via MTT Assay

In order to assess cell proliferation after compound treatment, 10×10^6 parasites were seeded in a 96-well plate (V-shape) and centrifuged at room temperature. As much medium as possible was carefully removed and replaced with 100 µl fresh RPMI without phenol red supplemented with 10 µl 12 mM MTT. A negative control without cells, consisting only of medium and MTT, was included. 4 h of incubation at 27°C followed. Plate was centrifuged again and all but 25 µl of medium was removed and replaced with 50 µl DMSO. After resuspension, the plate was incubated for 10 min at 37°C to dissolve formazan crystals. Samples were mixed again and absorbance was measured at 540 nm at Tecan Reader. All values were subtracted by negative control without cells and normalized to untreated parasites. Increased conversion of MTT to formazan crystals are indicative of an increased metabolic activity, which occur when parasites proliferate¹⁰⁸.

2.2.2.2. Phosphatidylserine Externalization via Annexin Binding Assay

Annexin A5 specifically binds negatively charged phospholipids, namely phosphatidylserine, at the surface of cell membranes¹⁰⁹. Therefore, the magnitude of phosphatidylserine externalization can be

measured by fluorescence intensity of bound FITC-labeled Annexin A5. Since binding of Annexin is dependent on calcium ions, a negative control without calcium ions was always included (PBS w/o Ca^{2+}).

1×10^6 parasites per well were seeded in a 96-well plate and centrifuged. Supernatant was discarded and the pellet was resuspended in 100 μl Ringer buffer, which contained calcium. The cells were stained with 1 μl AnnexinA5-FITC in 100 μl Ringer buffer and incubated for 20 min in the cold and dark. A washing step with 100 μl Ringer buffer followed. The samples were resuspended in 100 μl Ringer buffer and transferred to FACS tubes. Analysis was done via flow cytometry in FITC channel. The PBS control served as annexin A5 negative sample.

2.2.2.3. DNA Fragmentation via Cell Cycle Assay

Since propidiumiodide (PI) stochastically binds to DNA, it can be used to determine in which cell cycle phase a cell is situated¹¹⁰. The subG1 phase correlated with the percentage of cells that harbor fragmented DNA¹¹¹.

Parasites (1×10^6 /well) were centrifuged in a V-shaped 96-well plate and supernatant was discarded. Pellet was washed in 100 μl cold PBS and afterwards resuspended in 25 μl PBS. 175 μl EtOH 70% (v/v) was added and incubated at -20°C for at least 30 min for fixation and membrane permeabilization. Cells were centrifuged and washed in PBS supplemented with 50 mM EDTA. Staining solution, containing 1 $\mu\text{g/ml}$ PI and 5 $\mu\text{g/ml}$ RNase in 100 μl PBS/EDTA, was added to the cells, resuspended and transferred to FACS tubes. Cells were incubated for 30 min at 37°C . Analysis was done by flow cytometry in the PI channel. A digestion control was included, in which PI was not added, and used as negative control. Gating of the cells was done with the digestion control, which included the gating of *Leishmania*, single cells and stained cells (**Figure 7**). First, the *Leishmania* population was gated in the FSC-A/SSC-A. Next, the doublets were gated out using a single cell gate in the FSC-A/FSC-H channel. Finally, only the stained cells were considered through gating on PI+ cells. To determine the number of cells in the subG1 phase, every cell with a lower fluorescence than the biggest peak in the untreated parasites control, which corresponds to the G1 phase, was counted.

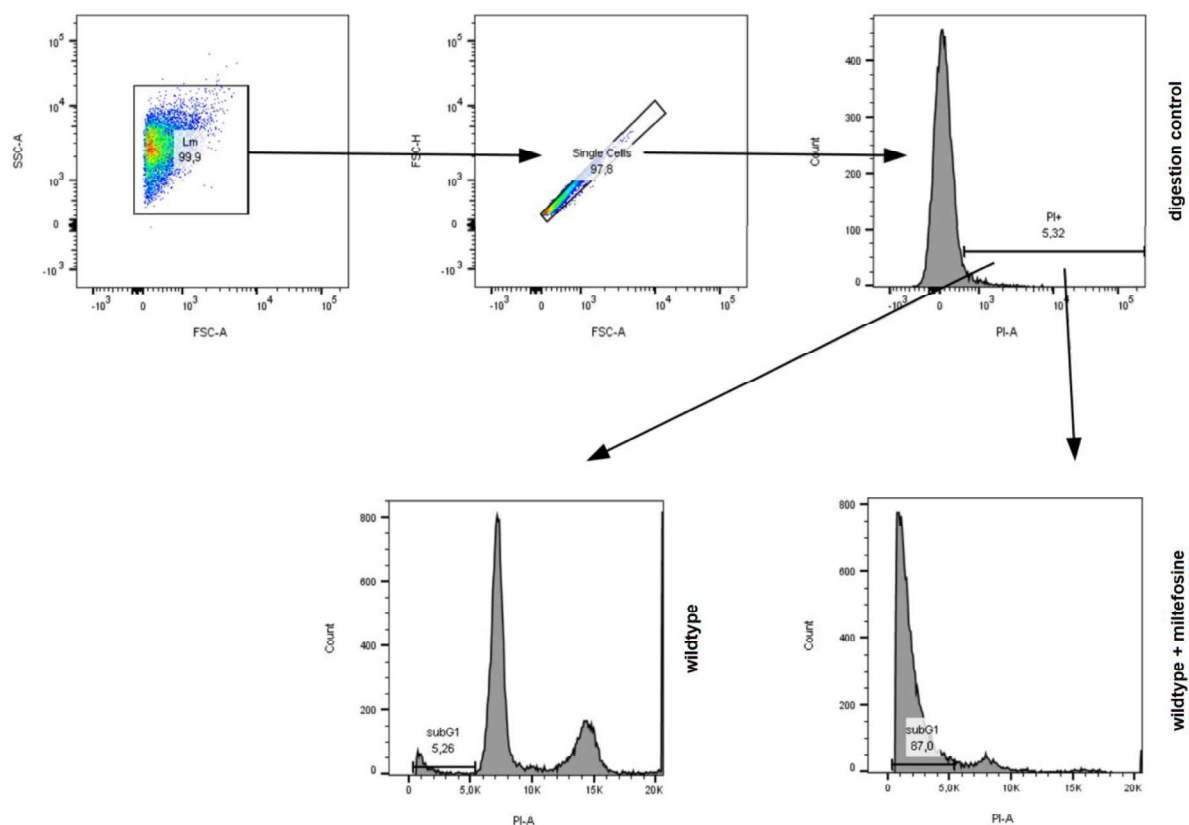


Figure 7. Gating strategy of cell cycle assay. The first three steps of gating were performed with the digestion control sample. Here, within the FSC-SSC it was gated on the *Leishmania* population. Next, using FSC-A and FSC-H it was gated on single cells and further on PI+ cells within the PI-A channel. The last gating step was done using stained but untreated parasites to gate on the subG1 phase. In miltefosine-treated parasites the number of cells in this gate was massively enhanced.

2.2.2.4. DNA Fragmentation via TUNEL Assay

A further method to determine DNA fragmentation is terminal deoxynucleotidyl transferase dUTP nick end labeling (TUNEL), in which the 3'-hydroxyl termini of DNA strand breaks are labeled¹¹².

For TUNEL assay, 1×10^6 parasites were seeded in a 96 well plate (V-shape) and the In Situ Cell Death Detection Kit from Sigma was used according to the manufacturer's instructions, leading to the labelling of free 3'-OH groups at DNA breaks with fluorescein-dUTP. For microscopy, the TUNEL staining was centrifuged to a Cytoslide (10 min at 1500 rpm). After that, a DAPI and an anti-*Leishmania* staining followed. For this, DAPI was mixed with anti-Lm serum and incubated with the parasites for 30 min at room temperature in the dark. After washing three times, a secondary anti-rabbit Alexa647 antibody was incubated for another 30 min in the dark. Further, three washing steps followed and parasites were embedded in Mowiol mounting medium and sealed with a cover slip and nail polish.

2.2.2.5. ROS Detection

The determination of reactive oxygen species (ROS) can be performed with different dyes, all detecting distinct species of ROS. H₂DCFDA can be used to detect H₂O₂, OH[•] and ONOO⁻, DHE is used for detection of O₂⁻ and DHR123 is used for H₂O₂, HOCl, ONOO⁻¹³.

1x10⁶ parasites were centrifuged and washed with 100 µl PBS. Staining solution of 1 µM H₂DCFDA, 50 µM DHE or 3 µM DHR123 in 100 µl PBS was prepared. The pellet was resuspended in 100 µl of the appropriate dye and incubated at 4°C in the dark for 20 min. Cells were washed with PBS and resuspended in 100 µl PBS for flow cytometry. An unstained control was included for each experiment. Readout was performed for DHE in the PE channel, for H₂DCFDA and DHR123 in the FITC channel. A parallel staining of H₂DCFDA and DHE was done. For this, a compensation of the fluorescent PE and FITC signals, using single-stained parasites, was performed.

2.2.3. Molecular Genetic Methods

2.2.3.1. Preparation of Chemically Competent Bacterial Cells

A 5 ml overnight culture of TOP10 F Prime *E. coli* cells was inoculated at 37°C. The culture was added to 100 ml fresh LB medium and optical density was measured in a cuvette at Nanodrop at 600 nm. After about 1.5 h, the optical density reached 0.5 and the culture was put on ice for 5 min. Cells were centrifuged at 3,600xg for 10 min at 4°C and supernatant was discarded. Next, the cells were resuspended in 40 ml TFB1 and put again on ice for 5 min. Bacteria were centrifuged again at 3,600xg for 10 min at 4°C and supernatant was discarded. 4 ml TFB2 were added, resuspended and put on ice for another 15 min. Competent cells were aliquoted on dry ice and stored at -80°C.

2.2.3.2. Transformation

TOP10 F Prime chemically competent *E. coli* cells were thawed on ice for 5 min. 1 – 5 µl of DNA was added to the cells and incubated on ice for 30 min. Subsequently, the cells were subjected to heat shock at 42° C for 1 min and placed immediately on ice for another 2 min. 250 µl of prewarmed S.O.C. medium was added to the cells and incubated at 37°C for 1 h. 1/10 of the cells were plated on one half of a selective agar plate and 9/10 were plated on the other half. The plate was incubated over night at 37°C.

2.2.3.3. Restriction Cloning

For restriction cloning, the insert was produced by PCR with primers containing the respective restriction sites. The following PCR reaction was prepared:

MATERIALS AND METHODS

gDNA 50 ng/ μ l	2 μ l
Primer fwd	1 μ l
Primer rev	1 μ l
H ₂ O	16 μ l
PWO Mastermix	20 μ l

The mix was incubated in a BioRad thermocycler with the following program, annealing temperature (highlighted in bold) was optimized for each insert:

95°C	3 min		
95°C	30 sec		
60°C	30 sec	}	25 cycles
72°C	1 min 30 sec		
72°C	10 min		
4°C	∞		

Restriction digest and subsequent dephosphorylation of a vector was performed with the respective restriction enzyme and the thermosensitive alkaline phosphatase (TSAP) or the quick calf intestinal phosphatase (CIP).

Vector DNA	1 μ g
Restriction enzyme	15 units
Buffer	1x
TSAP/CIP	1x
H ₂ O	ad 20 μ l

37°C	1 h
74°C / 80°C	15 min
4°C	∞

Restriction digest with insert was performed the same way as with the vector, but without dephosphorylation. Insert and vector were subjected to agarose gel electrophoresis. DNA was purified from gel pieces using the illustra GFX PCR DNA and Gel Band Purification Kit from GE Healthcare according to the manufacturer's instructions. The ratio of vector to insert was set to a molar ratio of 1:6, using 100 ng of the vector. Ligation of vector and insert was carried out with the Rapid DNA

Ligation Kit from Thermo Fisher according to the manufacturer's instructions. 5 µl of the ligation reaction was used for transformation of chemically competent *E. coli*.

Grown single-clone colonies were picked and incubated overnight at 37°C in 5 ml LB medium supplemented with ampicillin or kanamycin. 2 ml were used for Miniprep using the Qiaprep Spin Miniprep Kit according to the manufacturer's instructions. The isolated plasmid was digested with the respective restriction enzymes and loaded onto an agarose gel. If the vector and the released insert showed the expected size after gel electrophoresis, a proportion of the undigested plasmid was sent for sequence analysis at LGC genomics.

2.2.3.4. *Gibson Assembly*

10 µg of the vector was enzymatically digested as for restriction cloning. Insert overhangs, being homologous to 3' and 5' regions of the vector, were designed using the NEBuilder assembly tool (<https://nebuilder.neb.com/>). 30 - 40 bp overhangs were chosen and overhang-containing inserts were produced by PCR. Without further purification, the vector and inserts were assembled using the NEBuilder® HiFi DNA Assembly Master Mix according to the manufacturer's instructions.

2.2.3.5. *Stable Integration of Cas9/T7 in Leishmania*

4 µg pTB007 were linearized using PacI for 1 h and inactivated afterwards. Restriction was checked by agarose gel electrophoresis. 10×10^6 *Leishmania donovani* were washed in Zimmermann buffer and mixed with 2 µg of the linearized plasmid. Mixture was electroporated using the X-001 program at Amaxa Nucleofactor 2b. A MOCK control was included, in which the cells alone were electroporated without a plasmid. Parasites were transferred to a T25 flask with 5 ml LM. 12 – 16 h later 30µg/ml hygromycin supplemented with 10% FCS was added. When the MOCK control was completely dead, the parasites were centrifuged to get rid of the antibiotic and a clonal cell line was established by serial dilution. To confirm Cas9 expression, a PCR within the Cas9 CDS and a western blot for FLAG tag was performed.

2.2.3.6. *Stable Integration of eGFP and DiCre in Leishmania*

10 µg plasmid (pSSU-eGFP-SAT for eGFP and pGL2339 for DiCre) was linearized using PacI/PmeI for 1 h and inactivated afterwards. Restriction was checked by gel electrophoresis. 60×10^6 logarithmic phase *Leishmania* were used to electroporate them with the whole sample of the restriction digest. Therefore, the parasites were washed and resuspended in 200 µl Zimmerman buffer with the linearized plasmid and electroporated using the X-001 program at Amaxa Nucleofactor 2b. After electroporation, parasites were transferred to LM and incubated overnight at 27°C, 5% CO₂. At the next morning, the respective antibiotic (Nourseothricin/Blasticidin) was added to the parasites and

they were subjected to a serial dilution in blood agar plate. The expression of eGFP was confirmed by flow cytometry. The successful integration of DiCre was checked by PCR.

2.2.3.7. Generation of Knock-outs

For generation of knock-outs in *Leishmania* the necessary primers for homologous region (HR) and single guide RNA (sgRNA) were designed using LeishGEdit⁶², accessible on the following website: <http://www.leishgedit.net/Home.html>

In a first round of transfection, at least one allele of the gene of interest was replaced by a puromycin resistance gene. In the next round, the second allele was replaced by a blasticidin resistance gene, if necessary. For this, the pTPuro, pTBlast and pTNeo plasmids were used and homology arms were added up- and downstream of the resistance genes.

Oligonucleotides for HR and sgRNA were amplified via PCR:

- HR PCR:

pTPuro / pTBlast / pTNeo 15 ng/μl	2 μl
Fw HR primer 20 μM	2 μl
Rev HR primer 20 μM	2 μl
DMSO 100%	0.6 μl
MgCl ₂ 10 mM	2.76 μl
H ₂ O	0.65 μl
PWO Mastermix	10 μl

"HR" Program:

94°C	5 min	} 40 cycles
94°C	30 sec	
65°C	30 sec	
72°C	2 min 15 sec	
72°C	7 min	
4°C	∞	

- sgRNA PCR:

5' / 3' sgRNA Primer 20 μM	4 μl
Scaffold 10 μM	4 μl
H ₂ O	2 μl
PWO Mastermix	10 μl

“sgRNA” Program:

98°C	30 sec	}	35 cycles
98°C	10 sec		
60°C	30 sec		
72°C	15 sec		
4°C	∞		

2 µl of each PCR product was checked on a 1% agarose gel.

- “Steril” Program:

94°C	5 min
4°C	∞

60x10⁶ logarithmic phase promastigotes were used for electroporation and washed one time in 5 ml Zimmerman buffer. Pellet was resuspended in 200 µl Zimmerman buffer. 7.5µl of each PCR (HR and both sgRNAs) was pipetted on the bottom of an electroporation cuvette and the parasites were given to the DNA. Electroporation was done with Amaxa Nucleofector 2b in program X-001. Whole electroporation solution was pipetted into a T-25 flask with 5 ml of prewarmed LM. After 12 – 16 h the corresponding antibiotic was added to the flask, which was supplemented with 10% FCS.

For each electroporation, a MOCK control was done in parallel, in which the parasites were electroporated with the sgRNA but not the HR oligonucleotide. When the MOCK control was fully dead, the parasites were centrifuged and cultured in fresh LM supplemented with additional 10% FCS but without antibiotics.

After reaching normal growth behavior, the polyclonal mixture of knock-out parasites was either subjected to a serial dilution or it was plated on a M199 plate.

For serial dilution, 1x10⁶ parasites were resuspended in 1 ml LM and 125 µl parasites were pipetted in eight replicates into a blood agar plate. Starting with these sample, eleven 1:5 serial dilutions were pipetted into the same blood agar plate. The plate was incubated at 27°C for 7 – 10 days. In theory, after six serial dilution steps, a single-clone cell line is reached.

In parallel, the polyclonal parasites were plated out on M199 plates. For this, different amounts of parasites were plated onto the plates, ranging from 1,000 – 100,000 per plate. Plates were wrapped in parafilm and incubated at 27°C for several weeks. *Leishmania* colonies growing on these plates were assumed to originate from a single parasite, representing a single-cell clone.

2.2.3.8. *Generation of inducible Knock-outs*

Inducible KOs were generated in the same way as the common CRISPR/Cas9 KOs. The sgRNA PCR was performed accordingly. The HR PCR differed as follows:

- HR PCR:

pTNeoloxPeGFP / pGL2314 15 ng/μl	1 μl
Fw HR primer 20 μM	1 μl
Rev HR primer 20 μM	1 μl
GC Enhancer	4 μl
H ₂ O	3 μl
Platinum Mastermix	10 μl

"Platinum" Program:

98°C	30 sec	} 35 cycles
98°C	10 sec	
72°C	4 min / 3 min *	
72°C	5 min	
4°C	∞	

* Elongation time was 4 min for the 5' PCR and 3 min for the 3' PCR

For electroporation, 60×10^6 DiCre parasites were used with the PCR from 5' HR and 5' sgRNA. After selection of the neomycin resistance-carrying parasites, the electroporation with the 3' HR and 3' sgRNA followed. A further selection for puromycin resistance was done and a serial dilution for generation of single clones led to the parasites that were used in further experiments.

For the induction of the KO, 100 nM rapamycin was added to the cell culture medium. Parasites were subjected to flow cytometry daily and checked for eGFP and mCherry expression. For further counting at the flow cytometer, 123count™ eBeads counting beads were used. For this, 10 μl beads were mixed with 100 μl of parasite culture and measured at BD Symphony. At least 1000 events of beads were measured. Further calculation of parasite concentration was done according to the manufacturer's instructions.

2.2.3.9. Confirmation of Knock-outs

To confirm a successful gene knock-out in *Leishmania*, the genomic DNA was isolated using the DNeasy Blood and Tissue Kit from Qiagen according to the manufacturer's instructions. For each knock-out, four PCRs were established. Firstly, the forward (Primer 1) and reverse primer are positioned within the coding sequence (CDS) (Primer 2) of the gene of interest (GOI). For the second primer pair, the forward primer binds in the CDS (Primer 1) and the reverse primer downstream of the restriction site of Cas9 in the untranslated region (UTR) (Primer 3). The third primer pair detects an inserted blasticidin resistance with a forward blasticidin primer (Primer B) and a reverse UTR primer (Primer 3). Lastly, the fourth primer pair detects a puromycin resistance (Primer P), in comparable way as the blasticidin resistance.

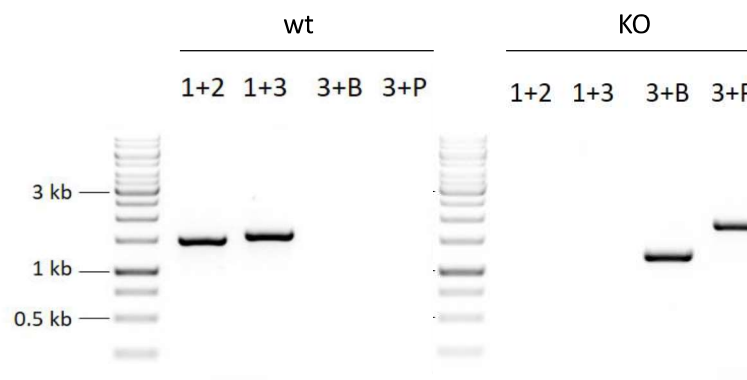


Figure 8. Confirmation of knock-out (KO) through PCR. A first PCR within the coding sequence of the gene of interest (GOI) was performed (1+2). The next PCR binds forward in the CDS and reverse in the UTR (1+3). The third PCR binds forward in the blasticidin resistance gene and reverse in the GOI UTR (3+B). The last PCR binds forward in the puromycin resistance gene and reverse in the GOI UTR (3+P). The example agarose gel shows the PCR products of wildtype (wt) left and EndoG KO right.

Thus, for wildtype gDNA, the PCR led to a DNA fragment amplified through primer pair one and two, but not for the two resistance genes. On the other hand, a successful knock-out led to no PCR product using the first two primer pairs, but shows a PCR product for the resistance genes (**Figure 8**).

gDNA 50 ng/ μ l	1 μ l
Fwd Primer	1 μ l
Rev Primer	1 μ l
H ₂ O	2 μ l
PWO Mastermix	5 μ l

“PWO” Program:

95°C	3 min	}	25 cycles
95°C	30 sec		
60°C *	30 sec		
72°C	1 min 30 sec		
72°C	10 min		
4°C	∞		

*Annealing temperature was optimized for each primer pair.

2.2.3.10. qRT-PCR

50 – 100x10⁶ *Leishmania* parasites were harvested and washed in cold PBS. For RNA Isolation, the RNeasy Plus Kit from Qiagen was used according to the manufacturer’s instructions. For DNA isolation, the DNeasy Blood and Tissue Kit from Qiagen was used according to the manufacturer’s instructions. The amount of RNA or DNA was measured at 260 nm using a NanoDrop and diluted to 100 µg/ml for RNA and 5 ng/µl for DNA.

Up to 10 µg of RNA was treated with 10 U DNase I and 40 U RNase Inhibitor at 37°C for 20 min and 75°C for 10 min. To perform quantitative real-time PCR (qRT-PCR), 100 ng RNA was used for synthesis of cDNA with the ImProm-II Reverse Transcription System from Promega according to the manufacturer’s instructions.

Detection of mRNA or gDNA was performed with the SYBR Green fluorophore. For this purpose, the MesaBlue qPCR MasterMix Plus from Eurogentec was used, according to the manufacturer’s instructions. For analysis, the 2^{-ΔΔCt} method was used, where kmp11 served as housekeeping gene.

2.2.4. Biochemical Methods

2.2.4.1. Western Blot

For confirmation of Cas9 expression, a Western blot to detect the FLAG-Cas9 fusion protein was performed. For this, 3x10⁶ parasites were harvested and resuspended in 20 µl 1 x Laemmli buffer. After heating for five minutes at 95°C, the lysate was loaded onto a 12% Sodium Dodecyl Sulfate (SDS) polyacrylamide gel. The proteins were separated by SDS-PAGE at a voltage of 80 V in the stacking gel and 120 V in the separating gel. Afterwards, the proteins were transferred onto a nitrocellulose membrane through semi-dry blotting in transfer buffer at 1.5 mA per cm² gel for 1 h. After transfer, the membrane was blocked for 1 h at RT in TBS-T + 5% milk. Next, the membrane was incubated with the primary antibody overnight at 4 °C. The membrane was washed three times with 10 ml PBS

supplemented with 0.1% TWEEN 20 for 5 min and then incubated with the corresponding secondary antibody for 1.5 h at RT. As described before, three washing steps followed. For detection of chemiluminescence, the membrane was incubated with the ECL substrate for 30 sec and detected in the digital gel-documentation device INTAS Chemostar.

2.2.4.2. Preparation of Mass Spectrometry Samples for Proteomic Analysis

25×10^6 promastigotes or amastigotes were seeded in a 12-well plate in 1 ml of LM or AAM, respectively. Parasites were treated with compounds for indicated time points and were sedimented by centrifugation. If the pellet contained too many rabbit erythrocytes from the blood agar plates (clearly visible by a red pellet), the pellet was resuspended in 1 ml of ammonium chloride and centrifuged immediately. Pellet was washed twice in 1 ml PBS and centrifuged again. Subsequently, the supernatant was discarded and the dry pellet was frozen at -80°C .

Mass spectrometric analysis was performed at the Core Facility of Mass Spectrometry at the University Medical Center Mainz in collaboration with Prof. Stefan Tenzer and PD Dr. Ute Distler. Samples were shipped on dry ice. Upon arrival, parasites were lysed in 7 M Urea, 2 M Thiourea, 2% CHAPS by sonication in a Bioruptor. The solubilized proteins were applied to tryptic digestion and further subjected to high-resolution nanoUPLC separation. Samples were analyzed using data-independent acquisition on the Waters Synapt G2-S platform. The rawdata was processed by PLGS searching the *Leishmania* reference proteome and label-free quantification was performed using the in-house developed software pipeline ISOQuant¹¹⁴. The mass spectrometry data was further analyzed using Partek®Flow®.

2.2.4.3. Preparation of Mass Spectrometry Samples for Lipidomic Analysis

A distinct number (between $3.3 - 8.4 \times 10^9$ parasites per measurement) of logarithmic (d3) and stationary phase (d10) promastigotes, and as a further control supernatant from blood agar plates without parasites, were sent to our cooperation partner Prof. Bernhard Spengler in Gießen. Here, lipids were extracted using the methyl-*tert*-butyl ether extraction method and resuspended in acetonitrile/water (60:40; v/v). The internal standard 1-palmitoyl-2-oleoyl-sn-glycero-3-phospho-L-serine was added and samples were subjected to ultra-high-performance liquid chromatography (Ultimate 3000 from Dionex) with isopropanol/acetonitrile (90:8) with 10 mM ammonium formate and 0.1% formic acid as second solvent. Afterwards, lipids were applied to high resolution hybrid quadrupole Orbitrap mass spectrometer (Q-Exactive HF-X from Thermo Fisher Scientific) in data dependent negative mode. The detected signals, which matched the masses of phosphatidylserine lipids were further validated by fragmentation. Converting and peak picking was performed using

Proteowizard, MZmine 2.5 and following identification was done with LipidDataAnalyzer and LipidMatch.

2.2.4.4. Enzyme-linked immunosorbent assay (ELISA)

Human monocyte derived macrophages type 1 were stimulated with 50 ng/ml IFN- γ or 100 ng/ml LPS with IFN- γ for 18 h. Afterwards, medium was replaced and exosomes were added for 24 h. Supernatants were frozen at -80°C until further use. The concentration of IL-10 or TNF α in cell supernatants was determined by ELISA in half area 96-well plates. Therefore, everything was done according to the manufacturer's instructions but with halved volumes.

2.2.5. Microscopy

To evaluate the morphology of macrophages and *Leishmania*, microscopic pictures were obtained via cytopins and following Diff-Quik staining. 100,000 macrophages or 1×10^6 parasites in 100 μ l medium were centrifuged on slides for 5 min at 500 rpm or for 10 min at 1500 rpm, respectively. Slides were dried on air and subjected to Diff-Quik staining. For this, cells were fixated for 2 min and stained in eosin (solution I) for 2 min and afterwards in thiazine (solution II) for 2 min. Slides were washed with water and dried on air. Pictures were obtained with ZEISS Axiophot in 400x magnification.

TUNEL staining of miltefosine-treated *Leishmania* was analyzed using the Leica SP8 LIGHTNING confocal laser scanning microscope. Therefore, fluorescein labeled DNA fragmentation were detected using the 488 laser and the FITC channel. The staining was complemented by nuclei staining with DAPI excited by 405 laser and detected in the DAPI channel and *Leishmania* were visualized by excitation with 633 laser and detection in the Alexa647 channel. Further examination was done using the Leica Application Suite X (LAS X) software. Here, same intensities were used to compare different *Leishmania* strains.

2.2.6. Statistical Analysis

Statistical analysis of mass spectrometry data was performed in Partek[®] Flow[®]. Here, proteins were considered as significantly regulated when the false discovery rate (FDR) was lower 0.05 and the fold change bigger 1.5 or lower -1.5. Remaining statistics were done using Two-Way ANOVA with Dunnett's multiple comparisons test in GraphPad Prism version 8. For P-values *p < 0.05, **p < 0.01, ***p < 0.001 and ****p < 0.0001 were considered to be statistically significant.

3. Results

In order to investigate apoptosis in *Leishmania*, I induced apoptosis in either promastigotes or amastigotes and subsequently assessed different characteristics of apoptosis. First, I checked for the decreasing metabolic activity by MTT assay and further for the early apoptosis characteristic phosphatidylserine externalization via annexin binding. Next, I investigated the late apoptosis characteristic DNA fragmentation, which can be tested by cell cycle assay, where the fragmented DNA accumulates in the subG1 phase.

3.1. Apoptosis Induction through different Compounds

I determined the potential of the compounds staurosporine, miltefosine, harmonine and compound 1o in apoptosis induction. Staurosporine is an unspecific kinase inhibitor that is also inducing apoptosis in mammalian cells¹¹⁵. Miltefosine is a drug used for the treatment of leishmaniasis, and it induces leishmanial apoptosis through disruption of the calcium homeostasis¹⁷. Harmonine and compound 1o are newly developed compounds with unknown target and working mechanism from our cooperation partners at the university in Gießen^{116,117}. To evaluate the potential of the anti-leishmanial drugs to inhibit or induce apoptosis in the parasites, I performed dose-response experiments and evaluated their efficacy by calculating an inhibitory concentration (IC) for the inhibition of the metabolic activity and an effective concentration (EC) for the induction of annexin binding. The IC/EC₅₀ represents the concentration, which leads to a response in the halfway between top and bottom response. It is expected that the IC₅₀ of the metabolic activity is always a little lower than the EC₅₀ of the annexin binding, since for the metabolic assays, an intact mitochondrion is crucial and the depolarization of the mitochondrion is one of the first steps of apoptosis induction, right before PS externalization¹¹⁸.

To do so, I incubated logarithmic phase *L. major* promastigotes with different concentrations of the compounds for 24 h and performed an MTT assay to measure the decrease of metabolic activity of the parasites after drug exposure (**Figure 9**).

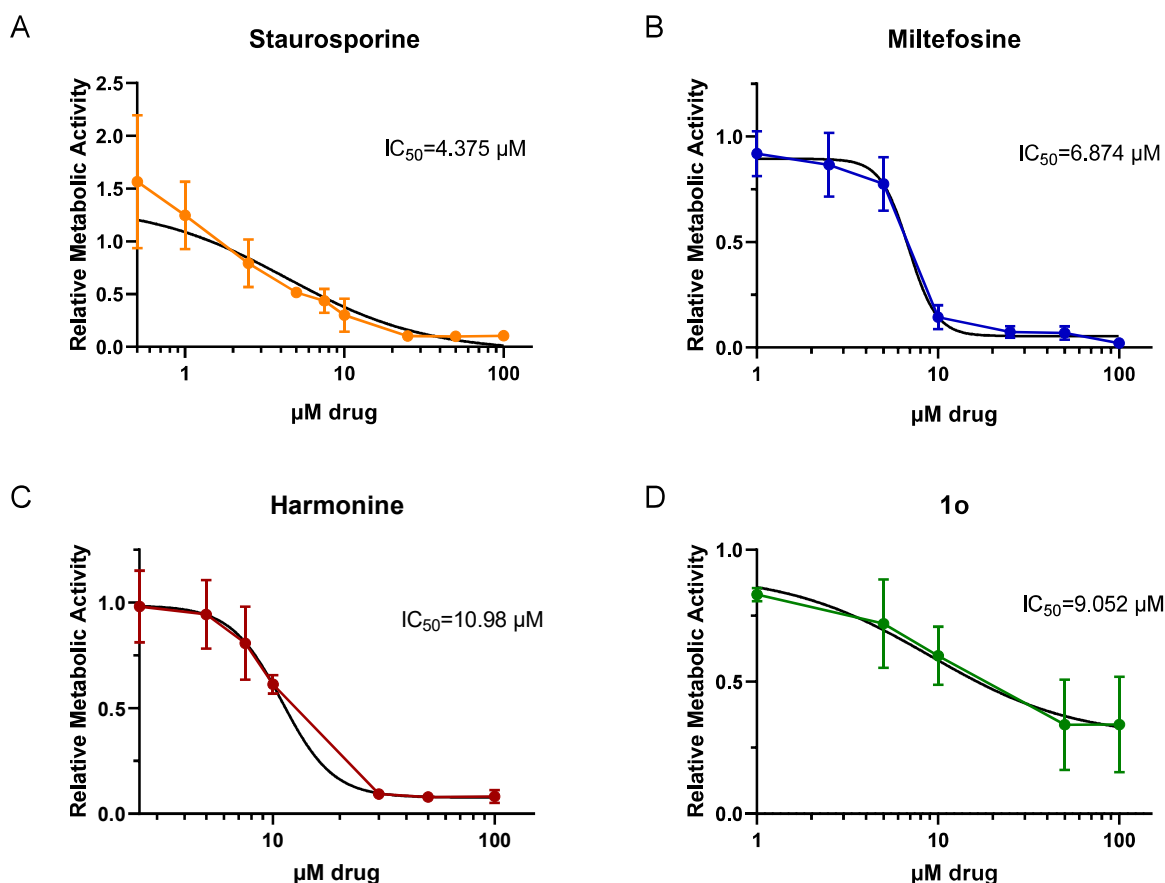


Figure 9. Staurosporine, miltefosine, harmonine and compound 1o show micromolar inhibitory concentrations (IC_{50}) of metabolic activity in *L. major* promastigotes. Logarithmic phase promastigotes of *L. major* were treated with different concentrations of staurosporine (A), miltefosine (B), harmonine (C) and compound 1o (D) for 24 h. MTT was added for 4 h and metabolic activity was assessed through normalizing to untreated control. IC_{50} values were determined by nonlinear regression in GraphPad prism. Mean \pm SD are shown and are representative for three independent experiments.

All compounds decreased the metabolic activity, while staurosporine showed with $4.4 \pm 1.9 \mu\text{M}$ the lowest IC_{50} , followed by miltefosine with $6.9 \pm 0.6 \mu\text{M}$, compound 1o with $9.1 \pm 6.1 \mu\text{M}$ and harmonine with $11.0 \pm 1.0 \mu\text{M}$. It is noteworthy, that even the highest concentrations with 1o did not decrease the metabolic activity to the same extent as the other compounds did. In sum, all drugs except compound 1o could diminish the metabolic activity of promastigotes and therefore kill the parasites.

I was further interested in the potential of the compounds to induce apoptosis, and for this I treated the promastigotes for 24 h and 48 h with the compounds before assessing annexin binding by using flow cytometry (**Figure 9**). A higher annexin binding means a higher externalization of PS and therefore induction of apoptosis⁷⁷.

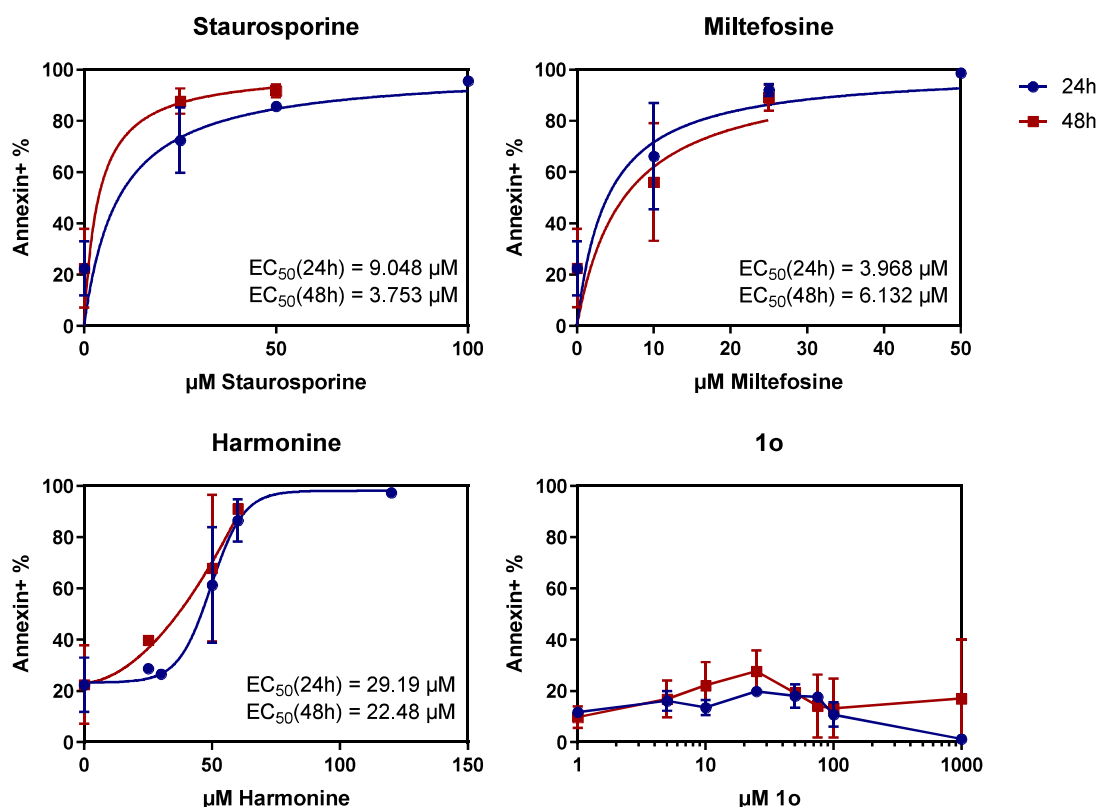


Figure 10.. Staurosporine, miltefosine and harmonine show micromolar effective concentrations (EC_{50}) of annexin binding in *L. major* promastigotes. Logarithmic phase promastigotes of *L. major* were treated with different concentrations of staurosporine, miltefosine, harmonine and compound 1o for 24 (blue) and 48 h (red). After indicated time points phosphatidylserine externalization was assessed through annexinA5 staining at BD LSR II. EC_{50} values were determined by nonlinear regression in GraphPad prism. (n=1-4)

Treatment of *L. major* promastigotes with 25 µM staurosporine led to over 60% annexin+ parasites for incubation times 24 h and 48 h. Incubation with 25 µM miltefosine led to over 80% annexin+ promastigotes for both incubation times. For harmonine, a concentration of 50 µM was necessary to obtain 60% annexin+ promastigotes. In all the tested concentrations, compound 1o reached no higher annexin+ cells than 40%. The percentages of annexin+ cells after 24 h and 48 h of treatment with the compounds was comparable. Effective concentration 50 (EC_{50}) of 24 h incubation was lowest for miltefosine treatment with $3.97 \pm 2.30 \mu M$, followed by staurosporine with $9.05 \pm 4.0 \mu M$ and harmonine with $29.19 \pm 10.80 \mu M$. After 48 h incubation, staurosporine showed the lowest EC_{50} ($3.75 \pm 3.26 \mu M$), followed by miltefosine ($6.13 \pm 3.79 \mu M$) and harmonine ($22.48 \pm 11.60 \mu M$). In summary, the results show that the most competent apoptosis inducer for promastigotes was miltefosine, followed by staurosporine and harmonine, while compound 1o was not able to induce apoptosis in promastigotes.

In addition to phosphatidylserine externalization, assessed by annexin binding and quantified as an early sign of apoptosis, I also quantified later apoptosis characteristics such as DNA fragmentation by using cell cycle analysis. Furthermore, since multiplying parasites in host macrophages are in the

RESULTS

amastigote stage, I used axenic amastigote cultures¹¹⁹ to assess early and late signs of apoptosis in this parasite stage in comparison to promastigotes (**Figure 11**).

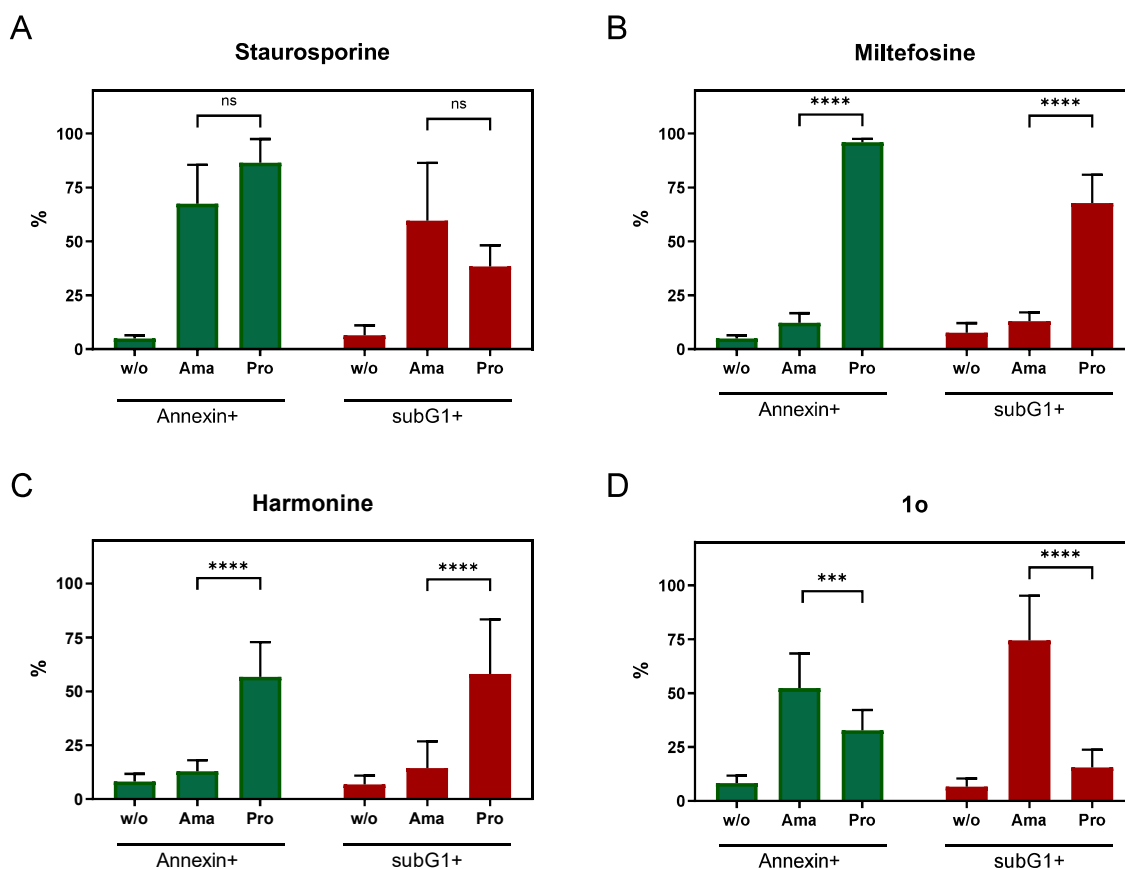


Figure 11. Staurosporine induces different apoptosis characteristics in *L. major* promastigotes and amastigotes, while miltefosine and harmonine is only active in promastigotes and 1o is active in amastigotes. *L. major* logarithmic phase promastigotes (Pro) and axenic amastigotes (Ama) were treated with 25 μ M staurosporine (A), 25 μ M miltefosine (B), 30 μ M harmonine (C) or 25 μ M compound 1o (D). After 24 h, phosphatidylserine externalization was measured via annexin A5 binding (Annexin+). Further, DNA fragmentation was measured by cell cycle analysis on the treated parasites and the proportion of sub-G1-phase parasites (corresponds to fragmented DNA) is shown (subG1+). Data shows mean + SD and is representative for at least 3 independent experiments. Significance was assessed by Two-Way ANOVA with *** $p < 0.001$ and **** $p < 0.0001$.

Staurosporine induced annexin binding as well as DNA accumulation in the subG1 phase in *Leishmania* promastigotes as well as amastigotes. Parasites were $67.45 \pm 18.03\%$ and $86.47 \pm 10.96\%$ annexin+ and $59.57 \pm 26.88\%$ and $38.43 \pm 9.75\%$ subG1+ for promastigotes and amastigotes, respectively. Miltefosine only induced PS externalization ($96.00 \pm 1.52\%$ annexin+) and DNA fragmentation ($67.70 \pm 13.27\%$ subG1+) in promastigotes but not in amastigotes ($12.24 \pm 4.47\%$ annexin+ and $13.03 \pm 4.02\%$ subG1+). For harmonine, the same was true but to a lower extent. Here, promastigotes showed annexin+ of $56.67 \pm 16.16\%$ and subG1+ of $58.03 \pm 25.38\%$, while the amastigotes were only $12.96 \pm 5.06\%$ annexin+ and $14.44 \pm 12.35\%$ subG1+. Compound 1o led to higher annexin binding in amastigotes ($52.28 \pm 16.09\%$) than in promastigotes ($32.70 \pm 9.47\%$) and to DNA fragmentation only in amastigotes ($74.40 \pm 20.74\%$) but not in promastigotes ($15.53 \pm 8.25\%$).

As I could determine by increased annexin and subG1+ parasites, staurosporine is a very effective apoptosis inducer in promastigotes as well as in amastigotes. Miltefosine was able to significantly increase annexin binding and DNA fragmentation in promastigotes, while in amastigotes the values were comparable to the untreated control. The difference between promastigotes and amastigotes was highly significant. Harmonine showed a comparable pattern to miltefosine, as apoptosis characteristics were only increased in the promastigote stage and not in the amastigote. However, the values were lower than after miltefosine treatment. Also here, the difference between promastigotes and amastigotes were significant. For compound 1o, annexin binding and DNA fragmentation assessed by cell cycle were higher in the amastigote form than in the promastigote stage. This was more pronounced for DNA fragmentation than for annexin binding, though significant for both. Overall, miltefosine and harmonine were determined to be potent apoptosis inducers in promastigotes, while compound 1o had an effect in amastigotes and staurosporine in both forms.

The newly developed compounds harmonine and 1o were only effective in either of the parasite life stages. Since promastigotes are cultured in medium with pH 7.4 and amastigotes are cultured in pH 5.5, to mimic the acidic environment of the phagolysosome, it is not clear if the compounds are only effective in the tested pH or if they are really only effective in one parasitic stage. To answer this question, promastigotes were cultured in amastigote medium pH 5.5 and amastigotes were cultured in promastigote medium pH 7.4 and were treated with 25 μ M compound 1o or 30 μ M harmonine for 24 h (Figure 12).

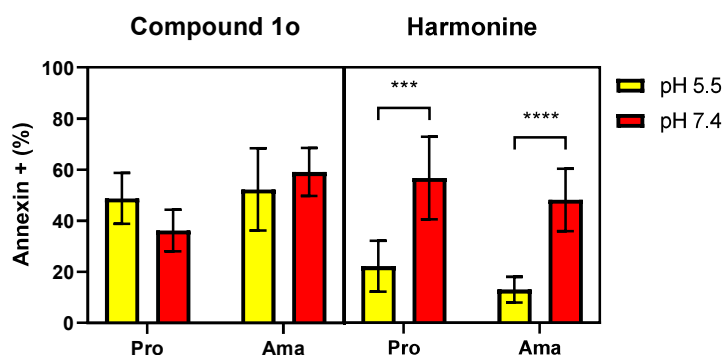


Figure 12. Harmonine is highly dependent on the pH of the environment. Compound 1o and harmonine were tested in two different media (AAM with pH 5.5 and LM with pH 7.4) for their phosphatidylserine exposure inducing activity in *L. major* promastigotes (Pro) and amastigotes (Ama). Parasites were incubated with 25 μ M 1o or 30 μ M harmonine for 24 h in amastigote medium (pH 5.5) or promastigote medium (pH 7.4) and then assessed via annexin staining for PS exposure. Data is representative for at least 3 independent experiments and shown as mean \pm SD. Significance was assessed by Two-Way ANOVA with *** p < 0.001 and **** p < 0.0001.

Compound 1o showed comparable activity at both pH values for promastigotes (pH 5.5: 48.77 \pm 9.92%; pH 7.4: 36.18 \pm 8.15%) and amastigotes (pH 5.5: 52.28 \pm 16.09%; pH 7.4: 59.10 \pm 9.38%).

At pH 5.5, harmonine led to 22.13 \pm 9.94% annexin+ promastigotes and to 12.96 \pm 5.06% annexin+ amastigotes, which is only slightly increased compared to untreated parasites (see Figure 11).

However, it showed almost as high annexin positivity for amastigote ($48.10 \pm 12.27\%$) as for promastigotes ($56.67 \pm 16.16\%$) at pH 7.4. Thus, harmonine is only active at a neutral pH and not at an acidic pH as found in a phagolysosomal compartment.

3.2. Mass Spectrometry Analysis of *Leishmania major*

As described above, various drugs, including those already used in the clinics, induce apoptosis in different parasite live stages by targeting different molecules and mechanisms. Since there is not much known about apoptosis regulation in *Leishmania*, I was aiming to identify proteins involved in apoptosis using a mass spectrometry approach. To this end, I induced apoptosis through the mentioned apoptosis-inducing agents. In order to identify initiators and executioners of apoptosis, I aimed to analyze the parasite's proteome at an early time point after treatment when apoptosis is just induced, and a later time point at which apoptosis is already fully activated.

3.2.1. Assessment of Time Points of Apoptosis Induction for Mass Spectrometry

As indicator for apoptosis induction, I assessed annexin binding for staurosporine, miltefosine, harmonine and compound 1o in promastigotes (**Figure 13**) and amastigotes (**Figure 14**). For this, different time points and two different concentrations were tested.

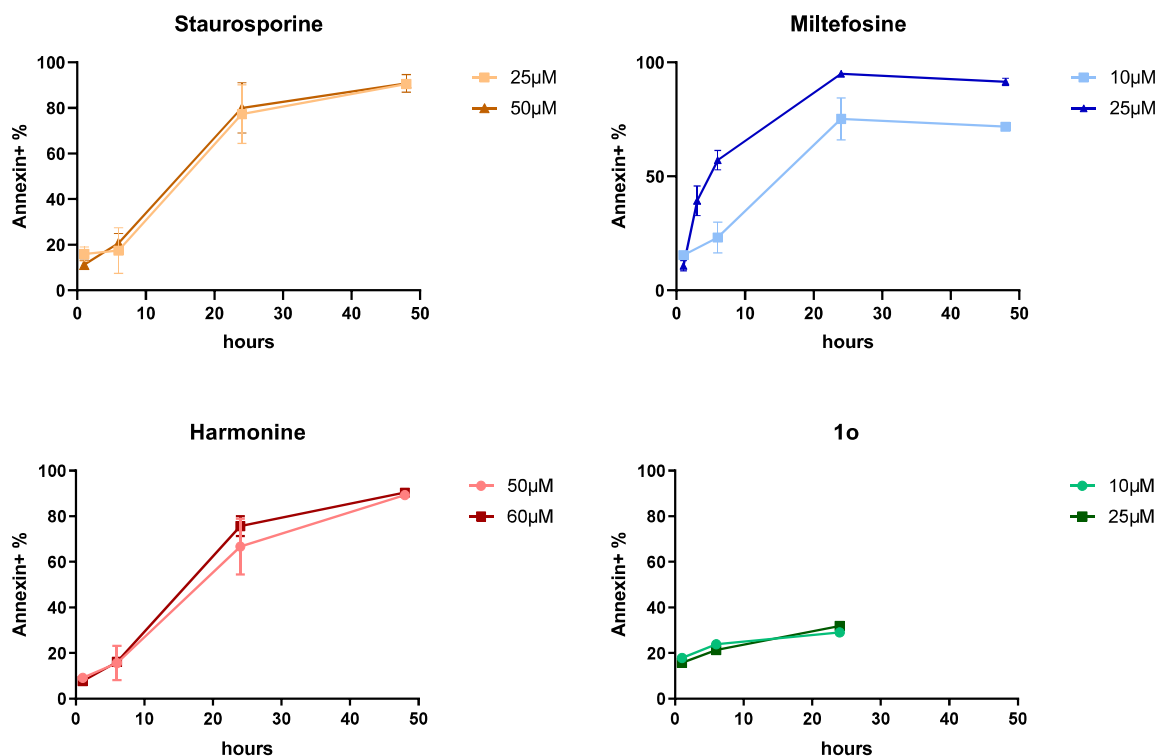


Figure 13. Staurosporine, miltefosine and harmonine but not 1o induce phosphatidylserine (PS) exposure in *L. major* promastigotes. PS exposure measured by annexin staining in *L. major* promastigotes was performed after incubation of different concentrations of staurosporine, miltefosine, harmonine and 1o. Annexin staining was carried out after indicated time points and measured at BD LSR II; n=1-3.

The percentage of annexin+ promastigotes increased slightly after 6 h staurosporine treatment and was approximately 80% after 24 h, independent of the concentration that was used. Miltefosine already showed annexin+ of $39.5 \pm 6.5\%$ at a concentration of $25 \mu\text{M}$ after 3 h. After 24 h at $25 \mu\text{M}$ miltefosine, $95.0 \pm 1.4\%$ were annexin+. Harmonine treatment caused slightly increasing apoptosis characteristics after 6 h and $66.8 \pm 12.3\%$ at a concentration of $50 \mu\text{M}$ after 24 h. Compound 1o did not induce apoptosis at all. After 24 h at a concentration of $25 \mu\text{M}$ compound 1o, 31.9% of the parasites were annexin+, which is negligible compared to 31.5% of the untreated parasites.

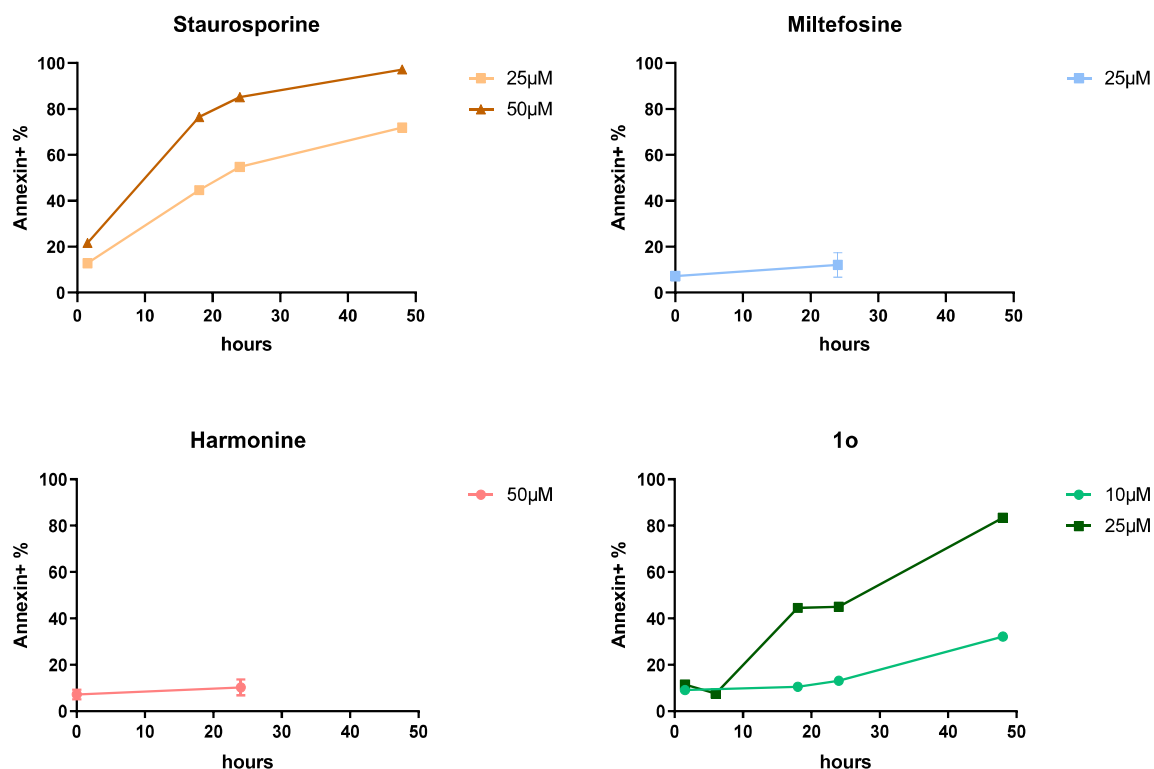


Figure 14. Staurosporine and 1o but not miltefosine and harmonine induce phosphatidylserine (PS) exposure in *L. major* amastigotes. PS exposure measured by annexin staining in *L. major* amastigotes was performed after incubation of different concentrations of staurosporine, miltefosine, harmonine and 1o. Annexin staining was carried out after indicated time points and measured at BD LSR II; n=1-3.

In amastigotes, 18 h of 25 µM staurosporine treatment increased the annexin binding from <20% in the untreated parasites to 44.6%, and after 24 h at 50 µM, 85.1% were reached. For miltefosine and harmonine, annexin binding did not increase after 24 h at 25 µM or 50 µM, respectively. At a concentration of 25 µM, compound 1o led to annexin binding of 44.5% after 18 h and 83.4% after 48 h.

In order to perform mass spectrometry analysis on the parasites, I decided to use an early time point after drug treatment, with a proportion of annexin+ parasites lower than 40%, and a late time point with annexin+ higher than 60%, see **Table 1**. For the compounds that did not induce apoptosis at all in the parasites, only one time point and concentration was chosen.

Table 1. Concentrations and time points of staurosporine, miltefosine, harmonine and compound 1o that were used to treat promastigotes and amastigotes of *L. major* for mass spectrometry analysis.

	Promastigotes		Amastigotes	
	Early Time point	Late Time point	Early Time point	Late Time point
Staurosporine	25 μ M 6 h	25 μ M 24 h	50 μ M 6 h	50 μ M 24 h
Miltefosine	25 μ M 3 h	25 μ M 24 h	-	25 μ M 24 h
Harmonine	50 μ M 6 h	50 μ M 24 h	-	50 μ M 24 h
Compound 1o	-	25 μ M 24 h	25 μ M 6 h	25 μ M 24 h

In addition, as a control of naturally dying parasites, *L. major* from the stationary growth phase were included in the mass spectrometry screen. In my experiments, $69.6 \pm 4.8\%$ of the parasites from this growth phase exhibited annexin-binding properties, confirming my expectation that the majority of the parasites in the stationary growth phase is already dead.

3.2.2. Analysis of Mass Spectrometry Data

Seven replicates of each of the differentially treated parasite samples were sent to Prof. Stefan Tenzer, Mainz and the parasites' proteome was analyzed via label free quantitative MS. Subsequent analysis of the MS data was performed using Partek®Flow® (**Figure 15**).

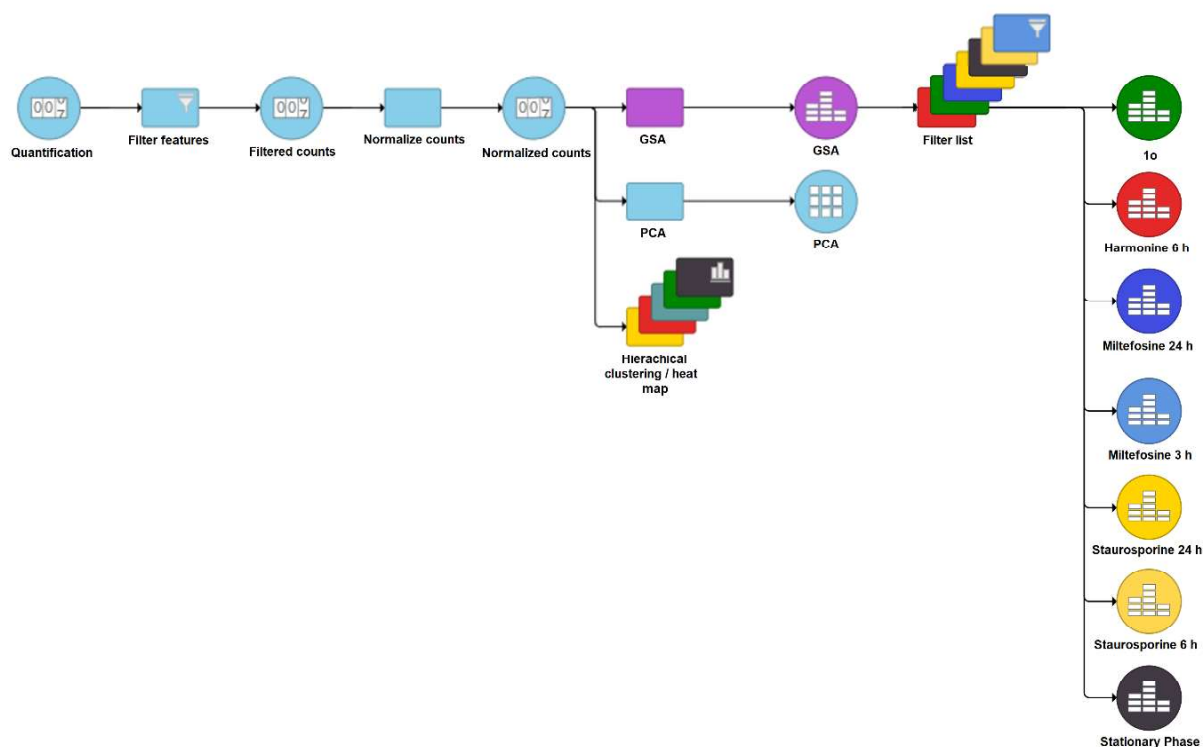


Figure 15. Pipeline for mass spectrometry data analysis in Partek®Flow®. Raw mass spectrometry data was uploaded to Partek® and filtered for control sequences and contaminants in a first step. Afterwards, they were normalized using counts per million (CPM) analysis and $1.0E-4$ was added to avoid zero values. To test for differential expression, a Gene Specific Analysis (GSA) was performed with the lowest average coverage of 1. Further, all conditions were compared to untreated control and considered as significant when the false discovery rate was lower 0.05 and the fold change bigger 1.5 or lower -1.5. Normalized counts were also used to perform a principal component analysis (PCA) and to do a hierarchical clustering.

The Partek®Flow® pipeline was comprised of filtering, normalization and differential expression analysis. In a first step, the control sequences that are used for MS and contaminants that arise during sample preparation were filtered out. This led us to the overall count of 4416 proteins in promastigotes and 2376 proteins in amastigotes. When considering 8038 predicted proteins in *L. major* proteome¹²⁰ this corresponds to 55% of the whole proteome for promastigotes and 30% for amastigotes that was found in our screen.

The filtered counts were normalized using the CPM (counts per million) method, in which $1.0E-4$ was added to avoid zero values. At this point, values were used to perform principal component analysis (PCA) and hierarchical clustering for heat maps. This was followed by the differential expression analysis using the gene specific analysis (GSA) method, in which the lowest average coverage of 1 was used. All of the treatment conditions were then compared to the untreated control. The up- or downregulation of proteins were considered as significant when the false discovery rate (FDR) was < 0.05 and the fold change was > 1.5 or < -1.5 .

During the analysis, I could see that the seven replicates of harmonine-treated promastigotes (24 h) differed. This could also be seen in the PCA, where the replicates did not cluster at all. Hence, I excluded this condition for further analysis.

The PCA of the promastigote dataset showed that, compared to the untreated sample, compound 1o shows similarly regulated proteins. In stationary phase promastigotes, slightly different proteins were regulated compared to untreated parasites. For the staurosporine 6 h treatment and the harmonine 6 h treatment, similar proteins were regulated that were different to the untreated control. 24 h of staurosporine treatment led to an altered up- or downregulation of distinct set of proteins. For the miltefosine 3 h treatment, four of the replicates were quite similar to the untreated promastigotes and three replicates differed. 24 h of miltefosine treatment had the biggest effect on the regulation of proteins compared to control. Here, the seven replicates clustered almost completely. This is in line with the expectation that small changes in apoptosis characteristics (e.g. compound 1o treatment) led to only a small subset of proteins that are differently regulated. On the other hand, big changes in apoptosis characteristics (for example miltefosine 24 h treatment) led to a large subset of differently regulated proteins (**Figure 16A**).

In the amastigote dataset, the untreated sample showed similarly regulated proteins as samples exposed to miltefosine or compound 1o (both time points). Staurosporine 6 h, 24 h and harmonine regulated specific proteins that were completely different to all other conditions. The replicates in the amastigote dataset did not cluster as strongly as the replicates in the promastigote dataset (**Figure 16B**).

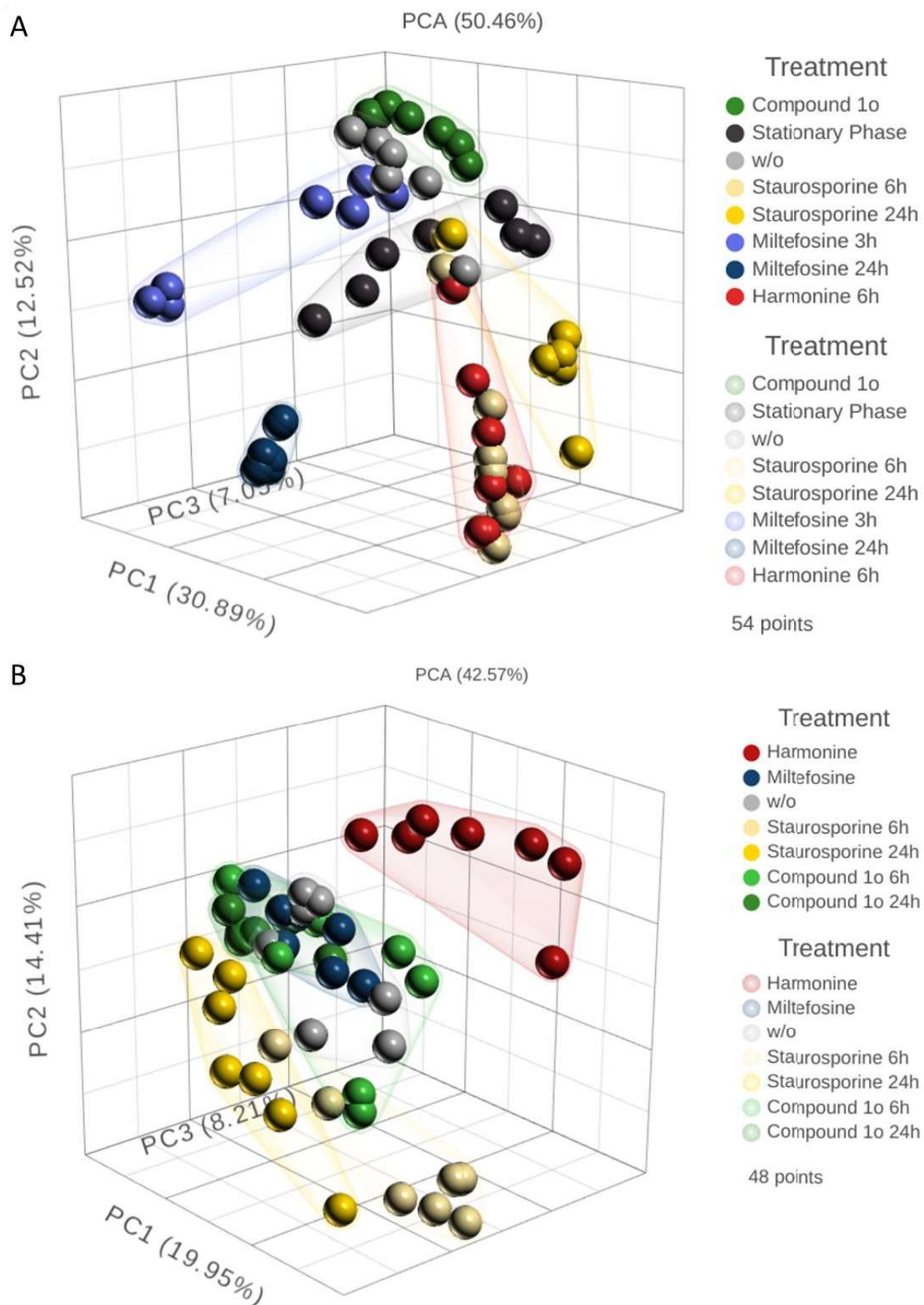


Figure 16. Proteins of *L. major* promastigotes and amastigotes are differentially regulated upon treatment with various apoptosis inducers. Principal component analysis (PCA) of mass spectrometry data obtained from promastigotes (A) or amastigotes (B) was performed in Partek®Flow®. Data was filtered for control sequences and contaminant and normalized before PCA was assessed in Partek®Flow®. For promastigotes 54 and for amastigotes 48 samples were included in the analysis.

3.2.2.1. Differential Expression Analysis of Promastigotes

Using Partek®Flow®, all compound-treated samples were compared to the untreated controls of promastigotes or amastigotes. To assess which proteins are significantly up- or downregulated in the treated samples compared to the untreated samples, I used the differential expression analysis. The regulated proteins were considered as significant when the false discovery rate (FDR) was lower 0.05 and the fold change was lower -1.5 for downregulation and bigger 1.5 for upregulation. All proteins were plotted in volcano plots, where each dot represents one protein. The grey dots indicate not significantly regulated proteins and the colored dots indicate regulated proteins. On the left side, they show a negative fold change and therefore a downregulation and on the right side a positive fold change and therefore upregulation. A Venn diagram shows further the overlap of proteins that are regulated in more than one condition.

The differential expression analysis for staurosporine-treated promastigotes showed that there are 75 proteins regulated after 6 h treatment. 18 h later, only 13 proteins were significantly regulated (**Figure 17A-C**). Only two proteins are differentially regulated (upregulated) in both time points (**Figure 17C**): ribosomal protein S2 and elongation factor 1-alpha (see **Supp. Table 2** and **Supp. Table 3**). It is noteworthy, that considering both time points, 80 proteins were downregulated and only 6 were upregulated. That means much more proteins were downregulated than upregulated.

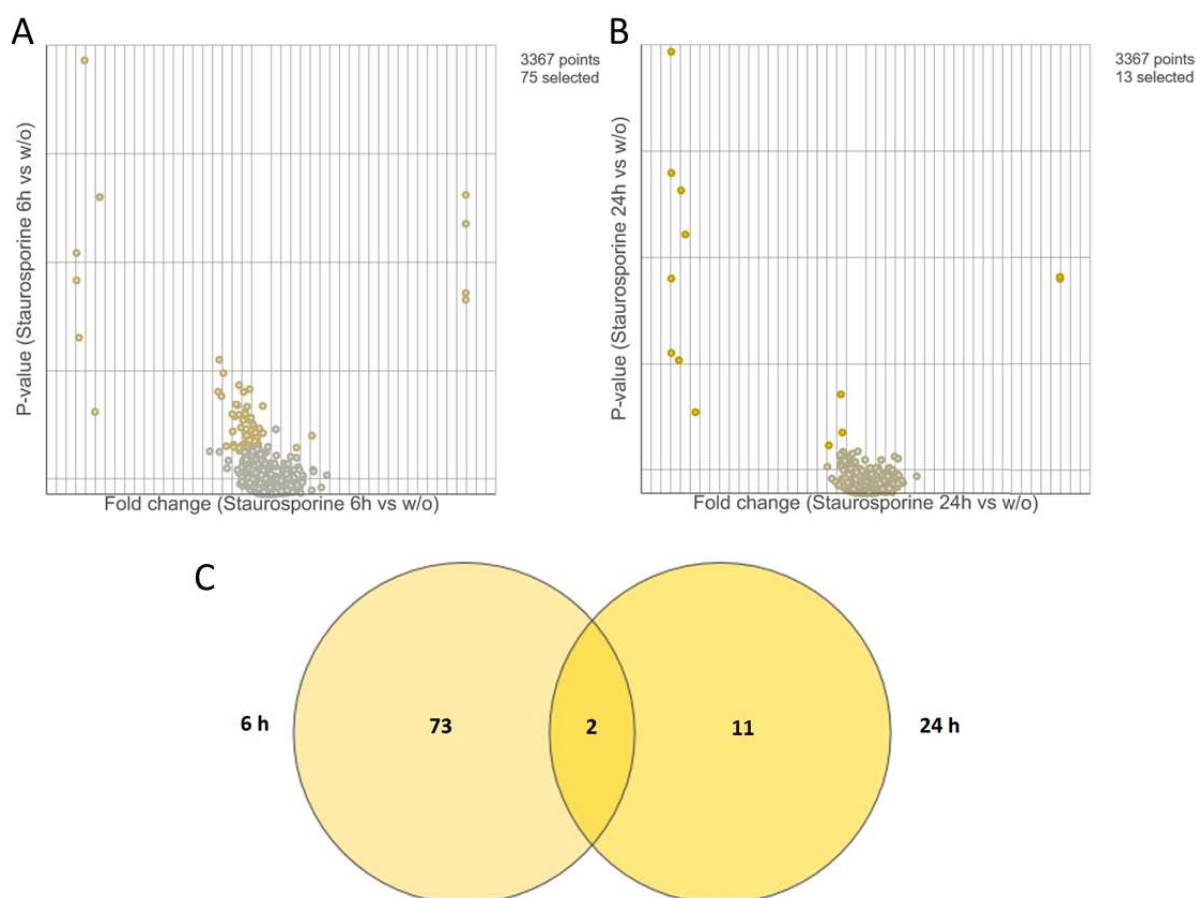


Figure 17. Specific proteins are regulated during staurosporine treatment in *L. major* promastigotes. Volcano plot of staurosporine treated promastigotes shows 75 regulated proteins after 6 h treatment (A) and 13 regulated proteins after

RESULTS

24 h treatment (B). Venn diagram shows 2 proteins that are regulated in both conditions (C). Figures were created in Partek®Flow® and considered as significant when the false discovery rate (FDR) was lower 0.05 and the fold change bigger 1.5 or lower -1.5. List of regulated proteins can be found in **Supp. Table 2** and **Supp. Table 3**.

The treatment of promastigotes with miltefosine for 3 h led to the upregulation of four proteins and the downregulation of four proteins (**Figure 18A**). 21 h later, 102 proteins were regulated, whereas 88 of them were downregulated (**Figure 18B**). Seven proteins were identified to be regulated at both time points (**Figure 18C**).

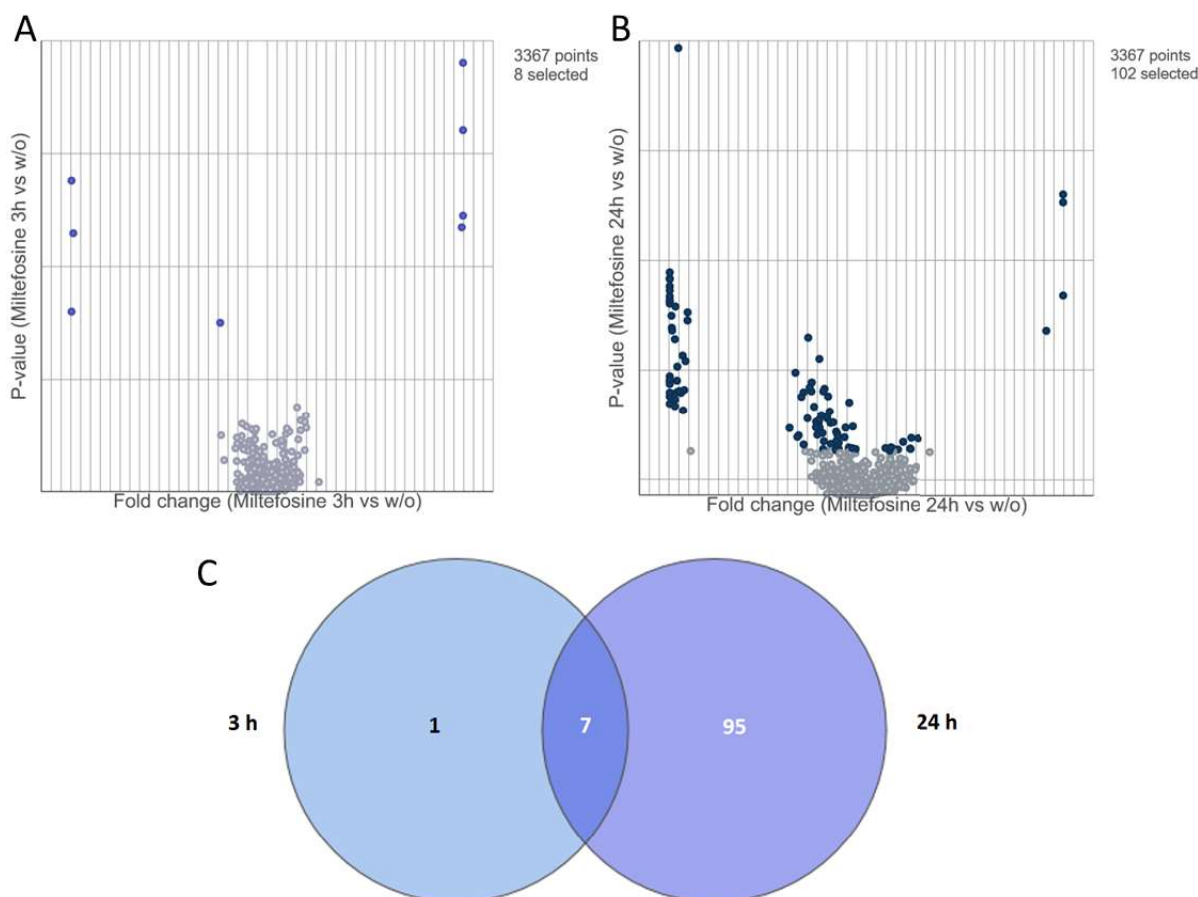


Figure 18. Specific proteins are regulated during miltefosine treatment in *L. major* promastigotes. Volcano plot of miltefosine treated promastigotes shows 8 regulated proteins after 3 h treatment (A) and 102 regulated proteins after 24 h treatment (B). Venn diagram shows 7 proteins that are regulated in both conditions. Figures were created in Partek®Flow® and considered as significant when the false discovery rate (FDR) was lower 0.05 and the fold change bigger 1.5 or lower -1.5. List of regulated proteins can be found in **Supp. Table 4** and **Supp. Table 5**.

Six hours of harmonine treatment led to the regulation of 49 proteins in promastigotes, of which 44 were downregulated and only five were upregulated (**Figure 19**). As already mentioned, the data for the 24 h treatment could not be analyzed, because it did not meet the quality standards.

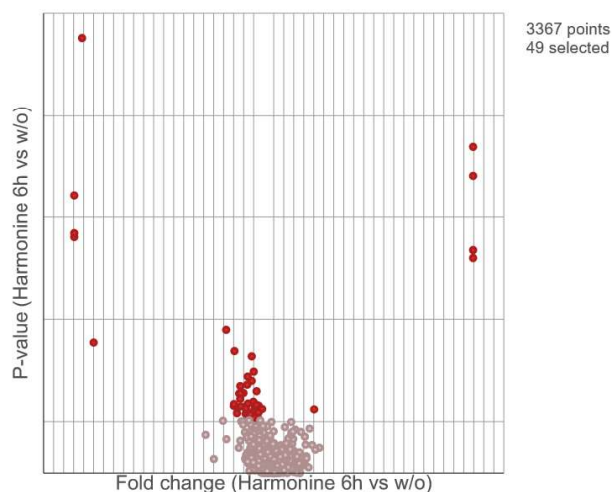


Figure 19. Volcano plot of harmonine-treated *L. major* promastigotes shows that 49 proteins are differentially regulated after 6 h. Figure was created in Partek®Flow® and considered as significant when the false discovery rate (FDR) was lower 0.05 and the fold change bigger 1.5 or lower -1.5. List of regulated proteins can be found in **Supp. Table 6**.

Compound 1o, which was the only compound tested that does not induce apoptosis in promastigotes, altered the measured abundance of only 12 proteins after 24 h of treatment compared to the untreated control. Here, three proteins were upregulated and nine downregulated (**Figure 20**).

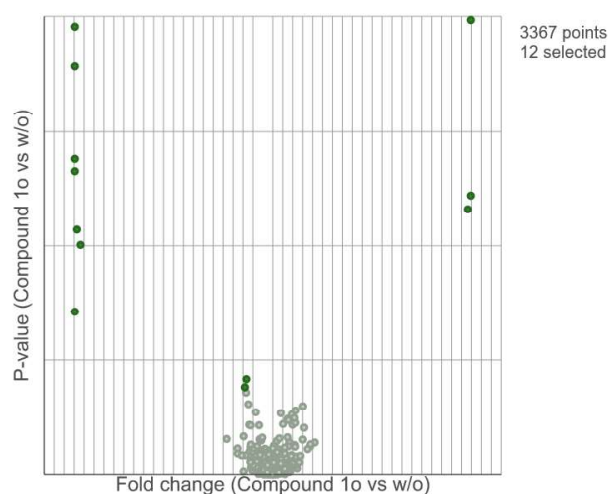


Figure 20. Volcano plot of compound 1o treated *L. major* promastigotes shows that twelve proteins are differentially regulated after 24 h. Figure was created in Partek®Flow® and considered as significant when the false discovery rate (FDR) was lower 0.05 and the fold change bigger 1.5 or lower -1.5. List of regulated proteins can be found in **Supp. Table 7**.

Promastigotes of the stationary growth phase showed the upregulation of three and the downregulation of five proteins compared to the promastigotes of the logarithmic growth phase (**Figure 21**).

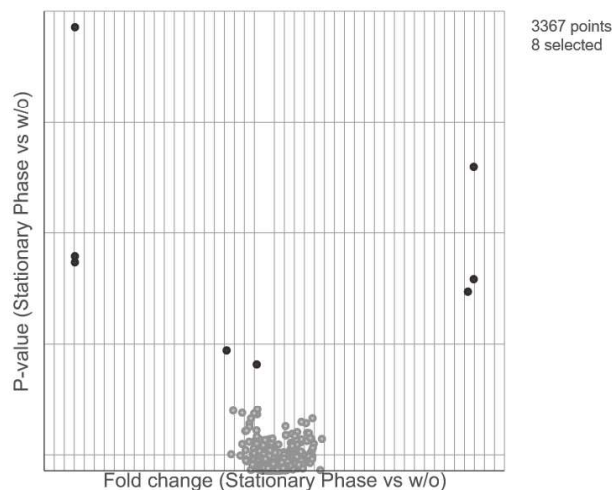


Figure 21. In the stationary phase of *L. major* promastigotes eight proteins were differentially regulated compared to the logarithmic phase. Figure was created in Partek®Flow® and considered as significant when the false discovery rate (FDR) was lower 0.05 and the fold change bigger 1.5 or lower -1.5. List of regulated proteins can be found in **Supp. Table 8**.

Taken together, the different compound treatments led to the regulation of specific proteins in early and late timepoints of apoptosis induction. The effect on downregulation of proteins was more pronounced than on protein upregulation.

3.2.2.2. *Differential Expression Analysis of Amastigotes*

When observing the differential expression analysis of the amastigote dataset it became clear that overall, there were more proteins significantly differentially regulated than in the promastigote dataset. For the staurosporine-treated amastigotes, there were 401 proteins regulated after 6 h (**Figure 22A**) and 735 after 24 h (**Figure 22B**). The overlap between the two time points was 194 proteins (**Figure 22C**).

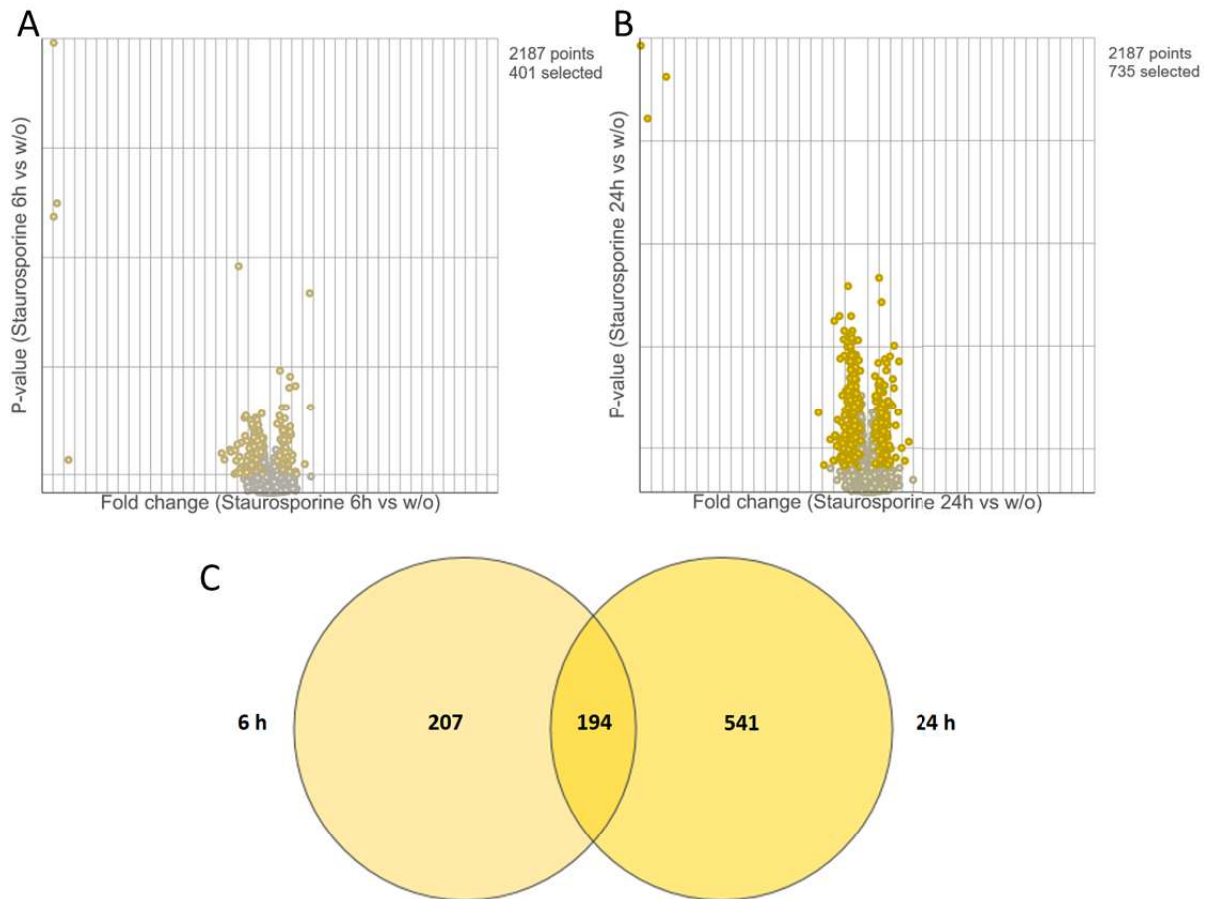


Figure 22. A high number of proteins are regulated during staurosporine treatment in *L. major* amastigotes. Volcano plot of staurosporine treated amastigotes shows 401 regulated proteins after 6 h treatment (A) and 735 regulated proteins after 24 h treatment (B). Venn diagram shows 194 proteins that are regulated in both conditions (C). Figures were created in Partek®Flow® and considered as significant when the false discovery rate (FDR) was lower 0.05 and the fold change bigger 1.5 or lower -1.5. List of regulated proteins can be found in **Supp. Table 9** and **Supp. Table 10**.

Miltefosine, which is not inducing apoptosis in amastigotes (see **Figure 11** and **Figure 14**), led to the differential regulation of 50 proteins, most of which were upregulated (**Figure 23**).

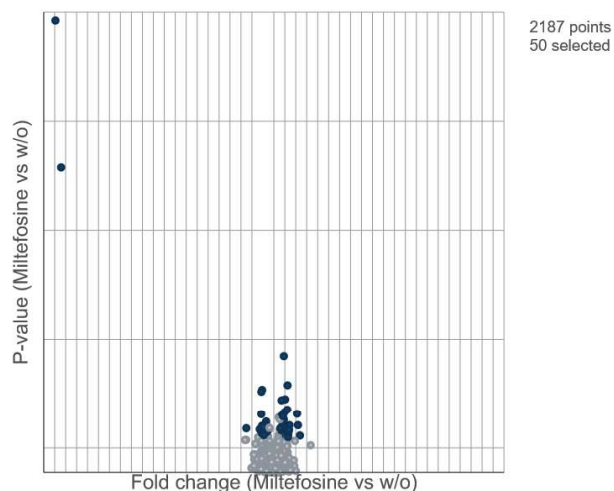


Figure 23. 50 proteins are regulated during 24 h miltefosine treatment in *L. major* amastigotes. Figures was created in Partek®Flow® and considered as significant when the false discovery rate (FDR) was lower 0.05 and the fold change bigger 1.5 or lower -1.5. List of regulated proteins can be found in **Supp. Table 11**.

RESULTS

The treatment of amastigotes with harmonine did not induce apoptosis but let to the differential regulation of 234 proteins (**Figure 24**).

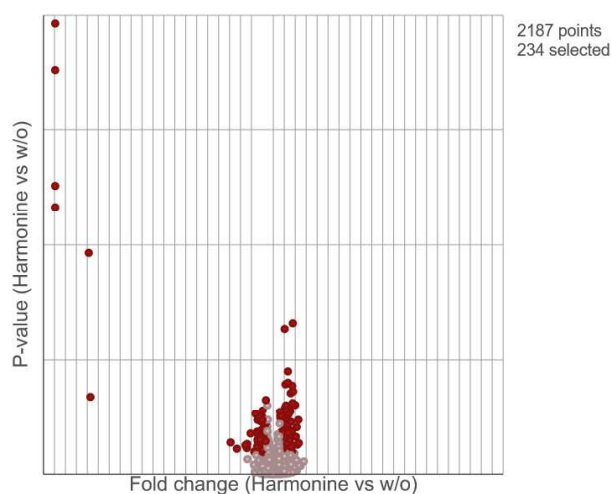


Figure 24. 234 proteins are regulated during 24 h harmonine treatment in *L. major* amastigotes. Figure was created in Partek®Flow® and considered as significant when the false discovery rate (FDR) was lower 0.05 and the fold change bigger 1.5 or lower -1.5. List of regulated proteins can be found in **Supp. Table 12**.

As shown before, compound 1o very strongly enhanced annexin binding in amastigotes (**Figure 14**). This induction of apoptosis led to the differential regulation of 34 proteins after 6 h of treatment with compound 1o (**Figure 25A**). After 24 h treatment, there were 442 proteins differentially regulated (**Figure 25B**). There were 31 proteins found to be differentially regulated in both timepoints (**Figure 25C**).

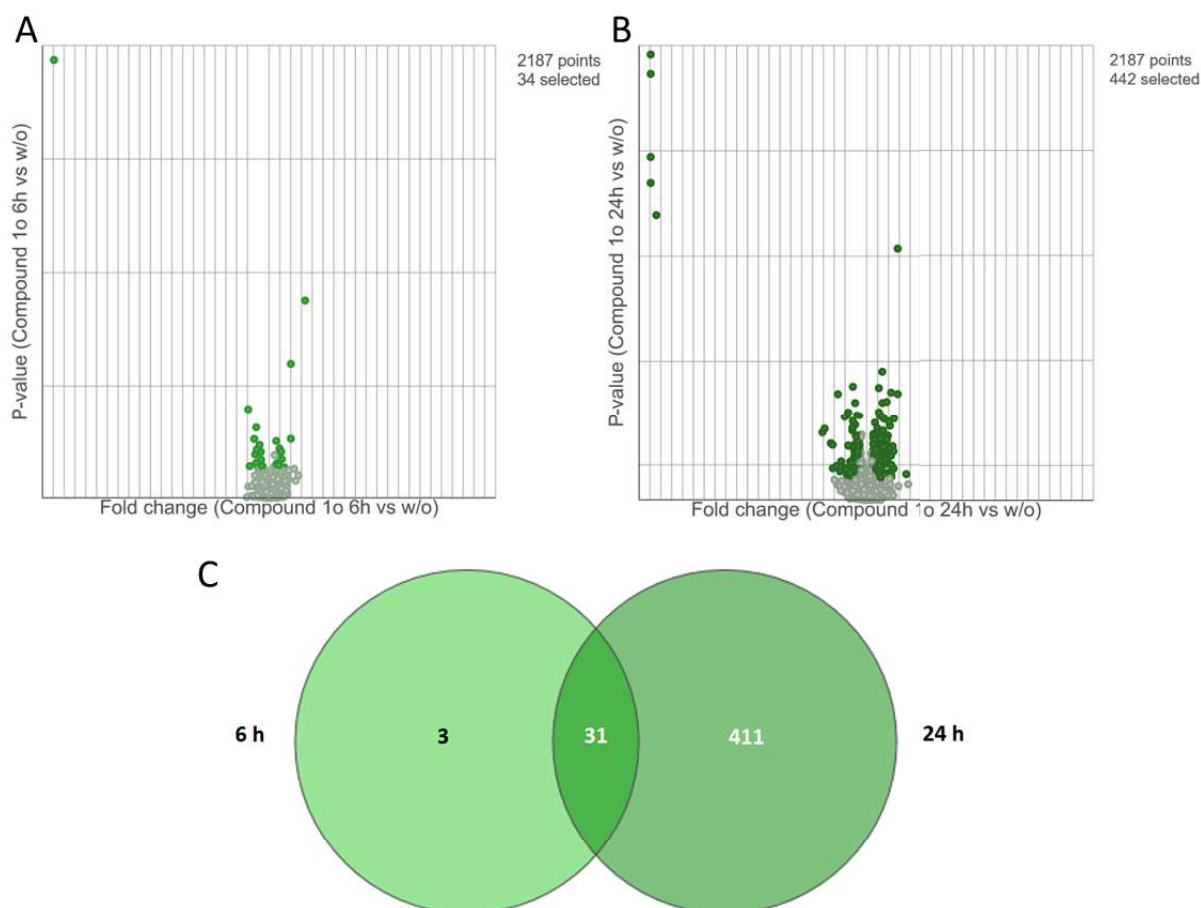


Figure 25. A high number of proteins are regulated during compound 1o treatment in *L. major* amastigotes. Volcano plot of compound 1o treated amastigotes shows 34 regulated proteins after 6 h treatment (A) and 442 regulated proteins after 24 h treatment (B). Venn diagram shows 31 proteins that are regulated in both time points. Figures were created in Partek®Flow® and considered as significant when the false discovery rate (FDR) was lower 0.05 and the fold change bigger 1.5 or lower -1.5. List of regulated proteins can be found in **Supp. Table 13** and **Supp. Table 14**.

Overall, there were explicitly more proteins changed in their abundance in the amastigote state than in the promastigote after compound treatment. Even the compounds that did not induce apoptosis in amastigotes, namely miltefosine and harmonine, led to the differential regulation of 50 and 234 proteins, respectively.

To identify proteins that play a major role during apoptosis, I investigated the conditions that elicited the induction of apoptosis in more detail. For promastigotes, the early time points of the different drug treatments (staurosporine 6 h, miltefosine 3 h and harmonine 6 h) were compared to each other (**Figure 26**).

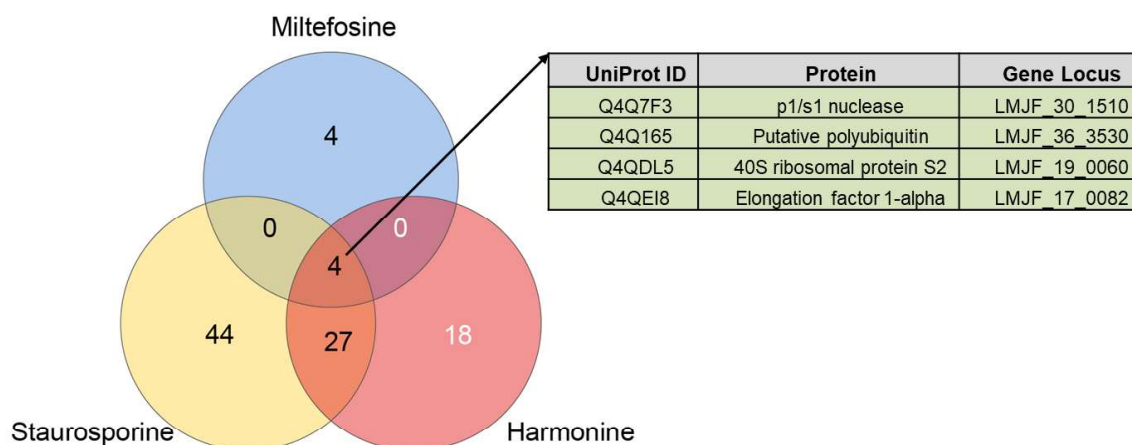


Figure 26. Four proteins were significantly upregulated in all early conditions of apoptosis induction in logarithmic phase *L. major* promastigotes. Venn diagram shows that 4 proteins are uniquely regulated through miltefosine, 44 through staurosporine and 18 through harmonine treatment. Staurosporine and harmonine have 27 proteins in common and all three conditions led to the upregulation of the four proteins, which are shown in the table. Venn diagram was created in Partek®Flow® and considered as significant when the false discovery rate (FDR) was lower 0.05 and the fold change bigger 1.5 or lower -1.5. Protein names and gene loci were retrieved through the online resource www.uniprot.org.

Upon these treatments, four proteins were differentially regulated in all conditions compared to the untreated control: p1/s1 nuclease, polyubiquitin, 40S ribosomal protein S2 and elongation factor 1-alpha. The proteins were all upregulated and no common downregulated proteins were observed. Since they were upregulated at early time points after treatment, they are likely to be important for apoptosis induction and I therefore considered them to be pro-apoptotic.

When comparing the later time points of apoptosis (stationary growth phase, 24 h staurosporine and miltefosine treatment), elongation factor 1-alpha was the only protein that was regulated in all conditions (**Figure 27**).

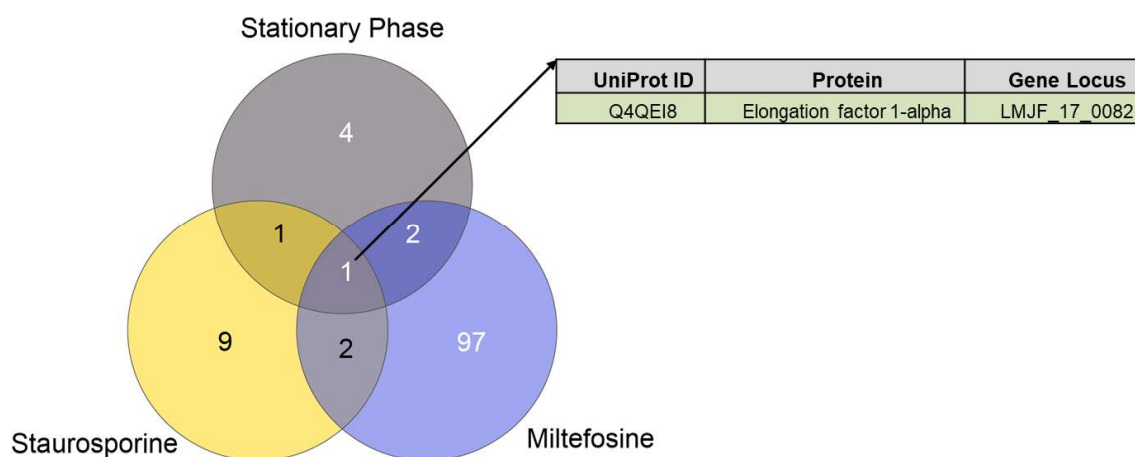


Figure 27. Elongation factor 1-alpha was upregulated in all late conditions of apoptosis induction in *L. major* promastigotes. Venn diagram shows that 4 proteins are uniquely regulated in stationary growth phase, 9 through staurosporine and 97 through miltefosine treatment. Stationary phase and staurosporine treatment have one protein in common, staurosporine and miltefosine 2 and miltefosine and stationary phase also 2 proteins. Venn diagram was created in Partek®Flow® and considered as significant when the false discovery rate (FDR) was lower 0.05 and the fold change bigger 1.5 or lower -1.5. Protein name and gene locus was retrieved through the online resource www.uniprot.org.

Taken together, we could quantify 4416 proteins in promastigotes and 2376 in amastigotes through the use of mass spectrometry. Within these, I found in apoptosis-inducing conditions 15 up- and 189 downregulated proteins in promastigotes and 455 up- and 633 downregulated proteins in amastigotes. In all apoptosis-inducing conditions of promastigotes, elongation factor 1-alpha was upregulated. This highlights the importance of this protein during the regulation of *Leishmania* cell death.

3.3. Knock-outs of Mass Spectrometry Targets

In order to confirm the importance during apoptosis induction of the identified proteins through mass spectrometry, I aimed to perform gene knock-outs (KOs) of the four initial targets I found comparing early timepoints of death stimuli, being p1/s1 nuclease, polyubiquitin, 40S ribosomal protein S2 and elongation factor 1-alpha.

The KOs were generated using a CRISPR/Cas9-based method that replaces the gene of interest (GOI) by an antibiotic resistance gene (see **Introduction**). Therefore, a puromycin resistance gene was inserted, replacing each single gene of the four targets and thereby potentially creating four single knock-out strains. For the deletion of the genes encoding polyubiquitin or 40S ribosomal protein S2, I did not yield living parasites, suggesting that this modification was lethal. For p1/s1 nuclease and elongation factor 1-alpha, a partial KO could be obtained: one gene copy could be replaced by the puromycin resistance cassette but there was still at least one copy of the gene left, since the second allele was not knocked out or the gene resides as multi-copy gene within the genome. The generation of full KOs, by subsequent replacement of the other copy through insertion of a blasticidin resistance gene, was not successful as culturing of the parasites in puromycin- and blasticidin-containing selection medium led to death of both knock-out candidates.

A more detailed investigation of the partial KOs showed that the gene-corresponding mRNA levels were highly reduced for both partial KOs (**Figure 28A**). Upon the deletion of elongation factor 1-alpha, the amount of mRNA was reduced to approximately 50% compared to the Cas9/T7 control. The mRNA level of p1/s1 nuclease was almost depleted in the respective gene knockout, but still above the detection limit. Since I could see a very strong reduction of mRNA level, I decided to determine the following apoptosis characteristics; reactive oxygen species (ROS), PS externalization and DNA fragmentation (**Figure 28B-F**). Different stainings for distinct ROS species were applied: H₂DCFDA detects H₂O₂, HO[•], ROO[•]; DHR123 detects ONOO⁻, H₂O₂ and HOCl and DHE detects O₂⁻¹¹³. Since I sought to detect apoptosis characteristics, it was necessary to induce apoptosis, which I did through the treatment with the different compounds.

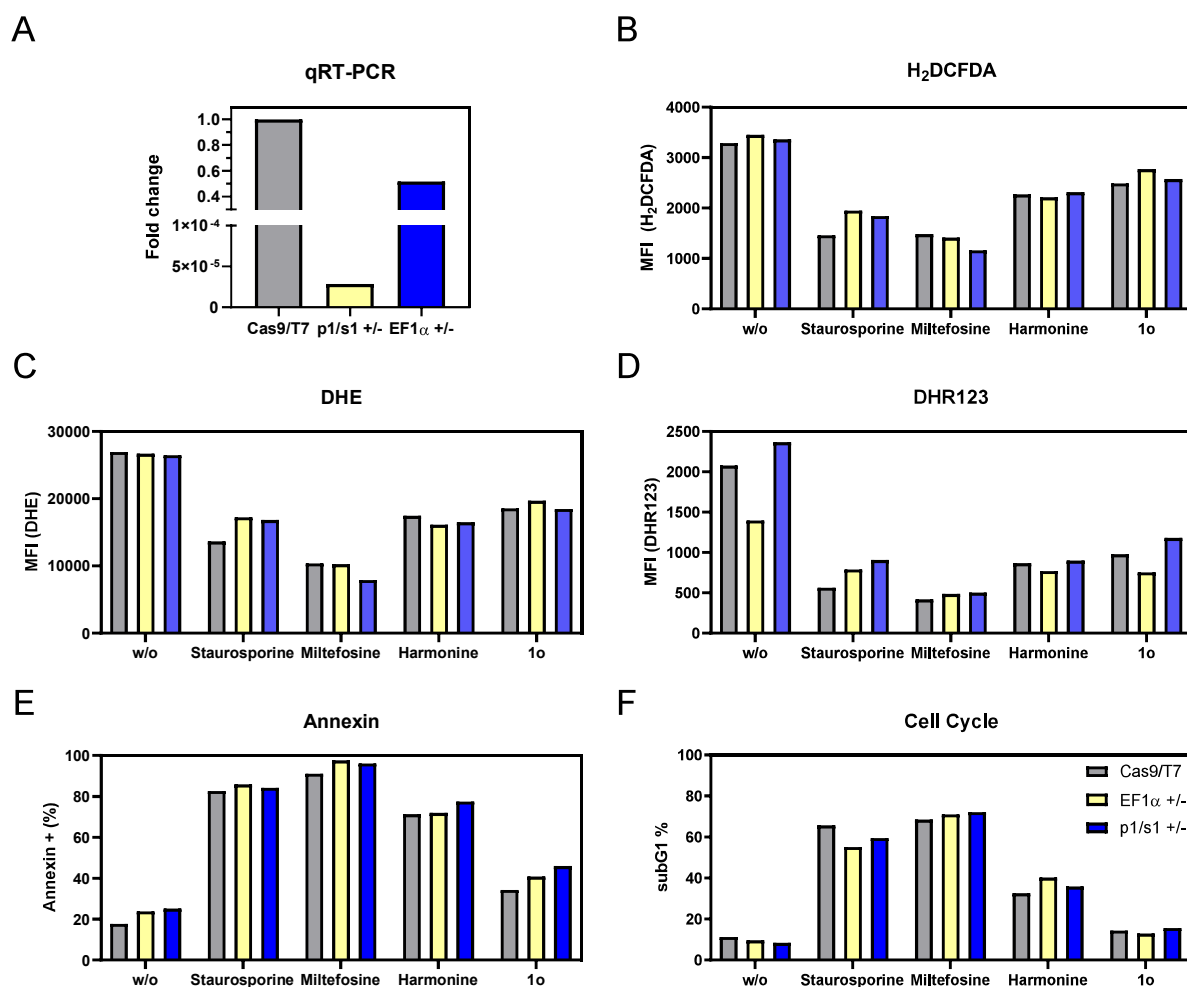


Figure 28. mRNA levels of the partial knock-outs (KO) of p1/s1 nuclease (p1/s1 +/-) and elongation factor 1-alpha (EF1α +/-) were reduced, which had no effect on apoptosis characteristics. mRNA levels of both KO were determined by $2^{-\Delta\Delta CT}$ method using kmp11 as housekeeping gene and normalization to Cas9/T7 control (A). Parasites were treated with 25 μM staurosporine, 25 μM miltefosine 30 μM harmonine or 25 μM compound 1o for 4 h and ROS levels were measured using H₂DCFDA (B), DHE (C) and DHR123 (D) staining at flow cytometer BD LSR II. PS externalization was assessed after treatment with compounds for 24 h by annexin A5-FITC binding and readout at flow cytometer BD LSR II (E). DNA fragmentation was determined after the mentioned treatments for 24 h and cell cycle assay at BD LSR II (F). Data shows the result of one experiment.

Even though the mRNA levels were reduced for both partial KO, there was no observable effect on different ROS species, PS externalization and DNA fragmentation (**Figure 28B-F**). Only the mean fluorescence intensity (MFI) of DHR123 was slightly reduced in the untreated partial KO of elongation factor 1-alpha compared to the control strain. However, after treatment with different compounds, there was no effect detectable anymore (**Figure 28D**).

As none of the above-described genes was determined suitable to explore apoptosis mechanisms in *L. major*, I decided to choose further potential targets based on the mass spectrometry dataset and also based on published data in literature (see **Table 2**). I sought to generate KO for all of the listed genes, but a full KO could only be obtained for DPP, MCA and EndoG as confirmed by PCR of the respective genetic locus (EndoG and MCA will be discussed in more detail in the next section). In

addition, the full KO of SMP4 was provided by Antonio Jiménez Ruiz for further investigations. For all other genes, I was only able to achieve partial KOs. A qRT-PCR showed that the mRNA level of the partial KOs of tryparedoxin peroxidase (TRYP4) and ATP-binding cassette protein subfamily G, member 2 (ABCG2) was reduced by half compared to the control. For the partial KOs pyruvate kinase (PK) and carboxypeptidase (CP), only small amounts of mRNA were still detectable, and for the partial KO of the uncharacterized protein (KO7), as for all full KOs, the mRNA level was below the detection limit (**Figure 29A**).

Table 2. List of KO Targets and the reason why there were chosen for experiments.

Abbreviation	UniProt ID	Protein	Gene Locus	Background
TRYP4	Q4QF74	Tryparedoxin peroxidase	LmjF.15.1060	MS: only detected in untreated promastigotes
KO7	Q4QDQ9	Uncharacterized protein (Probably transmembrane transporter according to uniprot.org)	LmjF.18.1300	MS: upregulated in apoptosis inducing conditions
PK	E9AEH9	Pyruvate kinase	LmjF.35.0020	MS: downregulated in both miltefosine time points in promastigotes
CP	Q4Q0D4	Putative carboxypeptidase	LmjF.36.6260	MS: only detected in early timepoints of apoptosis induction in promastigotes
SMP4	Q5SDH3	Putative small myristoylated protein 4 (former protein name: Calpain-like peptidase)	LmjF.20.1280	Earlier MS screen from J. Steinacker: upregulated in staurosporine treated promastigotes ¹²¹
DPP	Q4QJA6	Dipeptidyl peptidase 3	LmjF.05.0960	Earlier MS screen from J. Steinacker: downregulated in staurosporine treated amastigotes ¹²¹
ABCG2	Q4QJ70	Putative ATP-binding cassette protein subfamily G, member 2	LmjF.06.0090	Published to be involved in the externalization of phosphatidylserine ¹²²
EndoG	Q4QHF4	Putative endonuclease G	LmjF.10.0610	Published to be involved in <i>Leishmania</i> apoptosis ⁹⁸
MCA	E9AEY0 and B6DU86	Metacaspase	LmjF.35.1580	Published to be involved in <i>Leishmania</i> apoptosis ¹⁰⁴

RESULTS

Investigations of the different ROS species for the partial KOs of TRYP4, KO7, PK, CP and ABCG2 and of the full KOs of DPP, SMP4 were performed. Here, I could observe a strong increase of H₂DCFDA-detectable ROS for the ABCG2 +/- parasites compared to control Cas9/T7 parasites. This increase was strongest for untreated parasite. After treatment with the compounds staurosporine, miltefosine, harmonine and compound 1o, it was still observable but not to the same extend (**Figure 29B**). For the other KOs, there was no change seen in H₂DCFDA-detectable ROS levels. DHE and DHR123 staining showed no significant differences overall (**Figure 29C, D**).

The apoptosis characteristics PS externalization and DNA fragmentation were assessed through annexin binding and cell cycle assay, respectively. These parameters showed comparably high values for control parasites as for KOs in the untreated as well as in the apoptosis-induced conditions (**Figure 29E, F**).

Taken together, the KOs of polyubiquitin and 40S ribosomal protein S2 were lethal for the parasite. However, I could achieve a partial KO of p1/s1 nuclease, elongation factor 1 alpha as well as for the further targets TRYP4, KO7, PK, CP and ABCG2, and furthermore a full KO of DPP. The KOs led to a decrease of the respective gene-specific mRNA expression. Further investigations of the apoptosis characteristics ROS induction, PS externalization and DNA fragmentation were not altered except for an increase in H₂DCFDA-detectable ROS levels for ABCG2 partial KO.

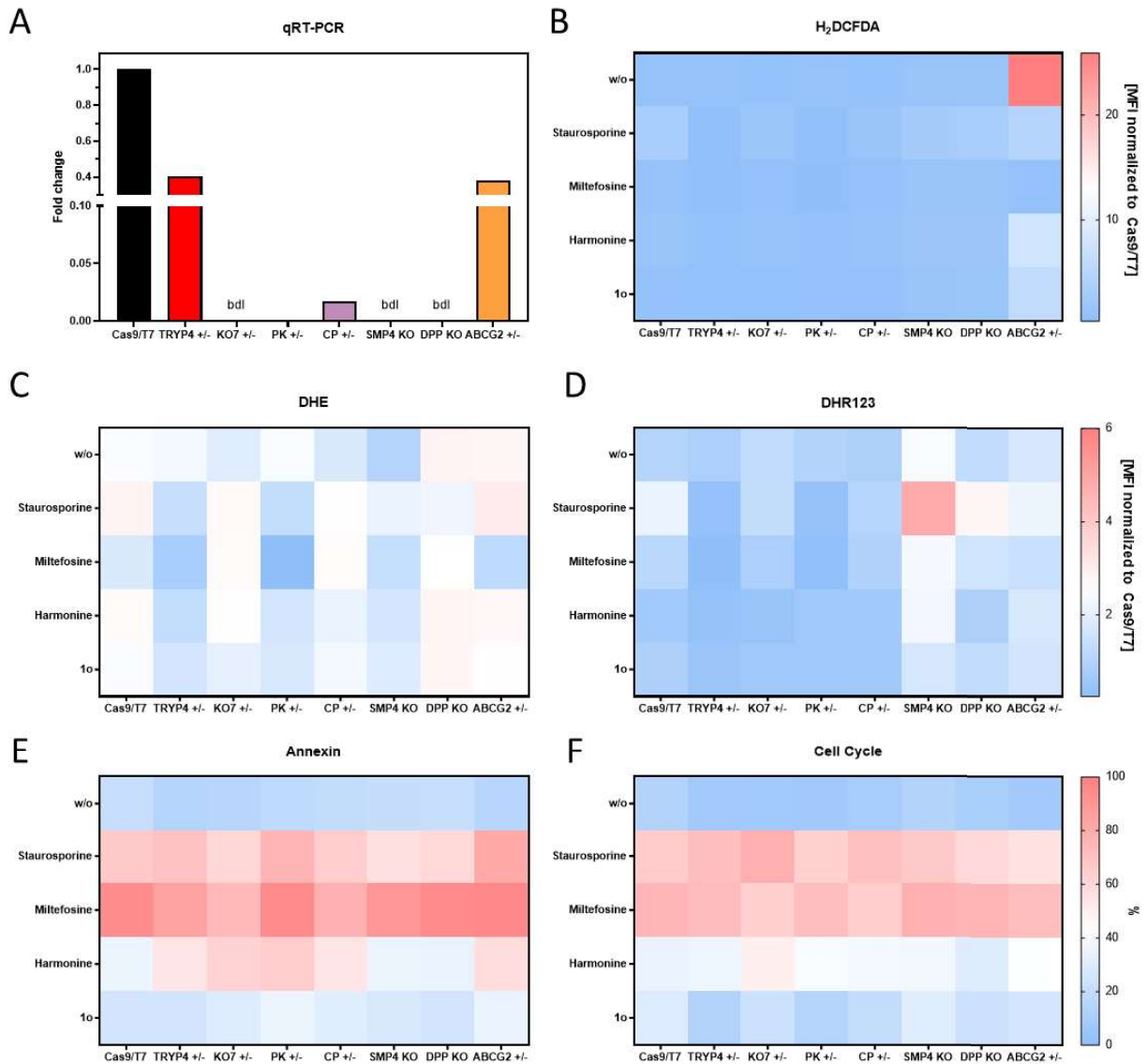


Figure 29. mRNA levels of the partial knock-outs (KO) of tryparedoxin peroxidase (TRYP4 +/-), pyruvat kinase (PK +/-), carboxypeptidase (CP +/-) and ATP-binding cassette protein subfamily G, member 2 (ABCG2 +/-) were reduced, while the mRNA levels of partial KO of uncharacterized protein (KO7 +/-) and full KO of small myristoylated protein 4 (SMP4) and Dipeptidyl peptidase 3 (DPP) were below the detection limit (bdl). mRNA levels of all KO were determined by $2^{-\Delta\Delta CT}$ method using *kmp11* as housekeeping gene and normalization to Cas9/T7 control (A). Parasites were treated with 25 μ M staurosporine, 25 μ M miltefosine, 30 μ M harmonine or 25 μ M compound 1o for 4 h and ROS levels were measured using H₂DCFDA (B), DHE (C) and DHR123 (D) staining at flow cytometer BD LSR II. PS externalization was assessed after treatment with 25 μ M staurosporine, 25 μ M miltefosine 30 μ M harmonine or 25 μ M compound 1o for 24 h by annexin A5-FITC binding and readout at flow cytometer BD LSR II (E). DNA fragmentation was determined after the mentioned treatments for 24 h by cell cycle assay and readout at flow cytometer BD LSR II (F). Data shows the results of one experiment (A) or one experiment for the partial KOs except ABCG2 +/-; full KOs and ABCG2 +/- were assessed in at least three independent experiments. Heat maps show the median of MFIs that were normalized to Cas9/T7 control (B-D), % annexin+ (E) and % subG1+ (F).

As ABCG2 partial KO promastigotes from the logarithmic growth phase showed a very strong upregulation of H₂DCFDA-detectable ROS species, I also investigated the corresponding stationary phase promastigotes and amastigotes for their ROS levels, in order to see if it is a stage specific effect (Figure 30).

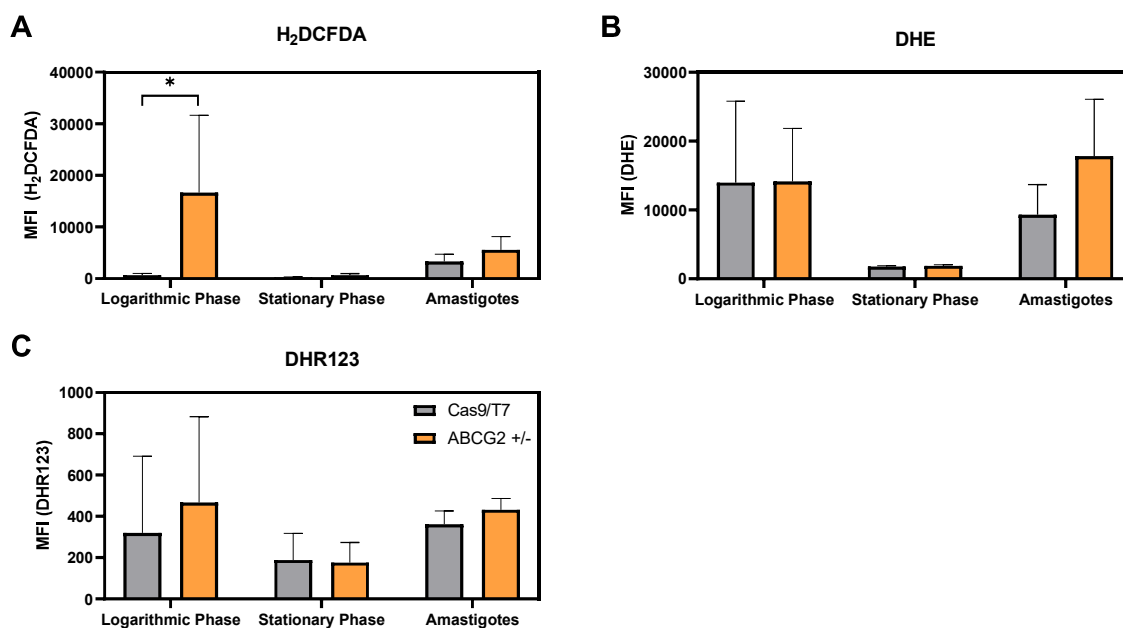


Figure 30. ROS levels of partial ATP-binding cassette protein subfamily G, member 2 knock-out (ABCG2 +/-) were only increased in logarithmic phase promastigotes. Untreated logarithmic and stationary phase promastigotes as well as amastigotes of Cas9/T7 and ABCG2 partial KO were stained with H₂DCFDA, DHE and DHR123 to detect ROS levels in the parasites. Data are shown as mean +SD and are representative for at least three independent experiments. Significance was assessed by Two-Way ANOVA with *p < 0.05.

For logarithmic phase promastigotes exhibiting the partial KO of ABCG2, there was a strong and significant increase (26-fold) in the H₂DCFDA-detectable ROS H₂O₂, HO[•] and ROO[•]. This could also be seen for stationary phase promastigotes (3.2-fold); however, it was not so pronounced since the ROS level in the stationary phase are clearly lower (compare the MFI 641.0 ± 370.0 in the Cas9/T7 logarithmic phase promastigotes to 209.0 ± 102.1 in the stationary phase promastigotes). There was only a minor increase in ROS for amastigotes (1.7-fold). The DHE assay, which stains O₂^{•-}, showed slightly increased values for amastigotes in the partial ABCG2 KO (1.9-fold) but not for the promastigotes in both growth phases. The DHR123 staining, which mainly detects ONOO⁻ but also H₂O₂ and HOCl, showed slightly increased values for logarithmic phase promastigotes (1.5-fold) and amastigotes (1.2-fold), but not for stationary phase promastigotes. Since ABCG2 is suggested to be involved in PS externalization¹²², I expected a decrease in annexin binding, which I could not see (see **Figure 29**). However, what I observed was an increase in ROS levels, which was the biggest increase for H₂DCFDA in living promastigotes of the ABCG2 partial KO compared to the control. This depicts a new role for ABCG2 in the defense against ROS in *Leishmania*.

Since apoptotic promastigotes are crucial for disease development⁴¹, I would expect less disease development after the deletion of a protein which induces *Leishmania* apoptosis, and an increased disease development after the deletion of a protein which impairs apoptosis in the parasite. In order to clarify if a protein indeed has a role in disease development, I first investigated the infection process. The model that we are using in the laboratory is the infection of primary human monocyte-derived

macrophages with *Leishmania*. I stained stationary phase promastigotes with the dye CFSE and infected human primary macrophages for 3 h at an MOI of 10. After 24 h, I checked for the percentage of infected macrophages, which were CFSE+, via flow cytometry (**Figure 31**).

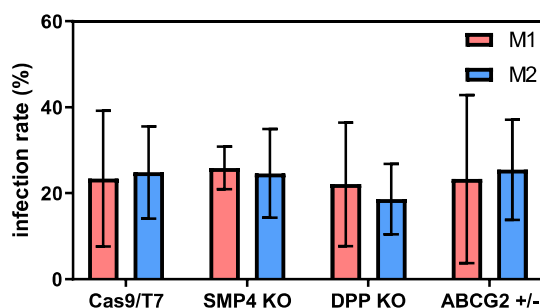


Figure 31. Infection rate of human primary macrophages is not altered for the KO of small myristoylated protein 4 (SMP4), dipeptidylpeptidase (DPP) and partial KO of ATP-binding cassette protein subfamily G, member 2 (ABCG2 +/-). Human primary macrophages type 1 and 2 (M1/M2) were infected with CFSE-stained stationary phase promastigotes for 3 h at an MOI of 10. 24 h later, infection rate was assessed by checking for CFSE+ macrophages via flow cytometry. For SMP4 KO infection n=2-3, rest n ≥5.

Around 20-25 % of type 1 or 2 macrophages were measured to be infected with the control parasites, and the infection rate did not significantly change when infection was performed using the SMP4 KO, DPP KO or the partial ABCG2 KO parasites. This means the KOs had no influence on the infectivity of the parasites.

3.4. Endonuclease G and Metacaspase

As already mentioned, I investigated as well the role of published apoptosis-involved proteins to get new insights in the apoptosis machinery of *Leishmania*. Since previously published data from multiple sources described a role of EndoG and MCA in apoptosis^{98,106}, I aimed to investigate their function in more detail. I created an EndoG KO, an MCA KO and also a KO for both genes, generating MCA/EndoG double-KO parasites. Whereas, I measured a certain amount of mRNA in the non-deletion control strain, the mRNA of the respective genes in the KO strains was below the detection limit (**Figure 32**).

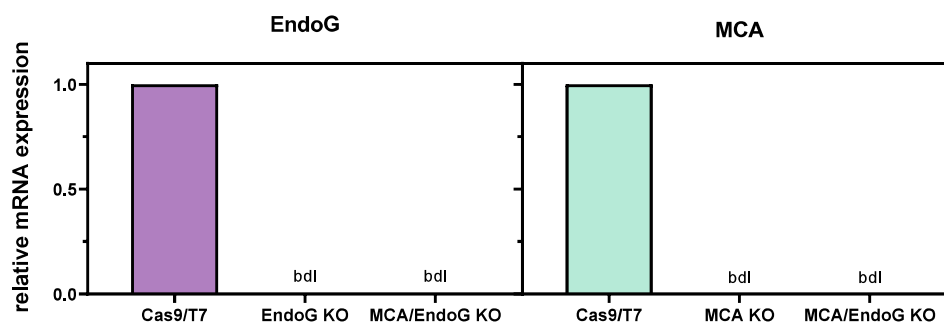


Figure 32. EndoG or MCA mRNA was not detectable in the respective KOs. RNA of the parasites was extracted and subjected to qRT-PCR. Ct values were normalized to the housekeeping gene *kmp11* and the relative mRNA expression was calculated using the Cas9/T7 expression of EndoG or MCA. RNA of the KOs was below detection limit (bdl). Data is representative of three independent experiments.

In order to characterize the KOs, I examined the growth behavior of all KO cell lines. When I analyzed the growth of the EndoG KO, I observed a reduced number of living parasites in the early logarithmic, as well as in the late stationary growth phase. In the later stationary growth phase, beginning six days after passaging, the number of dead parasites was significantly reduced as well (**Figure 33A**). The KO of MCA or MCA/EndoG did not affect the parasites' viability and growth behavior compared to the Cas9/T7 control. Morphologically, I could not observe a difference between the strains. All KO strains showed the same apoptotic shrinkage, beginning at day four after passaging (**Figure 33B-E**).

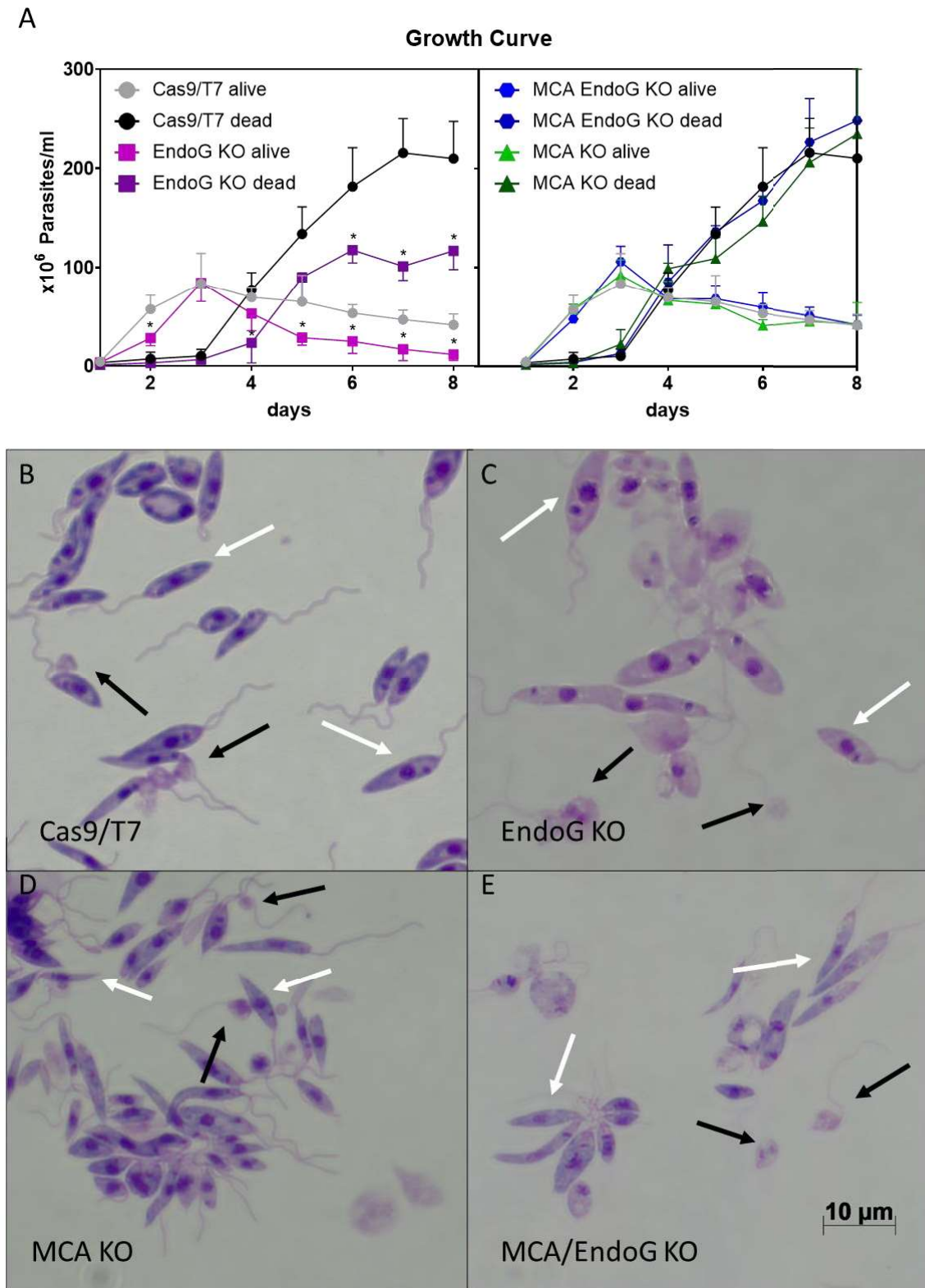


Figure 33. Double KO of EndoG and MCA does not affect viability of *L. major* promastigotes. *L. major* promastigotes were seeded with a density of 1×10^6 /ml living parasites into a blood agar plate and counted daily using a Neubauer chamber (A). Diff-Quik staining of late logarithmic phase Cas9/T7 (B), EndoG KO (C), MCA KO (D) and MCA/EndoG KO (E) parasites shows living (white arrows) and dead (black arrows) promastigotes. Data is representative of at least three independent experiments and is shown as mean \pm SD for dead and mean \pm SD for living parasites. Significance was assessed by Two-Way ANOVA with $*p < 0.05$.

I aimed to investigate alterations in the apoptosis machinery of the EndoG and MCA KO parasites. I used promastigotes and induced apoptosis through the addition of miltefosine. To further check for other endonucleases and metacaspases that could be involved in the apoptosis process, I pre-incubated the parasites for two hours with the endonuclease inhibitor ATA and the metacaspase inhibitor antipain. After three hours of miltefosine treatment, I investigated the decrease of the mitochondrial potential as a first step of apoptosis induction. The basal mitochondrial potential was slightly higher for the EndoG KO and slightly lower for the MCA KO and the MCA/EndoG KO compared to the control. After ATA or antipain pre-incubation the effect of lower mitochondrial potential became significant in the MCA KO. Interestingly, in the untreated control, the MCA KO showed a mitochondrial potential, which was as low as the potential in the apoptosis-induced condition (**Figure 34A**). This indicates a role of MCA together with other partners in the mitochondrial homeostasis.

As a next step of apoptosis, I investigated the ROS induction in the KO parasites after four hours. The basal level of ROS in the EndoG KO parasite was slightly enhanced compared to Cas9/T7 control, which was significant when pre-incubated with ATA. For the MCA KO and the MCA/EndoG KO, the ROS levels were not altered (**Figure 34B**). Meaning that EndoG might have a protective role against ROS in combination with other endonucleases.

After five hours of Miltefosine treatment, I performed an annexin binding assay to investigate the externalization of phosphatidylserine (PS). I observed a significant increase in PS externalization in the untreated double KO parasites. This effect was also present when the parasites were pre-incubated with ATA, but not for Antipain (**Figure 34C**).

As one of the later steps of apoptosis, I examined the DNA fragmentation via cell cycle assay after six hours. The basal level of DNA fragmentation was enhanced in the double KO ($18.27 \pm 2.48\%$ in the MCA/EndoG KO, compared to $7.24 \pm 3.92\%$ in the control parasites), which was highly significant after pre-incubation with antipain. Apoptosis induction through miltefosine showed significantly less DNA fragmentation in the EndoG KO as well as in the MCA/EndoG KO, but not in the MCA KO. This effect could also be observed after pre-incubation with ATA. When pre-incubated with antipain and treated with miltefosine, the DNA fragmentation was decreased to about 20 – 30% for control, MCA KO and MCA/EndoG KO parasites. In the EndoG KO parasites, the DNA fragmentation was comparable to untreated parasites (**Figure 34D**). EndoG KO parasites that were treated for six hours with miltefosine showed a reduced DNA fragmentation as well when TUNEL staining was performed compared to the Cas9/T7 parasites (**Figure 34E, F**). In these experiments, it could be shown that EndoG shows a major effect on DNA fragmentation, while MCA only had little effects.

It became evident that MCA has no effect on ROS, PS externalization and DNA fragmentation. However, combined with endonucleases or other metacaspases, it could have an effect on the mitochondrial potential. On the other hand, EndoG has no effect on the mitochondrial potential and PS externalization. Together with other endonucleases it could have an effect on ROS. The effect of EndoG on DNA fragmentation was clearly visible.

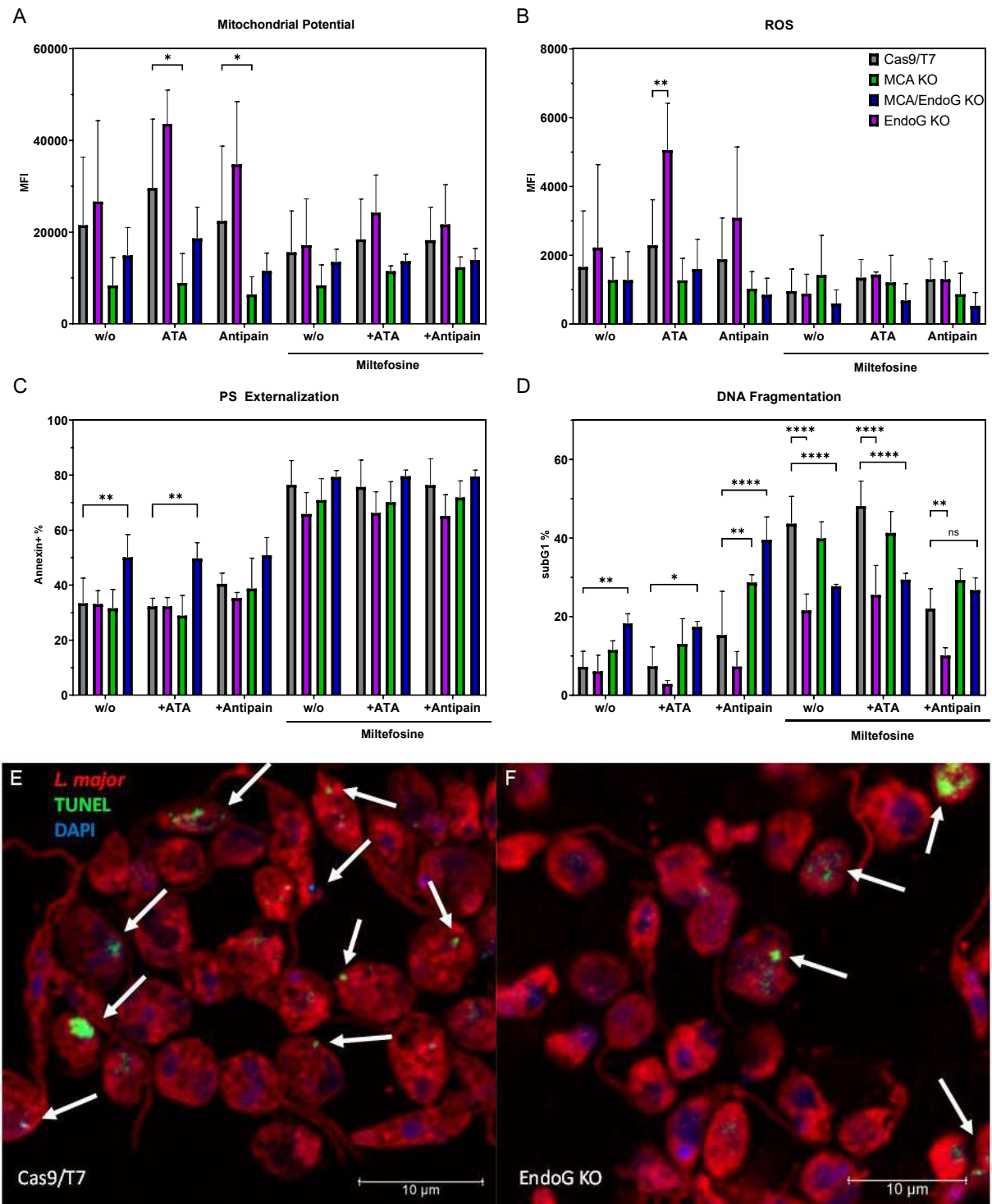


Figure 34. EndoG but not MCA KO leads to a significant decrease of DNA fragmentation after apoptosis induction through miltefosine. Promastigotes were pre-incubated with 50 μ M aurintricarboxylic acid (ATA) or 2 μ M antipain for two hours and then treated with 25 μ M miltefosine for apoptosis induction. After 3 h of miltefosine treatment, cells were stained with

RESULTS

rhodamine123 to observe the mitochondrial potential by flow cytometry (A). After 4 h apoptosis induction, parasites were stained with OxyBURST™ and investigated *via* flow cytometry for reactive oxygen species (ROS) (B). Phosphatidylserine (PS) externalization was determined through binding of fluorescent Annexin A5 after five hours miltefosine (C). After six hours miltefosine the amount of fragmented DNA was investigated through PI staining in a cell cycle assay (D). Fragmented DNA was further observed through terminal deoxynucleotidyl transferase dUTP nick end labeling (TUNEL). A staining with anti-*Leishmania* serum (red), DAPI (blue) and TUNEL (green) was performed in Cas9/T7 (E) and EndoG KO (F) parasites that were treated for six hours with miltefosine. A-D: Data is representative of at least three independent experiments and is shown as mean +SD. Significance was assessed by Two-Way ANOVA with *p < 0.05; **p < 0.01; ***p < 0.001; ****p < 0.0001.

After ATA treatment, there was a significant increase of ROS in the EndoG KO. Therefore, I investigated the different ROS in all life stages of EndoG KO parasites in more detail. In the H₂DCFDA detectable species, there was neither an effect between the controls and the EndoG KO in the logarithmic nor in the stationary growth phase nor in amastigotes. The DHE-detectable ROS (O₂⁻) (Figure 35B) was enhanced in amastigotes (2.4-fold), but not in promastigotes. For the DHR123-detectable species, the levels were decreased in the logarithmic phase (3.4-fold), but not for stationary phase or amastigotes.

Taken together, EndoG might have a more pronounced role in the protection against ROS in amastigotes than in promastigotes. To be precise, protection against O₂⁻.

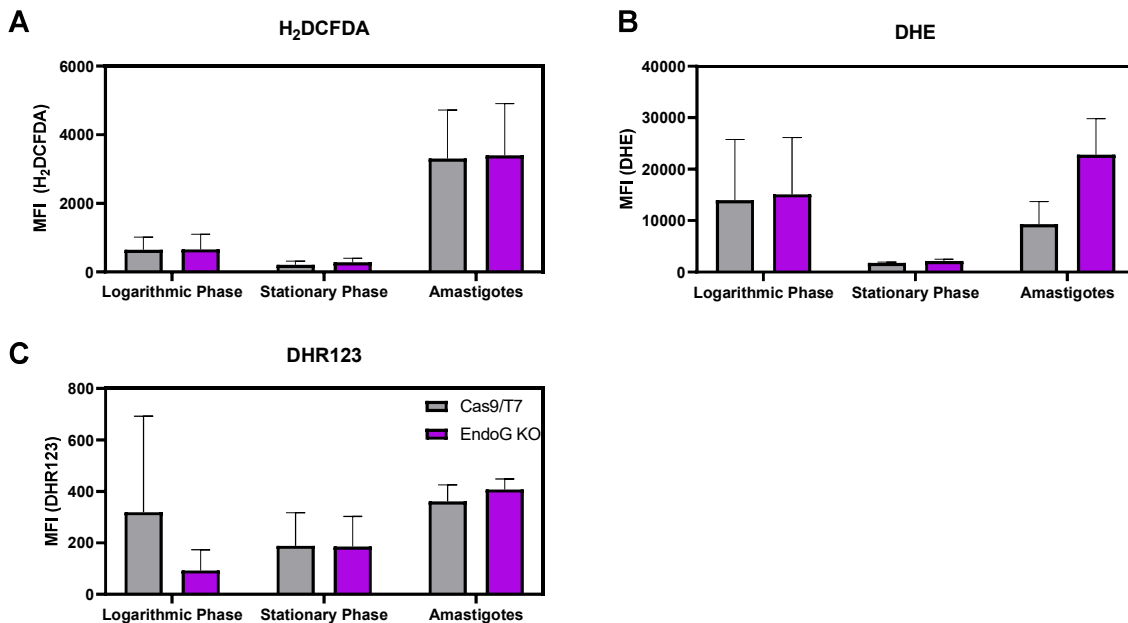


Figure 35. ROS levels are slightly enhanced in EndoG KO amastigotes but not in promastigotes. Untreated logarithmic and stationary phase promastigotes as well as amastigotes of Cas9/T7 and EndoG KO were stained with H₂DCFDA (A), DHE (B) and DHR123 (C) to detect ROS levels in the parasites. Data is representative of at least three independent experiments and is shown as mean +SD.

The biggest influence of the EndoG KO could be seen on DNA fragmentation. Therefore, I analyzed the significant effect of reduced DNA fragmentation after miltefosine treatment in the EndoG KO

(**Figure 34D**) in more detail. For this, I performed a cell cycle assay every two hours for 24 hours. I could see that there was less fragmented DNA after 4 to 12 hours. From 14 hours after miltefosine treatment there was no significant difference between the control cells and the EndoG KO (**Figure 36**). Other known apoptosis inducers were tested for DNA fragmentation as well. H₂O₂ treatment increased the DNA fragmentation in the Cas9/T7 parasites. In the EndoG KO this effect was significantly lower. MCA KO and MCA/EndoG KO showed the same level as the control parasite after H₂O₂ treatment. A pre-incubation with ATA enhanced the effect of reduced DNA fragmentation in the EndoG KO. H₂O₂ treatment led to more subG1+ Cas9/T7 parasites when pre-treated with antipain. This increased DNA fragmentation was significantly reduced in the EndoG KO parasites. For MCA and MCA/EndoG KO there was no difference compared to Cas9/T7. Staurosporine-induced DNA fragmentation showed the same effect of reduced DNA fragmentation in the EndoG KO compared to the control parasite. Here, the MCA KO and the MCA/EndoG KO showed an enhanced level of DNA fragmentation. This was not changed when pre-incubated with ATA or antipain. However, the reduced DNA fragmentation in the EndoG KO was not significant anymore when pre-incubated with antipain. Therefore, the involvement of EndoG in the DNA fragmentation is not only the case when apoptosis is induced through miltefosine, but also for hydrogen peroxide and staurosporine. Antipain could decrease the staurosporine-induced DNA fragmentation significantly. The further decrease through the KO of EndoG was not significant anymore when pre-incubated with antipain.

In order to test if the reduced DNA fragmentation can also be linked to a higher fitness of the parasites, I investigated the metabolic activity of EndoG KO parasites using MTT assay. Surprisingly, after 14 h and 16 h of miltefosine treatment, a lower metabolic activity of the EndoG KO could be observed (**Figure 36C**). Therefore, I could not link the reduced DNA fragmentation to higher fitness but observed a lower fitness. This indicates further roles of EndoG in cell survival or homeostasis.

RESULTS

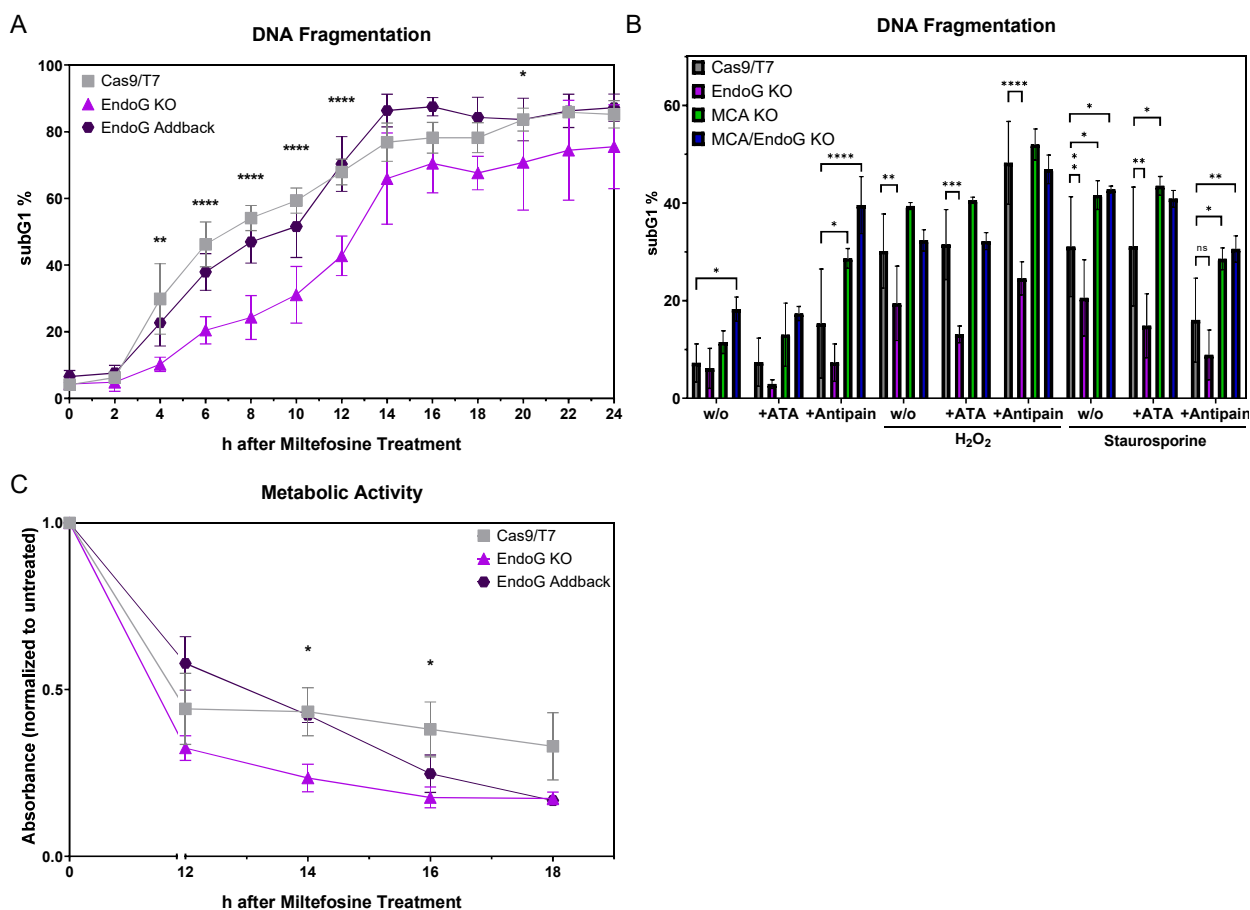


Figure 36. Reduced DNA fragmentation is a time-dependent and miltefosine unspecific effect. Cas9/T7, EndoG KO and EndoG addback parasites were treated for 24 h with 25 μ M miltefosine and subjected each two hours to PI staining in a cell cycle assay (A). Parasites were pre-incubated with 50 μ M aurintricarboxylic acid (ATA) or 2 μ M antipain for two hours and treated for six further hours with 25 μ M staurosporine or 2 mM H₂O₂ and analyzed via flow cytometry in a cell cycle assay (B). Cas9/T7, EndoG KO and EndoG addback parasites were treated with 25 μ M miltefosine and subjected after 12 h each two hours to an MTT assay. The measured absorbance was normalized to the respective untreated control (C). Data is representative of at least three independent experiments and is shown as mean \pm SD (A) \pm SD (B) \pm SEM (C). Significance was assessed by Two-Way ANOVA with * p < 0.05; ** p < 0.01; *** p < 0.001; **** p < 0.0001.

Leishmania apoptosis plays an important role for the infectivity of the parasites. Therefore, I investigated if the KO parasites also show an altered infectivity towards primary hMDM1/2. For this, I created fluorescent parasites that can be detected via flow cytometry. To do so, I integrated an eGFP to the ribosomal gene locus of the parasites and infected type 1 and 2 macrophages with the eGFP-expressing KO parasites. Since some of the effects were only seen after apoptosis induction, I also treated the infected macrophages with miltefosine. The cells were washed and examined for the infection rate (eGFP+ macrophages) after 12 h (d1) and after 96 h (d4) via flow cytometry. I could observe that the initial infection rate with Cas9/T7 parasites at day one was higher in type 2 macrophages (35.75 \pm 17.71%) than in type 1 (22.20 \pm 6.07%), and it was slightly decreased in both macrophage types when treated with miltefosine (M1: 15.56 \pm 11.23%; M2: 22.20 \pm 10.35%). The EndoG KO (M1: 20.73 \pm 9.55%; M2: 36.01 \pm 13.48%) was as infective as the Cas9/T7 control strain in

both types of macrophages. The MCA KO (M1: $18.52 \pm 13.97\%$; M2: $26.87 \pm 17.53\%$) and the MCA/EndoG double KO (M1: $9.93 \pm 7.12\%$; M2: $18.14 \pm 14.05\%$) showed lower infection rates, which were significant for the double KO in type 2 macrophages (**Figure 37A**). After 96 hours, this effect could also be seen in type 1 macrophages (**Figure 37B**). When pre-treated with miltefosine, there was no significant reduction in infectivity for the KO parasites compared to the control parasites. Besides the infection rate, I was also interested in the proliferation of the parasites. To this end, I measured the difference in mean fluorescence intensity of GFP+ parasites inside the macrophages by flow cytometry on day four and day one of infection and calculated the ratio. For the proliferation, I could not detect a significant decrease in the EndoG KO or MCA KO parasites, while it was significantly decreased for the double KO compared to the Cas9/T7 (**Figure 37C**). I visualized the infection of M1 cells with Cas9/T7 and MCA/EndoG KO parasites after 96 h via DiffQuik staining and observed less infected cells with less parasites inside the macrophages (parasite burden) when infected with the double KO (**Figure 37D, E**).

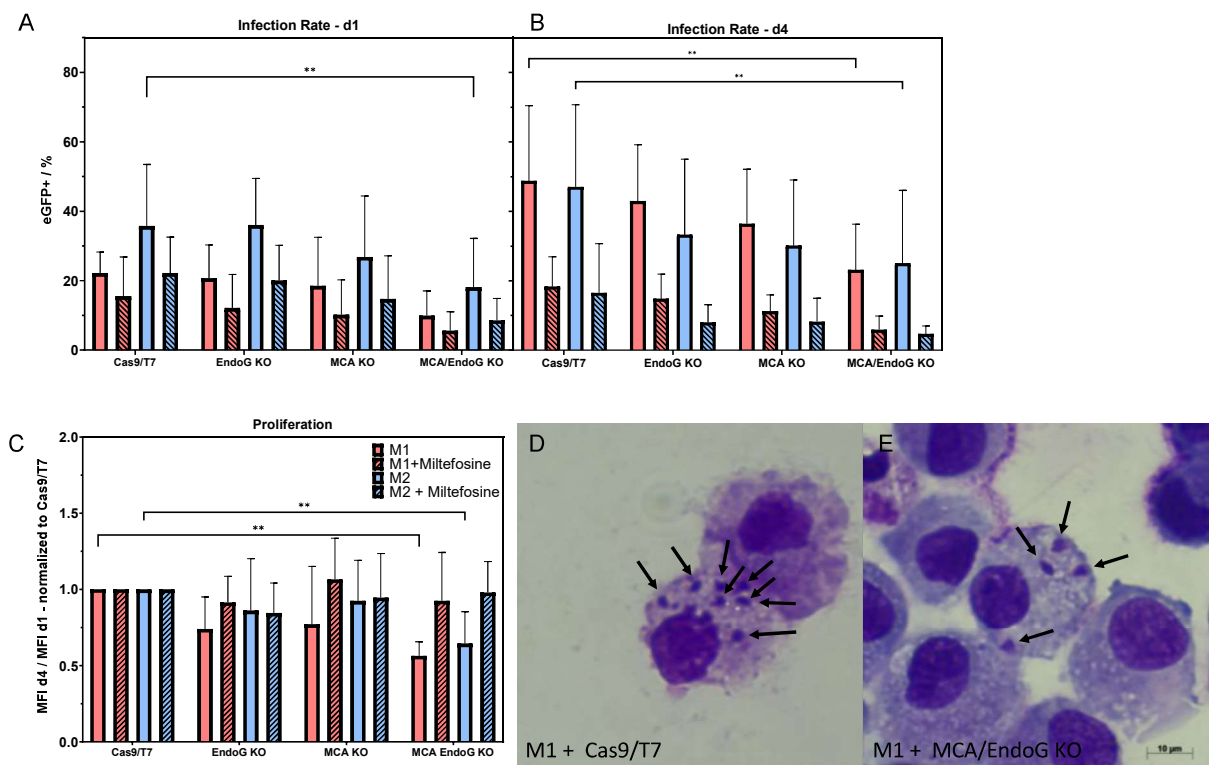


Figure 37. Double KO of MCA and EndoG leads to a reduced infection rate of hMDMs. Primary human monocyte-derived macrophages (hMDM) type 1 and 2 were infected with eGFP expressing parasites at a multiplicity of infection (MOI) 10. After 3 h of infection the extracellular parasites were removed and the infected macrophages were treated with $25 \mu\text{M}$ miltefosine for 12 h. Miltefosine was removed and macrophages were subjected to flow cytometry (A). Macrophages were cultured for another three days and investigated via flow cytometry for eGFP+ macrophages (B). Geometric mean of the macrophages from d1 and d4 were determined for both experiments and divided to determine the proliferation rate of the parasites (C). DiffQuik staining was performed of M1 macrophages infected with Cas9/T7 eGFP (D) and EndoG KO eGFP (E) parasites 96 h after infection. Black arrows indicate the intracellular parasites. Data is representative of at least three independent experiments and is shown as mean \pm SD; ** $p < 0.01$.

Taken together, the infection rate of EndoG KO or MCA KO parasites was not significantly changed in hMDM. However, the MCA/EndoG KO reduced the infection rate and the intracellular proliferation. Highlighting the role of both proteins in the intracellular survival of *Leishmania*.

3.5. Pentose Phosphate Pathway as Drug Target

The pentose phosphate pathway has previously been shown to be a promising drug target for other parasites like *Plasmodium falciparum*¹²³ or *Toxoplasma gondii*¹²⁴. Our cooperation partners in the group of Katja Becker at the university Gießen have been working on the two targets glucose-6-phosphate dehydrogenase (G6PD) and 6-phosphogluconat dehydrogenase (PGD) for many years. They developed several inhibitors against the G6PD from *Plasmodium*, one of them is SBI-750. I tested the potency of SBI-750 in killing of *L. major* in our laboratory. For this, I used dsRed-expressing parasites to determine the loss of fluorescence through cell death in addition to performing an annexin staining as assay for apoptosis induction (Figure 38).

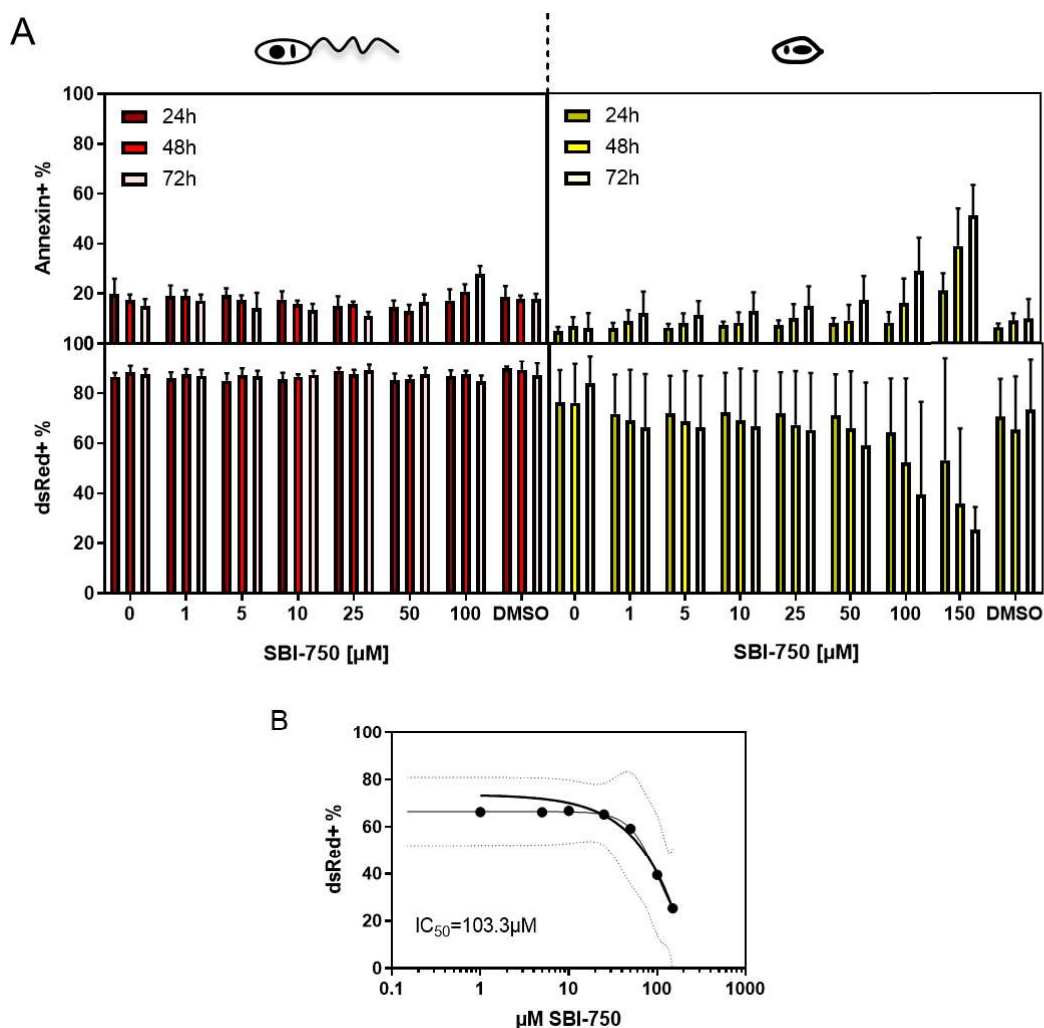


Figure 38. The G6PD inhibitor SBI-750 is more potent in *L. major* amastigotes than in promastigotes. Logarithmic phase promastigotes (left) or axenic amastigotes (right), which are expressing dsRed, were incubated with different concentrations

of SBI-750 for the indicated times (A). After incubation, the parasites were subjected to annexin assay and checked for dsRed decrease and annexin binding via flow cytometry. Data shows mean + SD and was collected in three independent experiments. dsRed+ values from 72 h of SBI-750 with amastigotes incubation was used to calculate an inhibitory concentration (IC) of the inhibitor (B). Sigmoidal fit was used in GraphPad Prism to determine the IC₅₀.

Promastigotes showed an increase from $17.69 \pm 2.24\%$ for the DMSO treated control to $27.75 \pm 3.29\%$ annexin+ parasites at a concentration of $100 \mu\text{M}$ SBI-750 after 72 h incubation. At the same concentration and incubation time there was no effect on dsRed+ parasites. On the other hand, amastigotes showed a more pronounced increase in the percentage of annexin+ parasites, from $12.5 \pm 7.01\%$ for DMSO control to $29.00 \pm 13.34\%$ for $100 \mu\text{M}$ SBI-750 and up to $51.05 \pm 12.37\%$ for $150 \mu\text{M}$ SBI-750 in case of 72 h incubation. A huge effect could also be seen for dsRed+ after 72 h of incubation with SBI-750. The DMSO control showed dsRed+ of $80.53 \pm 17.54\%$ down to $25.35 \pm 9.31\%$ for $150 \mu\text{M}$ SBI-750. The data from amastigotes and 72 h incubation were used to determine the IC₅₀ value for SBI-750 of $103.3 \pm 4.12 \mu\text{M}$ (**Figure 38B**). However, it was not possible to determine an IC₅₀ for the effectivity on promastigotes, since there were no decreasing dsRed+ values. These results indicate that G6PD plays a more important role for amastigotes than for promastigotes.

As my results showed the possibility to kill *L. major* amastigotes through a G6PD inhibitor, I started target validation of G6PD and PGD in *L. major* as well as in *L. donovani*, aiming to show the necessity of G6PD and/or PGD for parasite survival. To this end, I did several attempts to generate KOs of both genes but failed in achieving KO parasites. The lethality of this approach was a first hint that the genes might be essential. Next, I electroporated the parasites, introducing a G6PD expressing pIR plasmid (pIRLmG6PD), to carry out a rescued G6PD KO. On a genomic level, this could be proven by PCR products for G6PD CDS (1+2), G6PD UTR (1+3) and the existence of the nourseothricin resistance gene (SAT) in the parasites, which was localized on the plasmid (**Figure 39A**). With the additional copy of G6PD in *L. major*, it was possible to replace the both genomic alleles of G6PD by a blasticidin (3+B) and a puromycin (3+P) resistance gene. I tracked the growth behavior of the facilitated LmG6PD KO for eight passages always at day 7 in the blood agar plate and also cultured the parasites without antibiotics to accelerate the loss of the pIRLmG6PD plasmid. After eight passages with or without antibiotics, the growth of the parasites was stable and comparable to each other (**Figure 39B**). Moreover, I forced the transformation of promastigotes to amastigotes and back to promastigotes and then checked again for the loss of the pIRLmG6PD. The plasmid was still present in the parasites even after amastigote transformation. Thus, the loss of the only, plasmid-located, gene copy encoding for the G6PD seemed to be unfavorable for the parasites, pointing to its essential role for parasite survival.

For *L. donovani*, it was possible to create a partial G6PD KO. I tried to electroporate the parasites with a G6PD-encoding plasmid to be able to perform a full KO. The qRT-PCR showed approximately 40% of G6PD mRNA expression in the partial KO compared to the LdCas9/T7 control. Upon transfection with the pIRLdG6PD plasmid, the expression could be elevated to approximately 60% (**Figure 39C**).

RESULTS

However, even with G6PD expression from the plasmid, I were not able to obtain a full KO of the genomic G6PD genes in *L. donovani*.

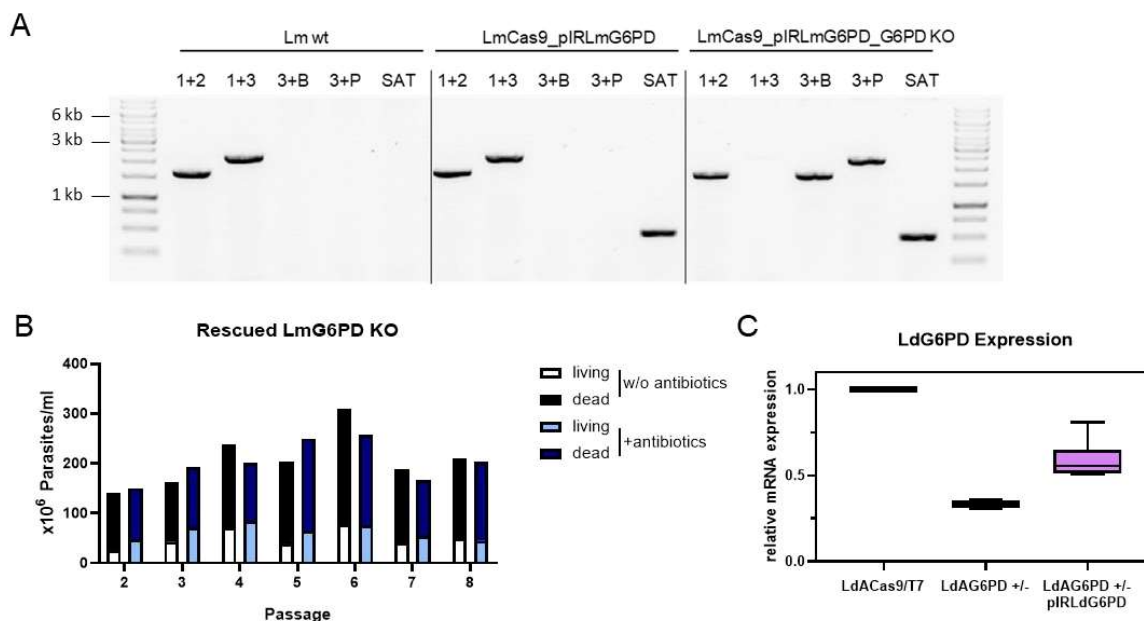


Figure 39. The KO of LmG6PD was only possible with an additional copy of G6PD in *L. major*. Agarose gel electrophoresis shows the PCR products of the G6PD CDS (1+2), G6PD UTR (1+3), blasticidin resistance gene within the G6PD CDS (3+B), puromycin resistance gene within the G6PD CDS (3+P) and nourseothricin resistance gene (SAT). PCRs were performed with the gDNA of *L. major* wild type (Lm wt), *L. major* Cas9/T7 carrying the pIRLmG6PD plasmid (LmCas9_pIRLmG6PD) and with the facilitated G6PD KO (LmCas9_pIR_LmG6PD_G6PD KO). GeneRuler 1 kb DNA Ladder (Thermo Fisher) was used. (A) The growth of the facilitated LmG6PD KO was tracked each week at day seven of culture for eight weeks using a Neubauer Chamber. Parasites were cultured with and without antibiotics (B). For *L. donovani* only a partial KO (LdAG6PD +/-) and a partial facilitated KO (LdAG6PD +/- pIRLdG6PD) could be achieved and the mRNA of the different clones were assessed by qRT-PCR. Kmp11 was used as housekeeping gene (C).

I further validated the role of PGD as drug target in *L. major* and *L. donovani*. Here, the KO of the gene was lethal as well. The transfection of a PGD expression plasmid in *L. major* was not successful, but I was able to insert another copy of the PGD within the 18S locus (**Figure 40A**). Using these parasites, I could generate a PGD genomic KO (**Figure 40A**). The PGD mRNA expression in these parasites was approximately 17x higher than in the control (**Figure 40B**). The growth of this overexpressing PGD parasite strain (PGD OE) was reduced compared to the Cas9/T7 control especially in the first days (2-6) (for example day 3: $155.00 \times 10^6 \pm 40.97 \times 10^6$ living Cas9/T7 parasites/ml compared to $34.65 \times 10^6 \pm 5.25 \times 10^6$ living PGD OE parasites/ml) (**Figure 40C**). This PGD overexpressing parasite strain was further used to delete the original genomic alleles of PGD by replacing them with a blasticidin resistance gene. The growth of these parasites was strongly reduced, they barely reached the concentration of 100×10^6 /ml. By qRT-PCR, it could be shown that the PGD mRNA expression in the rescued PGD KO parasites was about 10x higher than in the Cas9/T7 control parasites.

For *L. donovani* I was not able to generate the complete PGD KO. However, I could successfully insert a PGD expressing plasmid (pIRLmPGD) into these parasites upon which the rescued KO could be achieved. The growth of these parasites varied a lot with no clear trend with or without antibiotics.

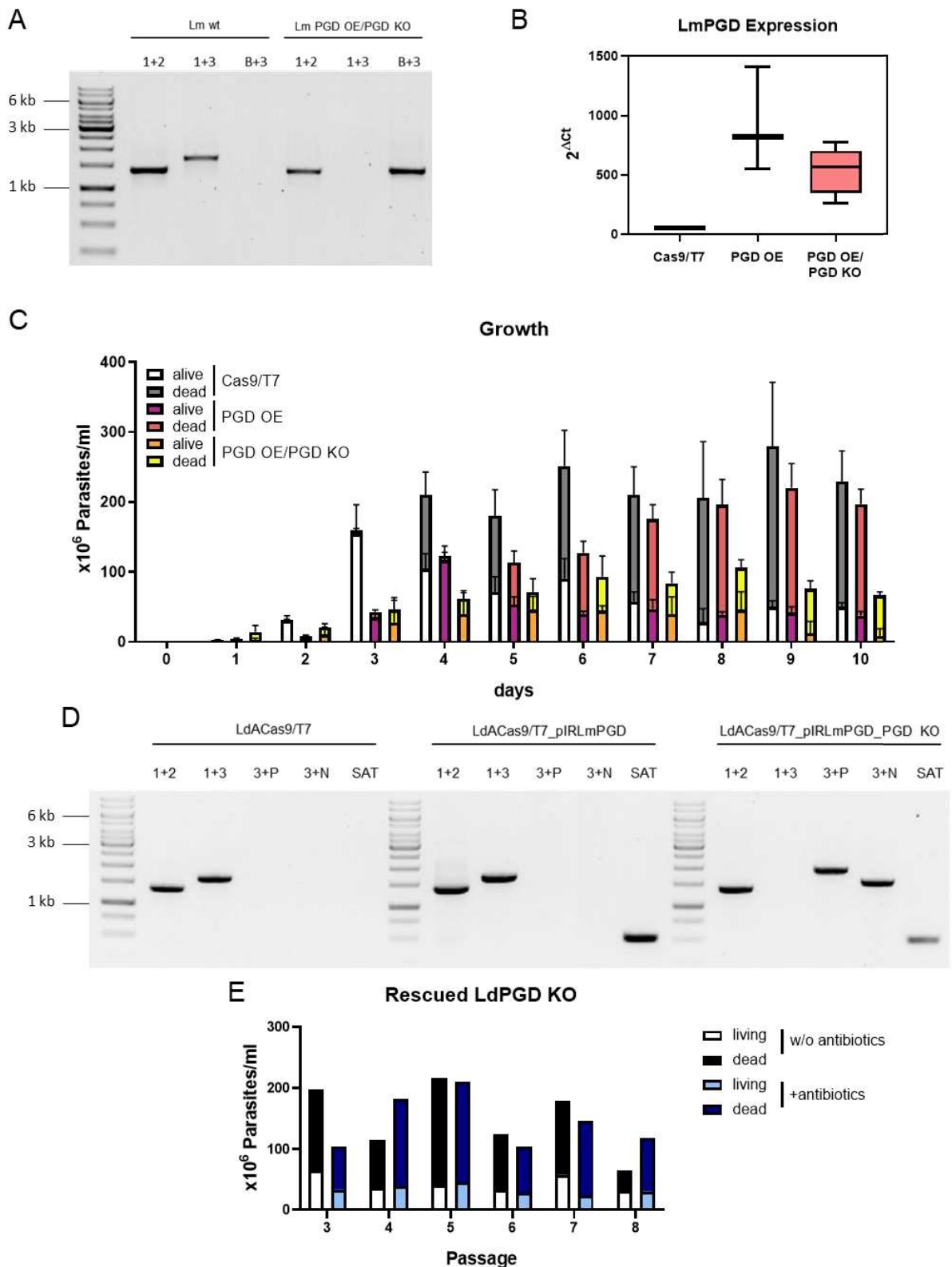


Figure 40. The KO of PGD was only achieved upon expression of an ectopic gene copy for *L. major* and *L. donovani*. Agarose gel electrophoresis shows the PCR products of the PGD CDS (1+2), PGD UTR (1+3) and blasticidin resistance gene within the PGD CDS (3+B). PCRs were performed using the gDNA of *L. major* wild type (Lm wt) and facilitated LmPGD KO (LmPGD OE/PGD KO) (A). By qRT-PCR the mRNA expression of PGD in different parasites were determined. The housekeeping gene *kmp11* was used (B). Parasites were seeded at a density of 1×10^6 /ml to a blood agar plate and counted daily using a Neubauer Chamber. Data is representative for at least 3 independent experiments and shown as mean + SD (C). Agarose gel electrophoresis shows the PCR products of the PGD CDS (1+2), PGD UTR (1+3), puromycin resistance gene within the PGD CDS (3+P), neomycin resistance gene within the PGD CDS (3+N) and nourseothricin resistance gene (SAT). PCRs were performed with the gDNA of *L. donovani* Cas9/T7, *L. donovani* Cas9/T7 carrying the pIRLmPGD plasmid and with the facilitated PGD KO

RESULTS

(LdACas9_pIR_LmPGD_PGD KO) (D). The growth of the fascilitated LdAPGD KO was tracked each week at day seven of culture for eight weeks using a Neubauer Chamber. Parasites were cultured with and without antibiotics (E). GeneRuler 1 kb DNA Ladder (Thermo Fisher) was used for agarose gel electrophoresis.

Together, these results indicate that G6PD and PGD might be important for parasite survival of *L. major* and *L. donovani*. However, to prove the vital necessity of the proteins, it is necessary to observe the direct effect of the KOs on the parasites. One possibility to do that is the induction of a KO through an inducible KO system. Hence, I established such a system in *L. major* and *L. donovani*.

3.6. Establishment of an Inducible Knock-out System

There are different systems already published that enable the induction of a gene deletion upon a specific stimulus. One of those systems is the dimerizable Cre recombinase (DiCre) system¹²⁵. Here, the parasites carry two inactive subunits of Cre that are fused to rapamycin-binding entities, and the GOI is flanked with LoxP sites. Through the addition of rapamycin, the Cre subunits dimerizes, which results in the activation of the enzyme. The active DiCre leads to the excision of the LoxP-flanked GOI. A further development of the system was the usage of CRISPR/Cas9 to integrate the loxP sites up- and downstream of the GOI¹²⁶.

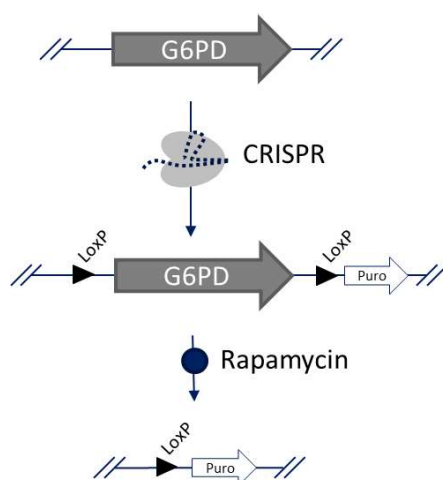


Figure 41. Usage of CRISPR/Cas9 in a DiCre inducible knock-out (KO) system. Through CRISPR/Cas9 the gene of interest (GOI), in this case G6PD, is flanked by LoxP sites and a puromycin resistance gene is introduced for selection. Adding rapamycin induce the KO and GOI becomes excised.

The published system requires cloning for each GOI and further PCR of the GOI carrying plasmid. The product then contains a loxP site, the GOI, another loxP site and a resistance gene. Without the GOI the construct is approximately 2 kb and can, especially in the case of multi-copy genes, increase up to 10 kb, depending on the size of the GOI. For such a large fragment it gets difficult to obtain a good PCR product amount¹²⁷. Therefore, I started to optimize this system. For the 5' loxP site, I cloned

a new plasmid using the pTNeo plasmid from Tom Beneke⁵² as backbone. I added a loxP site and an eGFP gene to the plasmid (pTNeoloxPeGFP) (**Figure 42A**). A plasmid (pGL2314) containing a loxP site, a puromycin resistance gene and a mCherry fluorescent protein gene was kindly provided by Jaziel Damasceno. This plasmid was further used for incorporation of the 3' loxP site in our setting (**Figure 42B**). Through PCR, a homologous region (HR) of 20 bp was added to each sequence that was planned to be integrated into the parasites.

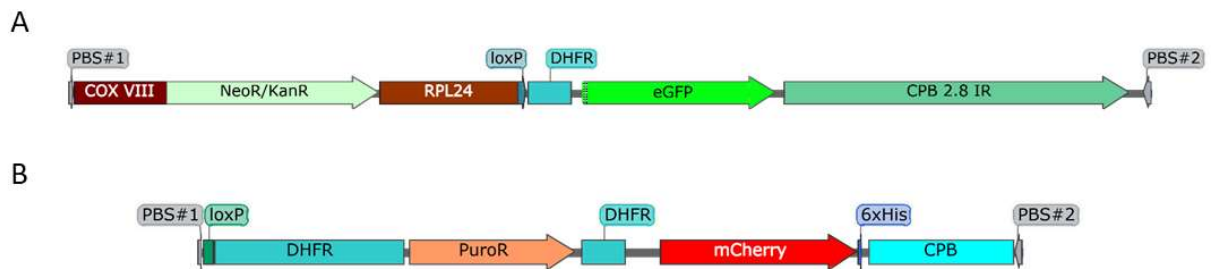


Figure 42. DNA sequences that are introduced into the untranslated regions (UTR) of a gene of interest in preparation of an inducible knock-out (KO). The plasmid pTNeoloxPeGFP containing of the UTRs COX VIII, RPL24, DHFR and CPB 2.8 IR for enhanced gene expression, neomycin resistance (NeoR) for antibiotic selection, loxP site for KO induction and eGFP for fluorescence detection are integrated in the 5' region of a GOI. (A). The pGL2314 containing loxP site for KO induction, the UTRs of DHFR and CPB for enhanced gene expression, puromycin resistance (PuroR) for antibiotic selection and mCherry for fluorescence detection are integrated in the 3' region of a GOI. (B) The DNA sequence is amplified through PCR with the primer binding sites (PBS) #1 for forward and #2 for reverse.

Electroporation of the parasites with sgRNA and together with the HR sequences led to the CRISPR/Cas9-induced integration of the sequences 5' and 3' of the GOI. The addition of rapamycin was used to initiate the excision of the GOI as well as the eGFP gene, while the mCherry gene is still present (**Figure 43**).

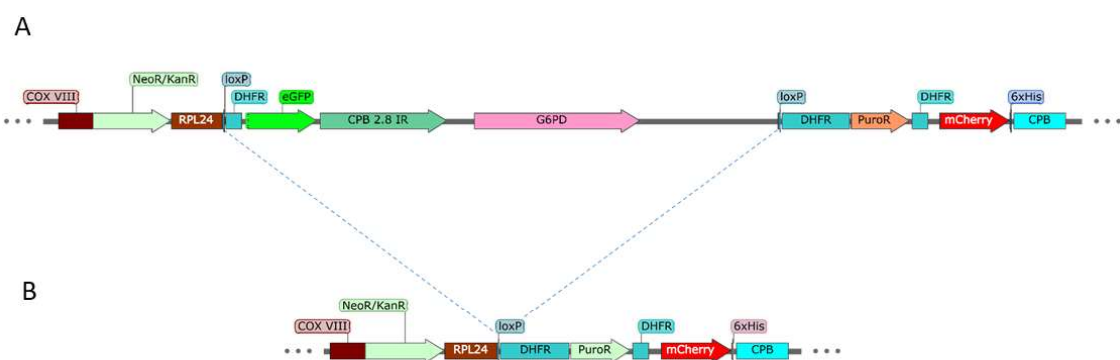


Figure 43. Genomic locus of G6PD during an inducible knock-out (KO). DNA sequences amplified from the plasmids pTNeoloxPeGFP and pGL2314 were introduced up- and downstream of the gene of interest G6PD, resulting in 5' and 3' integration of loxP site, resistance gene and fluorescent protein gene. (A) Genomic locus after rapamycin-induced deletion of the sequences between the loxP sites. (B)

RESULTS

I applied this system to perform the inducible KO of G6PD or PGD in *L. donovani* Cas9/T7/DiCre. After insertion of the required genomic modifications, 100 nM rapamycin was added to the parasites and the eGFP and mCherry fluorescence was tracked via flow cytometry for seven days (**Figure 44**).

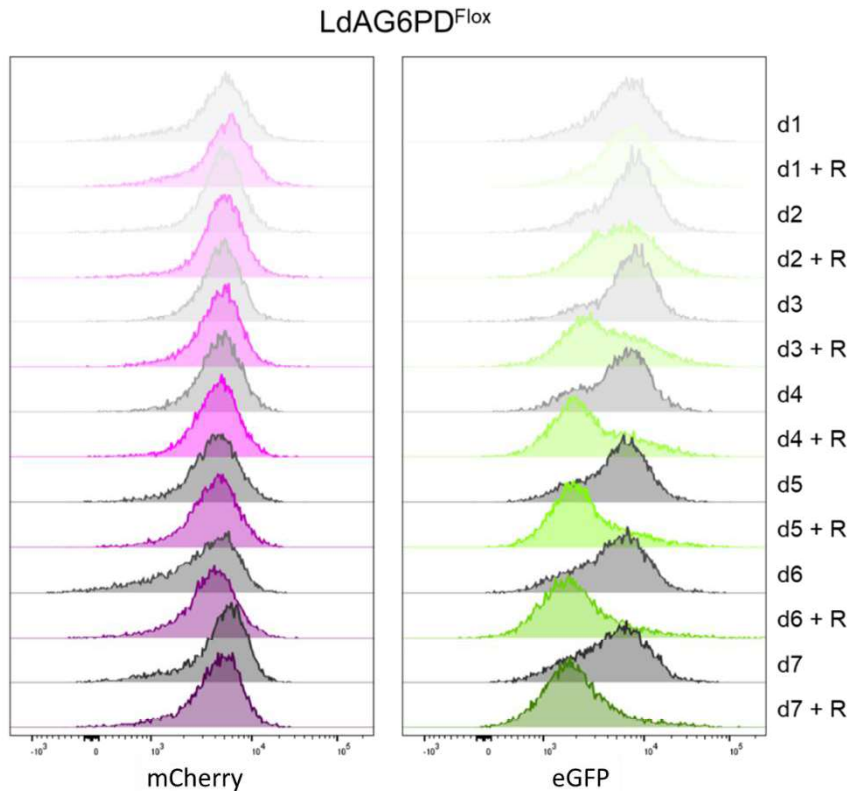


Figure 44. Through the addition of rapamycin, the eGFP signal decays while the mCherry signal remains. *LdAG6PD^{Flox}* were treated with 100 nM rapamycin and assessed by flow cytometry for eGFP and mCherry expression. Left shows the mCherry signal intensity and right the eGFP signal intensity. Figure was created in FlowJo and shows the representative image of three independent experiments.

The mCherry signal remained almost stable for seven days, as well as the eGFP signal of untreated *LdAG6PD^{Flox}*. Through rapamycin, the eGFP signal decreased after six days to approximately 35% (**Figure 45C**). The parasites were also counted by flow cytometry and a slightly reduced growth behavior could be seen after the induction of G6PD KO. The G6PD gDNA of the induced G6PD KO was decreased by about 90% compared to the untreated *G6PD^{Flox}* parasite's gDNA after seven days (**Figure 45B**).

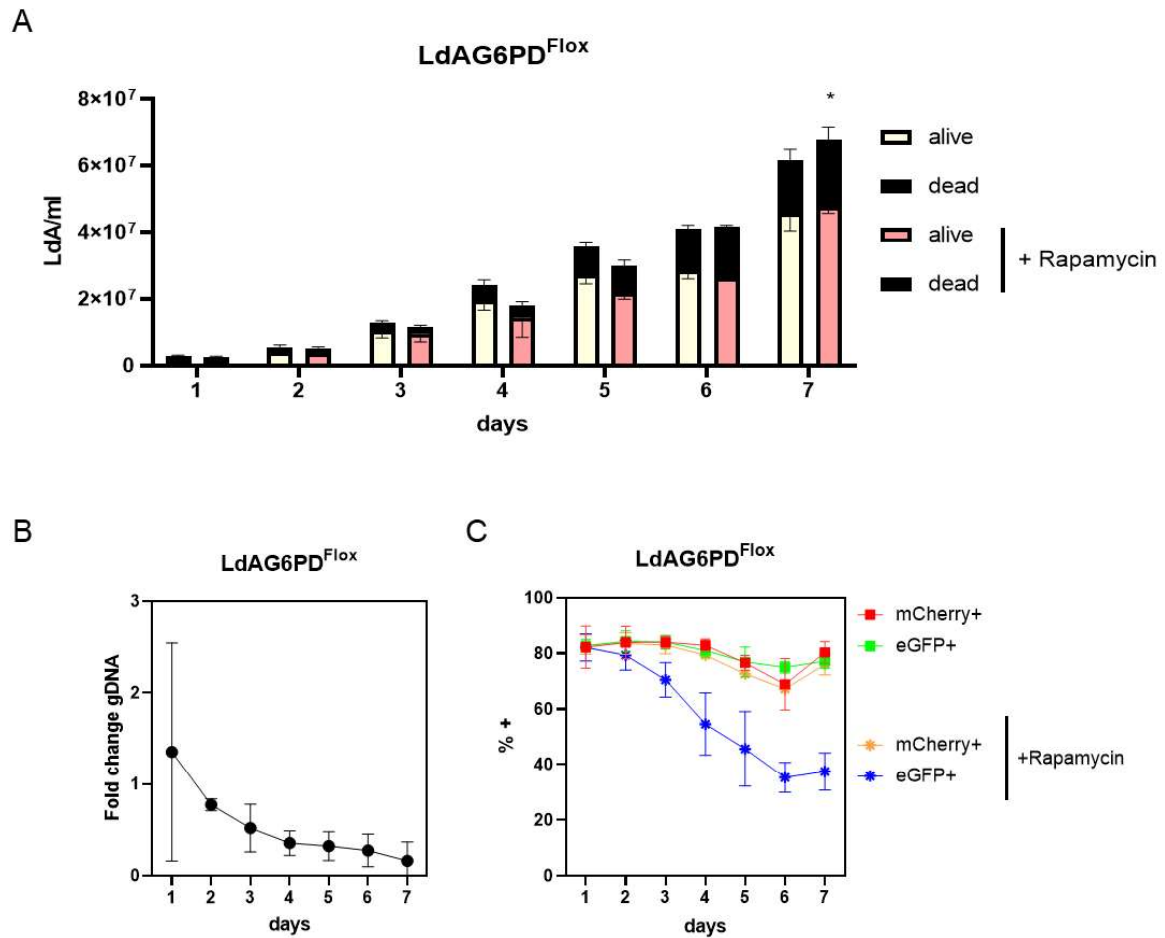


Figure 45. The KO induction of G6PD in *L. donovani* led to slightly lower growth. *L. donovani* G6PD^{Flox} was treated with 100 nM rapamycin and tracked for seven days via flow cytometry for growth (A) and eGFP and mCherry expression (C). Genomic DNA from untreated and rapamycin-treated *Leishmania* was extracted daily and investigated via qRT-PCR for G6PD. As housekeeping gene *kmp11* was used and data was normalized to untreated *Leishmania* (B). Data is representative for at least 3 independent experiments and shown as mean \pm SD. Significance was assessed by Two-Way ANOVA with * $p < 0.05$.

The same experiment was also performed for the inducible PGD KO in *L. donovani*. Here, the parasites only contained one allele that was floxed and one wildtype allele. This could probably be compensated by the parasites on a genomic level by gene duplication (**Figure 46B**). Other than for the G6PD KO, no decrease in eGFP+ cells could be observed. However, the parasites showed reduced growth behavior and a decrease in mCherry+ parasites (**Figure 46**).

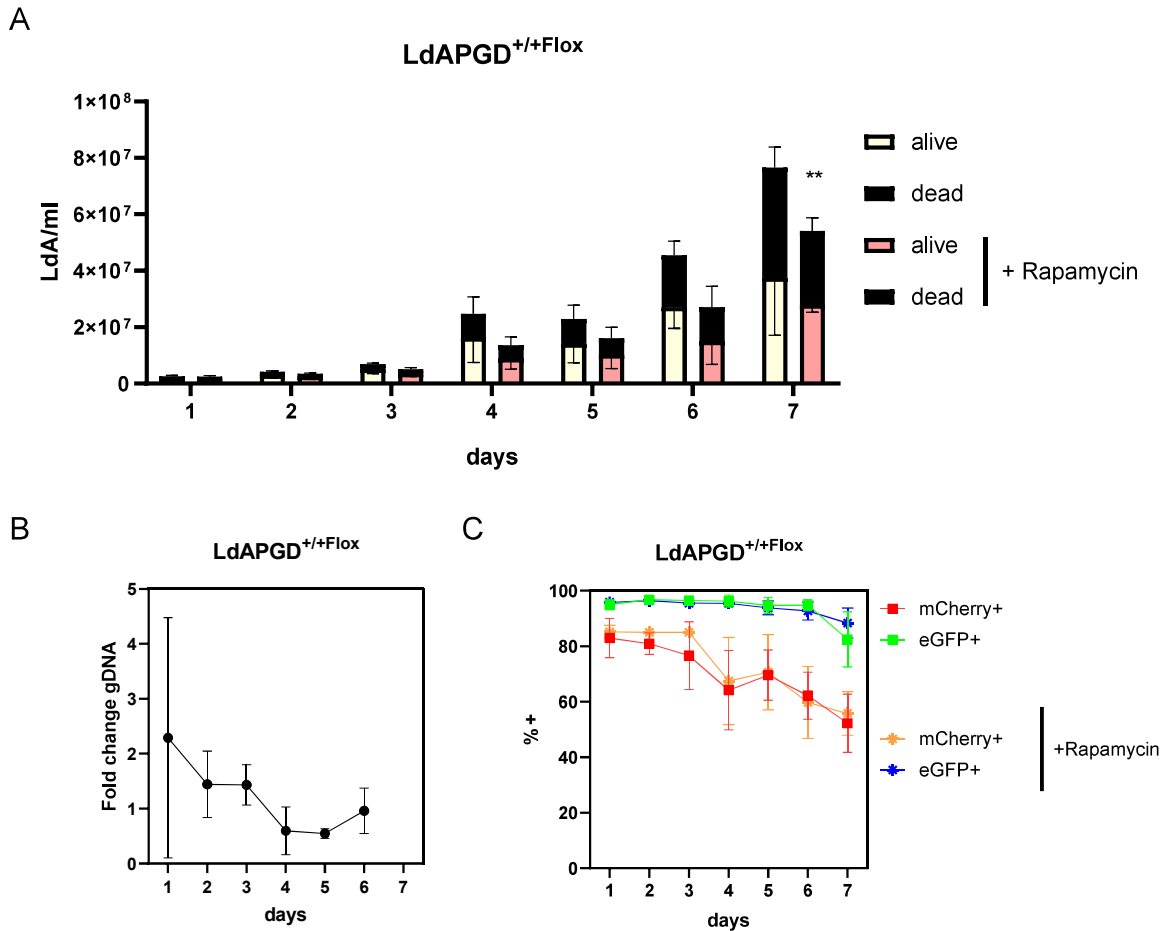


Figure 46. The KO induction of PGD in *L. donovani* led to slightly lower growth behavior. *L. donovani* PGD^{+/+Floxed} was treated with 100 nM rapamycin and tracked for seven days via flow cytometry for growth (A), gDNA (B) and eGFP and mCherry expression (C). Genomic DNA from untreated and rapamycin treated *Leishmania* was extracted daily and investigated via qRT-PCR for PGD. As housekeeping gene *kmp11* was used. Data is representative for at least 3 independent experiments and shown as mean ± SD. Significance was assessed by Two-Way ANOVA with **p < 0.01.

In summary, the KO of G6PD in *L. donovani* only showed a slight increase in dead parasites in late growth phases. However, the inducible partial KO of PGD had a greater influence on the growth behavior compared to G6PD. In essence, the results show that PGD could be a promising drug target in *Leishmania* although it has to be confirmed in a full inducible KO.

3.7. The Role of Leishmania PS on the Human Immune System

Leishmania parasites that expose annexin-binding lipids are crucial for disease development in mice due to the anti-inflammatory properties of apoptotic promastigotes. Since PS is known for its immune-silencing mechanism it was suggested that it is the main mediator of the anti-inflammatory response⁴¹. However, the existence of PS on *Leishmania* is still a matter of debate⁴³. To clarify this, I sent fixed samples of *L. major* promastigotes from logarithmic (d3) and late stationary (d10) growth phase to our collaborators from the group of Bernhard Spengler at the Universität Gießen, to perform a mass spectrometry analysis on the parasite's lipid composition.

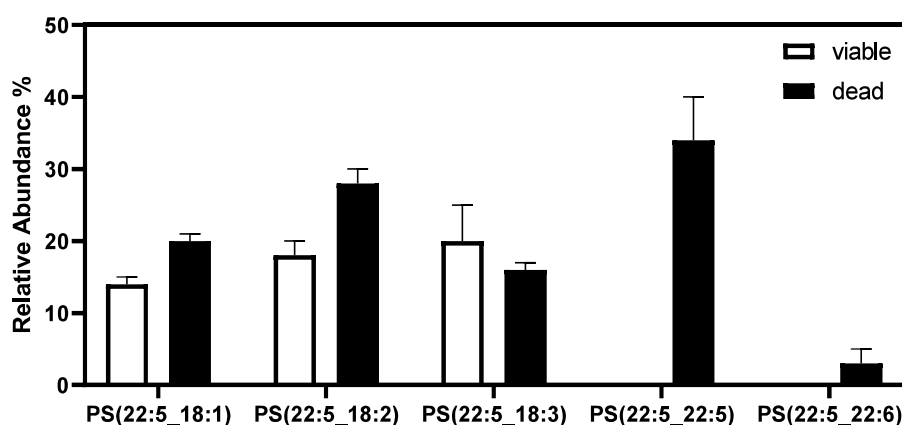


Figure 47. Dead *L. major* promastigotes harbor distinct species of phosphatidylserine (PS). Mass spectrometry analysis of logarithmic (viable) and late stationary (dead) growth phase parasites was performed by the group of Bernhard Spengler (Gießen). Chemically distinct PS species (with the specification of length and level of unsaturation) are shown with their relative abundance in the parasites as mean +SD of three measurements.

Mass spectrometry analysis found phosphatidylserine in viable as well as in dead promastigotes (**Figure 47**). Moreover, the analysis also showed that chemically distinct PS species can only be found in dead parasites. These species were mainly those with very long fatty acid chains and with a high number of double bonds.

I have the hypothesis that the distinct PS species on dead parasites play a major role in the immune-silencing mechanism that is found for apoptotic *L. major*⁴¹. To address this question, I chose a natural way to deliver lipids to host cells. For that purpose, I used the model of exosomes. I isolated exosomes from d3 and d10 promastigotes, harboring the distinct species of PS. By nanoparticle tracking analysis I could quantify and qualify the isolated exosomes (**Figure 48**).

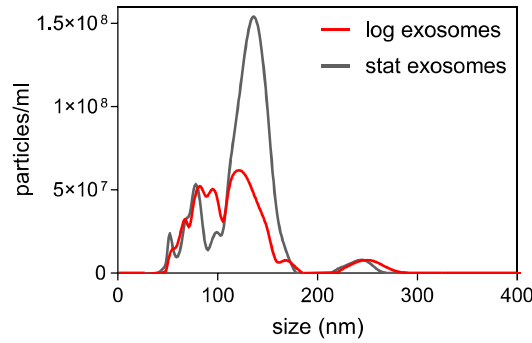


Figure 48. Logarithmic growth phase promastigotes secrete a larger number of exosomes with a size of 150 nm compared to promastigotes in the stationary phase. Exosomes from logarithmic (log) and stationary (stat) growth phase were isolated from *L. major* promastigotes through differential centrifugation. The harvested exosomes were further investigated by nanoparticle tracking analysis, where the concentration and sizes of the particles was measured.

After a basic characterization of the size and concentration of the exosomes, I tested the effect of them on human primary macrophages. I primed the macrophages with IFN γ or LPS+IFN γ for 18 h, added different concentrations of exosomes from the logarithmic or stationary growth phase for 24 h and then checked for TNF α and IL-10 secretion (**Figure 49**).

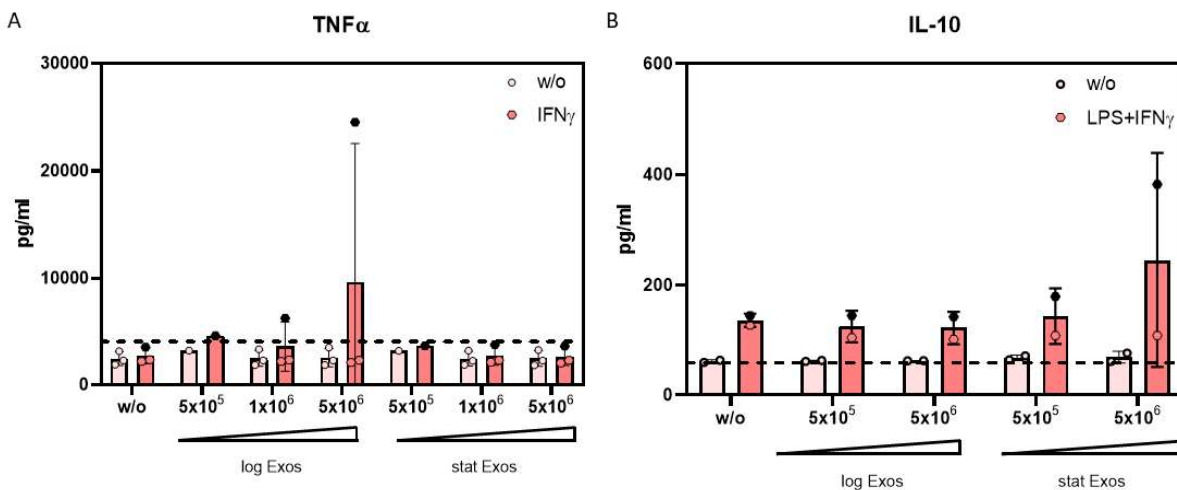


Figure 49. Exosomes from logarithmic and stationary growth phase are able to induce distinct cytokines. Type 1 human primary macrophages were primed with IFN γ or LPS+IFN γ for 18 h and further treated with exosomes from logarithmic (log Exos) and stationary (stat Exos) growth phase promastigotes. After 24 h, supernatants were collected and subjected to TNF α (A) or IL-10 (B) ELISA. Experiment was performed with 2-3 donors; each donor represents one spot (susceptible donor in black). Bars show the mean \pm SD.

One of the three donors that was tested for TNF α secretion showed an increasing amount of TNF α when incubated with increasing concentrations of logarithmic phase exosomes. Only primed macrophages were able to secrete TNF α . None of the donors showed a reaction to stationary phase exosomes. For IL-10 secretion, a similar pattern but vice versa could be seen. Here, only stationary phase exosomes were able to induce increasing amounts of IL-10 secretion for increasing amounts of exosomes in one of two donors. Logarithmic phase exosomes led not to a response and unprimed macrophages neither.

These experiments might be first hints that logarithmic phase exosomes can stimulate pro-inflammatory cytokine secretion, while stationary phase exosomes stimulate the anti-inflammatory cytokines in certain susceptible donors.

4. Discussion

It was my hypothesis that *Leishmania* induce and proceed apoptosis through a specialized mechanism, and I was seeking to elucidate this mechanism by the identification and characterization of proteins involved in its regulation. To perform KOs of potential candidates that are involved in apoptosis, I employed a CRISPR/Cas9 system and established it in our laboratory (**Figure 50-1**). I was also able to induce drug-mediated parasite apoptosis in order to identify potential promastigote- and amastigote-specific target proteins by label-free quantitative mass spectrometry and performed the gene specific analysis by Partek®Flow® (**Figure 50-2**). Overall, we identified 4416 proteins in promastigotes and 2376 proteins in amastigotes. I could determine proteome specific effects of the compounds miltefosine, harmonine and compound 1o on the different parasite life stage. Altogether, I found 15 up- and 189 downregulated proteins in promastigotes, and 455 up- and 633 downregulated proteins in amastigotes in the respective apoptosis-inducing conditions. I employed the CRISPR/Cas9 system to achieve gene KOs of first candidates that I identified to be potentially involved in apoptosis, either through the mass spectrometry screening or by literature research. For the majority of the respective genes only a partial KO could be achieved, meaning that one allele of a gene was still intact. A functional characterization of these gene KOs regarding their potential to undergo apoptosis, as well as the infectivity, followed (**Figure 50-3**). I could find specific alterations in apoptosis characteristics for some KOs (e.g., reduced DNA fragmentation in the EndoG KO), however for most of the KOs there was no clear phenotype observable. Therefore, I was not able to confirm yet potential drug or vaccine targets in this step. I investigated the potential of the two proteins G6PD and PGD as possible drug targets. Since I could not achieve a full KO of the respective genes, I employed rescued KOs of the candidates, which was not successful for G6PD from *L. donovani*. To overcome difficulties with performing KOs, I successfully established an inducible KO system that is coupled to the expression of fluorescent proteins (**Figure 50-4**). Further, I was able to show the existence of specific phosphatidylserine species on apoptotic *Leishmania*, which could help to understand the immune-silencing mechanism of apoptotic parasites (**Figure 50-5**). Although I could not identify a certain pathway that regulates the progression of apoptosis in *Leishmania*, I identified various potential protein candidates that might be involved in this mechanism that can be confirmed in further studies. The obtained results will be discussed in more detail in the following part.

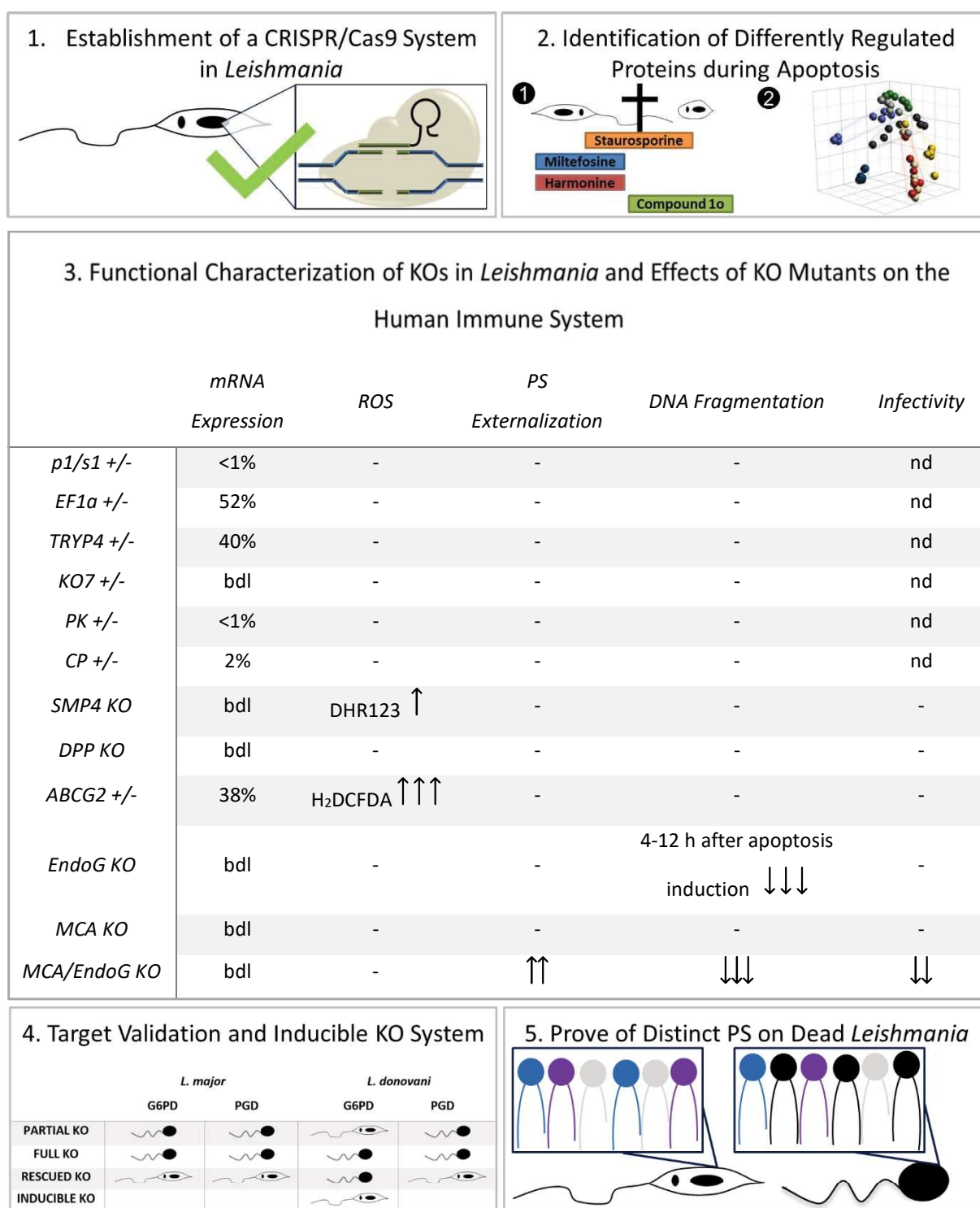


Figure 50. Major achievements that were done during this thesis. In a first step, a CRISPR/Cas9 system was established in *Leishmania*. Secondly, through the use of distinct compounds apoptosis was induced in the parasite and differently regulated proteins were identified by label-free quantitative mass spectrometry. Hereby, it could be shown that staurosporine is inducing apoptosis in promastigotes and amastigotes, while miltefosine and harmonine are only active in promastigotes and compound 1o is more active in amastigotes. In a next step, several KO strains of proteins from step 2 or from literature were created and functionally characterized. For partial KOs there was still mRNA expression detectable in the most cases, while for full KOs the mRNA expression was below the detection limit (bdl). Apoptosis characteristics ROS, phosphatidylserine (PS) externalization and DNA fragmentation were investigated as well as the infectivity of the KO strains in human monocyte derived macrophages and marked with an arrow if there was a significant difference compared to the control. In a next step, the target validation of G6PD and PGD from *L. major* and *L. donovani* was performed using genetic approaches. Thereby an inducible KO system was established in order to achieve full KOs for unobtainable candidates. During the last part of the thesis, we investigated the role of PS on apoptotic parasites in more detail. Here, we could show the occurrence of distinct long, rigid PS species on apoptotic *Leishmania*.

4.1. Induction of Apoptosis in *Leishmania*

Although showing all the typical characteristics of apoptosis, none of the human apoptosis-regulating proteins are found in *Leishmania*. To investigate apoptosis mechanisms in more detail, I made use of the two already established drugs staurosporine and miltefosine or the new compounds harmonine and compound 1o. I examined if these compounds are suitable to induce apoptosis in promastigotes or amastigotes for the further investigation of apoptosis in *Leishmania*.

Staurosporine is an unspecific ATP-competitive kinase inhibitor, which shows IC₅₀s in the nanomolar range for a lot of human protein kinases: PKA, PKC, cdc2 or EGFR¹⁰⁶. For *Leishmania*, it was shown that staurosporine derivatives inhibit the cyclin-dependent kinase CRK3 from *L. mexicana*¹¹⁶. This inhibition consequently leads to death of the parasite, since CRK3 was shown to be an essential gene¹¹⁷. However, staurosporine might also inhibit various other protein kinases and the cell death-inducible property is more a mixture of the unspecific potential. I determined the inhibitory concentration (IC) for the inhibition of the metabolic activity and the effective concentration (EC) for the induction of annexin binding for all compounds. Compared to human HeLa cells, which show a staurosporin EC₅₀ of 73 nM after 18 h¹¹⁹, the concentration for *Leishmania* of 9.05 µM is clearly higher. The easier inhibition of human cells can be explained with higher number of protein kinases, of which there are almost 500 in humans, while *L. major* only possess 179 predicted protein kinases¹²⁰. What also needs to be considered, is that the EC₅₀ value is highly dependent on assay conditions like cell number and can therefore differ very much to literature¹²¹. Because of the very low EC₅₀ for human cells, staurosporine is for sure no appropriate drug against *Leishmania*, however to study the apoptosis mechanism in the parasites it is very suitable. Apoptosis induction in the parasites was not only limited to promastigotes, but could also be seen in amastigotes (**Figure 11A**). Staurosporine treatment led to annexin binding and subG1+ cells in promastigotes and amastigotes, showing that early (PS externalization) and late (DNA fragmentation) apoptosis characteristics could be induced in both stages.

For miltefosine, the values from my experiments (EC₅₀ of 3.968 µM after 24h), are comparable to the EC₅₀s that are published in literature. These range for cell density experiments from 1.31 µM in *L. donovani* to 23.88 µM in *L. braziliensis*¹²⁸. On the other hand, the IC₅₀s in human cells are in the range of 66.7 µM, which enables the use of miltefosine as drug against leishmaniasis¹²⁹. Interestingly, my experiments also showed that miltefosine does not induce apoptosis in axenic amastigotes from *L. major* (**Figure 11B**). This is conflicting to all data found in published articles so far^{130,131}. However, the inhibiting effect of miltefosine in *L. major* amastigotes is always shown in intracellular or freshly isolated amastigotes from mice and therefore not directly comparable to our axenic amastigote model. Since miltefosine shows very good efficacy against *L. major in vivo*¹³², this might be a restriction of the *L. major* axenic amastigote model. One reason for the resistance of our axenic amastigotes could be found in alterations of the miltefosine transporter or the pyridoxal kinase. Both were mutated in

L. major strains with a miltefosine tolerance¹³³. Therefore, the sequencing of these genes in our axenic amastigotes should be done to find out if these alterations are the cause that miltefosine is not inducing apoptosis in the amastigotes in my experiments.

The compound harmonine is extracted out of the harlequin ladybird beetle *Harmonia axyridis* and shows growth inhibition against *Mycobacterium tuberculosis*, *Plasmodium falciparum* and *Schistosoma mansoni*^{116,134}. The mode of action is not fully solved but the inhibition of acetylcholinesterase was observed and therefore proposed as potential target of harmonine¹³⁴. The published IC₅₀ value for promastigotes (14.2 μM) matches quite well to my determined IC₅₀ (10.98 μM). However, in my experiments harmonine was not able to induce apoptosis in amastigotes (**Figure 11C**), contrary to literature where they found an IC₅₀ of 2.4 μM in intracellular amastigotes¹³⁰. I was able to link this to the finding that harmonine is not active at the low pH of 5.5 of our amastigote medium (**Figure 12**). The fact that harmonine was shown to be able to kill intracellular amastigotes questions the biological relevance of our *in vitro* finding. I would expect that a compound, which is not active in a low pH, is also not able to kill intracellular amastigotes *in vivo*, since they reside in the phagolysosomal compartment with a low pH. It was shown for several antibiotics that they are not antimicrobial active in phagolysosomes due to the low pH¹³⁵. Nevertheless, harmonine was shown to be active in intracellular amastigotes¹³⁰, so it might be possible that the compound is inactivated slowly in the acidic medium.

Compound 1o was found in a big screen of arylmethylamino steroids against *P. falciparum* and then showed also effects against *P. berghei* and *S. mansoni*¹¹⁷. In my experiments, the compound showed an inhibition of the metabolic activity of *L. major* promastigotes with an IC₅₀ of 9.052 μM. However, the compound could not diminish the metabolic activity of the parasites as the other drugs. For annexin binding in *L. major* promastigotes, I could not determine an EC₅₀, since even the very high concentrations of the compound were not able to induce annexin binding (**Figure 9**). On the other hand, for amastigotes I could observe an increased annexin binding and DNA fragmentation. This observation is notably, because this is the first compound, which shows a higher activity in *L. major* amastigotes than in promastigotes. Some minor modifications in the molecule of compound 1o could lead to a very effective drug against leishmaniasis. For example, it would be possible that one of the other tested arylmethylamino steroids from the screen in *Plasmodium* has a higher efficacy in *Leishmania* promastigotes and amastigotes.

I can conclude that staurosporine is an apoptosis inducer in both stages of *L. major*. Miltefosine and harmonine are suitable for the apoptosis induction in *L. major* promastigotes, but not in amastigotes. The compound 1o is more potent for apoptosis induction in *L. major* amastigotes than in promastigotes.

4.2. Search for New Proteins Involved in *Leishmania* Apoptosis

I was aiming to find new proteins involved in *Leishmania* apoptosis by the use of label-free quantitative mass spectrometry. This screen gave us first insights about the working mechanisms of the compounds. We found 4416 proteins in promastigotes and 2376 proteins in amastigotes. The proteome of *L. major* is comprised of 8038 predicted proteins¹²⁰, that means we could identify 55% of the whole proteome. In 2010, a former mass spectrometry analysis of the *L. major* proteome in our group could only identify 707 proteins¹²¹, meaning that the sensitivity of the MS approach increased massively.

As described above, compound 1o did not induce apoptosis in promastigotes. Therefore, I expected only a small number of proteins to be differently regulated and I would not expect to find apoptosis-involved proteins during the regulated proteins. Indeed, I found only 12 proteins to be regulated, which is less than for example miltefosine after the same incubation time. One of downregulated proteins was trypanothione peroxidase, which plays a pivotal role during combating ROS¹³⁶. This might indicate a new role of compound 1o in the response to ROS.

I included as well parasites from the stationary growth phase. Different studies suggest that parasites that enter the stationary phase rather undergo autophagy than apoptosis^{137,138}. However, even if the pathways are different, autophagic pressure over a prolonged time period will also result in death for the stationary phase promastigotes. Therefore, both pathways result in the end to the same characteristics like PS externalization, shrinkage and DNA fragmentation^{41,137}. I found uniquely regulated proteins in this condition. These proteins were: TPK_B1_binding domain-containing protein, Histone H2B, Putative RNA binding protein and nascent polypeptide associated complex subunit-like protein, copy 2 (see **Supp. Table 8**). Since all these proteins are downregulated during stationary growth phase, I can assume that the proteins are important for cell survival or homeostasis. The majority of the proteins are involved in transcription or translation. As already mentioned, for transcription processes in *Leishmania*, there are no promoter elements found, and therefore the expression of proteins, which subsequently ensure the transcription of distinct proteins might be an important mechanism. In *Trypanosoma brucei* it could be shown that histone H2B localizes to active genes and thus is important for unique functions in the cell¹³⁹.

The harmonine 6 h treated samples showed a complete overlap with those from staurosporine 6 h treatment in the PCA plot. This could also be seen when taking the upregulated proteins into account: except for one ribosomal protein, the upregulated proteins in both conditions matched completely. One of the proteins was only upregulated in harmonine and staurosporine (6 h) treatment: uncharacterized protein Q4Q1X2. By gene ontology, the protein was suggested to be part of the axoneme. A BLAST showed similarity with the coiled-coil domain-containing protein 189 (Ccdc189) from mouse and human, which is important for the motility of sperm¹⁴⁰. Therefore, this protein might

be also important for an increased motility of *L. major* and it is a response to the drug-induced stress in the early time point for the parasite. Although there were 25 proteins more downregulated for staurosporine-treated samples than for harmonine-treated samples, 26 proteins were downregulated in both conditions. Two of the downregulated proteins that could fulfill a similar role as initiator caspases are: calpain protease-like protein (Q4Q3Y6) and carboxypeptidase (Q4QDZ7) and shall be investigated in more detail in future studies.

After 3 h, the treatment of promastigotes with miltefosine led to two clusters as seen in the PCA plot: four of the seven replicates built a cluster close to the untreated samples and the cluster of the remaining three replicates could be found closer to the miltefosine 24 h treatment. Because of the short incubation time of 3 h, rapid and massive changes in the proteome composition occur and it might be possible that not all samples were in the exact same stage of apoptosis progression. Samples after the 24 h treatment showed a cluster that was most different when comparing to the untreated cluster in the PCA plot. This can also be seen in the volcano plot. Here, 102 proteins were significantly differently regulated. Many of them are connected with nuclease function (E9AC13, Q4Q1W1, Q4Q883, Q4QAA2, Q4QG27), which I would expect in this late timepoint of apoptosis.

Since mass spectrometry is a well-described method of target identification, I was expecting to get some new insights into the targets of harmonine and compound 1o. It could be shown that the potential targets of specific drugs are differently regulated after the treatment. In most cases the inhibited targets are upregulated in cells, but rarely also downregulated¹⁴¹. However, I could not determine a clear target.

For further apoptosis investigations, I focused on the proteins, which were commonly regulated in all promastigote apoptosis-inducing conditions of the early time points (miltefosine 3 h, harmonine 6 h, staurosporine 6 h). These were the upregulated proteins p1/s1 nuclease (Q4Q7F3), polyubiquitin (Q4Q165), 40S ribosomal protein S2 (Q4QDL5) and elongation factor 1-alpha (Q4QE18).

In 2004, the p1/s1 nuclease from *L. major* has been published to be a nuclease that exhibits similarity to other class 1 nucleases and that might be important for the salvage pathway of the parasites. *Leishmania* are not able to synthesize purines *de novo* and therefore they require a way to recycle ribonucleotides. The p1/s1 nuclease was suggested because of similarity to other class one nucleases and thus, was further cloned and characterized. It was suggested that the nuclease is stage-specific, because it could not be detected in promastigotes, but only in amastigotes¹⁴². Analogous findings could be obtained for P4 nuclease from *L. infantum*, which shows high similarity (64% identity) to the p1/s1 nuclease from *L. major*¹⁴³. Another published nuclease that exhibits the same length and similar DNA sequence is LdNuc⁵ from *L. donovani*. This nuclease was shown to be secreted from the parasite and is also proposed to be involved in the salvage pathway¹⁴⁴. However, the proof that these nucleases are involved in the salvage pathway are still missing. In our MS screen, we could not detect

p1/s1 nuclease in the untreated promastigotes, however it was present in high amounts in treated promastigotes as well as in all amastigote preparations. Because of its expression in amastigotes, p1/s1 nuclease was previously suggested to be essential for parasite survival and to be an attractive drug target¹⁴². As it is a very interesting candidate for further analysis, I sought to generate a KO of the corresponding gene. However, as it presents as a multi-copy gene, the KO is very difficult. I was able to knock out one copy of the gene, which resulted in highly reduced expression of the p1/s1 nuclease mRNA (**Figure 28A**). The KO had no effect on apoptosis characteristics like ROS, annexin binding and DNA fragmentation (**Figure 28B-F**). Only the DHR123-detectable ROS species were slightly reduced, which has to be confirmed in further experiments. Nevertheless, the mRNA expression should be checked after treatment with compounds, since the basal protein expression in promastigotes was not detectable via mass spectrometry. These results indicate that p1/s1 nuclease is not involved in *Leishmania* apoptosis, but nonetheless could be an essential protein. Further investigations of drug target validation should also include the alterations in the salvage pathway.

It was shown that ubiquitin is crucial for *Leishmania* life cycle progression and infection process^{145,146}. Further, because of the missing transcriptional regulation, ubiquitin becomes crucial in the post-translational control for degradation of certain proteins but also for recruiting proteins to sites of DNA damage¹⁴⁵. This makes it clear why in my experiments ubiquitin is upregulated in all conditions of drug treatment, where a response in the way of a changing protein expression is needed. My attempts to knock out the gene encoding polyubiquitin were lethal for the parasites. Knockdowns in human cells led to the inhibition of cell proliferation and the induction of apoptosis¹⁴⁷. Therefore, ubiquitin is an essential protein, however because of high sequence similarities between *Leishmania* and humans, it is not an appropriate drug target. Nevertheless, it might still be involved in apoptosis mechanisms and is worth further investigations.

Another protein, which was upregulated in all conditions of apoptosis induction, is 40S ribosomal protein S2 (RPS2). It belongs to the universal ribosomal protein uS5 family and is part of the small ribosomal subunit. The homolog in *E. coli*, ribosomal protein S5, is important for the assembly and the function of the 30S ribosomal subunit. Further, it was shown that mutations in the gene lead to increased translational error frequencies^{148,149}. RPS2 has a human homolog with 42% sequence identity. This protein has a conserved Arg/Gly-rich region, which can be methylated by PRMT3¹⁵⁰ or citrullinated by PAD4, which is suggested as a regulation mechanism¹⁵¹. For other proteins it has been shown that they are citrullinated after DNA damage¹⁵². Further, PRMT3 stabilizes RPS2 and prevents the protein from ubiquitin-mediated degradation¹⁵⁰. In *L. major*, I was not able to achieve a KO of RPS2. Since it was shown that the protein is very important for translation, especially for error-free translation, it might be the case that RPS2 is an essential protein. A similar regulation mechanism as in human cells could also be possible for *Leishmania*, since the parasite harbors also a homolog of PAD4.

Therefore, an upregulation during cell stress like DNA damage could lead to a citrullination and activation of RPS2, which in turn favors the translation of certain types of proteins. It was shown in *Schistosoma* that specific ribosomal proteins correspond to the translation of specific classes of proteins¹⁵³ and it is also suspected that this could be a general mechanism¹⁵⁴. This could link the upregulation of RPS2 to the apoptosis pathway in *Leishmania*.

In our mass spectrometry screen, elongation factor 1 alpha (EF1A) was significantly upregulated in all early and late conditions of apoptosis induction (**Figure 27**). The observed upregulation becomes clear when looking at the diverse and essential functions in the parasite. EF1A is important for the aminoacyl-tRNA binding to the ribosome during biosynthesis in a GTP-dependent manner¹⁵⁵. Apart from its role in translation, EF1A is also a well-known virulence factor. In infected cells, EF1A can be exported from the phagosome to the host cell's cytoplasm and is there able to bind and activate Src homology 2 domain containing tyrosine phosphatase-1 (SHP-1). It blocks the induction of nitric oxide synthase expression and therefore the *Leishmania* protein can deactivate the macrophage host cell. In the human host cell, there is a EF1A homolog with 75.1% sequence identity. However, it is not able to bind SHP-1¹⁵⁶. In contrary to *Leishmania* EF1A, mammalian EF1A harbors a hairpin loop, which is 12 amino acids long and offers structural differences that could serve the basis for drug target development¹⁵⁷. Further, it could be shown that there is a direct correlation of the EF1A expression level and the apoptosis rate in mice fibroblasts¹⁵⁸. It was suggested that EF1A is also associated with the cell shrinkage during apoptosis since it was shown that it is a microtubule-associated protein¹⁰⁶. It is not only important for apoptosis, but also for ubiquitination: there is an essential involvement of EF1A in the degradation of N-terminal acetylated proteins through the 26S proteasom¹⁵⁹. A further function is the role as activator by binding to the IFNG promoter together with TXK and PARP1 for the transcription of IFN γ in Th1 cells¹⁶⁰. *Leishmania* EF1A can also be delivered in exosomes to macrophages¹⁶¹. In a similar way, it was also tested as vaccine: recombinant EF1A was formulated in liposomes and determined in the effectiveness as vaccine in mice. It showed that there was a massive increase in T cells that protected the mice against visceral leishmaniasis¹⁶². In my experiments, it was not possible to achieve a full KO of EF1A. It was already earlier suggested that EF1A is essential for parasite survival^{157,163}. I could create a partial KO, in which the mRNA level decreased by 50% (**Figure 28**). Despite the involvement in the regulation of apoptosis I could not detect any influence of the partial KO on the apoptosis characteristics ROS, PS externalization and DNA fragmentation. It should be confirmed that the mRNA level is still decreased after apoptosis induction through the different drugs. EF1A is a housekeeping gene since it makes between 3 – 10% of the soluble proteins in the most cells¹⁶⁴. Therefore, even a 50% decreased level might be enough to initiate the apoptosis characteristics. To prove the role of EF1A in *Leishmania* apoptosis, an overexpression and but also an

inducible KO of the gene should be performed, to see the inevitable effects of a KO in the parasite, without the problems of lethality through the KO.

I propose distinct roles of the upregulated proteins EF1a, RPS2 and ubiquitin in the apoptosis pathway of *Leishmania* (Figure 51). Hereby, EF1a might have several roles, ranging from a direct effect on transcription and translation of pro-apoptotic proteins to the ubiquitin-dependent degradation of anti-apoptotic proteins. RPS2 probably has mainly an effect on translation of pro-apoptotic proteins and ubiquitin in the degradation of anti-apoptotic but also cell survival proteins.

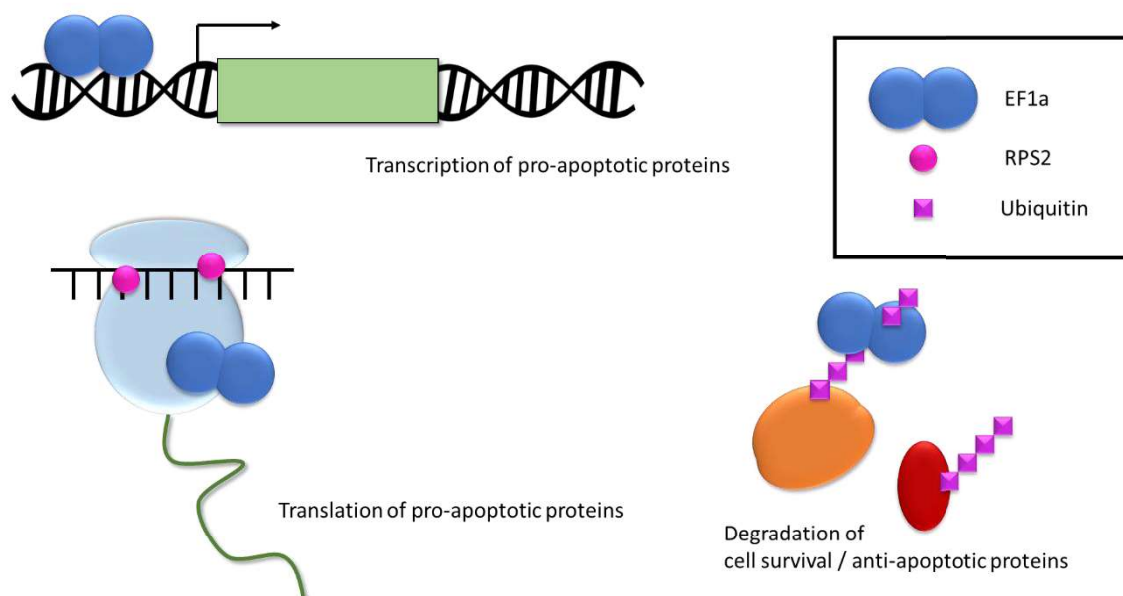


Figure 51. Proposed involvement of elongation factor 1 alpha (EF1a), ribosomal protein S2 (RPS2) and ubiquitin in *Leishmania* apoptosis. Possible mechanisms in the involvement of EF1a, RPS2 and ubiquitin can be found in the transcription and translation of pro-apoptotic proteins and in the degradation of cell survival or anti-apoptotic proteins.

Since I was not able to achieve KOs of the genes from newly identified proteins to investigate apoptosis mechanisms in *Leishmania* in more detail, I was seeking to characterize further proteins that we identified in the MS screen. These were: tryparedoxin peroxidase, an uncharacterized protein, pyruvate kinase and carboxypeptidase. Further, I chose two hits that were detected in an earlier MS screen during the MD thesis by Jochen Steinacker¹²¹: SMP4 and DPP. I decided to further include three more hits, which were published to be involved in apoptosis: ABCG2, EndoG, MCA.

Leishmania parasites must be able to deal with a broad range of reactive oxygen species to survive the ROS burst in the host macrophage. Although, enzymes like catalase and glutathione peroxidase are missing in the parasite, they harbor very special antioxidant compounds like trypanothione¹⁶⁵. The peroxidoxins were shown to be essential for the oxidative defense and survival of *Trypanosoma brucei*¹⁶⁶. Tryparedoxin peroxidase acts together with trypanothione/trypanothione reductase in the reduction of H_2O_2 ¹⁶⁵. A full KO of tryparedoxin peroxidase was not possible in my experiments; however, I could achieve a partial KO with approximately 40% of the TRYP4 mRNA expression compared to the Cas9/T7 control. Although I would expect highly enhanced ROS levels through the KO

of TRYP4, I could not see any effect in this regard. Especially the H₂O₂ level, which can be detected through staining with H₂DCFDA, should be highly increased through the KO. A higher H₂O₂ level would also lead to the increase of other ROS and in turn to lipid peroxidation, cytochrome c release and the externalization of phosphatidylserine^{167,168}. Theoretically, in case of a reduced ability to deal with ROS, I would also expect a lower ability to deal with the ROS burst during infection in the host macrophage. However, I could not observe any change in apoptosis characteristics. Since the protein was only detected in untreated promastigotes in our MS screen, it might have an effect on the ROS homeostasis, and during drug treatment, other tryparedoxin peroxidases take over the function of antioxidant defense. This can also be seen in the genomic organization of the TRYP4 gene, which is arranged as tandem array. It is possible that some of the genes are important for the basal reduction of ROS and the others are important for the response to various stimuli and the upregulation of certain ones can replace the others. Since a full KO of all tryparedoxin peroxidases is not possible¹³⁶, further investigations are difficult but could focus more on the distinct functions of the different tryparedoxin peroxidases.

A protein, which was upregulated during apoptosis is an uncharacterized protein: Q4QDQ9. According to the uniprot database, this protein is a transmembrane protein that could be important for malate, succinate, sulfate transport¹⁶⁹. Because of similarity to the *Trypanosoma brucei* homolog, it could be a mitochondrial carrier protein¹⁷⁰ and therefore crucial for the import of nutrition to the mitochondrion. A full KO of the gene was not possible in my experiments, however the partial KO led to a diminished gene-specific mRNA expression in the untreated promastigotes. Regarding the apoptosis characteristics ROS production, PS externalization and DNA fragmentation, there was no alterations observable upon the KO. In future, it should also be tested, if the expression is still diminished under apoptosis-induced conditions or if an upregulation occurs. Since the protein might also transport thiosulfate, it is possible that it delivers antioxidants to combat oxidative stress¹⁷¹. However, evidence for this is missing, since the KO experiments did not lead to any phenotype.

Pyruvate kinase was downregulated after miltefosine treatment in promastigotes. The protein catalyzes the last step of the glycolysis pathway. In human cells, it was shown that under oxidative stress, one isoform of the pyruvate kinase translocates to the mitochondrion and phosphorylates the anti-apoptotic protein Bcl2. This phosphorylation prevents Bcl2 from degradation. Therefore, the pyruvate kinase directly inhibits apoptosis in human cells¹⁷². The downregulation of pyruvate kinase in our MS screen would be in line with this observation in human cells. The published results describe pyruvate kinase as anti-apoptotic protein which is in accordance with its downregulation during apoptosis. The involvement of pyruvate kinase in apoptosis was shown in human cells and not in *Leishmania*, which is lacking a Bcl2 homolog¹⁷³. Another, more likely possibility is that the whole metabolism, including glycolysis, is downregulated. In my experiments, I could see a diminished mRNA

expression in the partial KO of pyruvate kinase, but no effect on apoptosis characteristics. This suggests that the downregulation of metabolism is the more pronounced effect than the regulation of apoptosis. However, here some metabolic assays could be performed to see if another protein is able to take over the function of the pyruvate kinase.

The putative carboxypeptidase Q4Q0D4 was more abundant in the early timepoints of apoptosis induction in promastigotes than in the untreated control. It is a metallo-carboxypeptidase. This type of protein was shown to be involved in apoptosis¹⁷⁴. I was able to create a partial KO of the gene, which almost completely impeded the mRNA expression. I could not observe any change of apoptosis characteristics in the partial KO. It is quite likely that the protein is important for other processes than apoptosis and this might be the reason why I did not observe a phenotype. It is also possible that the parasite is able to upregulate the protein expression from the remaining allele during apoptosis in such an amount that the partial KO is compensated.

In an earlier MS screen performed by Jochen Steinacker, in which promastigotes and amastigotes had been treated with staurosporine, he found Q5SDH3 to be upregulated in staurosporine-treated promastigotes¹²¹. When the screen was done in 2010, the protein was assigned as calpain-like peptidase. However, most of the protein name assignments are done based on similarity to other known proteins and therefore wrongly assigned proteins names are also found in the database. More recently, Q5SDH3, was assigned as putative small myristoylated protein 4 (SMP4). Myristoylations are co- or post-translational modifications, which allow a weak protein-protein or protein-lipid interaction. The modifications play an important role in signal transduction cascades¹⁷⁵. The enzyme, which conveys the myristoylation is called N-myristoyltransferase (NMT) and is discussed as a drug target for several years¹⁷⁶. The SMP1 from *L. major* is localized at the flagellum and a deletion leads to uncoordinated movements¹⁷⁷. For SMP4, it could be shown that the protein localizes to the cell body membrane but the function still remains elusive¹⁷⁸. In our recent MS screen, SMP4 was not significantly regulated in staurosporine-treated promastigotes, but it was downregulated in harmonine-treated promastigotes. A *Leishmania* strain with a full KO of the gene was kindly provided by the group of Antonio Jiménez Ruiz. I investigated the apoptosis characteristics in this KO but could not observe any phenotype. This is why I assume that SMP4 does not have a function in apoptosis.

A further hit from the screen by Jochen Steinacker was dipeptidyl peptidase 3, which was downregulated in staurosporine-treated amastigotes¹²¹. Because of its function as peptidase, it was suggested that DPP could play a similar role as caspases during cell death. DPP belongs to the family of M49 peptidases with homologs in bacteria, plants and animals¹⁷⁹⁻¹⁸¹. It is postulated that DPP plays a role in protein turnover. When proteins are ubiquitinated for proteasomal degradation, the resulting peptides are released into the cytosol, where peptidases degrade them further into amino acids. These amino acids are then used for protein synthesis or energy generation¹⁸². Together with other

peptidases, DPP degrades these peptides. Because of inhibitors of DPP, which reduced the viability of *L. braziliensis*, it was suggested as drug target¹⁸³. In our recent MS screen, DPP was not significantly up- or downregulated in any treated amastigote condition, however it was downregulated in 24 h miltefosine-treated promastigotes and in the stationary growth phase compared to untreated logarithmic phase promastigotes. The downregulation of the protein at the late timepoints after apoptosis induction would be in line with the published function, since the protein turnover for following protein synthesis is not an essential pathway anymore in the dying parasites. I was able to generate a full KO of DPP, which did not show any deficiencies in growth, thereby devaluing the role of DPP as drug target. The apoptosis characteristics were not changed after the KO of DPP. Consequently, the protein function is likely to be restored by other proteins.

I also aimed to investigate the role of published apoptosis-involved proteins to further characterize them as possible drug target or vaccine approach. The ATP-binding cassette protein subfamily G, member 2 (ABCG2) is a protein, which is published to be involved in the externalization of phosphatidylserine¹²². In the publication, the authors showed the impact of an inactive protein mutant, which led to reduced annexin binding. The lower annexin binding was accompanied by a decreased infection rate *in vitro* and the inability for disease development in mice when infected with the mutant *Leishmania*. Three years later, the same group published the role of ABCG2 in drug resistance. Here, overexpression experiments of the protein led to increased efflux of antimony¹⁸⁴. I attempted a KO of the ABCG2 gene, however were only able to achieve a partial KO with approximately 50% of the original gene expression. It was surprising that the published inactive version led to normally growing parasites but a full KO could not be achieved in my experiments. Because of the published involvement of the protein in PS externalization, I checked for annexin binding and infectivity but could not see a lower PS externalization or lower infection rate of macrophages with the partial KO, compared to the control. This was surprising, since I would at least expect a small change when the ABCG2 expression is decreased by 50%. Due to their ability to respond to environmental or genetic changes very quickly by adjusting the number of gene copies, it might be possible that *Leishmania* can compensate for a partial ABCG2 knockout by rapidly duplicating the gene locus within few rounds of replication. However, I cannot be certain about this, because I did not check if the gDNA amount was enhanced after apoptosis induction. I also determined the other apoptosis characteristics and there was a significant effect on the abundance of certain reactive oxygen species in the parasites. The most pronounced effect was the increase of H₂DCFDA-detectable ROS in logarithmic phase promastigotes, which are H₂O₂, HO· and ROO·. This means, the partial ABCG2 KO parasites are not able anymore to cope with oxidative stress. An unspecific efflux of antimony but also ROS could be a possible mechanism for the ABCG2 protein. Contradictory, the other apoptosis characteristics were not changed for the partial KO, which is unexpected since these characteristics are all connected. My data

indicates that ABCG2 has a similar role as the ABC-type efflux pump MacAB from *Salmonella*, which protects the bacterium from hydrogen peroxide by an active efflux¹⁸⁵. This has to be confirmed in further approaches with for example an inducible KO, since here the direct effect of a KO could be observed without the problems of lethality.

4.3. Endonuclease G and Metacaspase

Since EndoG and MCA are the proteins, which are discussed the most regarding *Leishmania* cell death¹³⁷, I investigated the role of these proteins in more detail. While a gene KO of MCA has previously been published⁹⁰, there was no KO available for EndoG, so far. Hence, I generated both KO strains in our lab. To also evaluate the interplay between both proteins or a reinforcing effect, I created a double KO of MCA and EndoG.

The KO of EndoG led to a slower growth compared to the Cas9/T7 parasites, which highlights the role of EndoG in cell survival. The pro-survival role of EndoG was previously reported by Rico et al⁹⁷. This observation is in line with the reduced viability of *L. infantum* promastigotes and amastigotes upon inhibition of EndoG^{97,103}. The EndoG KO showed a slightly higher mitochondrial membrane potential, which was not significant. In the published partial EndoG KO in *L. infantum* this effect was more pronounced⁹⁷. A higher mitochondrial membrane potential can be associated with higher energy capacity and a higher synthesis of ATP¹⁸⁶. However, in my experiment the opposite was true. I observed a lower metabolic activity in the EndoG KO. On the other side, the decreased metabolic activity is in line with the reduced growth behavior. Apart from the mitochondrial membrane potential, the ROS levels were also slightly increased, which was significant when pre-treated with ATA. Meaning that EndoG and other endonucleases potentially play a role in the defense against ROS. In human cells, it could recently be shown that ROS levels are enhanced in EndoG-deficient cells, especially observed for DHE staining, which is mainly detecting ROS within the mitochondrion¹⁸⁷. I could also show that mitochondrial ROS is enhanced in the EndoG KO parasites, but only in axenic amastigotes, not in promastigotes. For human EndoG it could previously be shown that the ROS levels within the mitochondrion lead to damage of the mtDNA and EndoG is involved in the clearance of mtDNA to initiate new replication of mtDNA¹⁸⁸. This is supported by the fact that an EndoG deficiency impairs the mtDNA replication¹⁸⁷. Therefore, EndoG might also have a pro-life role in the mitochondrion of *L. major*. ROS leads to lipid peroxidation, cytochrome c release and the externalization of phosphatidylserine¹⁶⁸. For the EndoG KO, there was no difference regarding PS externalization, but the lipid peroxidation probably also leads to the release of EndoG⁹⁸. Upon its release from the mitochondrion, EndoG locates to the nucleus, where it cleaves DNA⁹⁵. After apoptosis induction through miltefosine, the DNA fragmentation is significantly reduced for the EndoG KO compared to

the control. This was not dependent on inhibition of endonucleases. Since the DNA fragmentation is not decreased through the chemical endonuclease inhibitor ATA in the EndoG KO, it is unlikely that there are further endonucleases involved in DNA fragmentation at this point. However, since pre-incubation with the metacaspase inhibitor antipain could decrease DNA fragmentation in the EndoG KO to untreated values, and also the control parasites were reduced in DNA fragmentation, there are further antipain-inhibited proteins involved in the fragmentation of DNA. One of those proteins could be oligopeptidase B, which could be crystallized in complex with antipain¹⁸⁹. Also carboxypeptidase is a possible target, which is inhibited by antipain¹⁹⁰. Since EndoG is not inhibited by antipain, the difference between the Cas9/T7 and EndoG KO highlights the involvement of other proteins in DNA fragmentation.

This massive reduction of DNA fragmentation after 6 h could also be seen for other apoptosis inducers like staurosporine or hydrogen peroxide. This means EndoG is activated downstream of apoptosis inducers miltefosine, staurosporine and hydrogen peroxide. The effect of reduced DNA fragmentation was observable in case of miltefosine between 4 and 12 hours after treatment. Later, DNA fragmentation was still lower than in the control parasites, but not significant. Meaning other proteases/nucleases can compensate for EndoG at the later time points.

The infection rate of hMDMs was not changed for EndoG KO parasites, while proliferation of the parasites was slightly decreased in both type-1 and type-2 macrophages. This can be explained by the lower growth rate of the parasites. Previously, it could be shown that the overexpression of EndoG in *L. donovani* amastigotes leads to a reduced survival in hMDMs and that parasites are killed within 48 h⁹⁵. Therefore, the tight regulation of EndoG seems to be an important aspect for the survival of *Leishmania* within their mammalian host cell.

The KO of MCA did not change the growth of *L. major*, which could also be seen by Casanova et al⁹⁰, where wildtype showed the same growth rate as the MCA KO. The double KO of MCA and EndoG did not show the reduced growth observed for the EndoG KO, which could mean that MCA plays an indispensable role in the reduced growth behavior of the EndoG KO, probably through a cross-talk mechanism. MCA KO showed a lower mitochondrial membrane potential than control, which was significant after inhibition of endonucleases and metacaspases through ATA or antipain, respectively. MCA KO showed untreated such a low mitochondrial membrane potential as the control after apoptosis induction. This could indicate an important role in mitochondrial function, which is enhanced by ATA-inhibited and antipain-inhibited proteins, which could be in turn activators of MCA. The ROS levels were not changed for the MCA KO or for the MCA/EndoG KO. However, PS externalization and DNA fragmentation in the untreated parasites was significantly enhanced for the double KO, probably because of the dysregulation of the apoptosis machinery, since both KOs alone had no effect on PS externalization and DNA fragmentation in the untreated controls. When the parasites were pre-

treated with antipain, the DNA fragmentation was enhanced in the MCA and MCA/EndoG KO. This might indicate for a protective role of MCA on DNA fragmentation. After apoptosis induction, this effect could not be seen anymore. Therefore, a kind of housekeeping/homeostasis, as could be seen for EndoG, would be possible for MCA.

The rate of infected macrophages by MCA KO parasites was not changed compared to the control strain, however the MCA/EndoG KO led to a significant reduced infection rate of type 2 macrophages. M2 are anti-inflammatory macrophages, which are not able to deal with the infection in a proper way and show therefore higher infection rates as the inflammatory type 1 macrophages¹⁹¹. After four days, when the transformation of promastigotes to amastigotes took place¹⁹², the infection rate doubled for M1. Here, the parasites might have left the macrophages and infected further ones¹⁹³. The infection rate was significantly lower for the MCA/EndoG KO. However, the MCA/EndoG KO had an initially lower infection rate, which also doubled within the four days. Looking at the parasite burden using the geometric mean of eGFP, the MCA/EndoG KO parasites were not able to replicate as fast as the Cas9/T7 parasites, within both types of macrophages. Therefore, the small effects from both single KOs potentiated to a significant effect in the double KO.

My experiments showed that the function of both proteins MCA and EndoG are replaceable by other proteins and play only minor roles during *Leishmania* cell death. The DNA-fragmenting role of EndoG can be taken over by other proteins and for MCA I could not detect any significant involvement in apoptosis. However, there still seems to be a pro-life role of EndoG as well as for metacaspase when thinking of the growth behavior, infection of macrophages and parasite proliferation within the macrophages.

Through my experiments, I could show the roles of EndoG in DNA degradation and intracellular survival. For MCA I could also determine a role in the intracellular survival and I suspect a similar role for p1/s1 nuclease and EF1a. Although I could not proof the role of p1/s1 nuclease and EF1a experimentally in KO experiments, the upregulation in the MS screening and the reported functions in literature let us conclude that I can assign the proteins a function in intracellular survival. For ABCG2, I could show in our experiments a role in ROS defense. Because of differential regulation during cell death and the published findings, I suggest TRYP4 and Q4QDQ9 also to be involved in ROS defense. A further role of RPS2, EF1a and ubiquitin is proposed in apoptosis induction (**Figure 52**).

Taken together, I was able to identify several new proteins that are involved in apoptosis of *Leishmania*. Further, I could assign functions of new or already established proteins.

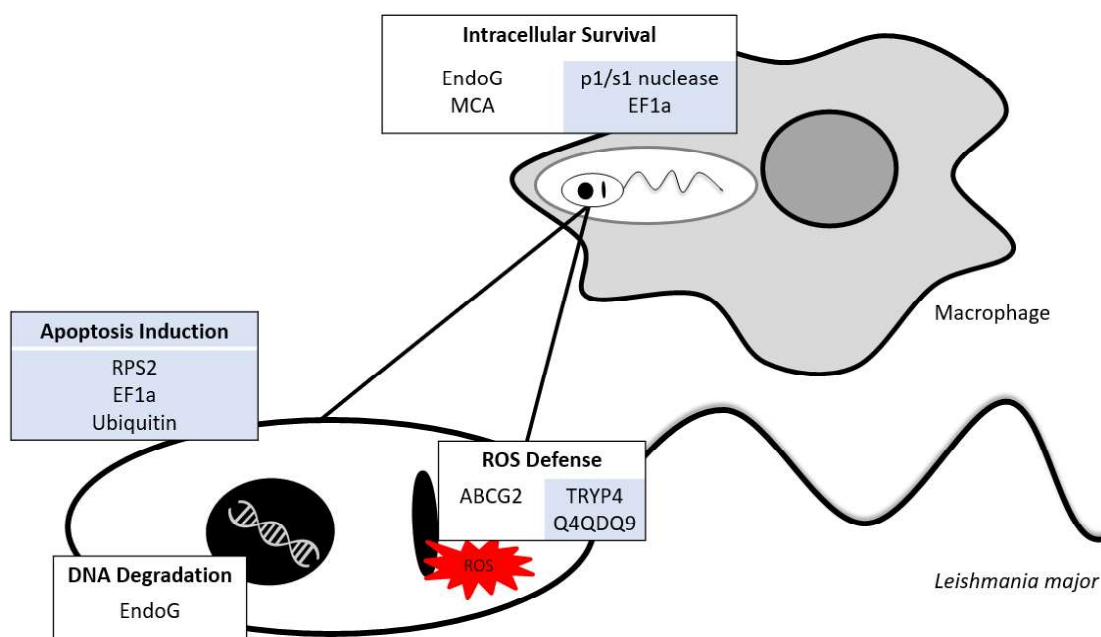


Figure 52. Proteins that are involved in the *Leishmania major* apoptosis pathway, which are proposed by us (blue) or experimentally proven by us (white). I could show the importance of EndoG in the DNA degradation and intracellular survival. MCA is important for the intracellular survival as well and ABCG2 in ROS defense. I suggest an essential role of RPS2, EF1a and ubiquitin in apoptosis induction and of TRYP4 and Q4QDQ9 in ROS defense. The role of p1/s1 nuclease and EF1a in intracellular survival is proposed.

4.4. Pentose Phosphate Pathway as Drug Target

The pentose phosphate pathway (PPP) is a key metabolic process, which uses glucose-6-phosphate in parallel to the glycolysis. It is divided in two distinct phases, the oxidative branch, which produces NADPH and the non-oxidative branch, which produces 5-carbon sugars. Thus, the main functions of the pathway are generation of reducing agents (for e.g., combating ROS) and generation of sugars that are important for further nucleotide or amino acid synthesis¹²⁴. The first enzyme in the pathway is the G6PD, being responsible for the reaction, in which the first NADPH molecule is catalyzed. RNA interference (RNAi) approaches showed that G6PD is an essential enzyme in *Trypanosoma brucei*, determined by severe growth deficiencies after G6PD knockdown¹⁹⁴. The essentiality of the gene was also determined in *P. falciparum*¹²³. In *L. major* mutant strains with antimony resistance, harboring several genomic aberrations, a KO of G6PD could be generated, which led to growth deficiencies and a decreased protection against ROS¹⁹⁵. All these observations highlight the role of G6PD as a possible drug target. The group of Katja Becker (University Gießen) already assessed the potency of several G6PD inhibitors in the use against *Plasmodium*. The inhibitor with the lowest IC₅₀ value was SBI-750 with 6.7 nM when tested on enzyme activity. Furthermore, the inhibitor was assessed to be selective, since it did not show inhibition of human G6PD¹⁹⁶. I tested the inhibitor in *L. major* promastigotes and amastigotes and could determine an IC₅₀ value of 103.3 μM for cell death measured by fluorescence loss of the dsRed-expressing parasites in the amastigote stage. The concentration of a suitable drug

should be in the nanomolar range, since higher concentrations might induce off-target effects¹⁹⁷. This means SBI-750 is not a suitable drug for the treatment of *Leishmania*, however it can be used to study the potential of G6PD as drug target in the parasite. Since I could not see any effects on annexin binding or fluorescence loss even for high concentrations of SBI-750 in promastigotes but in amastigotes, I can conclude that G6PD seems to be more important in the amastigote stage than in the promastigote stage. This could be the case because amastigotes have to deal with a large amount of oxidative stress within the macrophage host cell, which could be alleviated by the generation of reducing agents through G6PD activity¹⁹⁸.

I was aiming to create G6PD KOs in *L. major* and *L. donovani* strains with a stable integration of Cas9/T7. All attempts of transfecting the KO constructs into the parasites and further selection of parasites via antibiotics led to death in *L. major*. This could either be due to experimental problems, which did not lead to a KO, or due to the fact that the gene is essential for parasite survival. One experimental issue could be an inefficient sgRNA binding and consequently an inefficient cutting of the DNA through the Cas9. Another possibility is that the HRs do not fit to a required extent to the UTRs of the GOI. We are working with *L. major* FEBNI, which is not sequenced, and therefore the oligonucleotide design is performed with the reference genome of *L. major* Friedlin. Hence, it is possible that there are minor differences in the gene sequences that result in an impaired binding of the designed oligonucleotide to the target gene. However, it could be shown that the genome of different *Leishmania* strains is very similar. For example, there are only 15 out of all 8,405 protein-coding genes more between *L. major* and *L. donovani*. Thus, between different species the difference is only in pseudogene formation and gene copy number variations but not in the overall genomic sequence¹⁹⁹. Since we work in the same species but different strain, I expect only very small genomic alterations. What refutes the point of inefficient oligonucleotide binding is that I was able to perform a KO in the G6PD overexpressing *L. major*. Even after eight passages with and without selection pressure and the further transformation to amastigotes, the parasites did not lose the G6PD expressing plasmid. I would expect that the parasites get rid of a plasmid, which expresses a gene that is not essential for parasite survival. Since RNA interference cannot be performed in *Leishmania*, this procedure was the gold standard to discover essential genes in *Leishmania* before the establishment of inducible KOs²⁰⁰. This experiment shows the importance of G6PD for the survival of *L. major* and the potential usage as a drug target.

In *L. donovani*, I was able to obtain the partial KO of G6PD. Although the G6PD mRNA expression was reduced to less than 40%, this did not influence the survival of the parasites. However, I could not achieve a full KO of G6PD in *L. donovani*. Therefore, I applied the same approach as for *L. major*: I introduced a plasmid for G6PD overexpression in the partial G6PD KO of *L. donovani* and attempted the full G6PD genomic KO. All my attempts for a rescued full G6PD KO failed, probably because the

partial KO harboring the overexpression plasmid only showed a G6PD mRNA expression of about 60% compared to wildtype *L. donovani*. It is not clear why the plasmid led only to this small increase in expression. Although the plasmid is designed with promotor-like regions from *L. major* its use in *L. donovani* was shown as well²⁰¹. Nonetheless, I was neither able to create a full G6PD KO nor a rescued G6PD KO in *L. donovani*. This could be bypassed through the usage of an inducible KO system, since the lethality of the genetic modification can be excluded and the direct effects of the KO can be observed.

PGD is the second enzyme in the PPP, which produces a NADPH molecule. Therefore, PGD is also highly discussed as a drug target^{124,202}. Using RNAi, which led to growth deficiencies, it could be shown that it is an essential protein in *T. brucei*²⁰³. I applied the same drug target validation strategy for PGD as I did for G6PD in *L. major* and *L. donovani*. Initial KO of the PGD was lethal in both strains. Therefore, I decided for a rescued PGD KO with the integration of a plasmid for PGD overexpression (OE). This was not successful in a first attempt in *L. major*, however the stable integration of an additional copy of PGD in the ribosomal locus worked immediately. The PGD OE parasites showed a very strong upregulation of PGD mRNA. This enabled the full KO of the genomic PGD locus, which showed a lower mRNA expression than the PGD OE parasites but still much higher expression than the control parasites. Therefore, conclusions about reduced amounts of PGD cannot be made. Anyway, I could see a change in the phenotype for the PGD OE and the rescued PGD KO. The PGD OE led to a highly reduced growth behavior in the logarithmic phase. This was even more pronounced in the rescued PGD KO, especially in the late stationary growth phase. This shows that an endogenous control of the PGD is very important for proper growth of *Leishmania*. In human carcinoma cells, a PGD overexpression leads to a higher survival²⁰⁴. Moreover, the overexpression of PGD is a known mechanism of cancer cells to gain metabolic advantages, why it is also a target for cancer therapy²⁰⁵.

L. donovani did not lose the PGD OE plasmid within the rescued PGD KO after eight passages. A following transformation of promastigotes to axenic amastigotes would be the next step to achieve the eventual loss of the plasmid in case it is not essential for parasite survival, since during the transformation step the highest genomic adaptations occur (unpublished results from our group). However, I was not able to perform the transformation, since it is very difficult to achieve *in vitro*. Thus, the amastigote generation *in vivo* in a mouse would be the appropriate alternative, which could be performed next. Taken together, I cannot be sure, if PGD is an essential gene in *L. donovani*. It is necessary to perform further experiments to finish the target validation. A suitable alternative method for this would be an inducible KO of the gene, since here the direct effects of the KO could be observed, without the issues of the KO performance.

4.5. Establishment of an Inducible Knock-out System

The main obstacle to face during this thesis was that I did not obtain a full KO for the majority of my target genes. Since I can never be sure if a KO did not work because of problems during experiment performance or because the parasite dies upon deletion of a gene, there is the urgent need for a better way to deal with essential genes. As already mentioned, a solution for most of my target genes would be an inducible KO. With this system, the KO can be induced through the addition of a drug (in my case rapamycin), which leads to the removal of the GOI. The advantage of the method lies in the fact that the parasites do not die through the genetic modification, but if they die after rapamycin addition, one can be sure that it is because of the loss of the gene. I was able to establish such a system in our laboratory, which uses two fluorescent proteins for the tracking of efficient removal of the GOI (eGFP) and also for the viability of the parasite (mCherry).

I used the inducible KO system for the drug target validation of G6PD in *L. donovani*. After the addition of rapamycin, I could see an increase in the G6PD gDNA on the first day. This is a well described mechanism of *Leishmania* to deal with environmental changes. The parasites deal with stress through variations of the gene copy number²⁰⁶. However, the increase of the gene copy number is only possible as long there are still copies of the G6PD left, which is only on the first day. Later, the gDNA is constantly decreasing down to approximately 10% at day 7. Therefore, the method is working very efficiently. The observed eGFP fluorescence decreased in the same fashion but showed levels at approximately 30% from day 7 on. The amount of eGFP decreases slower than the gDNA abundance, since there is a delay due to the half-life of the protein. I could only see minor differences after the induction of the G6PD KO in *L. donovani*. The only significant difference was the number of dead parasites at day 7, which was increased after KO induction. For an essential gene, I would expect highly decreased growth. Based on these experiments, I can conclude that G6PD is dispensable for the survival of *L. donovani* promastigotes. Nonetheless, as seen for the inhibitor experiments, the role of G6PD KO in amastigotes should be investigated in more detail, since I would expect a bigger effect there.

For inducible PGD KO experiments in *L. donovani*, I was not able to integrate the loxP site on both alleles but since I could not achieve this through the non-inducible KO method, I investigated this inducible partial PGD KO in more detail. In this inducible KO I could see the effect of gene copy number variation much more pronounced. At day one after induction, the PGD gDNA was up to 4x the number compared to control. Only at day 4 and 5 the gene copy number decreased to lower than one, but increased later. This shows again the genomic plasticity of *Leishmania*. Through the duplications of the chromosomes, the parasite was able to keep an almost constant expression of eGFP and therefore also PGD. Therefore, the growth differences were not significant, though constantly decreased for the induced partial PGD KO. Altogether, I can say that a full inducible PGD KO would be very promising and should be focused on in the future, since this could be a good drug target. The question arises, why

PGD shows higher growth defects in a partial KO than G6PD in a full KO. A reason could be that, apart from the NADPH production, a deficiency in PGD leads also to the accumulation of 6-phosphogluconate. This accumulation is toxic for the cell, since it inhibits the phosphoglucose isomerase and consequently glycolysis¹²⁴. A further readout to track the induction of the KO could also be the metabolic consumption and ROS levels in the parasite.

4.6. The Role of *Leishmania* PS on the Human Immune System

Although it was shown that annexin-binding lipids on the parasites' surface play a crucial role in the disease development of leishmaniasis⁴¹, it is still a matter of debate which annexin-binding lipids are responsible for this effect⁴³. It was suggested that PS is the sought-after lipid, since it plays a role in many other immune-silencing mechanisms²⁰⁷. However, in the publication of Weingärtner et al.⁴³, the researchers used several biophysical methods to detect PS in *L. donovani* promastigotes but failed to do so. They detected other lipids like phosphatidylglycerol, phosphatidylethanolamine or phosphatidylinositol, which are all able to bind annexin⁴³. One critical point in their publication is that they used logarithmic phase promastigotes, which do not externalize PS and it is not clear if this life-stage of *Leishmania* synthesizes PS, although PS is an inherent part of the plasma membrane of most eukaryotes. PS synthesis could be shown in *T. brucei*, which use the phosphatidylserine synthase to produce PS through serine²⁰⁸. A putative phosphatidylserine synthase is also found in the *Leishmania* genome however, experimental evidence is missing if the protein is functional. In our MS screen, we could not detect the synthase in any of the conditions, and a KO attempt did not lead to living parasites (data not shown). Though, there are other ways proposed how *Leishmania* might acquire PS, for example from the FCS in the culture medium⁴³. Therefore, we were aiming to solve the question if *Leishmania* harbors PS, together with our cooperation partners. We were able to identify distinct species of PS on living and dead parasites. Moreover, certain species of PS can only be found on dead parasites, strikingly the PS with very long fatty acid chains and a high number of double bonds. Rats that were fed with PS_{22:6} showed reduced oxidative stress pathways through lower TNF α and IL-1 β production in the brain²⁰⁹. It is my hypothesis that these distinct PS species on dead parasites play a major role in the immune-silencing mechanism when infecting host cells. Because of their low stability in aqueous solutions²¹⁰, it is not trivial to deliver lipids to cells in a way that they can recognize them, I used the physiological model of exosomes to deliver the lipids. I was successful in purifying exosomes derived from logarithmic and stationary phase promastigotes. As expected, logarithmic phase promastigotes produced more exosomes than stationary phase promastigotes, which is conclusive, since the production of exosomes is an active process²¹¹. By definition, exosomes vary in their size between 50 and 150 nm²¹². With a measured mode size of 124 nm for logarithmic and 136 nm for

stationary phase exosomes, I am in the range for exosomes. It could be shown that *Leishmania* secrete exosomes during all life stages, even within the sand fly's midgut. These exosomes were shown to facilitate a *Leishmania* infection of the mammalian host cells through the induction of several cytokines like IL-4, IL-17a or IL-10²¹¹. *Leishmania* exosomes are packed with the proteins EF1a, different heat shock proteins, GP63 and histones²¹³. However, the lipidome of *Leishmania* exosomes remain elusive.

When I incubated hMDMs with logarithmic or stationary phase exosomes, I could not see an effect on cytokine secretion for non-activated macrophages. However, when the macrophages were primed with IFN γ /LPS, I could see an effect for distinct donors. This stimulus is quite physiological, since CD4⁺ T cells secrete IFN γ in order to establish a proper Th1 type immune response against *Leishmania*²¹⁴. Regarding the second stimulus, it was shown that through the bite of an infected sand fly, bacteria of the genera *Tsukamurella*, *Lysinibacillus*, *Paenibacillus*, *Solibacillus*, *Myroides* and *Bacillus* were found to be transmitted alongside with *L. donovani*. The bacteria lead to IL-1 β secretion at the site of the sand fly bite, which leads to inflammasome activation and further neutrophil infiltration. When the sand fly was pre-treated with antibiotics, there was no parasite dissemination *in vivo*²¹⁵. Therefore, a bacteria-derived stimulus (LPS) together with a stimulus derived from other lymphocytes (IFN γ) is a physiological system²¹⁶.

I could see an increase for logarithmic exosomes in TNF production and an increase in IL-10 production for stationary phase exosomes. It could be shown that the infection of hMDMs with logarithmic phase promastigote facilitate the secretion of the pro-inflammatory cytokines TNF, IL-6 and IL-1 β , while stationary phase promastigotes lead to the anti-inflammatory cytokine secretion of IL-10⁴⁴. Therefore, the observed cytokine secretion fits to my hypothesis but only in some donors. The macrophages, we use for experiments are derived from human blood donors, and were shown to exhibit a substantial donor-to-donor variance when infected with several pathogens^{217,218}. These differences are based on the gender, the genetic variability but also the local environment in the donor and can be assayed through for example different cytokine profiles, but also differences in intracellular proliferation of pathogens²¹⁷.

Another important point to mention is that the exosomes do not only consist of lipids but also of proteins and nucleic acids²¹⁹. Thus, it is also possible that the cytokine secretion observed in distinct donors is due to the other substances in the vesicles and I cannot assign the observed effects to the lipids. To proof the lipid-induced effects, it would be necessary to synthesize the PS species, especially PS(22:5_22:5) and constitute them as liposomes.

Further, a greater number of donors should be tested and also, a more suitable polarization of the macrophages should be considered. I could observe TNF and IL-10 secretion for the M1 macrophages, which were activated with LPS+IFN γ (activated M1) or IFN γ alone (M1-). The type 1 macrophages play a major role in the microbicidal activity¹⁹¹. However, since type 1 macrophages are pro-inflammatory

cells and are very effective in TNF secretion, the type 2 macrophages are more prone for anti-inflammatory cytokine secretion like IL-10. Therefore, the M2 macrophages could be activated with IL-10 or TGF- β to achieve a M2c phenotype, which is able to secrete large amounts of IL-10²²⁰. This phenotype is also relevant for *Leishmania* infection, since it could be shown that through the sand fly saliva an M2 phenotype is favored²²¹. Therefore, a more physiological type of macrophage would possibly lead to a more pronounced cytokine response against the exosomes.

Taken together, we could prove the existence of PS in *Leishmania* and moreover of distinct PS species, which only occur on dead parasites. Further, I saw that exosomes, derived from living or dead parasites, are able to induce the secretion of pro- or anti-inflammatory cytokines, respectively. Thus, it might be possible that distinct PS species can trigger the secretion of anti-inflammatory (immune-silencing) cytokines, which need to be proven in further experiments.

4.7. Conclusion and Outlook

Overall, this thesis gave some new insights in the specialized mechanism of apoptosis in *Leishmania*. I identified several new proteins that might be involved in the cell death process and characterized selected ones of them. The work that was conducted during this thesis also highlights the difficult genetic background of *Leishmania* parasites. Tandem repeats or gene duplications of genes that are important for parasite survival is a common mechanism in the parasite. But also, several proteins with similar functions make it harder to discriminate a function of a specific protein, since a KO can always be compensated through other proteins for this kind of proteins. One way to examine essential proteins is the use of an inducible KO system. I could see how good this system works in the parasite and it should therefore also be used for all the investigated partial KOs, which did not lead to a clear phenotype.

Regarding the investigated KOs of EndoG and MCA, it should be considered to get them out of the focus of apoptosis investigations in *Leishmania*. Both proteins belong to the most investigated ones in cell death mechanisms of the parasites. However, they show only small effects and both can be compensated quite good. Further investigations should consider new proteins, for example those from the conducted mass spectrometry screen. I focused mainly on those from the promastigotes but also the regulated proteins in the amastigote stage are very important, since this is the form, which occurs inside the infected host cells.

A search for genes that might be involved in PS synthesis or externalization in *Leishmania* revealed that the human ATP11 has a homolog in *L. major* with 30.59% identity called phospholipid-transporting ATPase 1-like protein (Q4QG01/LMJF.13.1530). A KO of this protein should also be considered, because it could be possible that these KO parasites do not show anti-inflammatory properties. Without the

DISCUSSION

anti-inflammatory properties a proper T cell response would be possible⁴⁴ and therefore ATP11 might be a good vaccine target. Furthermore, an inducible KO of PS synthase would be very interesting. The chances are quite high that it would lead to death immediately after KO induction but maybe a first decrease in PS content (annexin binding) could be detected. Even so, the other side would be worth investigating: how the macrophage mediates the anti-inflammatory properties. As mentioned in the introduction, there is a broad range of receptors present on phagocytes, which can recognize PS⁸¹. *Leishmania* infections in TIM4^{-/-} or MerTK^{-/-} mice could solve this open question, which receptor is responsible for mediating the anti-inflammatory response.

Altogether, this work can be the next starting point to fully understand the apoptosis mechanisms in *Leishmania*. The huge dataset of differentially regulated proteins during cell death can bring a lot of information about that and reveal further drug targets to combat leishmaniasis. The here described system of inducible KOs can be used to investigate this further.

5. References

1. Leishmaniasis. <https://www.who.int/news-room/fact-sheets/detail/leishmaniasis> (accessed 04/06/2021)
2. World Health Organization. Photos on leishmaniasis for download. https://www.who.int/leishmaniasis/resources/photo_gallery/gallery/en/ (accessed 04/06/2021)
3. Gomes CM, Paula NA de, Morais OO de, Soares KA, Roselino AM, Sampaio RNR. Complementary exams in the diagnosis of American tegumentary leishmaniasis. *Anais brasileiros de dermatologia* 2014; 89: 701–9
4. Leishmaniasis. https://www.who.int/health-topics/leishmaniasis#tab=tab_2 (accessed 04/06/2021)
5. Talmi-Frank D, Nasereddin A, Schnur LF, *et al.* Detection and identification of old world *Leishmania* by high resolution melt analysis. *PLoS Neglected Tropical Diseases* 2010; 4: e581
6. Ronet C, Beverley SM, Fasel N. Muco-cutaneous leishmaniasis in the New World: the ultimate subversion. *Virulence* 2011; 2: 547–52
7. Sundar S. Drug resistance in Indian visceral leishmaniasis. *Tropical medicine & international health : TM & IH* 2001; 6: 849–54
8. Peters W. The treatment of kala-azar—new approaches to an old problem. *The Indian journal of medical research* 1981; 73 Suppl: 1–18
9. Baiocco P, Colotti G, Franceschini S, Ilari A. Molecular basis of antimony treatment in leishmaniasis. *Journal of medicinal chemistry* 2009; 52: 2603–12
10. Sundar S, Sinha PR, Agrawal NK, *et al.* A cluster of cases of severe cardiotoxicity among kala-azar patients treated with a high-osmolarity lot of sodium antimony gluconate. *The American journal of tropical medicine and hygiene* 1998; 59: 139–43
11. Sundar S, Murray HW. Cure of antimony-unresponsive Indian visceral leishmaniasis with amphotericin B lipid complex. *The Journal of infectious diseases* 1996; 173: 762–5
12. Kumar Saha A, Mukherjee T, Bhaduri A. Mechanism of action of amphotericin B on *Leishmania donovani* promastigotes. *Molecular and biochemical parasitology* 1986; 19: 195–200

13. Kuhlencord A, Maniera T, Eibl H, Unger C. Hexadecylphosphocholine: oral treatment of visceral leishmaniasis in mice. *Antimicrobial agents and chemotherapy* 1992; 36: 1630–4
14. Sundar S, Olliaro PL. Miltefosine in the treatment of leishmaniasis: Clinical evidence for informed clinical risk management. *Therapeutics and Clinical Risk Management* 2007; 3: 733–40
15. Mondelaers A, Sanchez-Cañete MP, Hendrickx S, *et al.* Genomic and Molecular Characterization of Miltefosine Resistance in *Leishmania infantum* Strains with Either Natural or Acquired Resistance through Experimental Selection of Intracellular Amastigotes. *PloS one* 2016; 11: e0154101
16. Luque-Ortega JR, Rivas L. Miltefosine (hexadecylphosphocholine) inhibits cytochrome c oxidase in *Leishmania donovani* promastigotes. *Antimicrobial Agents and Chemotherapy* 2007; 51: 1327–32
17. Pinto-Martinez AK, Rodriguez-Durán J, Serrano-Martin X, Hernandez-Rodriguez V, Benaim G. Mechanism of Action of Miltefosine on *Leishmania donovani* Involves the Impairment of Acidocalcisome Function and the Activation of the Sphingosine-Dependent Plasma Membrane Ca²⁺ Channel. *Antimicrobial agents and chemotherapy* 2018; 62
18. Ghorbani M, Farhoudi R. Leishmaniasis in humans: drug or vaccine therapy? *Drug Design, Development and Therapy* 2018; 12: 25–40
19. Mohebbali M, Nadim A, Khamesipour A. An overview of leishmanization experience: A successful control measure and a tool to evaluate candidate vaccines. *Acta tropica* 2019; 200: 105173
20. Serebriakov VA, Karakhodzhaeva SK, Ni GV, Belozerovala OD, Safarov GI. Pervyi opyt organizatsii i provedeniia massovykh leishmaniinykh privivok sel'skomu naseleniiu. *Meditinskaiia parazitologiiia i parazitarnye bolezni* 1968; 37: 651–4
21. Nadim A, Javadian E, Tahvildar-Bidrui G, Ghorbani M. Effectiveness of leishmanization in the control of cutaneous leishmaniasis. *Bulletin de la Societe de pathologie exotique et de ses filiales* 1983; 76: 377–83
22. Khamesipour A, Dowlati Y, Asilian A, *et al.* Leishmanization: use of an old method for evaluation of candidate vaccines against leishmaniasis. *Vaccine* 2005; 23: 3642–8
23. Pacheco-Fernandez T, Volpedo G, Gannavaram S, *et al.* Revival of Leishmanization and Leishmanin. *Frontiers in Cellular and Infection Microbiology* 2021; 11: 639801

24. Teixeira MCA, Oliveira GGdS, Santos POM, *et al.* An experimental protocol for the establishment of dogs with long-term cellular immune reactions to *Leishmania* antigens. *Memorias do Instituto Oswaldo Cruz* 2011; 106: 182–9
25. Moafi M, Rezvan H, Sherkat R, Taleban R. *Leishmania* Vaccines Entered in Clinical Trials: A Review of Literature. *International Journal of Preventive Medicine* 2019; 10: 95
26. Regina-Silva S, Feres AMLT, França-Silva JC, *et al.* Field randomized trial to evaluate the efficacy of the Leish-Tec® vaccine against canine visceral leishmaniasis in an endemic area of Brazil. *Vaccine* 2016; 34: 2233–9
27. Osman M, Mistry A, Keding A, *et al.* A third generation vaccine for human visceral leishmaniasis and post kala azar dermal leishmaniasis: First-in-human trial of ChAd63-KH. *PLoS Neglected Tropical Diseases* 2017; 11: e0005527
28. Muyombwe A, Olivier M, Harvie P, Bergeron MG, Ouellette M, Papadopoulou B. Protection against *Leishmania* major challenge infection in mice vaccinated with live recombinant parasites expressing a cytotoxic gene. *The Journal of infectious diseases* 1998; 177: 188–95
29. Banerjee A, Bhattacharya P, Dagur PK, *et al.* Live Attenuated *Leishmania donovani* Centrin Gene-Deleted Parasites Induce IL-23-Dependent IL-17-Protective Immune Response against Visceral Leishmaniasis in a Murine Model. *Journal of immunology (Baltimore, Md. : 1950)* 2018; 200: 163–76
30. Alexander J, Coombs GH, Mottram JC. *Leishmania mexicana* cysteine proteinase-deficient mutants have attenuated virulence for mice and potentiate a Th1 response. *Journal of immunology (Baltimore, Md. : 1950)* 1998; 161: 6794–801
31. Leishman WB. On the possibility of the occurrence of trypanosomiasis in India. *BMJ* 1903: 1252–4
32. Donovan C. On the possibility of the occurrence of trypanosomiasis in India. *BMJ* 1903: 79
33. Ross R. NOTE ON THE BODIES RECENTLY DESCRIBED BY LEISHMAN AND DONOVAN. *BMJ* 1903: 1261–2
34. Loría-Cervera EN, Andrade-Narváez FJ. Animal models for the study of leishmaniasis immunology. *Revista do Instituto de Medicina Tropical de Sao Paulo* 2014; 56: 1–11
35. Prasanna P, Upadhyay A. Heat Shock Proteins as the Druggable Targets in Leishmaniasis: Promises and Perils. *Infection and immunity* 2021; 89

36. Müller K, van Zandbergen G, Hansen B, *et al.* Chemokines, natural killer cells and granulocytes in the early course of *Leishmania major* infection in mice. *Medical microbiology and immunology* 2001; 190: 73–6
37. Laufs H, Müller K, Fleischer J, *et al.* Intracellular survival of *Leishmania major* in neutrophil granulocytes after uptake in the absence of heat-labile serum factors. *Infection and immunity* 2002; 70: 826–35
38. Aga E, Katschinski DM, van Zandbergen G, *et al.* Inhibition of the spontaneous apoptosis of neutrophil granulocytes by the intracellular parasite *Leishmania major*. *Journal of immunology (Baltimore, Md. : 1950)* 2002; 169: 898–905
39. Laskay T, van Zandbergen G, Solbach W. Neutrophil granulocytes – Trojan horses for *Leishmania major* and other intracellular microbes? *Trends in Microbiology* 2003; 11: 210–4
40. van Zandbergen G, Klinger M, Mueller A, *et al.* Cutting edge: neutrophil granulocyte serves as a vector for *Leishmania* entry into macrophages. *Journal of immunology (Baltimore, Md. : 1950)* 2004; 173: 6521–5
41. van Zandbergen G, Bollinger A, Wenzel A, *et al.* *Leishmania* disease development depends on the presence of apoptotic promastigotes in the virulent inoculum. *PNAS* 2006; 37: 13837–42
42. Warburg A, Schlein Y. The effect of post-bloodmeal nutrition of *Phlebotomus papatasi* on the transmission of *Leishmania major*. *The American journal of tropical medicine and hygiene* 1986; 35: 926–30
43. Weingärtner A, Kemmer G, Müller FD, *et al.* *Leishmania* promastigotes lack phosphatidylserine but bind annexin V upon permeabilization or miltefosine treatment. *PloS one* 2012; 7: e42070
44. Crauwels P, Bohn R, Thomas M, *et al.* Apoptotic-like *Leishmania* exploit the host's autophagy machinery to reduce T-cell-mediated parasite elimination. *Autophagy* 2015; 11: 285–97
45. Wincker P, Ravel C, Blaineau C, *et al.* The *Leishmania* genome comprises 36 chromosomes conserved across widely divergent human pathogenic species. *Nucleic Acids Research* 1996; 9: 1688–94
46. Ivens A, Lewis S, Bagherzadeh A, Zhang L, Chan H, Smith D. A Physical Map of the *Leishmania major* Friedlin Genome. *Genome Research* 1998: 135–45

47. Britto C, Ravel C, Bastien P, *et al.* Conserved linkage groups associated with large-scale chromosomal rearrangements between Old World and New World *Leishmania* genomes. *Gene* 1998: 107–17
48. Dumetz F, Imamura H, Sanders M, *et al.* Modulation of Aneuploidy in *Leishmania donovani* during Adaptation to Different In Vitro and In Vivo Environments and Its Impact on Gene Expression. *mBio* 2017; 8
49. Rogers MB, Hilley JD, Dickens NJ, *et al.* Chromosome and gene copy number variation allow major structural change between species and strains of *Leishmania*. *Genome Research* 2011; 21: 2129–42
50. Damasceno JD, Marques CA, Beraldi D, *et al.* Genome duplication in *Leishmania major* relies on DNA replication outside S phase, Vol 2, 2019
51. Myler PJ, Audleman L, DeVos T, *et al.* *Leishmania major* Friedlin chromosome 1 has an unusual distribution of protein-coding genes. *PNAS* 1999: 2902–6
52. Beneke T, Madden R, Makin L, Valli J, Sunter J, Gluenz E. A CRISPR Cas9 high-throughput genome editing toolkit for kinetoplastids. *Royal Society open science* 2017; 4: 170095
53. Lye L-F, Owens K, Shi H, *et al.* Retention and loss of RNA interference pathways in trypanosomatid protozoans. *PLOS Pathogens* 2010; 6: e1001161
54. Boothroyd JC, Cross G. Transcripts coding for variant surface glycoproteins of *Trypanosoma brucei* have a short, identical exon at their 5' end. *Gene* 1982; 2: 281–9
55. Milhausen M, Nelson RG, Sather S, Selkirk M, Agabian N. Identification of a Small RNA Containing the Trypanosome Spliced Leader: A Donor of Shared 5' Sequences of Trypanosomatid mRNAs? *Cell* 1984: 721–9
56. Boothroyd JC, Cross G. Transcripts coding for variant surface glycoproteins of *Trypanosoma brucei* have a short, identical exon at their 5' end. *Gene* 1982; 2: 281–9
57. Sutton RE, Boothroyd JC. Evidence for Trans Splicing in Trypanosomes. *Cell* 1986: 527–35
58. LeBowitz JH, Smith HQ, Rusche L, Beverley SM. Coupling of poly(A) site selection and trans-splicing in *Leishmania*. *Genes & Development* 1993: 996–1007
59. Donelson JE, Gardner MJ, El-Sayed NM. More surprises from Kinetoplastida. *PNAS* 1999: 2579–81
60. Boucher N, Wu Y, Dumas C, *et al.* A common mechanism of stage-regulated gene expression in *Leishmania* mediated by a conserved 3'-untranslated region element. *The Journal of biological chemistry* 2002; 277: 19511–20

61. Louradour I, Ferreira TR, Ghosh K, Shaik J, Sacks D. In Vitro Generation of Leishmania Hybrids. *Cell Reports* 2020; 31: 107507
62. Beneke T, Gluenz E. LeishGEdit: A Method for Rapid Gene Knockout and Tagging Using CRISPR-Cas9. *Methods in molecular biology (Clifton, N.J.)* 2019; 1971: 189–210
63. Kerr JFR, Wyllie AH, Currie AR. Apoptosis: a basic biological phenomenon with wideranging implications in tissue kinetics. *Br. J. Cancer* 1972; 26: 239–57
64. Horvitz HR. Genetic Control of Programmed Cell Death in the Nematode *Caenorhabditis elegans*. *Cancer Research* 1999: 1701–6
65. Martin SJ, Cotter TG. Ultraviolet B irradiation of human leukaemia HL-60 cells in vitro induces apoptosis. *International journal of radiation biology* 1991; 59: 1001–16
66. Itoh N, Yonehara S, Ishii A, *et al.* The polypeptide encoded by the cDNA for human cell surface antigen Fas can mediate apoptosis. *Cell* 1991; 66: 233–43
67. Carswell EA, Old LJ, Kassel RL, Green S, Fiore N, Williamson B. An endotoxin-induced serum factor that causes necrosis of tumors. *Proc. Nat. Acad. Sci. USA* 1975; 9: 3666–70
68. Cohen GM. Caspases: Executioners of Apoptosis. In: *Pathobiology of Human Disease*: Elsevier, 2014: 145–52
69. Liu X, Kim CN, Yang J, Jemmerson R, Wang X. Induction of Apoptotic Program in Cell-Free Extracts: Requirement for dATP and Cytochrome c. *Cell* 1996; 86: 147–57
70. Susin SA, Zamzami N, Castedo M, *et al.* Bcl-2 inhibits the mitochondrial release of an apoptogenic protease. *The Journal of experimental medicine* 1996; 184: 1331–41
71. Li LY, Luo X, Wang X. Endonuclease G is an apoptotic DNase when released from mitochondria. *Nature* 2001; 412: 95–9
72. Zou H, Li Y, Liu X, Wang X. An APAF-1.cytochrome c multimeric complex is a functional apoptosome that activates procaspase-9. *The Journal of biological chemistry* 1999; 274: 11549–56
73. Medema JP, Scaffidi C, Kischkel FC, *et al.* FLICE is activated by association with the CD95 death-inducing signaling complex (DISC). *The EMBO journal* 1997; 16: 2794–804
74. Luo X, Budihardjo I, Zou H, Slaughter C, Wang X. Bid, a Bcl2 Interacting Protein, Mediates Cytochrome c Release from Mitochondria in Response to Activation of Cell Surface Death Receptors. *Cell* 1998; 94: 481–90

75. Walker PR, Smith C, Youdale T, Leblanc J, Whitfield JF, Sikorska M. Topoisomerase II-reactive Chemotherapeutic Drugs Induce Apoptosis in Thymocyte. *Cancer Research* 1991; 1078–85
76. Ichim G, Tait SWG. A fate worse than death: apoptosis as an oncogenic process. *Nature Reviews Cancer* 2016; 16: 539–48
77. Bratton DL, Fadok VA, Richter DA, Kailey JM, Guthrie LA, Henson PM. Appearance of phosphatidylserine on apoptotic cells requires calcium-mediated nonspecific flip-flop and is enhanced by loss of the aminophospholipid translocase. *The Journal of biological chemistry* 1997; 272: 26159–65
78. Yabas M, Teh CE, Frankenreiter S, *et al.* ATP11C is critical for the internalization of phosphatidylserine and differentiation of B lymphocytes. *Nature immunology* 2011; 12: 441–9
79. Suzuki J, Denning DP, Imanishi E, Horvitz HR, Nagata S. Xk-related protein 8 and CED-8 promote phosphatidylserine exposure in apoptotic cells. *Science (New York, N.Y.)* 2013; 341: 403–6
80. Duvall E, Wyllie H, Morris RG. Macrophage recognition of cells undergoing programmed cell death (apoptosis). *Immunology* 1985; 56: 351–8
81. Boada-Romero E, Martinez J, Heckmann BL, Green DR. The clearance of dead cells by efferocytosis. *Nature reviews. Molecular cell biology* 2020; 21: 398–414
82. Majno G, Joris I. Apoptosis, Oncosis, and Necrosis. *American Journal of Pathology* 1995; 1: 3–15
83. Aubrey BJ, Kelly GL, Janic A, Herold MJ, Strasser A. How does p53 induce apoptosis and how does this relate to p53-mediated tumour suppression? *Cell Death & Differentiation* 2018; 25: 104–13
84. Alam JJ. Apoptosis: target for novel drugs. *Trends in Biotechnology* 2003; 21: 479–83
85. Fischer U, Schulze-Osthoff K. Apoptosis-based therapies and drug targets. *Cell Death & Differentiation* 2005; 12 Suppl 1: 942–61
86. Kim JL, Lee D-H, Jeong S, *et al.* Imatinib-induced apoptosis of gastric cancer cells is mediated by endoplasmic reticulum stress. *Oncology Reports* 2019; 41: 1616–26
87. Yang Y, Yi J, Pan M, Hu B, Duan H. Edaravone Alleviated Propofol-Induced Neurotoxicity in Developing Hippocampus by mBDNF/TrkB/PI3K Pathway. *Drug Design, Development and Therapy* 2021; 15: 1409–22

88. Alzate JF, Arias A, Mollinedo F, Rico E, La Iglesia-Vicente J de, Jiménez-Ruiz A. Edelfosine induces an apoptotic process in *Leishmania infantum* that is regulated by the ectopic expression of Bcl-XL and Hrk. *Antimicrobial agents and chemotherapy* 2008; 52: 3779–82
89. Jiménez-Ruiz A, Alzate JF, Macleod ET, Lüder CGK, Fasel N, Hurd H. Apoptotic markers in protozoan parasites. *Parasites & vectors* 2010; 3: 104
90. Casanova M, Gonzalez IJ, Sprissler C, *et al.* Implication of different domains of the *Leishmania major* metacaspase in cell death and autophagy. *Cell death & disease* 2015; 6: e1933
91. Proto WR, Coombs GH, Mottram JC. Cell death in parasitic protozoa: regulated or incidental? *Nature reviews. Microbiology* 2013; 11: 58–66
92. Kumar R, Tiwari K, Dubey VK. Methionine aminopeptidase 2 is a key regulator of apoptotic like cell death in *Leishmania donovani*. *Scientific reports* 2017; 7: 95
93. Genes CM, Lucio H de, González VM, *et al.* A functional BH3 domain in an aquaporin from *Leishmania infantum*. *Cell death discovery* 2016; 2: 16043
94. El-Fadili AK, Zangger H, Desponds C, *et al.* Cathepsin B-like and cell death in the unicellular human pathogen *Leishmania*. *Cell death & disease* 2010; 1: e71
95. Gannavaram S, Vedvyas C, Debrabant A. Conservation of the pro-apoptotic nuclease activity of endonuclease G in unicellular trypanosomatid parasites. *Journal of cell science* 2008; 121: 99–109
96. Rico E, Alzate JF, Arias AA, *et al.* *Leishmania infantum* expresses a mitochondrial nuclease homologous to EndoG that migrates to the nucleus in response to an apoptotic stimulus. *Molecular and biochemical parasitology* 2009; 163: 28–38
97. Rico E, Oliva C, Gutierrez KJ, *et al.* *Leishmania infantum* EndoG is an endo/exo-nuclease essential for parasite survival. *PloS one* 2014; 9: e89526
98. BoseDasgupta S, Das BB, Sengupta S, *et al.* The caspase-independent algorithm of programmed cell death in *Leishmania* induced by baicalein: the role of LdEndoG, LdFEN-1 and LdTatD as a DNA ‘degradesome’. *Cell Death and Differentiation* 2008: 1629–40
99. Schönian G. Genetics and Evolution of *Leishmania* parasites. *Infection, genetics and evolution : journal of molecular epidemiology and evolutionary genetics in infectious diseases* 2017; 50: 93–4
100. Oliva C, Sánchez-Murcia PA, Rico E, *et al.* Structure-based domain assignment in *Leishmania infantum* EndoG: characterization of a pH-dependent regulatory switch and a

- C-terminal extension that largely dictates DNA substrate preferences. *Nucleic Acids Research* 2017; 45: 9030–45
101. Dolai S, Pal S, Yadav RK, Adak S. Endoplasmic reticulum stress-induced apoptosis in *Leishmania* through Ca²⁺-dependent and caspase-independent mechanism. *The Journal of biological chemistry* 2011; 286: 13638–46
102. Chowdhury S, Mukherjee T, Chowdhury SR, *et al.* Disuccinyl betulin triggers metacaspase-dependent endonuclease G-mediated cell death in unicellular protozoan parasite *Leishmania donovani*. *Antimicrobial agents and chemotherapy* 2014; 58: 2186–201
103. Casanova E, Moreno D, Gigante A, *et al.* 5'-Trityl-substituted thymidine derivatives as a novel class of antileishmanial agents: *Leishmania infantum* EndoG as a potential target. *ChemMedChem* 2013; 8: 1161–74
104. González IJ, Desponds C, Schaff C, Mottram JC, Fasel N. *Leishmania major* metacaspase can replace yeast metacaspase in programmed cell death and has arginine-specific cysteine peptidase activity. *International Journal for Parasitology* 2007; 37: 161–72
105. Lee N, Gannavaram S, Selvapandiyan A, Debrabant A. Characterization of metacaspases with trypsin-like activity and their putative role in programmed cell death in the protozoan parasite *Leishmania*. *Eukaryotic cell* 2007; 6: 1745–57
106. Ambit A, Fasel N, Coombs GH, Mottram JC. An essential role for the *Leishmania major* metacaspase in cell cycle progression. *Cell Death & Differentiation* 2008; 15: 113–22
107. Verreck FAW, Boer T de, Langenberg DML, *et al.* Human IL-23-producing type 1 macrophages promote but IL-10-producing type 2 macrophages subvert immunity to (myco)bacteria. *Proceedings of the National Academy of Sciences of the United States of America* 2004; 101: 4560–5
108. Mosmann T. Rapid colorimetric assay for cellular growth and survival: Application to proliferation and cytotoxicity assays. *Journal of Immunological Methods* 1983; 65: 55–63
109. van Genderen HO, Kenis H, Hofstra L, Narula J, Reutelingsperger CPM. Extracellular annexin A5: functions of phosphatidylserine-binding and two-dimensional crystallization. *Biochimica et biophysica acta* 2008; 1783: 953–63
110. Krishan A. Rapid flow cytofluorometric analysis of mammalian cell cycle by propidium iodide staining. *Journal of Cell Biology* 1975; 66: 188–93

111. Fujikawa-Yamamoto K, Teraoka K, Zong ZP, Yamagishi H, Odashima S. Apoptosis by demecolcine in V79 cells. *Cell Structure and Function* 1994; 19: 391–6
112. Gavrieli Y, Sherman Y, Ben-Sasson SA. Identification of programmed cell death in situ via specific labeling of nuclear DNA fragmentation. *Journal of Cell Biology* 1992; 119: 493–501
113. Gomes A, Fernandes E, Lima JLFC. Fluorescence probes used for detection of reactive oxygen species. *Journal of Biochemical and Biophysical Methods* 2005; 65: 45–80
114. Distler U, Kuharev J, Navarro P, Tenzer S. Label-free quantification in ion mobility-enhanced data-independent acquisition proteomics. *Nature Protocols* 2016; 11: 795–812
115. Meggio F, Donella Deana A, Ruzzene M, *et al.* Different susceptibility of protein kinases to staurosporine inhibition. Kinetic studies and molecular bases for the resistance of protein kinase CK2. *European Journal of Biochemistry* 1995; 234: 317–22
116. Röhrich CR, Ngwa CJ, Wiesner J, *et al.* Harmonine, a defence compound from the harlequin ladybird, inhibits mycobacterial growth and demonstrates multi-stage antimalarial activity. *Biology Letters* 2012; 8: 308–11
117. Krieg R, Jortzik E, Goetz A-A, *et al.* Arylmethylamino steroids as antiparasitic agents. *Nature Communications* 2017; 8: 14478
118. Sun AY, Draczynska-Lusiak B, Sun GY. Oxidized lipoproteins, beta amyloid peptides and Alzheimer's disease. *Neurotoxicity Research* 2001; 3: 167–78
119. Wenzel UA, Bank E, Florian C, *et al.* Leishmania major parasite stage-dependent host cell invasion and immune evasion. *The FASEB Journal* 2012; 26: 29–39
120. Sanchiz Á, López-García D, García-García C, Ozaez I, Aguado B, Requena JM. Proteins interacting with Leishmania major PUF1: A proteomic dataset. *Data in Brief* 2020; 33: 106594
121. Steinacker JP. Detektion und Analyse molekularer Mechanismen der Apoptose in humanpathogenen Protozoen der Gattung Leishmania. Dissertation. Ulm, 2012
122. Campos-Salinas J, León-Guerrero D, González-Rey E, *et al.* LABCG2, a new ABC transporter implicated in phosphatidylserine exposure, is involved in the infectivity and pathogenicity of Leishmania. *PLoS Neglected Tropical Diseases* 2013; 7: e2179
123. Allen SM, Lim EE, Jortzik E, *et al.* Plasmodium falciparum glucose-6-phosphate dehydrogenase 6-phosphogluconolactonase is a potential drug target. *FEBS Journal* 2015; 282: 3808–23

124. Loureiro I, Faria J, Santarem N, Smith TK, Tavares J, Cordeiro-da-Silva A. Potential Drug Targets in the Pentose Phosphate Pathway of Trypanosomatids. *Current Medicinal Chemistry* 2018; 25: 5239–65
125. Duncan SM, Myburgh E, Alves-Ferreira EV, Mottram JC. DiCre-Based Inducible Disruption of Leishmania Genes. In: Clos J, ed. *Leishmania. Methods in Molecular Biology*. Vol 1971. New York, NY: Springer New York, 2019: 211–24
126. Damasceno JD, Reis-Cunha J, Crouch K, *et al.* Conditional knockout of RAD51-related genes in *Leishmania major* reveals a critical role for homologous recombination during genome replication. *PLOS Genetics* 2020; 16: e1008828
127. Yagoubat A, Crobu L, Berry L, *et al.* Universal highly efficient conditional knockout system in *Leishmania*, with a focus on untranscribed region preservation. *Cellular Microbiology* 2020; 22: e13159
128. dos Santos MG, Muxel SM, Zampieri RA, Pomorski TG, Floeter-Winter LM. Transbilayer dynamics of phospholipids in the plasma membrane of the *Leishmania* genus. *PloS one* 2013; 8: e55604
129. Muñoz-Martínez F, Torres C, Castanys S, Gamarro F. The anti-tumor alkylphospholipid perifosine is internalized by an ATP-dependent translocase activity across the plasma membrane of human KB carcinoma cells. *Biochimica et biophysica acta* 2008; 1778: 530–40
130. Nagel NC, Masic A, Schurigt U, Boland W. Efficient synthesis of (R)-harmonine—the toxic principle of the multicolored Asian lady beetle (*Harmonia axyridis*). *Organic & biomolecular chemistry* 2015; 13: 5139–46
131. Khademvatan S, Gharavi MJ, Rahim F, Saki J. Miltefosine-induced apoptotic cell death on *Leishmania major* and *L. tropica* strains. *The Korean Journal of Parasitology* 2011; 49: 17–23
132. Schmidt-Ott R, Klenner T, Overath P, Aebischer T. Topical treatment with hexadecylphosphocholine (Miltex®) efficiently reduces parasite burden in experimental cutaneous leishmaniasis. *Transactions of the Royal Society of Tropical Medicine and Hygiene* 1999; 93: 85–90
133. Coelho AC, Boisvert S, Mukherjee A, Leprohon P, Corbeil J, Ouellette M. Multiple mutations in heterogeneous miltefosine-resistant *Leishmania major* population as

- determined by whole genome sequencing. *PLoS Neglected Tropical Diseases* 2012; 6: e1512
134. Kellershohn J, Thomas L, Hahnel SR, *et al.* Insects in anthelmintics research: Lady beetle-derived harmonine affects survival, reproduction and stem cell proliferation of *Schistosoma mansoni*. *PLoS Neglected Tropical Diseases* 2019; 13: e0007240
135. Maurin M, Benoliel AM, Bongrand P, Raoult D. Phagolysosomal Alkalinization and the Bactericidal Effect of Antibiotics: The *Coxiella burnetii* Paradigm. *The Journal of infectious diseases*; 1992: 1097–102
136. Iyer JP, Kaprakkaden A, Choudhary ML, Shaha C. Crucial role of cytosolic trypanothione peroxidase in *Leishmania donovani* survival, drug response and virulence. *Molecular microbiology* 2008; 68: 372–91
137. Basmaciyan L, Casanova M. La mort cellulaire chez *Leishmania*. *Parasite* 2019; 26: 71
138. Besteiro S, Williams RAM, Morrison LS, Coombs GH, Mottram JC. Endosome sorting and autophagy are essential for differentiation and virulence of *Leishmania major*. *Journal of Biological Chemistry* 2006; 281: 11384–96
139. Lowell JE, Kaiser F, Janzen CJ, Cross GAM. Histone H2AZ dimerizes with a novel variant H2B and is enriched at repetitive DNA in *Trypanosoma brucei*. *Journal of cell science* 2005; 118: 5721–30
140. Iso-Touru T, Wurmser C, Venhoranta H, *et al.* A splice donor variant in CCDC189 is associated with asthenospermia in Nordic Red dairy cattle. *BMC Genomics* 2019; 20: 286
141. Chernobrovkin A, Marin-Vicente C, Visa N, Zubarev RA. Functional Identification of Target by Expression Proteomics (FITExP) reveals protein targets and highlights mechanisms of action of small molecule drugs. *Scientific Reports* 2015; 5: 11176
142. Farajnia S, Alimohammadian MH, Reiner NE, Karimi M, Ajdari S, Mahboudi F. Molecular characterization of a novel amastigote stage specific Class I nuclease from *Leishmania major*. *International Journal for Parasitology* 2004; 34: 899–908
143. Farajnia S, Rahbarnia L, Maleki Zanjani B, *et al.* Molecular Cloning and Characterization of P4 Nuclease from *Leishmania infantum*. *Enzyme research* 2011; 2011: 970983
144. Joshi MB, Dwyer DM. Molecular and functional analyses of a novel class I secretory nuclease from the human pathogen, *Leishmania donovani*. *Journal of Biological Chemistry* 2007; 282: 10079–95

145. Burge RJ, Damianou A, Wilkinson AJ, Rodenko B, Mottram JC. Leishmania differentiation requires ubiquitin conjugation mediated by a UBC2-UEV1 E2 complex. *PLOS Pathogens* 2020; 16: e1008784
146. Damianou A, Burge RJ, Catta-Preta CMC, *et al.* Essential roles for deubiquitination in Leishmania life cycle progression. *PLOS Pathogens* 2020; 16: e1008455
147. Oh C, Park S, Lee EK, Yoo YJ. Downregulation of ubiquitin level via knockdown of polyubiquitin gene Ubb as potential cancer therapeutic intervention. *Scientific Reports* 2013; 3: 2623
148. Vallabhaneni H, Farabaugh PJ. Accuracy modulating mutations of the ribosomal protein S4-S5 interface do not necessarily destabilize the rps4-rps5 protein-protein interaction. *RNA* 2009; 15: 1100–9
149. Ramakrishnan V, White SW. The structure of ribosomal protein S5 reveals sites of interaction with 16S rRNA. *Nature* 1992; 358: 768–71
150. Choi S, Jung C-R, Kim J-Y, Im D-S. PRMT3 inhibits ubiquitination of ribosomal protein S2 and together forms an active enzyme complex. *Biochimica et biophysica acta* 2008; 1780: 1062–9
151. Guo Q, Bedford MT, Fast W. Discovery of peptidylarginine deiminase-4 substrates by protein array: antagonistic citrullination and methylation of human ribosomal protein S2. *Molecular BioSystems* 2011; 7: 2286–95
152. Tanikawa C, Ueda K, Nakagawa H, Yoshida N, Nakamura Y, Matsuda K. Regulation of protein Citrullination through p53/PADI4 network in DNA damage response. *Cancer Research* 2009; 69: 8761–9
153. Sun J, Li C, Wang S. The Up-Regulation of Ribosomal Proteins Further Regulates Protein Expression Profile in Female *Schistosoma japonicum* after Pairing. *PLoS one* 2015; 10: e0129626
154. Gilbert WV. Functional specialization of ribosomes? *Trends in Biochemical Sciences* 2011; 36: 127–32
155. Negrutskii BS, El'skaya AV. Eukaryotic Translation Elongation Factor 1 α : Structure, Expression, Functions, and Possible Role in Aminoacyl-tRNA Channeling. In: Moldave K, ed. *Progress in Nucleic Acid Research and Molecular Biology*, 1st edn. Progress in Nucleic Acid Research and Molecular Biology. v.60. s.l.: Elsevier textbooks, 1998: 47–78

156. Nandan D, Yi T, Lopez M, Lai C, Reiner NE. Leishmania EF-1alpha activates the Src homology 2 domain containing tyrosine phosphatase SHP-1 leading to macrophage deactivation. *Journal of Biological Chemistry* 2002; 277: 50190–7
157. Nandan D, Cherkasov A, Sabouti R, Yi T, Reiner NE. Molecular cloning, biochemical and structural analysis of elongation factor-1 α from *Leishmania donovani*: comparison with the mammalian homologue. *Biochemical and Biophysical Research Communications* 2003; 302: 646–52
158. Duttaroy A, Bourbeau D, Wang XL, Wang E. Apoptosis rate can be accelerated or decelerated by overexpression or reduction of the level of elongation factor-1 alpha. *Experimental Cell Research* 1998; 238: 168–76
159. Gonen H, Smith CE, Siegel NR, *et al.* Protein synthesis elongation factor EF-1 alpha is essential for ubiquitin-dependent degradation of certain N alpha-acetylated proteins and may be substituted for by the bacterial elongation factor EF-Tu. *Proceedings of the National Academy of Sciences of the United States of America* 1994; 91: 7648–52
160. Maruyama T, Nara K, Yoshikawa H, Suzuki N. Txk, a member of the non-receptor tyrosine kinase of the Tec family, forms a complex with poly(ADP-ribose) polymerase 1 and elongation factor 1alpha and regulates interferon-gamma gene transcription in Th1 cells. *Clinical & Experimental Immunology* 2007; 147: 164–75
161. Silverman JM, Reiner NE. *Leishmania* exosomes deliver preemptive strikes to create an environment permissive for early infection. *Frontiers in Cellular and Infection Microbiology* 2011; 1: 26
162. Sabur A, Bhowmick S, Chhajer R, *et al.* Liposomal Elongation Factor-1 α Triggers Effector CD4 and CD8 T Cells for Induction of Long-Lasting Protective Immunity against Visceral Leishmaniasis. *Frontiers in Immunology* 2018; 9: 18
163. Lopez M, Cherkasov A, Nandan D. Molecular architecture of *leishmania* EF-1alpha reveals a novel site that may modulate protein translation: a possible target for drug development. *Biochemical and Biophysical Research Communications* 2007; 356: 886–92
164. Ouaisi A. Apoptosis-like death in trypanosomatids: search for putative pathways and genes involved. *Kinetoplastid Biology and Disease* 2003; 2: 5
165. Levick MP, Tetaud E, Fairlamb AH, Blackwell JM. Identification and characterisation of a functional peroxidoxin from *Leishmania major*1Note: Nucleotide sequence data reported in this paper are available in the EMBL, GenBank™ and DDJB databases under

- the accession number AF069386.1. *Molecular and biochemical parasitology* 1998; 96: 125–37
166. Wilkinson SR, Horn D, Prathalingam SR, Kelly JM. RNA interference identifies two hydroperoxide metabolizing enzymes that are essential to the bloodstream form of the african trypanosome. *Journal of Biological Chemistry* 2003; 278: 31640–6
167. Saudagar P, Dubey VK. Molecular mechanisms of in vitro betulin-induced apoptosis of *Leishmania donovani*. *The American journal of tropical medicine and hygiene* 2014; 90: 354–60
168. Tyurina Y, Shvedova A, Kawai K, *et al.* Phospholipid signaling in apoptosis: peroxidation and externalization of phosphatidylserine. *Toxicology* 2000; 148: 93–101
169. LMJF_18_1300 - Uncharacterized protein - *Leishmania major* - LMJF_18_1300 gene & protein. <https://www.uniprot.org/uniprot/Q4QDQ9> (accessed 08/29/2021)
170. Tb10.389.0690 - Mitochondrial carrier protein, putative - *Trypanosoma brucei brucei* (strain 927/4 GUTat10.1) - Tb10.389.0690 gene & protein. <https://www.uniprot.org/uniprot/Q388W2> (accessed 08/29/2021)
171. Bijarnia RK, Bachtler M, Chandak PG, van Goor H, Pasch A. Sodium thiosulfate ameliorates oxidative stress and preserves renal function in hyperoxaluric rats. *PloS one* 2015; 10: e0124881
172. Liang J, Cao R, Wang X, *et al.* Mitochondrial PKM2 regulates oxidative stress-induced apoptosis by stabilizing Bcl2. *Cell Research* 2017; 27: 329–51
173. Gannavaram S, Debrabant A. Programmed cell death in *Leishmania*: biochemical evidence and role in parasite infectivity. *Frontiers in Cellular and Infection Microbiology* 2012; 2: 95
174. Fu Y, Su L, Cai M, *et al.* Downregulation of CPA4 inhibits non small-cell lung cancer growth by suppressing the AKT/c-MYC pathway. *Molecular Carcinogenesis* 2019; 58: 2026–39
175. Farazi TA, Waksman G, Gordon JI. The biology and enzymology of protein N-myristoylation. *Journal of Biological Chemistry* 2001; 276: 39501–4
176. Wright MH, Paape D, Storck EM, Serwa RA, Smith DF, Tate EW. Global analysis of protein N-myristoylation and exploration of N-myristoyltransferase as a drug target in the neglected human pathogen *Leishmania donovani*. *Chemistry & Biology* 2015; 22: 342–54

177. Tull D, Naderer T, Spurck T, *et al.* Membrane protein SMP-1 is required for normal flagellum function in *Leishmania*. *Journal of cell science* 2010; 123: 544–54
178. Tull D, Heng J, Gooley PR, Naderer T, McConville MJ. Acylation-dependent and-independent membrane targeting and distinct functions of small myristoylated proteins (SMPs) in *Leishmania major*. *International Journal for Parasitology* 2012; 42: 239–47
179. Sabljic I, Meštrović N, Vukelić B, *et al.* Crystal structure of dipeptidyl peptidase III from the human gut symbiont *Bacteroides thetaiotaomicron*. *PLoS one* 2017; 12: e0187295
180. Karačić Z, Vukelić B, Ho GH, *et al.* A novel plant enzyme with dual activity: an atypical Nudix hydrolase and a dipeptidyl peptidase III. *Biological Chemistry* 2017; 398: 101–12
181. Shimamori Y, Watanabe Y, Fujimoto Y. Purification and characterization of dipeptidyl aminopeptidase III from human placenta. *Chemical and Pharmaceutical Bulletin* 1986; 34: 3333–40
182. Prajapati SC, Chauhan SS. Dipeptidyl peptidase III: a multifaceted oligopeptide N-end cutter. *FEBS Journal* 2011; 278: 3256–76
183. Diaz JR, Ramírez CA, Nocua PA, Guzman F, Requena JM, Puerta CJ. Dipeptidyl peptidase 3, a novel protease from *Leishmania braziliensis*. *PLoS one* 2018; 13: e0190618
184. Perea A, Manzano JI, Castanys S, Gamarro F. The LABC2G2 Transporter from the Protozoan Parasite *Leishmania* Is Involved in Antimony Resistance. *Antimicrobial Agents and Chemotherapy* 2016; 60: 3489–96
185. Bogomolnaya LM, Andrews KD, Talamantes M, *et al.* The ABC-type efflux pump MacAB protects *Salmonella enterica* serovar typhimurium from oxidative stress. *mBio* 2013; 4: e00630-13
186. Zorova LD, Popkov VA, Plotnikov EY, *et al.* Mitochondrial membrane potential. *Analytical Biochemistry* 2018; 552: 50–9
187. Blasco N, Beà A, Barés G, *et al.* Involvement of the mitochondrial nuclease EndoG in the regulation of cell proliferation through the control of reactive oxygen species. *Redox Biology* 2020; 37: 101736
188. Wiehe RS, Gole B, Chatre L, *et al.* Endonuclease G promotes mitochondrial genome cleavage and replication. *Oncotarget* 2018; 9: 18309–26
189. McLuskey K, Paterson NG, Bland ND, Isaacs NW, Mottram JC. Crystal structure of *Leishmania major* oligopeptidase B gives insight into the enzymatic properties of a

- trypanosomatid virulence factor. *The Journal of biological chemistry* 2010; 285: 39249–59
190. Bullock TL, Breddam K, Remington SJ. Peptide aldehyde complexes with wheat serine carboxypeptidase II: implications for the catalytic mechanism and substrate specificity. *Journal of molecular biology* 1996; 255: 714–25
191. Tomiotto-Pellissier F, Da Bortoleti BTS, Assolini JP, *et al.* Macrophage Polarization in Leishmaniasis: Broadening Horizons. *Frontiers in Immunology* 2018; 9: 2529
192. Vermeersch M, da Luz RI, Toté K, Timmermans J-P, Cos P, Maes L. In vitro susceptibilities of *Leishmania donovani* promastigote and amastigote stages to antileishmanial reference drugs: practical relevance of stage-specific differences. *Antimicrobial Agents and Chemotherapy* 2009; 53: 3855–9
193. Real F, Florentino PTV, Reis LC, *et al.* Cell-to-cell transfer of *Leishmania amazonensis* amastigotes is mediated by immunomodulatory LAMP-rich parasitophorous extrusions. *Cellular Microbiology* 2014; 16: 1549–64
194. Cordeiro AT, Thiemann OH, Michels PAM. Inhibition of *Trypanosoma brucei* glucose-6-phosphate dehydrogenase by human steroids and their effects on the viability of cultured parasites. *Bioorganic & Medicinal Chemistry* 2009; 17: 2483–9
195. Mukherjee A, Boisvert S, Monte-Neto RLd, *et al.* Telomeric gene deletion and intrachromosomal amplification in antimony-resistant *Leishmania*. *Molecular microbiology* 2013; 88: 189–202
196. Häußler KME. Characterization and inhibition of NADPH-producing enzymes from the pentose phosphate pathway of *Plasmodium* parasites 2018
197. Song X, Chen J, Zhao M, *et al.* Development of potent small-molecule inhibitors to drug the undruggable steroid receptor coactivator-3. *Proceedings of the National Academy of Sciences of the United States of America* 2016; 113: 4970–5
198. Maugeri DA, Cazzulo JJ, Burchmore RJ, Barrett MP, Ogbunude PO. Pentose phosphate metabolism in *Leishmania mexicana*. *Molecular and biochemical parasitology* 2003; 130: 117–25
199. Camacho E, La González-de Fuente S, Rastrojo A, *et al.* Complete assembly of the *Leishmania donovani* (HU3 strain) genome and transcriptome annotation. *Scientific Reports* 2019; 9: 6127

200. Späth GF, Clos J. Joining forces: first application of a rapamycin-induced dimerizable Cre system for conditional null mutant analysis in *Leishmania*. *Molecular microbiology* 2016; 100: 923–7
201. Hoyer C, Zander D, Fleischer S, *et al.* A *Leishmania donovani* gene that confers accelerated recovery from stationary phase growth arrest. *International Journal for Parasitology* 2004; 34: 803–11
202. Jakkula P, Narsimulu B, Qureshi IA. Biochemical and structural insights into 6-phosphogluconate dehydrogenase from *Leishmania donovani*. *Applied Microbiology and Biotechnology* 2021; 105: 5471–89
203. Kerkhoven EJ, Achcar F, Alibu VP, *et al.* Handling uncertainty in dynamic models: the pentose phosphate pathway in *Trypanosoma brucei*. *PLoS Computational Biology* 2013; 9: e1003371
204. Chen H, Wu D, Bao L, *et al.* 6PGD inhibition sensitizes hepatocellular carcinoma to chemotherapy via AMPK activation and metabolic reprogramming. *Biomedicine & pharmacotherapy = Biomedecine & pharmacotherapie* 2019; 111: 1353–8
205. Sarfraz I, Rasul A, Hussain G, *et al.* 6-Phosphogluconate dehydrogenase fuels multiple aspects of cancer cells: From cancer initiation to metastasis and chemoresistance. *BioFactors* 2020; 46: 550–62
206. Bussotti G, Gouzelou E, Côrtes Boité M, *et al.* *Leishmania* Genome Dynamics during Environmental Adaptation Reveal Strain-Specific Differences in Gene Copy Number Variation, Karyotype Instability, and Telomeric Amplification. *mBio* 2018; 9
207. Henson PM, Bratton DL, Fadok VA. Apoptotic cell removal. *Current Biology* 2001; 11: R795-R805
208. RICHMOND GS, GIBELLINI F, YOUNG SA, *et al.* Lipidomic analysis of bloodstream and procyclic form *Trypanosoma brucei*. *Parasitology* 2010; 137: 1357–92
209. Wen M, Ding L, Zhang L, *et al.* DHA-PC and DHA-PS improved A β 1–40 induced cognitive deficiency uncoupled with an increase in brain DHA in rats. *Journal of Functional Foods* 2016; 22: 417–30
210. Grit M, Smidt JH de, Struijke A, Crommelin DJ. Hydrolysis of phosphatidylcholine in aqueous liposome dispersions. *International Journal of Pharmaceutics* 1989; 50: 1–6

211. Atayde VD, Aslan H, Townsend S, Hassani K, Kamhawi S, Olivier M. Exosome Secretion by the Parasitic Protozoan *Leishmania* within the Sand Fly Midgut. *Cell Reports* 2015; 13: 957–67
212. Li Y, Zhang Y, Li Z, Zhou K, Feng N. Exosomes as Carriers for Antitumor Therapy. *ACS Biomaterials Science & Engineering* 2019; 5: 4870–81
213. Silverman JM, Clos J, Horakova E, *et al.* *Leishmania* exosomes modulate innate and adaptive immune responses through effects on monocytes and dendritic cells. *Journal of immunology (Baltimore, Md. : 1950)* 2010; 185: 5011–22
214. Pinheiro RO, Rossi-Bergmann B. Interferon-gamma is required for the late but not early control of *Leishmania amazonensis* infection in C57Bl/6 mice. *Memorias do Instituto Oswaldo Cruz* 2007; 102: 79–82
215. Dey R, Joshi AB, Oliveira F, *et al.* Gut Microbes Egested during Bites of Infected Sand Flies Augment Severity of Leishmaniasis via Inflammasome-Derived IL-1 β . *Cell Host & Microbe* 2018; 23: 134-143.e6
216. Kima PE, Soong L. Interferon gamma in leishmaniasis. *Frontiers in Immunology* 2013; 4: 156
217. Garelnabi M, Taylor-Smith LM, Bielska E, Hall RA, Stones D, May RC. Quantifying donor-to-donor variation in macrophage responses to the human fungal pathogen *Cryptococcus neoformans*. *PloS one* 2018; 13: e0194615
218. Crauwels P, Bank E, Walber B, *et al.* Cathelicidin Contributes to the Restriction of *Leishmania* in Human Host Macrophages. *Frontiers in Immunology* 2019; 10: 2697
219. Lambertz U, Oviedo Ovando ME, Vasconcelos EJR, Unrau PJ, Myler PJ, Reiner NE. Small RNAs derived from tRNAs and rRNAs are highly enriched in exosomes from both old and new world *Leishmania* providing evidence for conserved exosomal RNA Packaging. *BMC Genomics* 2015; 16: 151
220. Iqbal S, Kumar A. Characterization of In vitro Generated Human Polarized Macrophages. *Journal of Clinical & Cellular Immunology* 2015; 06
221. Mbow ML, Bleyenbergh JA, Hall LR, Titus RG. *Phlebotomus papatasi* sand fly salivary gland lysate down-regulates a Th1, but up-regulates a Th2, response in mice infected with *Leishmania major*. *Journal of immunology (Baltimore, Md. : 1950)* 1998; 161: 5571–7

6. Supplement

Supp. Table 1. Primers that were used for the generation and confirmation of CRISPR/Cas9 KOs.

Nr.	Target	Gene ID	Primer Name	Sequenz 5'--> 3'
C1_1	Dipeptidyl peptidase 3	LmjF.05.0960	LmjF.05.0960 fw	ACCGTAACCCCTAACCCTCCGgtataatgcagacctgtgc
C1_2			LmjF.05.0960 rev	TTTCCACTACTGCTGTCCCGGTTGCCcCaatttgagagacctgtgc
C1_3			LmjF.05.0960 sg fw	gaaattaatagcactcactataggAGCACAAAGCACGGGATCTGTgttttaga gctagaaatagc
C1_4			LmjF.05.0960 sg rev	gaaattaatagcactcactataggTAGGAGCGTCTCCCGCATGgttttagag ctagaaatagc
C1_5			LmjF.05.0960_Primer 1_2	TGTCGCACAACACGCTTTAC
C1_6			LmjF.05.0960_Primer 2_2	CCATGATGATGTCGCGGTAGT
C1_7			LmjF.05.0960_Primer 3_2	GTTTCCACTACTGCTCTGC
C2_1	Putative ATP- binding cassette protein subfamily G,member 2	LmjF.06.0090	LmjF.06.0090 fw	CTTCCACTGGCTTCTCGTTCGCCGGCGCCGgtataatgcagacctgtgc
C2_2			LmjF.06.0090 rev	CCGCAAAACAGAAAGCTCGAAGCTTCGCCAcCaatttgagagacctgtg c
C2_3			LmjF.06.0090 sg fw	gaaattaatagcactcactataggAAGGCAGAGTGTACGGGGAgtttag agctagaaatagc
C2_4			LmjF.06.0090 sg rev	gaaattaatagcactcactataggTCGGGTGAAAATGGTGACTGgttttaga gctagaaatagc
C2_6			LmjF.06.0090_Primer 2	ATGCAGCCCCACCATCCAGT
C2_8			LmjF.06.0090_Primer 1_new	TACAGAGGACACCTACACCGACTACT
C2_11			LmjF.06.0090_Primer 3_NTI	ATCACAGCTGCCAGATGCG
C3_1	EndoG	LmjF.10.0610	LmjF.10.0610 fw	AAGAGTCCCTCGCAGTGTCTGCTCCCTGTCCgtataatgcagacctgtgc
C3_2			LmjF.10.0610 rev	GCACACAAGTGATGGCGTTGTGGTGTCTCCAcCaatttgagagacctgtg c
C3_3			LmjF.10.0610 sg fw	gaaattaatagcactcactataggGTTGCGGAAACGATTCATCgttttaga gctagaaatagc
C3_4			LmjF.10.0610 sg rev	gaaattaatagcactcactataggTTGCCCTCGTTGCTGTTACGgttttagag ctagaaatagc
C3_5			LmjF.10.0610_Primer 1	CGCAGCCTCTGTTGGTCTCTTC
C3_6			LmjF.10.0610_Primer 2	TCGCTCTGCCTGGTCGATCA
C3_7			LmjF.10.0610_Primer 3	TGTGTGTCGAGGTGCTTTCCGT
C3_8			LmjF.10.0610_Addbac k_fw	CC CTCGAG ATGATCGCCCGG
C3_9			LmjF.10.0610_Addbac k_rev	GGAATTCcatagTCAGCGTCTCT
C4_1			Putative phosphatidyl serine synthase	LmjF.14.1200
C4_2	LmjF.14.1200 rev	TGAGCTGCCACCCACCCACCCCTCcaatttgagagacctgtgc		
C4_3	LmjF.14.1200 sg fw	gaaattaatagcactcactataggTGCCTGATGCGTGTATGTAgtttaga gctagaaatagc		
C4_4	LmjF.14.1200 sg rev	gaaattaatagcactcactataggAGAGAAGGCGACGGACAACGgttttag agctagaaatagc		
C4_5	LmjF.14.1200_Primer 1	ATGCGTCGAGGTCCGGATGA		
C4_6	LmjF.14.1200_Primer 2	CGTACAGCTCTCGAAGCACGA		
C4_7	LmjF.14.1200_Primer 3	ATGAGAGAAGGAAGGTGGAGCAGAC		
C5_1		LmjF.15.1060	LmjF.15.1060 fwd	CCCATCTTTGTTTTCTCTCTCCCGCGCCGgtataatgcagacctgtgc

C5_2	Tryparedoxin peroxidase		LmjF.15.1060 rev	ACGGTAAAGAGGCAGGTGTGTGGCCGTCCAcCaatttgagagacctgtgc
C5_3			LmjF.15.1060 sg fwd	gaaattaatacagactcactataggGCTGGCTGGTGGCTGCGAGGgttttagagctagaataagc
C5_4			LmjF.15.1060 sg rev	gaaattaatacagactcactataggTGTCTGAGCTCACTTACAGCgttttagagctagaataagc
C5_5			LmjF.15.1060_Primer 1	CATGTCCTGCGGTAACGCCA
C5_6			LmjF.15.1060_Primer 2	ACGGTGATCTGACGCAGCATG
C5_7			LmjF.15.1060_Primer 3	CCGACGTACATCCTCCTCCAGC
C6_1			Elongation factor 1-alpha	LmjF.17.0082
C6_2	LmjF.17.0082 rev	GCGTGGGGGAGGGATACAAGCGAAAAGAAAcCaatttgagagacctgtgc		
C6_3	LmjF.17.0082 sg fwd	gaaattaatacagactcactataggCGTGATGTTAGATAGCGAGCgttttagagctagaataagc		
C6_4	LmjF.17.0082 sg rev	gaaattaatacagactcactataggGGGGTGGAGGGAGGGGGCGCgttttagagctagaataagc		
C6_5	LmjF.17.0082_Primer 1	ATGGGCAAGGATAAAGGTGCATGA		
C6_6	LmjF.17.0082_Primer 2	TTACTTCTCGAAGCCTTCGCGGC		
C6_7	LmjF.17.0082_Primer 3	GGGGGAAAAGAGGAGAGGCC		
C6_8	LmjF.17.0082_Primer 3_2	TTTGGGGAAAAGAGGAGAGGTCC		
C7_1	Uncharacterized protein	LmjF.18.1300		
C7_2			LmjF.18.1300 rev	AACACAGCGCTACTCCTGCATCGCTCCCTccaatttgagagacctgtgc
C7_3			LmjF.18.1300 sg fwd	gaaattaatacagactcactataggTGGAGCGAGGCGTAAAGAGgttttagagctagaataagc
C7_4			LmjF.18.1300 sg rev	gaaattaatacagactcactataggGGCTGCGTGGGTGTAGGGAGgttttagagctagaataagc
C7_5			LmjF.18.1300_Primer 1	ATGTCTCCACAGACCGCTTCAGC
C7_6			LmjF.18.1300_Primer 2	CCTCCACTGGCATCGTCACAATG
C7_7			LmjF.18.1300_Primer 3	ATACACCACCGTCCGACACT
C8_1	40S ribosomal protein S2	LmjF.19.0060	LmjF.19.0060 fwd	CGCACACAAACCGGAACTCCATATGTCCAgataatgcagacctgtgc
C8_2			LmjF.19.0060 rev	AATGACTGTCACCCTTGAGGTAAGACCTccaatttgagagacctgtgc
C8_3			LmjF.19.0060 sg fwd	gaaattaatacagactcactataggTCTAGGAGAAGACAGCTCGTgttttagagctagaataagc
C8_4			LmjF.19.0060 sg rev	gaaattaatacagactcactataggTAAGGCTTGATAGCAGAGAgtttttagagctagaataagc
C8_5			LmjF.19.0060_Primer 1	CAGATACTCAGCCTGCTCAGGAGG
C8_6			LmjF.19.0060_Primer 2	CGGCAAACCTCGAGGATCTTCTTG
C8_7			LmjF.19.0060_Primer 3	AGCGTACTCGACCAATATGCGACT
C9_1			p1/s1 nuclease	LmjF.30.1510
C9_2	LmjF.30.1510 rev	CAGGTGCAGGCACACTCCGCATCGGTGCGCccaatttgagagacctgtgc		
C9_8	LmjF.30.1510 rev NEU	CTGTGCAATTCATCAGCAAGCCCGTGCAGTccaatttgagagacctgtgc		
C9_3	LmjF.30.1510 sg fwd	gaaattaatacagactcactataggAGTGCAGCACTGTTGAGGCGgttttttagagctagaataagc		
C9_9	LmjF.30.1510 sg fwd NEU	gaaattaatacagactcactataggGTGCGCGCAGAGGATAGAAATGGgttttagagctagaataagc		

SUPPLEMENT

C9_10			LmjF.30.1510 sg rev NEU	gaaattaatacgactcactataggGTAGGCACATGACCTGTCCATCGGgtt ttagagctagaataatagc
C9_5			LmjF.30.1510_Primer 1	TCCGTCTGCCTCTCACAGTGCT
C9_6			LmjF.30.1510_Primer 2	CTCCTCGTGAATCGCCACCA
C9_7			LmjF.30.1510_Primer 3	TCAGCCCTTCGTCGCTTTCC
C9_11			LmjF.30.1510_Primer 4	GCTTCGTTTGTCTCTGTACCATTTTCT
C10_1	Pyruvate kinase	LmjF.35.0020	LmjF.35.0020 fwd	ATCGGTCCCAGCACGCAGAGTGTGGAGGCGgtataatgcagacctgct gc
C10_2			LmjF.35.0020 rev	TGGACATGAGAACTTCAAAGTCATCGCCGccaatttgagagacctgtg c
C10_3			LmjF.35.0020 sg fwd	gaaattaatacgactcactataggCTGAAGGGGCTGATTGAGAGgttttaga gctagaataatagc
C10_4			LmjF.35.0020 sg rev	gaaattaatacgactcactataggGTACACAACCTTTGCGGCAAgttttaga gctagaataatagc
C10_5			LmjF.35.0020_Primer 1	GTCTGTTGCGCGCATGAACTTC
C10_6			LmjF.35.0020_Primer 2	GAACACACTCTCCACGCTTGTG
C10_7			LmjF.35.0020_Primer 3	GGCACATACGAGGAAAGATCACAGA
C11_1	Putative polyubiquitin	LmjF.36.3530	LmjF.36.3530 fwd	TGCCTTTCATTCTTGCGTCTTGCATTCCGgtataatgcagacctgctgc
C11_2			LmjF.36.3530 rev	CATCGTAGTGACAGAAAAAGCAAAAACACCCccaatttgagagacctgtg c
C11_3			LmjF.36.3530 sg fwd	gaaattaatacgactcactataggAAGAACGAGGGTAAACGgttttag agctagaataatagc
C11_4			LmjF.36.3530 sg rev	gaaattaatacgactcactataggGGCTGAAGCGCTGTAGCCAAgttttaga gctagaataatagc
C11_5			LmjF.36.3530 Primer 1	CGTGAAGACGCTGACCGCAAG
C11_6			LmjF.36.3530 Primer 2	GTGCAGCGTGGACTCCTTCTGG
C11_7			LmjF.36.3530 Primer 3	CAACACTAACCCGCTTCGAGACAAT
C12_1	Putative carboxypepti dase	LmjF.36.6260	LmjF.36.6260 fwd	TGCCTCCTGTTGAAGGAGGCGCTGCTGGTgtataatgcagacctgctg c
C12_2			LmjF.36.6260 rev	ACGGACCTGATCCTCAACAATTTCCGAGTGccaatttgagagacctgtgc
C12_3			LmjF.36.6260 sg fwd	gaaattaatacgactcactataggTAAGGACGAACTCGCCGAGGgttttaga gctagaataatagc
C12_4			LmjF.36.6260 sg rev	gaaattaatacgactcactataggCAAACGAGCAAATGGAAAACgttttaga gctagaataatagc
C12_5			LmjF.36.6260_Primer 1	ATGGTGCCTGTCACAAACTTGC
C12_6			LmjF.36.6260_Primer 2	TCCTGTAGGCAACCGAGGTCGT
C12_7			LmjF.36.6260_Primer 3	GCGCGGTTGTGCTTCGTTTT
C13_1	Superoxide dismutase	LmjF.32.1820	LmjF.32.1820 fwd	ATTCCGTTCTCACGGTTCTTCTACATCCCTgtataatgcagacctgctgc
C13_2			LmjF.32.1820 rev	ACTCGCTCGGCCTCTCTCTCGTGAACCTCCAccaatttgagagacctgtgc
C13_3			LmjF.32.1820 sg fwd	gaaattaatacgactcactataggCGCACGAACAGAAAGTAAGCgttttaga gctagaataatagc
C13_4			LmjF.32.1820 sg rev	gaaattaatacgactcactataggGTTGTCTGCGATACACAGTgttttagag ctagaataatagc
C13_5 .1			LmjF.32.1820_Primer 1 neu	CGCTGTTGAGCCGCTGCCGTA
C13_6 .1			LmjF.32.1820_Primer 2 neu	TAGAGGCGAAATTCAGTCCACCATGTT
C13_7 .1			LmjF.32.1820_Primer 3 neu	GCTCCTTCTACTATACCGTTCGCTACTT

C14_5	SMP4	LmjF.20.1280	LmjF.20.1280_Primer 1	ATGGGGAACAAGCAGTCACACGC
C14_6			LmjF.20.1280_Primer 2	CTACCGCGTGCTACTGCCGAG
C14_7			LmjF.20.1280_Primer 3	TGGGTGCACTTCTCCACATGAGATCT
C15_1	G6PD	LmjF.34.0080	LmjF.34.0080_fwd	AATCTCGTTCGGTGTTCCTCCGGCTGCCAgtataatgcagacctgctgc
C15_2			LmjF.34.0080_rev	TGCCTCTCTCGCTGTCGTCGACAGGGCCCTccaatttgagagacctgtgc
C15_3			LmjF.34.0080_sg_fwd	gaaattaatagactcactataggGGATAACGCCGATCAATATAgttttagagctagaaatagc
C15_4			LmjF.34.0080_sg_rev	gaaattaatagactcactataggGACATTGCAGTCTGTTTCACgttttagagctagaaatagc
C15_5			LmjF.34.0080_Primer 1	AGCAGTCTCATGCTGATCAGGATGC
C15_6			LmjF.34.0080_Primer 2	TTCGAGGGAAGCCATTGGTAGCCTT
C15_7			LmjF.34.0080_Primer 3	CCTTCCCTTGCCAACACCCAC
C16_1	PGD	LmjF.35.3340	LmjF.35.3340_fwd	TTCACTGGCGCTTAGTTCATCATACACCCgtataatgcagacctgctgc
C16_2			LmjF.35.3340_rev	GGGTGAAGGGAAGCGGTTGAGCGGCTACCTccaatttgagagacctgtgc
C16_3			LmjF.35.3340_sg_fwd	gaaattaatagactcactataggGTGTGTGTGAAAAGGGTGTGtttttagagctagaaatagc
C16_4			LmjF.35.3340_sg_rev	gaaattaatagactcactataggGCTCTCACCTAGCCGCTCTGtttttagagctagaaatagc
C16_5.1			LmjF.35.3340_Primer 1 NEU	GCGCGAATCTCGCCCTGAACATC
C16_6.1			LmjF.35.3340_Primer 2 NEU	CATTCGAACGACTCACGACCGTCC
C16_7.1			LmjF.35.3340_Primer 3 NEU	CTTGTCAGTGGAGGTGTTTCTGTGTG
C17_1	Metacaspase	LmjF.35.1580	LmjF.35.1580_fwd	CTCCCTCCGCTTCTCGTTCAGTGCCTCCgtataatgcagacctgctgc
C17_2			LmjF.35.1580_rev	AAAGAGGTGGTGTGGGCGGTGACACACCTccaatttgagagacctgtgc
C17_3			LmjF.35.1580_sg_fwd	gaaattaatagactcactataggCGTATTGTCCTTCGTTGTGCtttttagagctagaaatagc
C17_4			LmjF.35.1580_sg_rev	gaaattaatagactcactataggAGATACATCAGAACGTGTGTtttttagagctagaaatagc
C17_5			LmjF.35.1580_Primer 1	ATGGCAGACCTTTTGTATTTGGGGG
C17_6			LmjF.35.1580_Primer 2	GAACGTGTAAGGCTGGAGG
C17_7			LmjF.35.1580_Primer 3	ACATCGTCTCTCCACCCCTC
C19_1	G6PD	LdBPK_340080.1	LdBPK_340080.1_fwd	CCTTGTTCCTCCGGCTACCATATATTGATgtataatgcagacctgctgc
C19_2			LdBPK_340080.1_rev	ATAGGCACGCATCCAGTGTATAACACCCTGccaatttgagagacctgtgc
C19_3			LdBPK_340080.1_sg_fwd	gaaattaatagactcactataggTGGTGTATACAAATCAAGTtttttagagctagaaatagc
C19_4			LdBPK_340080.1_sg_rev	gaaattaatagactcactataggACTCTCTCGTGTGTCGACgtttttagagctagaaatagc
C19_5			LdBPK_340080.1_Primer 1	GTCCGAAGAGCAGTCTCATGCTG
C19_6			LdBPK_340080.1_Primer 2	ACGGAAGCCAGTGGTAGCCT
C19_7			LdBPK_340080.1_Primer 3	CAGAGCGGACCACGTGATT
C20_1	PGD	LdBPK_353390.1	LdBPK_353390.1_fwd	GCGCTTAGTCCCATCATACACCCACACCCgtataatgcagacctgctgc
C20_2			LdBPK_353390.1_rev	CTCAACTGGCAGAGGGGGAGAAGGGAACCGccaatttgagagacctgtgc
C20_5			LdBPK_353390.1_rev_phleo	CTCAACTGGCAGAGGGGGAGAAGGGAACCGcttgcgtctcgaacgctgt

SUPPLEMENT

C20_3		LdBPK_353390.1_sg fwd	gaaattaatagcactactataggTCTGTGTGTGTGTGAAAAgttttaga gctagaatagc	
C20_4		LdBPK_353390.1_sg rev	gaaattaatagcactactataggGTTGAGCGGCTAGCTGAGAGgttttaga gctagaatagc	
Scaffold			Aaaagcaccgactcgggtgccacttttcaagttgataaccgactagcctattttaact tgctatttctagctctaaaac	
	LdG6PD	LdBPK_340080.1	LdG6PD_Neo_rev	GCATGAGACTGCTCTTCGGACATGGTGCCTGCACAGGTCTCTCAA ATTGG
			LdG6PD_Puro_fwd	CAGACATTGCAGTCTGTTTCACAGTACCCTgcccattacgcatgatcta
			LdG6PD_Puro_rev	ATAGGCACGCATCCAGTGTATAACACCCTGaagaaagctgggtccatg g
	LdPGD	LdBPK_353390.1	LdPGD_rev_Neo	GTCGTTTCGACATAGAGAATAAGGGATTCTGTGCACAGGTCTCTCA AATTGG
			LdPGD_fwd_Puro	CTGCAGTAGACAGCCGCTCTCACCTAGCCGccccattacgcatgatct a
			LdPGD_rev_Puro	CTCAACTGGCAGAGGGGGAGAAGGGAACCGaagaaagctgggtcca tgg

Supp. Table 2. Proteins that were upregulated (green) or downregulated (red) in promastigotes that were treated with staurosporine for 6 hours.

Entry	Protein names	Gene names
Q4Q1X2	Uncharacterized protein	LMJF_36_1040
Q4QIE1	Putative ribosomal protein L2	LMJF_08_0280
Q4QEI8	Elongation factor 1-alpha	LMJF_17_0082
Q4QDL5	40S ribosomal protein S2	LMJF_19_0060
Q4Q165	Putative polyubiquitin	LMJF_36_3530
Q4Q7F3	p1/s1 nuclease	LMJF_30_1510
E9ACF1	D-3-phosphoglycerate dehydrogenase-like protein, EC 1.1.1.95	LMJF_03_0030
E9ACN5	Putative peter pan protein	LMJF_03_0900
E9ACW8	Pre-mRNA-processing factor 19, EC 2.3.2.27	LMJF_27_2480
E9ACY7	Protein kinase domain-containing protein	LMJF_27_0100
E9ACY8	Uncharacterized protein	LMJF_27_0110
E9AD18	Putative heat shock protein DNAJ	LMJF_27_0410
E9AE43	Putative Tob55	LMJF_29_1820
E9AE93	Enoyl-CoA hydratase/isomerase-like protein	LMJF_29_2310
E9AEB7	Uncharacterized protein	LMJF_29_2550
E9AEW0	Uncharacterized protein	LMJF_35_1370
P35549	rRNA 2'-O-methyltransferase fibrillarin, EC 2.1.1.- (Histone-glutamine methyltransferase)	
P69201	Ubiquitin-60S ribosomal protein L40 [Cleaved into: Ubiquitin; 60S ribosomal protein L40 (CEP52)]	UB-EP52, LmjF31.1900, LmjF_31_1900, LmjF31.2030, LmjF_31_2030
P90628	Cathepsin L-like protease	
Q4Q1W4	Uncharacterized protein	LMJF_36_1120
Q4Q2E4	AP-1 complex subunit gamma	LMJF_34_3970
Q4Q2T0	Uncharacterized protein	LMJF_34_2650
Q4Q3A0	SET domain-containing protein	LMJF_34_1050

Q4Q3H0	Uncharacterized protein	LMJF_34_0380
Q4Q3U9	Putative Golgi reassembly stacking protein	LMJF_33_2380
Q4Q3Y6	Calpain protease-like protein, EC 3.4.22.-, EC 3.4.22.33	LMJF_33_2010
Q4Q3Z5	Uncharacterized protein	LMJF_33_1920
Q4Q4C7	FCP1 homology domain-containing protein	LMJF_33_0780
Q4Q4U6	Glucosamine-6-phosphate isomerase, EC 3.5.99.6 (Glucosamine-6-phosphate deaminase)	LMJF_32_3260
Q4Q5K3	Uncharacterized protein	LMJF_32_0790
Q4Q5L0	Pan3_PK domain-containing protein	LMJF_32_0720
Q4Q5L4	Ribosomal_S4 domain-containing protein	LMJF_32_0690
Q4Q5Z0	Phosphatidylinositol-4-phosphate 5-kinase-like protein	LMJF_31_2710
Q4Q6B4	Uncharacterized protein	LMJF_31_1480
Q4Q6X3	Meiosis-specific nuclear structural protein 1	LMJF_30_3170
Q4Q7N8	Putative nuclear movement protein	LMJF_30_0700
Q4Q8P1	Uncharacterized protein	LMJF_28_0290
Q4Q8S4	Putative ATP-binding cassette protein subfamily B, member 2	ABCB2 LMJF_26_2670
Q4Q9D6	ApaG domain-containing protein	LMJF_26_0580
Q4Q9E1	Uncharacterized protein	LMJF_26_0500
Q4Q9W6	Uncharacterized protein	LMJF_25_1270
Q4Q187	Actin-like protein 2 (Putative actin-like protein)	ALP2 LMJF_36_3310
Q4Q189	Uncharacterized protein	LMJF_36_3290
Q4Q220	Uncharacterized protein	LMJF_36_0560
Q4Q281	Putative 1,2-Dihydroxy-3-keto-5-methylthiopentene dioxygenase, EC 1.13.11.54	LMJF_34_4600
Q4Q367	Uncharacterized protein	LMJF_34_1350
Q4Q455	Cysteine conjugate beta-lyase,aminotransferase-like protein	LMJF_33_1330
Q4Q463	Uncharacterized protein	LMJF_33_1260
Q4Q471	Uncharacterized protein	LMJF_33_1190
Q4Q596	Superoxide dismutase, EC 1.15.1.1	SODB2, LMJF_32_1830
Q4Q713	Uncharacterized protein	LMJF_30_2800
Q4Q941	RRM domain-containing protein	LMJF_26_1530
Q4Q984	Uncharacterized protein	LMJF_26_1100
Q4QA82	Uncharacterized protein	LMJF_25_0140
Q4QAK4	Amastin-like surface protein-like protein	LMJF_24_1280
Q4QCF0	Uncharacterized protein	LMJF_21_0650
Q4QD96	Uncharacterized protein	LMJF_19_1190
Q4QDZ0	Uncharacterized protein	LMJF_18_0520
Q4QDZ3	BTB_2 domain-containing protein	LMJF_18_0490
Q4QDZ7	Carboxypeptidase, EC 3.4.16.-	LMJF_18_0450
Q4QEAO	Uncharacterized protein	LMJF_17_0900

SUPPLEMENT

Q4QEC8	Uncharacterized protein	LMJF_17_0760
Q4QEF9	Dus domain-containing protein	LMJF_17_0350
Q4QF67	TFIIB_C_1 domain-containing protein	LMJF_15_1170
Q4QFA4	Peroxisomal membrane protein PEX16	LMJF_15_0810
Q4QFG4	Cytochrome b5 heme-binding domain-containing protein	LMJF_15_0190
Q4QGJ9	Putative surface antigen protein 2	LMJF_12_0760
Q4QHU2	AAA domain-containing protein	LMJF_09_0820
Q4QID2	Uncharacterized protein	LMJF_08_0370
Q4QIH8	Uncharacterized protein	LMJF_07_1080
Q4QIQ0	Putative 3-hydroxyacyl-ACP dehydratase, EC 4.2.1.-	HTD2-2, LMJF_07_0430
Q4QJ92	Methyltransfer_dom domain-containing protein	LMJF_05_1100
Q4QJ99	Uncharacterized protein	LMJF_05_1030
Q4QJC4	Uncharacterized protein	LMJF_05_0780
Q9N857	Putative exosome complex exonuclease RRP40	LMJF_04_0120

Supp. Table 3. Proteins that were upregulated (green) or downregulated (red) in promastigotes that were treated with staurosporine for 24 hours.

Entry	Protein names	Gene names
Q4QEI8	Elongation factor 1-alpha	LMJF_17_0082
Q4QDL5	40S ribosomal protein S2	LMJF_19_0060
Q4QDS7	RING-type domain-containing protein	LMJF_18_1150
Q4QHH2	Leishmanolysin, EC 3.4.24.36	GP63-1 LMJF_10_0460
Q4QIZ7	Uncharacterized protein	LMJF_06_0800
Q9XYH4	Prolyl endopeptidase, EC 3.4.21.-	opb
Q4Q4U3	Uncharacterized protein	LMJF_32_3290
Q4Q5P0	40S ribosomal protein S2	LMJF_32_0450
Q4Q6Z4	Glyceraldehyde-3-phosphate dehydrogenase, EC 1.2.1.12	LMJF_30_2980
Q4QAB3	Uncharacterized protein	LMJF_24_2170
Q4QAM1	Uncharacterized protein	LMJF_24_1120
Q4QBR7	Uncharacterized protein	LMJF_22_0800
Q25317	100 kDa heat shock protein (Hsp100)	

Supp. Table 4. Proteins that were upregulated (green) or downregulated (red) in promastigotes that were treated with miltefosine for 3 hours.

Entry	Protein names	Gene names
Q4QEI8	Elongation factor 1-alpha	LMJF_17_0082
Q4Q7F3	p1/s1 nuclease	LMJF_30_1510
Q4Q165	Putative polyubiquitin	LMJF_36_3530
Q4QDL5	40S ribosomal protein S2	LMJF_19_0060
Q4Q4Z5	Uncharacterized protein	LMJF_32_2800
Q4Q6Z4	Glyceraldehyde-3-phosphate dehydrogenase, EC 1.2.1.12	LMJF_30_2980

Q4QDX2	Citrate synthase	LMJF_18_0670
Q4QE9	ATP pyrophosphate-lyase (Adenylyl cyclase)	RAC-B4 LMJF_17_0237

Supp. Table 5. Proteins that were upregulated (green) or downregulated (red) in promastigotes that were treated with miltefosine for 24 hours.

Entry	Protein names	Gene names
Q4QEI8	Elongation factor 1-alpha	LMJF_17_0082
Q4Q7F3	p1/s1 nuclease	LMJF_30_1510
Q4QDL5	40S ribosomal protein S2	LMJF_19_0060
Q4Q165	Putative polyubiquitin	LMJF_36_3530
Q9NED9	Uncharacterized protein	LMJF_04_0630
Q4QIS6	Uncharacterized protein	LMJF_07_0180
Q4QF48	Uncharacterized protein	LMJF_15_1340
Q4Q3H6	Uncharacterized protein	LMJF_34_0320
Q4QHD9	Uncharacterized protein	LMJF_10_0750
P35549	rRNA 2'-O-methyltransferase fibrillarin, EC 2.1.1.- (Histone-glutamine methyltransferase)	LMJF_27_0100
Q4Q4D3	Putative 60S ribosomal protein L6	LMJF_33_0720
Q4QIE1	Putative ribosomal protein L2	LMJF_08_0280
Q4QFR7	Elongation of fatty acids protein, EC 2.3.1.199 (Very-long-chain 3-oxoacyl-CoA synthase)	ELO2 LMJF_14_0670
Q4Q1X2	Uncharacterized protein	LMJF_36_1040
Q4Q463	Uncharacterized protein	LMJF_33_1260
Q4Q0D6	Uncharacterized protein	LMJF_36_6240
Q4Q1T7	Uncharacterized protein	LMJF_36_1390
Q4QGM9	PriCT_2 domain-containing protein	LMJF_12_0640
O97206	Uncharacterized protein	LMJF_04_0490
Q4Q3Q8	Putative ubiquitin-conjugating enzyme, EC 6.3.2.19	LMJF_33_2770
Q4Q3B2	Uncharacterized protein	LMJF_34_0930
Q4QC17	Uncharacterized protein	LMJF_21_1670
Q4Q8B9	Qa-SNARE protein	LMJF_28_1470
Q4QBA5	Uncharacterized protein	LMJF_23_0580
Q4QJ11	Uncharacterized protein	LMJF_06_0670
Q4QIB7	Uncharacterized protein	LMJF_08_0520
Q4QE31	Uncharacterized protein	LMJF_18_0110
Q4Q3L0	ABC transporter family-like protein	LMJF_33_3260
Q4Q6K5	Putative amino acid transporter aATP11	AAT25.2 LMJF_31_0580
Q4QHB1	RNA-binding protein-like protein	LMJF_10_1030
Q4Q5F9	Putative ADP-ribosylation factor GTPase activating protein 1	LMJF_32_1230
Q4QEC7	EF-hand domain-containing protein	LMJF_17_0750
Q4QD77	Uncharacterized protein	LMJF_19_1347

SUPPLEMENT

Q4Q8S1	6-phosphogluconolactonase, 6PGL, EC 3.1.1.31	LMJF_26_2700
Q4Q227	Putative mitochondrial carrier protein	LMJF_36_0510
Q4QAT1	Uncharacterized protein	LMJF_24_0500
Q4Q768	Conserved zinc-finger protein	LMJF_30_2250
Q4QIS8	Protein kinase domain-containing protein	LMJF_07_0160
Q9XYH9	Putative glycoprotein	
Q4Q0N6	Putative adaptin	LMJF_36_5260
Q4Q7M6	Uncharacterized protein	LMJF_30_0790
Q4QBP4	Uncharacterized protein	LMJF_22_1030
Q4QAZ9	Putative Qb-SNARE protein	LMJF_23_1740
Q4QB42	Uncharacterized protein	LMJF_23_1140
Q4Q233	Uncharacterized protein	LMJF_36_0450
Q4QFI2	Uncharacterized protein	LMJF_15_0020
Q4QB64	Uncharacterized protein	LMJF_23_0990
Q9GRN2	Uncharacterized protein L8530.04	L8530.04 LMJF_33_2150
Q4Q222	Putative ubiquitin-like protein	LMJF_36_0540
Q4QD96	Uncharacterized protein	LMJF_19_1190
Q4QDS4	Uncharacterized protein	LMJF_18_1180
Q4QDH4	Putative nuclear cap binding complex subunit CBP30	CBP30 LMJF_19_0470
Q4QG27	DNA/RNA non-specific endonuclease-like protein	LMJF_13_1270
Q4Q9S0	Uncharacterized protein	LMJF_25_1700
Q4Q1I0	Cullin_Nedd8 domain-containing protein	LMJF_36_2410
Q4Q3P2	Uncharacterized protein	LMJF_33_2930
Q4QBS1	Uncharacterized protein	LMJF_22_0760
Q4Q6Z4	Glyceraldehyde-3-phosphate dehydrogenase, EC 1.2.1.12	LMJF_30_2980
Q4Q2L9	Putative pyruvate/indole-pyruvate carboxylase, EC 4.1.1.74	LMJF_34_3250
Q4QJD2	Uncharacterized protein	LMJF_05_0700
Q4Q883	DNA repair protein-like protein	LMJF_28_1830
E9AEN3	Conserved SNF-7-like protein	LMJF_35_0580
Q4Q842	2,3-bisphosphoglycerate-independent phosphoglycerate mutase-like, EC 5.4.2.1	LMJF_28_2220
Q4QF27	Uncharacterized protein	LMJF_15_1520
Q4Q9P4	Putative kinesin, EC 3.6.4.4	LMJF_25_1950
Q4QGT2	Uncharacterized protein	LMJF_12_0110
Q4QED3	Uncharacterized protein	LMJF_17_0610
Q4Q6S9	40S ribosomal protein S14	LMJF_30_3590
Q4QI51	Pre-mRNA-splicing factor SLU7	LMJF_08_1180
Q4Q4W6	Uncharacterized protein	LMJF_32_3060
Q4Q3N2	ABC transporter family-like protein	LMJF_33_3040
Q4QCA1	PDCD2_C domain-containing protein	LMJF_21_0950

Q4Q105	Glycosyl hydrolase-like protein	LMJF_36_4100
Q4QHY9	Putative DNA photolyase, EC 4.1.99.3	LMJF_09_0360
Q1X7J8	Excreted/secreted protein 31	
E9AC13	Putative DNA excision/repair protein SNF2	LMJF_01_0240
Q4Q5Y5	Uncharacterized protein	LMJF_31_2750
E9AC97	Phosphoglycan beta 1,2 arabinosyltransferase	SCA1 LMJF_02_0220
Q4QEB7	Uncharacterized protein	LMJF_17_0690
Q4Q9G1	Aminopeptidase, EC 3.4.11.-	LMJF_26_0300
Q4Q5D0	YqaJ domain-containing protein	LMJF_32_1510
Q4QAL6	Uncharacterized protein	LMJF_24_1160
Q4QAA2	General transcription and DNA repair factor IIH helicase subunit XPD, EC 3.6.4.12	LMJF_24_2280
P08148	Leishmanolysin, EC 3.4.24.36 (Cell surface protease) (Major surface glycoprotein) (Major surface protease) (Promastigote surface endopeptidase) (Protein gp63)	gp63
Q4QE9H	ATP pyrophosphate-lyase (Adenylyl cyclase)	RAC-B4 LMJF_17_0237
E9AE05	Uncharacterized protein	LMJF_29_1460
Q4Q1P6	Uncharacterized protein	LMJF_36_1780
E9AC30	Uncharacterized protein	LMJF_01_0390
Q4QBH9	Phosphoinositide phospholipase C, EC 3.1.4.11	LMJF_22_1680
E9ADP8	Uncharacterized protein	LMJF_29_0470
Q4Q3K1	Glucose-6-phosphate 1-dehydrogenase, EC 1.1.1.49	G6PD LMJF_34_0080
Q4QDX2	Citrate synthase	LMJF_18_0670
E9AD66	Putative phosphatidylinositol (3,5) kinase	LMJF_27_0890
Q4QH22	Uncharacterized protein	LMJF_09_0340
Q4Q1W1	Putative endonuclease/exonuclease/phosphatase	LMJF_36_1150
Q4Q1B2	Fibrillarlin	LMJF_36_3070
Q4Q3A1	Putative uracil phosphoribosyltransferase, EC 2.4.2.9	LMJF_34_1040
Q4QEL8	Putative kinesin, EC 3.6.4.4	LMJF_16_1470
Q4QER1	Ubiquitin-fold modifier 1	LMJF_16_1065
A1Y2D9	Prostaglandin f2-alpha synthase	
Q4Q966	Uncharacterized protein	LMJF_26_1280
E9AFX4	Protein kinase domain-containing protein	LMJF_35_5010

Supp. Table 6. Proteins that were upregulated (green) or downregulated (red) in promastigotes that were treated with harmonine 6 hours.

Entry	Protein names	Gene names
Q4Q1X2	Uncharacterized protein	LMJF_36_1040
Q4QEI8	Elongation factor 1-alpha	LMJF_17_0082
Q4QDL5	40S ribosomal protein S2	LMJF_19_0060
Q4Q165	Putative polyubiquitin	LMJF_36_3530

SUPPLEMENT

Q4Q7F3	p1/s1 nuclease	LMJF_30_1510
E9ACF1	D-3-phosphoglycerate dehydrogenase-like protein, EC 1.1.1.95	LMJF_03_0030
E9ACH4	FYVE-type domain-containing protein	LMJF_03_0270
E9ACY7	Protein kinase domain-containing protein	LMJF_27_0100
E9AE43	Putative Tob55	LMJF_29_1820
E9AE93	Enoyl-CoA hydratase/isomerase-like protein	LMJF_29_2310
E9AEI7	Uncharacterized protein	LMJF_35_0100
E9AF27	60S ribosomal protein L32	LMJF_35_2050
E9AF54	Uncharacterized protein	LMJF_35_2300
E9AFB4	Uncharacterized protein	LMJF_35_2900
E9AFL9	Uncharacterized protein	LMJF_35_3940
O97007	Uncharacterized protein	LMJF_04_0900
P69201	Ubiquitin-60S ribosomal protein L40 [Cleaved into: Ubiquitin; 60S ribosomal protein L40 (CEP52)]	UB-EP52 LmjF31.1900, LmjF_31_1900, LmjF31.2030, LmjF_31_2030
Q4Q3U9	Putative Golgi reassembly stacking protein	LMJF_33_2380
Q4Q3Y6	Calpain protease-like protein, EC 3.4.22.-, EC 3.4.22.33	LMJF_33_2010
Q4Q4P6	Putative enolase, EC 4.2.1.11	LMJF_32_3760
Q4Q5L0	Pan3_PK domain-containing protein	LMJF_32_0720
Q4Q5Z0	Phosphatidylinositol-4-phosphate 5-kinase-like protein	LMJF_31_2710
Q4Q7Y9	Uncharacterized protein	LMJF_28_2730
Q4Q8P1	Uncharacterized protein	LMJF_28_0290
Q4Q189	Uncharacterized protein	LMJF_36_3290
Q4Q220	Uncharacterized protein	LMJF_36_0560
Q4Q377	Putative NLI-interacting factor	LMJF_34_1250
Q4Q455	Cysteine conjugate beta-lyase,aminotransferase-like protein	LMJF_33_1330
Q4Q708	Uncharacterized protein	LMJF_30_2845
Q4Q747	Putative heat shock 70-related protein 1, mitochondrial	LMJF_30_2460
Q4Q984	Uncharacterized protein	LMJF_26_1100
Q4QAK4	Amastin-like surface protein-like protein	LMJF_24_1280
Q4QCF0	Uncharacterized protein	LMJF_21_0650
Q4QCQ0	Uncharacterized protein	LMJF_20_1440
Q4QD96	Uncharacterized protein	LMJF_19_1190
Q4QDZ0	Uncharacterized protein	LMJF_18_0520
Q4QDZ7	Carboxypeptidase, EC 3.4.16.-	LMJF_18_0450
Q4QE04	Uncharacterized protein	LMJF_18_0380
Q4QEA0	Uncharacterized protein	LMJF_17_0900
Q4QEC8	Uncharacterized protein	LMJF_17_0760
Q4QEL9	Putative kinesin, EC 3.6.4.4	LMJF_16_1460
Q4QF67	TFIIB_C_1 domain-containing protein	LMJF_15_1170

Q4QFG4	Cytochrome b5 heme-binding domain-containing protein	LMJF_15_0190
Q4QFZ2	Squalene monooxygenase, EC 1.14.14.17	LMJF_13_1620
Q4QH58	4a-hydroxytetrahydrobiopterin dehydratase, EC 4.2.1.96	LMJF_11_0220
Q4QI39	Uncharacterized protein	LMJF_08_1222, LMJF_08_1260
Q4QIH8	Uncharacterized protein	LMJF_07_1080
Q4QJ92	Methyltransfer_dom domain-containing protein	LMJF_05_1100
Q4QJC4	Uncharacterized protein	LMJF_05_0780

Supp. Table 7. Proteins that were upregulated (green) or downregulated (red) in promastigotes that were treated with compound 1o for 24 hours.

Entry	Protein names	Gene names
Q4Q7F3	p1/s1 nuclease	LMJF_30_1510
Q4Q165	Putative polyubiquitin	LMJF_36_3530
Q4QEI8	Elongation factor 1-alpha	LMJF_17_0082
Q4QEI9	Elongation factor 1-alpha	LMJF_17_0080, LMJF_17_0081, LMJF_17_0083, LMJF_17_0084, LMJF_17_0085
Q4QF68	Thiol specific antioxidant (Tryparedoxin peroxidase)	TRYP7, TRYP5, TSA, LMJF_15_1120, LMJF_15_1160
Q4QG20	Uncharacterized protein	LMJF_13_1340
Q9BJC7	Histone H2B	H2B
E9AF00	DNA polymerase II subunit 2	LMJF_35_1790
P08148	Leishmanolysin, EC 3.4.24.36 (Cell surface protease) (Major surface glycoprotein) (Major surface protease) (Promastigote surface endopeptidase) (Protein gp63)	gp63
Q4Q2Z6	ATP-dependent RNA helicase, EC 3.6.4.13	LMJF_34_2050
Q4Q6Z5	Glyceraldehyde-3-phosphate dehydrogenase, EC 1.2.1.12	LMJF_30_2970
Q4Q141	Putative 60S ribosomal protein L34	LMJF_36_3740

Supp. Table 8. Proteins that were upregulated (green) or downregulated (red) in promastigotes from the stationary growth phase.

Entry	Protein names	Gene names
Q4Q165	Putative polyubiquitin	LMJF_36_3530
Q4Q7F3	p1/s1 nuclease	LMJF_30_1510
Q4QEI8	Elongation factor 1-alpha	LMJF_17_0082
Q4QG30	TPK_B1_binding domain-containing protein	LMJF_13_1240

Q4QDL6	Histone H2B	H2B; LMJF_19_0030; LMJF_19_0040; LMJF_19_0050
E9ADZ9	Putative RNA binding protein	LMJF_29_1400
Q9XYH4	Oligopeptidase B (EC 3.4.21.83)	Opb
O97212	Nascent polypeptide associated complex subunit-like protein, copy 2	LMJF_04_0760

Supp. Table 9. Proteins that were upregulated (green) or downregulated (red) in amastigotes treated with staurosporine for 6 h.

Entry	Protein names	Gene names
A9LJZ6	Thiol-specific antioxidant antigen	TSA
P12076	Heat shock 70-related protein 1, mitochondrial	HSP70.1
Q4Q5Z0	Phosphatidylinositol-4-phosphate 5-kinase-like protein	LMJF_31_2710
Q4QCG2	Uncharacterized protein	LMJF_21_0530
Q4QBW9	zf-Tim10_DDP domain-containing protein	LMJF_22_0270
Q25306	Guanine nucleotide-binding protein subunit beta-like protein (Antigen LACK)	
E9ACL9	Putative cytochrome c oxidase copper chaperone	LMJF_03_0740
Q4QEV9	Putative histone H3	LMJF_16_0600
Q4Q793	Uncharacterized protein	LMJF_30_2010
Q25312	DNA-directed RNA polymerase subunit, EC 2.7.7.6	RPOIILS
Q4Q9Y5	RRM domain-containing protein	LMJF_25_1080
Q9GU34	Elongation factor 2	EF2-1
Q4QCL6	Putative ring-box protein 1	LMJF_21_0023
Q4Q2E8	Non-specific serine/threonine protein kinase, EC 2.7.11.1	TOR3 LMJF_34_3940
Q25317	100 kDa heat shock protein (Hsp100)	
Q4QCC2	Xanthine phosphoribosyltransferase, EC 2.4.2.22, EC 2.4.2.8	XRPT LMJF_21_0850
Q4Q267	Uncharacterized protein	LMJF_36_0110
Q4Q6R7	Putative CPSF-domain protein	LMJF_30_3710
Q4QCM6	Putative N-acyl-L-amino acid amidohydrolase, EC 3.5.1.14	LMJF_20_1550
Q4Q3U2	Uncharacterized protein	LMJF_33_2450
Q4Q0C1	Rab-GAP TBC domain-containing protein	LMJF_36_6370
Q4Q6Y4	Putative kinesin, EC 3.6.4.4	LMJF_30_3060
Q4QCA4	Histone H2A	LMJF_21_0915, LMJF_21_0920, LMJF_21_0930
Q4Q3J2	Malate dehydrogenase, EC 1.1.1.37	mMDH LMJF_34_0160
Q9XYH4	Prolyl endopeptidase, EC 3.4.21.-	opb
Q4QF49	ALP5 (Putative actin-like protein)	ALP5 LMJF_15_1330
Q4QIP4	DHC_N2 domain-containing protein	LMJF_07_0480

Q4Q9Y8	Ferroxidase, EC 1.16.3.1	LMJF_25_1050
Q4Q2Y2	Uncharacterized protein	LMJF_34_2180
Q25323	Glycoprotein 96-92	GP 96-92
E9ACK6	Kinase-like protein	LMJF_03_0610
E9AD29	Putative radial spoke protein 3	LMJF_27_0520
Q4Q3D3	Protein phosphatase, EC 3.1.3.16	LMJF_34_0730
Q4Q8L7	RAD50 DNA repair-like protein	LMJF_28_0530
Q4QBI7	Putative ser/thr protein phosphatase	LMJF_22_1600
Q4Q615	Putative lipase, EC 3.1.1.3	LMJF_31_2460
Q4Q2M1	RNA editing associated helicase 2,putativewith=GeneDB:Tb927.4.1500	REH2 LMJF_34_3230
Q4QER3	Stealth_CR3 domain-containing protein	LMJF_16_1050
Q4Q6Q1	Uncharacterized protein	LMJF_31_0130
Q4Q7J2	Putative RNA-binding protein	LMJF_30_1110
E9ADF2	Putative dynein heavy chain	LMJF_27_1750
Q4Q0E9	Putative centrin	LMJF_36_6110
Q4QG19	Uncharacterized protein	LMJF_13_1350
Q4Q0F5	Uncharacterized protein	LMJF_36_6050
Q4QDW0	Uncharacterized protein	LMJF_18_0820
Q4Q5B5	Uncharacterized protein	LMJF_32_1650
A0A0B4ULI4	Phosphopyruvate hydratase, EC 4.2.1.11	
Q4Q626	Symplekin_C domain-containing protein	LMJF_31_2350
Q4Q8K9	Putative dynein heavy chain	LMJF_28_0610
Q4Q2D0	Uncharacterized protein	LMJF_34_4110
Q4QD15	Protein-serine/threonine kinase, EC 2.7.11.-	LMJF_20_0280
Q4QIS2	Uncharacterized protein	LMJF_07_0220
Q4QAT7	Hypothetical predicted transmembrane protein	LMJF_24_0440
Q4QH99	TPH domain-containing protein	LMJF_10_1150
E9AG12	Uncharacterized protein	LMJF_35_5390
Q6UQ31	Inorganic diphosphatase, EC 3.6.1.1	
E9AE23	Uncharacterized protein	LMJF_29_1610
P90627	Cathepsin B-like protease	
E9AF26	Putative ankyrin repeat protein	LMJF_35_2040
Q4Q5Q2	Uncharacterized protein	LMJF_32_0330
Q4Q1Z8	Calpain catalytic domain-containing protein	LMJF_36_0780
Q4Q7J6	Succinate dehydrogenase assembly factor 2, mitochondrial, SDH assembly factor 2, SDHAF2	LMJF_30_1070
Q4QER2	Uncharacterized protein	LMJF_16_1060
Q4QJB0	Putative paraflagellar rod protein	LMJF_05_0920

SUPPLEMENT

E9ADV5	Putative kinesin, EC 3.6.4.4	LMJF_29_0970
Q4Q0D2	Glucose transporter, Iugt3	LMJF_36_6280
O97194	Uncharacterized protein	LMJF_04_1150
Q4Q0B7	HU-CCDC81_euk_2 domain-containing protein	LMJF_36_6410
Q4QC01	60S ribosomal protein L37a (Putative 60S ribosomal protein L37a)	LMJF_21_1820, LMJF_36_1925
P39095	60S ribosomal protein L30	RPL30
Q4QJI2	Uncharacterized protein	LMJF_05_0210
Q4QF09	APH domain-containing protein	LMJF_16_0110
Q4QB24	Uncharacterized protein	LMJF_23_1280
Q4QFM2	Putative kinesin K39	LMJF_14_1120
E9AEQ8	FAD:protein FMN transferase, EC 2.7.1.180 (Flavin transferase)	LMJF_35_0830
Q4Q5U0	Uncharacterized protein	LMJF_31_3150
Q4Q801	Uncharacterized protein	LMJF_28_2610
Q4Q1Y1	Putative dynein heavy chain	LMJF_36_0950
E9AES4	Uncharacterized protein	LMJF_35_0990
Q4QG35	Adenylosuccinate synthetase, AMPsase, AdSS, EC 6.3.4.4 (IMP-- aspartate ligase)	Lmjf13.1190, Lmjf_13_1190
Q4QCW2	Cytochrome c oxidase assembly factor-like protein, EC 1.9.3.1	LMJF_20_0840
E9ADG8	Uncharacterized protein	LMJF_27_1895
E9ADH2	Uncharacterized protein	LMJF_27_1930
Q4QE92	Uncharacterized protein	LMJF_17_0990
Q4Q8E1	Uncharacterized protein	LMJF_28_1250
E9AD88	Uncharacterized protein	LMJF_27_1100
E9ACM1	Uncharacterized protein	LMJF_03_0760
Q4Q0C8	Serine/threonine-protein kinase TOR, EC 2.7.11.1	TOR1 LMJF_36_6320
Q4Q1P9	Uncharacterized protein	LMJF_36_1750
Q4QEN3	Uncharacterized protein	LMJF_16_1340
B8YDG1	Leishmanolysin, EC 3.4.24.36	
Q4Q325	Putative amastin-like surface protein	LMJF_34_1700, LMJF_34_1760, LMJF_34_1780, LMJF_34_1800, LMJF_34_1820
Q4QB21	Putative dynein heavy chain	LMJF_23_1310
Q4QE98	Putative ATP-dependent RNA helicase	LMJF_17_0920
E9AD28	Putative calpain-like cysteine peptidase	LMJF_27_0510
K7P5C3	Cathepsin L-like protease	Cpb
Q4QC61	V-type proton ATPase subunit H	LMJF_21_1340
Q4Q510	SpoU_methylase domain-containing protein	LMJF_32_2650

E9ADP6	Uncharacterized protein	LMJF_29_0450
Q4QHN3	Uncharacterized protein	LMJF_09_1420
Q4QGT2	Uncharacterized protein	LMJF_12_0110
Q4Q6Z4	Glyceraldehyde-3-phosphate dehydrogenase, EC 1.2.1.12	LMJF_30_2980
E9AEH9	Pyruvate kinase, EC 2.7.1.40	LMJF_35_0020
E9ADH0	Uncharacterized protein	LMJF_27_1910
Q4QJ94	Uncharacterized protein	LMJF_05_1080
Q4Q8V4	Uncharacterized protein	LMJF_26_2370
E9AEZ5	Ubiquitinyl hydrolase 1, EC 3.4.19.12	LMJF_35_1740
Q4QCF1	Putative phosphoglucomutase, EC 5.4.2.2	LMJF_21_0640
Q4QIR6	Putative ubiquitin-protein ligase-like, EC 6.3.2.19	LMJF_07_0280
Q4Q131	Diadenosine tetraphosphate synthetase, EC 6.1.1.14	LMJF_36_3840
Q4QEA3	META domain containing protein	META2 LMJF_17_0870
Q4QGZ8	Uncharacterized protein	LMJF_11_0810
E9AFF5	LRRcap domain-containing protein	LMJF_35_3310
E9AD65	Oxoglutarate dehydrogenase (succinyl-transferring), EC 1.2.4.2	LMJF_27_0880
Q4Q2V7	DNAj-like protein	LMJF_34_2430
Q4QC72	Guanine nucleotide-binding protein subunit beta-like protein	LMJF_21_1240
Q4QGR1	Myotubularin phosphatase domain-containing protein	LMJF_12_0320
Q4QB73	Uncharacterized protein	LMJF_23_0900
Q4Q4D7	Putative sterol C-24 reductase, EC 1.3.1.71	LMJF_33_0680
Q4QD18	Midasin	LMJF_20_0260
Q4QA84	Electron transfer flavoprotein subunit beta, Beta-ETF	LMJF_25_0120
Q4Q800	Coatomer subunit gamma	LMJF_28_2620
Q4QD14	ZZ-type domain-containing protein	LMJF_20_0290
Q4Q9Z6	Putative dynein heavy chain	LMJF_25_0980
Q4Q0J9	Isoleucyl-tRNA synthetase, EC 6.1.1.5	ILERS LMJF_36_5620
Q4Q2Z3	Uncharacterized protein	LMJF_34_2080
Q4Q644	Uncharacterized protein	LMJF_31_2170
Q4Q4E7	Uncharacterized protein	LMJF_33_0590
Q4QJJ7	Major vault protein	LMJF_05_0060
Q4QIQ5	Uncharacterized protein	LMJF_07_0380
Q4Q937	Putative thimet oligopeptidase, EC 3.4.24.15	LMJF_26_1570
Q4QIT7	Uncharacterized protein	LMJF_07_0070
Q4QDA0	Uncharacterized protein	LMJF_19_1150
Q6XFB3	Serine palmitoyltransferase 1 (Serine palmitoyltransferase-like protein, EC 2.3.1.50)	SPT1 LMJF_34_3740
Q4Q182	Bromo domain-containing protein	LMJF_36_3360

Q4QEM2	Paraflagellar rod protein 2C	LMJF_16_1425, LMJF_16_1427, LMJF_16_1430
Q4QAI4	Guanine nucleotide-binding protein subunit beta-like protein	LMJF_24_1470
Q4Q3V0	Uncharacterized protein	LMJF_33_2370
Q4Q3M7	Uncharacterized protein	LMJF_33_3090
Q4QCC1	Protein kinase domain-containing protein	LMJF_21_0853
Q4QAZ3	TPH domain-containing protein	LMJF_23_1450
Q4Q3P5	Uncharacterized protein	LMJF_33_2900
Q4QDF1	Putative kinesin, EC 3.6.4.4	LMJF_19_0700
Q4QHU8	Uncharacterized protein	LMJF_09_0760
Q4Q0I5	RAB3GAP2_N domain-containing protein	LMJF_36_5760
Q4QJA4	NADH dehydrogenase [ubiquinone] flavoprotein 1, mitochondrial, EC 7.1.1.2	LMJF_05_0980
Q4Q6E2	RanBP2-type domain-containing protein	LMJF_31_1210
Q6S4V7	Dihydrolipoyl dehydrogenase, EC 1.8.1.4	Lpd
Q4QCI1	Metallo-peptidase, Clan ME, Family M16	LMJF_21_0340
Q4Q2U9	Uncharacterized protein	LMJF_34_2480
E9AFQ7	Uncharacterized protein	LMJF_35_4300
Q4Q5U3	Methylcrotonoyl-coa carboxylase biotinylated subunitprotein-like protein, EC 6.4.1.4	LMJF_31_3130
Q4Q276	Uncharacterized protein	LMJF_36_0030
Q4QII7	RNA binding protein-like protein	LMJF_07_1000
Q4QJA6	Dipeptidyl peptidase 3, EC 3.4.14.4 (Dipeptidyl aminopeptidase III) (Dipeptidyl peptidase III)	LMJF_05_0960
E9AFW8	Uncharacterized protein	LMJF_35_4940
E9AFL1	Putative nucleoside diphosphate kinase, EC 2.7.4.6	LMJF_35_3870
E9AE04	Putative phosphatidylinositol 4-kinase alpha, EC 2.7.1.67	LMJF_29_1450
Q4Q7S9	Uncharacterized protein	LMJF_30_0300
Q4Q2E0	Uncharacterized protein	LMJF_34_4010
Q4Q1C5	Non-specific serine/threonine protein kinase, EC 2.7.11.1	LMJF_36_2940
Q4QDB6	4-coumarate:coa ligase-like protein, EC 6.2.1.12	LMJF_19_0995
Q9NJT7	Heat shock protein	
Q4QIW6	Uncharacterized protein	LMJF_06_1100
Q4Q6F8	Uncharacterized protein	LMJF_31_1050
E9ACK9	Uncharacterized protein	LMJF_03_0640
E9AEW4	Threonyl-tRNA synthetase, EC 6.1.1.3	LMJF_35_1410
Q4Q821	Vacuolar proton pump subunit B, V-ATPase subunit B (Vacuolar proton pump subunit B)	LMJF_28_2430
Q4QAC4	Transketolase, EC 2.2.1.1	LMJF_24_2060

Q4QIW9	2-deoxy-D-ribose 5-phosphate aldolase, EC 4.1.2.4 (Phosphodeoxyriboaldolase)	LMJF_06_1070
Q4Q0P8	VHS domain-containing protein	LMJF_36_5140
Q4Q5X2	Uncharacterized protein	LMJF_31_2870
Q4Q6U8	Guanine nucleotide-binding protein subunit beta-like protein	LMJF_30_3410
Q4QDA2	Uncharacterized protein	LMJF_19_1130
Q4Q9Z5	Uncharacterized protein	LMJF_25_0990
E9ADI3	Putative branched-chain amino acid aminotransferase, EC 2.6.1.42	LMJF_27_2030
E9ADQ2	ADF/Cofilin	LMJF_29_0510
Q4Q3T7	Uncharacterized protein	LMJF_33_2500
Q4Q1A4	Putative ADP-ribosylation factor GTPase activating protein	LMJF_36_3150
E9ADU3	Uncharacterized protein	LMJF_29_0870
Q4QDL5	40S ribosomal protein S2	LMJF_19_0060
Q4Q8G0	Uncharacterized protein	LMJF_28_1070
E9ADT8	Putative high mobility group protein homolog tdp-1	LMJF_29_0850
Q4Q9E8	Cytosolic Fe-S cluster assembly factor NUBP2 homolog	LMJF_26_0430
P48157	60S ribosomal protein L11	RPL11 P1421.04, LmjF22.0030
Q4Q0P7	Kinesin motor domain-containing protein	LMJF_36_5150
Q868B1	40S ribosomal protein S5 (40S ribosomal protein S5A) (40S ribosomal protein S5B)	LMJF_11_0960, LMJF_11_0970
Q4QEH4	Putative peptidase t, EC 3.4.11.14	LMJF_17_0140
Q4Q579	Uncharacterized protein	LMJF_32_1975
Q9BJ51	Phosphoglycerate kinase, EC 2.7.2.3	
Q4QAP8	Triosephosphate isomerase, EC 5.3.1.1	LMJF_24_0850
Q4Q7H9	Pyridoxal kinase, EC 2.7.1.35	LMJF_30_1250
Q9BJ48	Uncharacterized protein	
Q4QDA3	Putative proteasome regulatory non-ATP-ase subunit	LMJF_19_1120
Q4QCL4	Uncharacterized protein	LMJF_21_0030
Q4Q090	Phosphoglycerate mutase (2,3-diphosphoglycerate-independent), EC 5.4.2.12	PGAM LMJF_36_6650
Q4Q485	Uncharacterized protein	LMJF_33_1050
Q4QJE6	Uncharacterized protein	LMJF_05_0560
E9AD84	Cysteine desulfurase, EC 2.8.1.7	LMJF_27_1060
Q4QFV7	Uncharacterized protein	LMJF_14_0280
Q4QBS0	Putative NADH-cytochrome b5 reductase, EC 1.6.2.2	LMJF_22_0770
Q4Q9W6	Uncharacterized protein	LMJF_25_1270
Q4Q1M7	Phosphomannomutase, EC 5.4.2.8	PMM LMJF_36_1960
Q4QIK0	Splicing factor ptrs1-like protein	LMJF_07_0870
Q4Q573	Putative ras-related protein rab-2a	LMJF_32_2030

SUPPLEMENT

Q4Q8Q9	Proteasome subunit beta	LMJF_28_0110
Q4QEL8	Putative kinesin, EC 3.6.4.4	LMJF_16_1470
E9AFQ4	Uncharacterized protein	LMJF_35_4270
Q4QDS0	Prolyl-tRNA synthetase, EC 6.1.1.15	LMJF_18_1220
Q4Q9A5	Putative 40S ribosomal protein S16 (Ribosomal protein S16)	LMJF_26_0880, LMJF_26_0890
Q4Q7E6	PH domain-containing protein	LMJF_30_1580
Q4QBD6	Putative ATP-binding cassette protein subfamily	ABCG5 LMJF_23_0380
Q4QER5	Uncharacterized protein	LMJF_16_1030
E9ACZ8	Uncharacterized protein	LMJF_27_0210
Q9XZW6	Cysteine proteinase A	cpa
Q4Q9S9	Uncharacterized protein	LMJF_25_1620
Q4QED4	Putative P-type ATPase	LMJF_17_0600
Q4Q8L6	40S ribosomal protein S26	LMJF_28_0540
Q4Q2Q6	Putative ribosomal protein L3 (Ribosomal protein L3)	LMJF_32_3130, LMJF_34_2870, LMJF_34_2880, LMJF_34_2890, LMJF_34_2900
E9AD42	Uncharacterized protein	LMJF_27_0650
Q4QEL2	Putative endoplasmic reticulum oxidoreductin	LMJF_16_1530
Q4Q812	Putative acyl-CoA dehydrogenase, EC 1.3.99.3	LMJF_28_2510
E9ADW9	Uncharacterized protein	LMJF_29_1110
E9AEJ6	FCP1 homology domain-containing protein	LMJF_35_0190
P14834	Heat shock 70 kDa protein	HSP70
Q4Q3G4	40S ribosomal protein S25	S25 LMJF_34_0440
Q4Q0M8	Uncharacterized protein	LMJF_36_5340
Q4Q0G7	Uncharacterized protein	LMJF_36_5930
A0A1B2BGM7	Putative lanosterol 14-alpha-demethylase	
Q4Q8F2	Electron transfer flavoprotein subunit alpha, Alpha-ETF	LMJF_28_1140
Q4QBD7	Putative cytochrome c oxidase subunit 10, EC 1.9.3.1	LMJF_23_0370
Q4Q9Q5	Uncharacterized protein	LMJF_25_1840
Q4QA23	Uncharacterized protein	LMJF_25_0715
E9AFK0	Putative 60S ribosomal protein L27A/L29	LMJF_35_3760, LMJF_35_3780
Q4QGW6	WD_REPEATS_REGION domain-containing protein	LMJF_11_1160
Q4QFG2	Putative 60S ribosomal protein L13a	LMJF_15_0200
Q4Q3B9	Putative 60S ribosomal protein L13a	LMJF_34_0860
Q4Q1W0	Uncharacterized protein	LMJF_36_1160
Q4Q112	Methyltransferase, EC 2.1.1.-	LmSMT LMJF_36_2390

Q4QDK5	Putative aminopeptidase	LMJF_19_0160
Q4QGE5	Metallo-peptidase, Clan MA(E), family 32	LMJF_13_0090
Q6YIR7	Quinonoid dihydropteridine reductase QDPR	
E9AE93	Enoyl-CoA hydratase/isomerase-like protein	LMJF_29_2310
Q4QID2	Uncharacterized protein	LMJF_08_0370
Q4QFM4	Putative kinesin K39	LMJF_14_1100
Q4QBJ1	Putative 40S ribosomal protein L14	LMJF_22_1520, LMJF_22_1560
E9ADL3	C2 DOCK-type domain-containing protein	LMJF_29_0110
Q4Q557	CSN8_PSD8_EIF3K domain-containing protein	LMJF_32_2180
Q9U5N8	Dolichyl-diphosphooligosaccharide--protein glycotransferase, EC 2.4.99.18	stt3
Q4QBY9	Uncharacterized protein	LMJF_22_0050
Q4Q598	Uncharacterized protein	LMJF_32_1810
Q4Q1P8	Putative aldehyde dehydrogenase, EC 1.2.1.3	LMJF_36_1760
Q4Q7F9	Putative kinesin, EC 3.6.4.4	LMJF_30_1450
Q4Q6S8	Putative ATP synthase, epsilon chain, EC 3.6.3.14	LMJF_30_3600
E9AFX7	Polyadenylate-binding protein, PABP	PABP1 LMJF_35_5040
O96606	Polyadenylate-binding protein, PABP	PAB1
Q4Q6U6	Uncharacterized protein	LMJF_30_3430
Q4QCX5	Putative serine/threonine protein phosphatase 2A regulatory subunit	LMJF_20_0660
Q4Q4U6	Glucosamine-6-phosphate isomerase, EC 3.5.99.6 (Glucosamine-6-phosphate deaminase)	LMJF_32_3260
Q4QDB1	Phenylalanyl-tRNA synthetase beta subunit, EC 6.1.1.20	LMJF_19_1040
Q4QH17	Putative aminopeptidase, EC 3.4.11.-	LMJF_11_0630
Q4QFY6	Pyrroline-5-carboxylate reductase, EC 1.5.1.2	P5CR LMJF_13_1680
Q6IMM3	ADP-ribosylation factor 1 (Putative ADP-ribosylation factor)	ARF1 LMJF_31_2280
Q4Q2N9	Cytochrome b5 heme-binding domain-containing protein	LMJF_34_3050
Q4QIQ9	Putative ATP-dependent DEAD/H RNA helicase	LMJF_07_0340
Q4QEJ1	ADP-ribosylation factor-like protein 1	ARL-1 LMJF_17_0070
Q4Q0Q8	Uncharacterized protein	LMJF_36_5040
E9AD18	Putative heat shock protein DNAJ	LMJF_27_0410
E9AG04	Putative GTP-binding protein	LMJF_35_5310
Q4QDU3	UTP--glucose-1-phosphate uridylyltransferase, EC 2.7.7.9	UGP LMJF_18_0990
Q4Q6T6	S-adenosylmethionine synthase, EC 2.5.1.6	METK2 METK1, LMJF_30_3500, LMJF_30_3520
Q4Q756	ADP-ribosylation factor-like protein	LMJF_30_2370
Q4QBE9	ABC-thiol transporter, EC 3.6.3.44	MRPA LMJF_23_0250

Q4Q806	Putative 40S ribosomal protein S17	LMJF_28_2555, LMJF_28_2560
E9ACG6	Putative U2 splicing auxiliary factor	LMJF_03_0190
Q4QD68	Cysteine peptidase A (CPA)	CPA LMJF_19_1420
P25204	40S ribosomal protein S8	RPS8A, RPS8, LmjF24.2070, LmjF_24_2070, RPS8B, RPS8, LmjF24.2080, LmjF_24_2080
C6KJD0	Actin	
E9ADC7	Putative proteasome regulatory non-ATP-ase subunit 3	LMJF_27_1460
Q4Q0P4	Aldehyde dehydrogenase	LMJF_36_5180
Q4Q3S6	Putative enoyl-CoA hydratase/Enoyl-CoA isomerase/3-hydroxyacyl-CoA dehydrogenase, EC 1.1.1.35, EC 4.2.1.17	LMJF_33_2600
Q4QH21	Putative 3-methylcrotonoyl-CoA carboxylase beta subunit, EC 6.4.1.4	LMJF_11_0590
Q4Q424	Peptidyl-prolyl cis-trans isomerase, PPIase, EC 5.2.1.8	CYP4 LMJF_33_1630
E9ACL5	Uncharacterized protein	LMJF_03_0700
Q4QDB7	4-coumarate:coa ligase-like protein, EC 6.2.1.12	LMJF_19_0985
Q4QCD4	Ras-related protein Rab-21	LMJF_21_0790
E9AEU8	Thioredoxin-like protein	LMJF_35_1250
E9AC95	Phosphoglycan beta 1,3 galactosyltransferase	SCGR3 LMJF_02_0200
Q4QIA5	Uncharacterized protein	LMJF_08_0640
Q4FX73	40S ribosomal protein S3a (LmS3a-related protein, LmS3arp)	LmjF.35.0400, LmjF.35.0410, LmjF.35.0420
E9AEK1	60S ribosomal protein L30	LMJF_35_0240
Q4QH85	Uncharacterized protein	LMJF_10_1270
E9ADM2	Uncharacterized protein	LMJF_29_0200
Q4QD91	Uncharacterized protein	LMJF_19_1240
E9AF45	Kinetoplast membrane protein 11 (Kinetoplastid membrane protein-11)	KMP11-1 KMP11-2, LMJF_35_2210, LMJF_35_2220
Q4Q3T1	Putative Unc104-like kinesin	LMJF_33_2560
Q4QHU7	Prolyl endopeptidase, EC 3.4.21.-	OPB LMJF_09_0770
Q4QFZ6	Ubiquitin-conjugating enzyme-like protein, EC 6.3.2.19	LMJF_13_1580
Q4Q5C3	Mannose-6-phosphate isomerase, EC 5.3.1.8	PMI LMJF_32_1580
Q4QE03	Uncharacterized protein	LMJF_18_0390
Q4QE64	Uncharacterized protein	LMJF_17_1270
Q4Q4E4	Uncharacterized protein	LMJF_33_0610

Q4Q6K7	Mevalonate kinase, MK, EC 2.7.1.36	LMJF_31_0560
Q4Q111	Uncharacterized protein	LMJF_36_4040
Q4Q8G4	Putative ribosomal protein S20	LMJF_28_1010, LMJF_28_1030
Q4QCN7	Putative 40S ribosomal protein S11 (Ribosomal protein S11 homolog)	LMJF_20_1650, LMJF_21_1550
Q868G9	Inhibitor of cysteine peptidase	icp LMJF_24_1770
Q4Q3M1	Putative 40S ribosomal protein S13	LMJF_19_0390, LMJF_33_3150
Q4QHW8	Uncharacterized protein	LMJF_09_0560
Q4QDM2	Glutamate--cysteine ligase, EC 6.3.2.2 (Gamma-ECS) (Gamma-glutamylcysteine synthetase)	GSH1 LMJF_18_1660
E9ACN8	Amidohydro_3 domain-containing protein	LMJF_03_0930
Q4Q288	Serine/threonine-protein kinase TOR, EC 2.7.11.1	TOR2 LMJF_34_4530
Q4FWX5	Putative 60S ribosomal protein L2	LMJF_32_3900, LMJF_35_1430, LMJF_35_1440
Q4Q2J7	Uncharacterized protein	LMJF_34_3470
Q4Q1Y3	Putative 40S ribosomal protein S18 (Ribosomal protein S18)	LMJF_36_0930
E9AFM5	Uncharacterized protein	LMJF_35_4000
Q4QJG7	N(1),N(8)-bis(glutathionyl)spermidine reductase, EC 1.8.1.12 (Trypanothione reductase)	TRYR LMJF_05_0350
O43943	Guanine nucleotide-binding protein subunit beta-like protein	
E9AEJ7	Uncharacterized protein	LMJF_35_0200
Q4Q1D7	Putative dead/h helicase	LMJF_36_2830
Q4QFI0	Uncharacterized protein	LMJF_15_0040
Q4Q9V6	Uncharacterized protein	LMJF_25_1370
Q4QCI6	Uncharacterized protein	LMJF_21_0290
Q4Q273	Putative L-ribulokinase, EC 2.7.1.16	LMJF_36_0060
Q4Q5J4	60S ribosomal protein L18a	LMJF_32_0880, LMJF_35_0600
Q4Q0F7	Uncharacterized protein	LMJF_36_6030
Q4QG48	NADH-cytochrome b5 reductase, EC 1.6.2.2	LMJF_13_1060
Q4Q8S0	Putative glutamate 5-kinase, EC 2.7.2.11	LMJF_26_2710
Q4QJ04	Putative serine-threonine dehydratase, EC 4.3.1.19	LMJF_06_0730
Q4QFR7	Elongation of fatty acids protein, EC 2.3.1.199 (Very-long-chain 3-oxoacyl-CoA synthase)	ELO2 LMJF_14_0670
Q4Q170	Small acidic protein	LMJF_36_3480
Q4Q7S8	Uncharacterized protein	LMJF_30_0310
Q4Q819	DUF676 domain-containing protein	LMJF_28_2445

SUPPLEMENT

E9ADC5	Uncharacterized protein	LMJF_27_1440
E9AFW9	C3H1-type domain-containing protein	LMJF_35_4950
E9ADX4	Tryparedoxin	TXN1 LMJF_29_1160
E9AD15	Putative nucleoporin	LMJF_27_0380
Q4Q534	Uncharacterized protein	LMJF_32_2410
E9AEJ1	Uncharacterized protein	LMJF_35_0140
Q4Q4A0	Putative 40S ribosomal protein S3	LMJF_15_0950, LMJF_33_0920
Q4QCU9	1,2-dihydroxy-3-keto-5-methylthiopentene dioxygenase, EC 1.13.11.54 (Acireductone dioxygenase (Fe(2+)-requiring), ARD, Fe-ARD)	LMJF_20_0970
E9AE59	Uncharacterized protein	LMJF_29_1980
E9ACG2	Uncharacterized protein	LMJF_03_0150
Q4Q0A7	Uncharacterized protein	LMJF_36_6500
Q4QGT7	Ribonuclease mar1	MAR1 LMJF_12_0060
Q4QGW3	Putative 40S ribosomal protein S15A	LMJF_11_1190, LMJF_29_1800
Q4Q2F9	Uncharacterized protein	LMJF_34_3830
E9AFR9	Putative mitochondrial phosphate transporter	LMJF_35_4420
Q4Q1Y7	Eukaryotic translation initiation factor 6, eIF-6	EIF6 LMJF_36_0890
Q4QA83	Putative elongation factor	LMJF_25_0130
Q4Q9V1	GTP-binding nuclear protein	LMJF_25_1420
E9AE92	Ubiquitin carboxyl-terminal hydrolase, EC 3.4.19.12	LMJF_29_2300
Q4Q6U7	Uncharacterized protein	LMJF_30_3420
Q4QE21	Aha1_N domain-containing protein	LMJF_18_0210
Q1PC45	Adenylate kinase	ADK
Q4Q270	Leucine carboxyl methyltransferase 1, EC 2.1.1.233	LMJF_36_0080
Q4QEG0	Uncharacterized protein	LMJF_17_0340
Q4Q1E9	Metallo-peptidase, Clan MA(E), Family M41	LMJF_36_2710
Q4QG66	Uncharacterized protein	LMJF_13_0880
Q4QJ19	RNA helicase, EC 3.6.4.13	LMJF_05_0140
E9AD06	Acyl carrier protein	ACP LMJF_27_0290
Q4Q2Y8	Ubiquitin-like protein	LMJF_34_2125
Q4Q138	Nascent polypeptide-associated complex subunit beta	LMJF_36_3770
Q4Q990	Peptidase_M28 domain-containing protein	LMJF_26_1040
Q4QC74	Uncharacterized protein	LMJF_21_1220
Q4Q6J3	Putative ATP-dependent zinc metallopeptidase, EC 3.4.24.-	LMJF_31_0700
Q4QCE1	Putative 60S Ribosomal protein L36	LMJF_21_0730
Q4Q9M8	TPR_REGION domain-containing protein	LMJF_25_2100
Q4QF85	Putative succinate dehydrogenase	LMJF_15_0990

Q4Q2G5	Phosphomannomutase-like protein	LMJF_34_3780
Q4Q471	Uncharacterized protein	LMJF_33_1190
Q4QFG4	Cytochrome b5 heme-binding domain-containing protein	LMJF_15_0190
Q5SDH5	Putative calpain-like cysteine peptidase (Small myristoylated protein 1)	SMP-1 LMJF_20_1310
Q4Q3J3	Malate dehydrogenase, EC 1.1.1.37	LMJF_34_0150
Q4QH32	mRNA (guanine-N(7)-)-methyltransferase, EC 2.1.1.56	LMJF_11_0480
Q4Q5K7	Putative RNA binding protein	LMJF_32_0750
E9ACY8	Uncharacterized protein	LMJF_27_0110
E9AE89	PlsC domain-containing protein	LMJF_29_2270
Q4QF32	Ribonucleoprotein	LMJF_15_1470
Q4Q2H9	Putative 60S ribosomal protein L21	LMJF_34_3650
Q4QBU9	tRNA-binding domain-containing protein	LMJF_22_0470
Q4Q1X7	Putative 40S ribosomal protein S10	LMJF_36_0980, LMJF_36_0990
Q4Q7U1	Protein YIPF	LMJF_30_0140
Q4Q1G6	Uncharacterized protein	LMJF_36_2550
Q4QFF3	Putative replication Factor A 28 kDa subunit	LMJF_15_0270
Q4Q956	Prefoldin subunit 3	LMJF_26_1380
E9AEY7	Uncharacterized protein	LMJF_35_1650
Q4QI62	Cathepsin L-like protease	LMJF_08_1070
Q4Q203	Uncharacterized protein	LMJF_36_0730
Q4Q702	Putative aldehyde dehydrogenase, EC 1.2.1.3	LMJF_30_2900
E9AF69	HECT domain-containing protein	LMJF_35_2450
Q4QDI4	Uncharacterized protein	LMJF_19_0370
Q4Q5J3	CTP:phosphoethanolamine cytidyltransferase, EC 2.7.7.14	LMJF_32_0890
Q4Q6N2	CRAL-TRIO domain-containing protein	LMJF_31_0310
Q4Q0F0	Uncharacterized protein	LMJF_36_6100
Q4QE09	J domain-containing protein	LMJF_18_0330
Q4Q7V1	Uncharacterized protein	LMJF_30_0200
E9AEN3	Conserved SNF-7-like protein	LMJF_35_0580
Q4Q439	Uncharacterized protein	LMJF_33_1490
A0A2P0XMV4	Monoglyceride lipase, EC 3.1.1.23	
Q4Q747	Putative heat shock 70-related protein 1, mitochondrial	LMJF_30_2460

Supp. Table 10. Proteins that were upregulated (green) or downregulated (red) in amastigotes treated with staurosporine for 24 h.

Entry	Protein names	Gene names
Q4Q5Z0	Phosphatidylinositol-4-phosphate 5-kinase-like protein	LMJF_31_2710
Q4Q2Y5	Protein kinase domain-containing protein	LMJF_34_2150

SUPPLEMENT

Q4QCG2	Uncharacterized protein	LMJF_21_0530
Q4QD15	Protein-serine/threonine kinase, EC 2.7.11.-	LMJF_20_0280
Q4QEV9	Putative histone H3	LMJF_16_0600
Q4QCL6	Putative ring-box protein 1	LMJF_21_0023
Q4QIJ4	Uncharacterized protein	LMJF_07_0930
E9ADF2	Putative dynein heavy chain	LMJF_27_1750
Q4Q197	Uncharacterized protein	LMJF_36_3220
Q4QIS2	Uncharacterized protein	LMJF_07_0220
Q4Q0B9	Methylenetetrahydrofolate reductase (NAD(P)H), EC 1.5.1.20	LMJF_36_6390
Q4QE94	Uncharacterized protein	LMJF_17_0960
E9AD01	Kinetoplast-associated protein-like protein	LMJF_27_0240
Q4Q615	Putative lipase, EC 3.1.1.3	LMJF_31_2460
Q4QER3	Stealth_CR3 domain-containing protein	LMJF_16_1050
Q4QHT2	Calmodulin	LMJF_09_0910, LMJF_09_0920, LMJF_09_0930
Q4QF88	Sulfhydryl oxidase, EC 1.8.3.2	LMJF_15_0960
Q25312	DNA-directed RNA polymerase subunit, EC 2.7.7.6	RPOIILS
Q4Q2M1	RNA editing associated helicase 2, putative with=GeneDB:Tb927.4.1500	REH2 LMJF_34_3230
Q4QHV2	Putative cleavage and polyadenylation specificity factor 30 kDa subunit	LMJF_09_0720
Q4Q2E8	Non-specific serine/threonine protein kinase, EC 2.7.11.1	TOR3 LMJF_34_3940
Q4Q3W0	Uncharacterized protein	LMJF_33_2270
Q4QFM3	Putative kinesin K39	LMJF_14_1110
Q4Q0H3	Uncharacterized protein	LMJF_36_5870
Q4QGC8	Putative N-acetyltransferase subunit ARD1	LMJF_13_0260
Q4Q3U2	Uncharacterized protein	LMJF_33_2450
Q4Q793	Uncharacterized protein	LMJF_30_2010
Q4Q0D2	Glucose transporter, lmgT3	LMJF_36_6280
Q4Q6R7	Putative CPSF-domain protein	LMJF_30_3710
Q4Q695	Uncharacterized protein	LMJF_31_1670
Q4Q847	Uncharacterized protein	LMJF_28_2180
Q4QC45	Uncharacterized protein	LMJF_21_1500
E9ACM1	Uncharacterized protein	LMJF_03_0760
Q4QEQ4	Tyrosyl or methionyl-tRNA synthetase-like protein, EC 6.1.1.-	LMJF_16_1130
E9ACD7	Gamma-glutamyl phosphate reductase-like protein	LMJF_02_0630
E9ACK6	Kinase-like protein	LMJF_03_0610
Q4Q3P4	Uncharacterized protein	LMJF_33_2910
Q4Q3H2	DNA-directed RNA polymerase subunit, EC 2.7.7.6	LMJF_34_0360

E9AED0	Uncharacterized protein	LMJF_29_2680
E9AD88	Uncharacterized protein	LMJF_27_1100
E9AD29	Putative radial spoke protein 3	LMJF_27_0520
Q4Q2Y2	Uncharacterized protein	LMJF_34_2180
Q4Q3E6	Putative enoyl-[acyl-carrier-protein] reductase	LMJF_34_0610
Q4QH24	Putative transcription modulator/accessory protein	LMJF_11_0560
Q4QC39	Uncharacterized protein	LMJF_21_1560
Q4Q1Z8	Calpain catalytic domain-containing protein	LMJF_36_0780
Q4Q7J2	Putative RNA-binding protein	LMJF_30_1110
E9ACL9	Putative cytochrome c oxidase copper chaperone	LMJF_03_0740
Q4Q933	Proline dehydrogenase, EC 1.5.5.2	LMJF_26_1610
Q4QGN0	Alanine aminotransferase, EC 2.6.1.2	ALAT LMJF_12_0630
Q4QJB0	Putative paraflagellar rod protein	LMJF_05_0920
Q4Q4E0	Uncharacterized protein	LMJF_33_0650
Q4QCS8	Putative calpain-like cysteine peptidase, EC 3.4.22.-, EC 3.4.22.33	LMJF_20_1185
Q4QJ83	Uncharacterized protein	LMJF_05_1190
Q4QDF2	Putative kinesin, EC 3.6.4.4	LMJF_19_0690
Q4QC71	Putative adenylate kinase, EC 2.7.4.3	LMJF_21_1250
Q4QCW2	Cytochrome c oxidase assembly factor-like protein, EC 1.9.3.1	LMJF_20_0840
Q4Q3I4	CARD domain-containing protein	LMJF_34_0240
E9ACG3	Putative ATP-binding cassette protein subfamily F member 1	ABCF1 LMJF_03_0160
Q4QID5	Uncharacterized protein	LMJF_08_0340
E9ACK4	Putative DNA repair helicase	LMJF_03_0590
E9AE36	Putative paraflagellar rod protein 1D	LMJF_29_1750
Q4QDN6	Putative kinesin, EC 3.6.4.4	LMJF_18_1530
E9AFQ2	Ubiquinone biosynthesis O-methyltransferase, mitochondrial (3-demethylubiquinol 3-O-methyltransferase, EC 2.1.1.64) (Polyprenyldihydroxybenzoate methyltransferase, EC 2.1.1.114)	LMJF_35_4250
Q4QAQ6	Putative malic enzyme, EC 1.1.1.38	LMJF_24_0770
Q4QFK1	Uncharacterized protein	LMJF_14_1330
Q4QF09	APH domain-containing protein	LMJF_16_0110
Q4Q8N1	Uncharacterized protein	LMJF_28_0390
Q4Q747	Putative heat shock 70-related protein 1, mitochondrial	LMJF_30_2460
Q4QGR1	Myotubularin phosphatase domain-containing protein	LMJF_12_0320
Q4Q8Y0	Uncharacterized protein	LMJF_26_2120
Q4QHH8	Putative folate/biopterin transporter	LMJF_10_0390
Q4QAV5	Uncharacterized protein	LMJF_24_0260
B8YDG1	Leishmanolysin, EC 3.4.24.36	

SUPPLEMENT

Q4Q801	Uncharacterized protein	LMJF_28_2610
E9ADG8	Uncharacterized protein	LMJF_27_1895
E9AFQ7	Uncharacterized protein	LMJF_35_4300
Q4QCM5	Putative N-acyl-L-amino acid amidohydrolase, EC 3.5.1.14	LMJF_20_1560
Q4Q1Y1	Putative dynein heavy chain	LMJF_36_0950
Q4QIW4	Uncharacterized protein	LMJF_06_1120
Q95Z93	Calcium-transporting ATPase, EC 7.2.2.10	LMJF_04_0010
Q4QHX9	Uncharacterized protein	LMJF_09_0450
Q4QBK6	Ca ²⁺ -binding EF-hand protein	LMJF_22_1410
Q4QE77	WW domain-containing protein	LMJF_17_1140
Q4Q6D5	Putative ATP-binding cassette protein subfamily C,member 5	ABCC5 LMJF_31_1280
Q4QFL2	Uncharacterized protein	LMJF_14_1220
Q4QC37	Uncharacterized protein	LMJF_21_1555
E9AFG9	Putative DNA-repair protein	LMJF_35_3450
Q4QCC2	Xanthine phosphoribosyltransferase, EC 2.4.2.22, EC 2.4.2.8	XRPT LMJF_21_0850
Q4QIW5	Uncharacterized protein	LMJF_06_1110
Q4QGZ8	Uncharacterized protein	LMJF_11_0810
Q4QIT8	Putative cytochrome c1, heme protein,mitochondrial, EC 1.10.2.2	LMJF_07_0060
Q4QEK4	Prohibitin	LMJF_16_1610
Q4QDR6	Uncharacterized protein	LMJF_18_1260
E9ADH2	Uncharacterized protein	LMJF_27_1930
Q4QAA6	Corrinoid adenosyltransferase, EC 2.5.1.17	LMJF_24_2240
Q4QBP8	Uncharacterized protein	LMJF_22_0990
Q4QHP3	Putative paraflagellar rod component	LMJF_09_1320
Q4Q8C7	Uncharacterized protein	LMJF_28_1390
E9ADX5	EF-hand domain-containing protein	LMJF_29_1170
Q25317	100 kDa heat shock protein (Hsp100)	
Q4QIP4	DHC_N2 domain-containing protein	LMJF_07_0480
Q4Q0W2	Uncharacterized protein	LMJF_36_4520
Q4Q459	Putative ABC transporter	LMJF_33_1300
Q4Q2V7	DNAj-like protein	LMJF_34_2430
Q4Q0Z1	Uncharacterized protein	LMJF_36_4230
Q4QHR3	Mitochondrial RNA binding protein 2	LMJF_09_1120
Q4QGA0	Uncharacterized protein	LMJF_13_0540
P12076	Heat shock 70-related protein 1, mitochondrial	HSP70.1
Q4Q6Q1	Uncharacterized protein	LMJF_31_0130
Q4QBF3	Putative ATP-binding cassette protein subfamily C,member 2	ABCC2 LMJF_23_0220
E9AEX6	Putative reiske iron-sulfur protein, EC 1.10.2.2	LMJF_35_1540

Q7KF27	Cytosolic leucyl aminopeptidase, EC 3.4.11.1	lap LAP, LMJF_23_0950
Q4QFT3	Uncharacterized protein	LMJF_14_0520
E9ACA6	Uncharacterized protein	LMJF_02_0310
Q4QHC2	Uncharacterized protein	LMJF_10_0920
E9AFU0	J domain-containing protein	LMJF_35_4630
Q4QEM2	Paraflagellar rod protein 2C	LMJF_16_1425, LMJF_16_1427, LMJF_16_1430
Q4QIX1	Protein disulfide isomerase, EC 5.3.4.1	PDI-1 LMJF_06_1050
Q4QCI1	Metallo-peptidase, Clan ME, Family M16	LMJF_21_0340
Q4Q3R8	Uncharacterized protein	LMJF_33_2680
Q4Q6E9	Putative monoglyceride lipase, EC 3.1.1.23	LMJF_31_1140
Q4Q510	SpoU_methylase domain-containing protein	LMJF_32_2650
Q4QEW8	Uncharacterized protein	LMJF_16_0520
E9AFH5	Structural maintenance of chromosomes protein	LMJF_35_3510
Q4QCF1	Putative phosphoglucomutase, EC 5.4.2.2	LMJF_21_0640
O97194	Uncharacterized protein	LMJF_04_1150
Q4Q6Z3	Uncharacterized protein	LMJF_30_2990
Q4Q166	Uncharacterized protein	LMJF_36_3520
Q4Q9N0	Uncharacterized protein	LMJF_25_2090
Q4QDG9	Uncharacterized protein	LMJF_19_0520
Q4QDH0	Uncharacterized protein	LMJF_19_0510
Q4Q4E7	Uncharacterized protein	LMJF_33_0590
Q4QFM2	Putative kinesin K39	LMJF_14_1120
Q4Q3D8	Uncharacterized protein	LMJF_34_0690
E9ADV5	Putative kinesin, EC 3.6.4.4	LMJF_29_0970
Q4Q5Q0	Uncharacterized protein	LMJF_32_0350
Q4QC01	60S ribosomal protein L37a (Putative 60S ribosomal protein L37a)	LMJF_21_1820, LMJF_36_1925
Q4QDW0	Uncharacterized protein	LMJF_18_0820
Q4Q7B3	Uncharacterized protein	LMJF_30_1810
Q4QFZ4	Uncharacterized protein	LMJF_13_1600
Q4QCE3	Uncharacterized protein	LMJF_21_0720
Q4QFF6	Putative sterol carrier protein	LMJF_15_0240
Q4Q922	Putative cytochrome c oxidase subunit V, EC 1.9.3.1	LMJF_26_1710
Q4Q699	Putative 3-ketoacyl-CoA thiolase-like protein, EC 2.3.1.16	LMJF_31_1630
Q4QGJ3	Uncharacterized protein	LMJF_12_0820
E9AFL1	Putative nucleoside diphosphate kinase, EC 2.7.4.6	LMJF_35_3870
Q4QJ11	Uncharacterized protein	LMJF_06_0670

SUPPLEMENT

Q4Q219	Elongation factor G, mitochondrial, EF-Gmt (Elongation factor G 1, mitochondrial, mEF-G 1) (Elongation factor G1)	MEFG LMJF_36_0570
E9AD28	Putative calpain-like cysteine peptidase	LMJF_27_0510
Q4QGX0	Putative lanosterol 14-alpha-demethylase, EC 1.14.13.70	LMJF_11_1100
Q4Q6Z4	Glyceraldehyde-3-phosphate dehydrogenase, EC 1.2.1.12	LMJF_30_2980
E9ACC9	Uncharacterized protein	LMJF_02_0550
Q4Q9Y0	Putative cytochrome c oxidase VII, EC 1.9.3.1	LMJF_25_1130
Q4QDK0	ADP/ATP translocase (ADP, ATP carrier protein)	ANC2 ANC1, LMJF_19_0200, LMJF_19_0210
Q4QAV4	SER_THR_PHOSPHATASE domain-containing protein	LMJF_24_0270
Q4QIT4	Pitrilysin-like metalloprotease	LMJF_07_0100
Q4Q8F5	Guanine nucleotide-binding protein subunit beta-like protein	LMJF_28_1110
Q4Q845	Uncharacterized protein	LMJF_28_2200
Q4Q1Q2	Uncharacterized protein	LMJF_36_1720
Q4QAT7	Hypothetical predicted transmembrane protein	LMJF_24_0440
Q4Q5U3	Methylcrotonoyl-coa carboxylase biotinylated subunitprotein-like protein, EC 6.4.1.4	LMJF_31_3130
Q4QJ15	Dihydrolipoamide acetyltransferase component of pyruvate dehydrogenase complex, EC 2.3.1.-	LMJF_05_0180
E9ADY8	Uncharacterized protein	LMJF_29_1300
Q4Q8K9	Putative dynein heavy chain	LMJF_28_0610
Q4FXY8	Elongation factor Ts, mitochondrial, EF-Ts, EF-TsMt	Lmjf.29.0720
Q4QB10	Fer2_3 domain-containing protein	LMJF_23_1410
Q4Q7J6	Succinate dehydrogenase assembly factor 2, mitochondrial, SDH assembly factor 2, SDHAF2	LMJF_30_1070
Q4Q963	Uncharacterized protein	LMJF_26_1310
Q4Q0T5	Uncharacterized protein	LMJF_36_4780
Q4QH77	Uncharacterized protein	LMJF_11_0030
Q4Q6S8	Putative ATP synthase, epsilon chain, EC 3.6.3.14	LMJF_30_3600
Q4Q131	Diadenosine tetraphosphate synthetase, EC 6.1.1.14	LMJF_36_3840
Q4Q0W8	Uncharacterized protein	LMJF_36_4460
Q4QIR6	Putative ubiquitin-protein ligase-like, EC 6.3.2.19	LMJF_07_0280
E9AFU6	Uncharacterized protein	LMJF_35_4690
Q4Q8M1	Putative propionyl-coa carboxylase beta chain, EC 6.4.1.3	LMJF_28_0490
Q4Q828	Serine hydroxymethyltransferase, EC 2.1.2.1	SHMT-L LMJF_28_2370
Q4Q8V4	Uncharacterized protein	LMJF_26_2370
E9ABZ5	Uncharacterized protein	LMJF_01_0060
E9ABZ4	Propanoyl-CoA:carbon dioxide ligase subunit alpha, EC 6.4.1.3 (Propionyl-CoA carboxylase alpha chain, mitochondrial)	LMJF_01_0050
Q9XZY9	ADH_N domain-containing protein	LMJF_04_0290

E9AD84	Cysteine desulfurase, EC 2.8.1.7	LMJF_27_1060
Q4QE43	META domain containing protein	META2 LMJF_17_0870
Q4Q8N2	Sacchrp_dh_NADP domain-containing protein	LMJF_28_0380
Q4Q0F5	Uncharacterized protein	LMJF_36_6050
Q4Q3D3	Protein phosphatase, EC 3.1.3.16	LMJF_34_0730
Q4QJF0	Nuclear receptor binding factor-like protein	LMJF_05_0520
E9ADF0	Uncharacterized protein	LMJF_27_1730
Q4QF49	ALP5 (Putative actin-like protein)	ALP5 LMJF_15_1330
Q4Q2I7	Uncharacterized protein	LMJF_34_3570
E9AE23	Uncharacterized protein	LMJF_29_1610
Q4QER8	Stealth_CR3 domain-containing protein	LMJF_16_1010
E9ADU9	Letm1 RBD domain-containing protein	LMJF_29_0920
P90552	HASPA1 (Hydrophilic acylated surface protein a) (Hydrophilic surface protein 2)	haspa2 HASPA1, HASPA2, LMJF_23_1040, LMJF_23_1082, LMJF_23_1088
Q4Q5V3	Uncharacterized protein	LMJF_31_3040
Q4Q2N4	Uncharacterized protein	LMJF_34_3100
E9AEW1	Metallo-peptidase, Clan ME, Family M16, EC 1.10.2.2	LMJF_35_1380
Q4QEH6	ER membrane protein complex subunit 2	LMJF_17_0120
Q4QGN3	Uncharacterized protein	LMJF_12_0600
E9AEB3	ATP-dependent 6-phosphofructokinase, ATP-PFK, Phosphofructokinase, EC 2.7.1.11 (Phosphohexokinase)	pfk LMJF_29_2510
Q4QDB6	4-coumarate: coa ligase-like protein, EC 6.2.1.12	LMJF_19_0995
Q4QCC9	Uncharacterized protein	LMJF_21_0825
Q4Q137	Uncharacterized protein	LMJF_36_3780
Q4QD20	Uncharacterized protein	LMJF_20_0240
Q4Q2P9	Uncharacterized protein	LMJF_34_2950
E9ACCO	Uncharacterized protein	LMJF_02_0460
E9ACP2	Uncharacterized protein	LMJF_03_0970
Q4QDA9	Uncharacterized protein	LMJF_19_1060
Q4QDQ9	Uncharacterized protein	LMJF_18_1300
Q4Q2W6	Asparagine--tRNA ligase, EC 6.1.1.22	LMJF_34_2340
Q4QE33	Putative alpha glucosidase II subunit, EC 3.2.1.20	LMJF_18_0090
Q9U1E6	Putative outer dynein arm docking complex (Uncharacterized protein L1648.02)	L1648.02 DC2, LMJF_32_2900
Q4QJ32	ATP-NAD kinase-like protein, EC 2.7.1.23	LMJF_06_0460
Q9U0T9	Putative calpain-like cysteine peptidase, EC 3.4.22.-	LMJF_04_0450
Q4QIZ6	Uncharacterized protein	LMJF_06_0810
E9AE37	Putative paraflagellar rod protein 1D	LMJF_29_1760, LMJF_29_1770
Q4Q5B5	Uncharacterized protein	LMJF_32_1650

SUPPLEMENT

E9AFU8	Uncharacterized protein	LMJF_35_4710
Q4QJA4	NADH dehydrogenase [ubiquinone] flavoprotein 1, mitochondrial, EC 7.1.1.2	LMJF_05_0980
Q4Q7N4	GrpE protein homolog	LMJF_30_0730
E9ACK8	Uncharacterized protein	LMJF_03_0630
Q4Q4V4	Uncharacterized protein	LMJF_32_3180
Q4Q7L0	DUF4139 domain-containing protein	LMJF_30_0930
Q4Q353	Uncharacterized protein	LMJF_34_1490
Q4Q0L5	DAO domain-containing protein	LMJF_36_5460
Q4Q057	Uncharacterized protein	LMJF_36_6960
Q4QD86	PHB domain-containing protein	LMJF_19_1290
E9AFR9	Putative mitochondrial phosphate transporter	LMJF_35_4420
E9AFW8	Uncharacterized protein	LMJF_35_4940
Q4Q1I3	Methyltransferase, EC 2.1.1.-	LMJF_36_2380
E9AES4	Uncharacterized protein	LMJF_35_0990
Q4Q5H6	Guanine nucleotide-binding protein subunit beta-like protein	LMJF_32_1060
E9AEX9	Uncharacterized protein	LMJF_35_1570
A0A2R4SDU4	Phosphogluconate dehydrogenase (NADP(+)-dependent, decarboxylating), EC 1.1.1.44	6PGD
E9AE73	Uncharacterized protein	LMJF_29_2110
E9AFR1	Uncharacterized protein	LMJF_35_4340
Q4Q363	Uncharacterized protein	LMJF_34_1390
Q4QIR3	Uncharacterized protein	LMJF_07_0310
E9ADL7	Uncharacterized protein	LMJF_29_0150
Q4QJ94	Uncharacterized protein	LMJF_05_1080
Q4QDX3	Probable citrate synthase, mitochondrial, EC 2.3.3.16	LmjF18.0680, LmjF_18_0680
Q4QAW6	Glycosomal membrane like protein	LMJF_24_0150
Q4Q830	Uncharacterized protein	LMJF_28_2350
E9AE30	Uncharacterized protein	LMJF_29_1690
Q4QGR8	Cysteinyl-tRNA synthetase, EC 6.1.1.16	LMJF_12_0250
E9ADU3	Uncharacterized protein	LMJF_29_0870
Q4Q0G1	Uncharacterized protein	LMJF_36_5990
Q4QBT2	Mitochondrial guide RNA binding complex subunit 1	GRBC1 LMJF_22_0650
Q4Q7S9	Uncharacterized protein	LMJF_30_0300
Q4QH21	Putative 3-methylcrotonoyl-CoA carboxylase beta subunit, EC 6.4.1.4	LMJF_11_0590
Q4QDF0	Malate dehydrogenase, EC 1.1.1.37	gMDH LMJF_19_0710
Q4Q0W9	Putative mitochondrial intermediate peptidase, EC 3.4.24.59	LMJF_36_4450
Q4QH88	Uncharacterized protein	LMJF_10_1240

E9ADS8	Putative lipophosphoglycan biosynthetic protein	LPG3 LMJF_29_0760
Q4QD14	ZZ-type domain-containing protein	LMJF_20_0290
Q4Q9I9	Methylmalonyl-coa epimerase-like protein, EC 5.1.99.1	LMJF_26_0020
Q4QFH9	NADH-cytochrome b5 reductase, EC 1.6.2.2	LMJF_15_0050
Q4Q8B0	Uncharacterized protein	LMJF_28_1550
Q4Q666	Tryparedoxin-like protein	LMJF_31_1960
Q25325	Heat shock protein 70-related protein	hsp70.4
Q4QE86	Hydrolase-like protein	LMJF_17_1050
Q4QGM6	Cytochrome c oxidase subunit IV, EC 1.9.3.1	LMJF_12_0670
Q4QI59	Uncharacterized protein	LMJF_08_1100
Q4QJ98	Stomatin-like protein	LMJF_05_1040
E9AG12	Uncharacterized protein	LMJF_35_5390
Q4QG87	Putative lectin	LMJF_13_0670
Q4QAC7	Putative 3-oxoacyl-(Acyl-carrier protein) reductase, EC 1.1.1.100	LMJF_24_2030
E9AD61	Uncharacterized protein	LMJF_27_0840
Q9U0W1	Acetyl-coenzyme A synthetase, EC 6.2.1.1	L7836.01 LMJF_23_0710
Q4QJ88	V-type proton ATPase subunit	LMJF_05_1140
Q4QFH6	Uncharacterized protein	LMJF_15_0080
Q4Q2E0	Uncharacterized protein	LMJF_34_4010
Q4Q3V3	Succinyl-CoA:3-ketoacid-coenzyme A transferase, EC 2.8.3.5	LMJF_33_2340
Q4QE41	Uncharacterized protein	LMJF_18_0010
Q4Q134	Aminomethyltransferase, EC 2.1.2.10 (Glycine cleavage system T protein)	GCVT-2 LMJF_36_3810
Q4QDE0	Vps53_N domain-containing protein	LMJF_19_0810
Q4Q0J6	Uncharacterized protein	LMJF_36_5650
Q4Q804	Putative splicing factor 3B subunit 1	LMJF_28_2570
Q4Q3U8	Putative heat shock protein	LMJF_33_2390
Q4Q601	Calreticulin	LMJF_31_2600
Q4Q214	Uncharacterized protein	LMJF_36_0620
Q4Q5U0	Uncharacterized protein	LMJF_31_3150
Q4Q2C8	ER membrane protein complex subunit 1	LMJF_34_4130
Q4QFQ1	Excreted/secreted protein 9.1	LMJF_14_0820
E9AD64	Uncharacterized protein	LMJF_27_0870
Q25306	Guanine nucleotide-binding protein subunit beta-like protein (Antigen LACK)	
Q4QAI4	Guanine nucleotide-binding protein subunit beta-like protein	LMJF_24_1470
Q4Q8P6	Glycerol-3-phosphate dehydrogenase, EC 1.1.5.3	LMJF_28_0240
Q4Q7F3	p1/s1 nuclease	LMJF_30_1510

SUPPLEMENT

Q4Q3Z5	Uncharacterized protein	LMJF_33_1920
Q4QB73	Uncharacterized protein	LMJF_23_0900
Q4QDB0	Uncharacterized protein	LMJF_19_1050
E9AD65	Oxoglutarate dehydrogenase (succinyl-transferring), EC 1.2.4.2	LMJF_27_0880
Q4Q6C6	SPRY domain-containing protein	LMJF_31_1370
Q4Q4V5	Putative NADH dehydrogenase subunit NI8M, EC 1.6.5.3	LMJF_32_3170
Q4QAG8	Succinate dehydrogenase [ubiquinone] flavoprotein subunit, mitochondrial, EC 1.3.5.1	LMJF_24_1630
E9ADX3	Tryparedoxin	TXN2 LMJF_29_1150
E9ACB9	Putative voltage-dependent anion-selective channel	LMJF_02_0450
Q4QG67	Metallo-peptidase, Clan ME, Family M16, EC 3.4.24.6, EC 3.4.24.64	LMJF_13_0870
Q4QA69	Uncharacterized protein	LMJF_25_0270
Q4VT70	Phosphotransferase, EC 2.7.1.-	HK LMJF_21_0240
Q4QIW6	Uncharacterized protein	LMJF_06_1100
Q4QI03	Putative ATP-dependent hsl protease ATP-binding subunit hslU	HSLU LMJF_09_0230
Q4QGV7	Putative ATP-binding cassette protein subfamily A, member4	ABCA4 LMJF_11_1250
Q4Q116	Hs1vu complex proteolytic subunit-like, EC 3.4.25.-	LMJF_36_3990
Q4QED3	Uncharacterized protein	LMJF_17_0610
Q4Q9Z6	Putative dynein heavy chain	LMJF_25_0980
Q4Q5D1	Putative ATP-dependent zinc metallopeptidase, EC 3.4.24.-	LMJF_32_1500
P90627	Cathepsin B-like protease	
Q4QAB4	GP-PDE domain-containing protein	LMJF_24_2160
Q4Q242	ER membrane protein complex subunit 3	LMJF_36_0360
E9AFC2	Putative chaperone protein DNAj	LMJF_35_2980
Q4QC72	Guanine nucleotide-binding protein subunit beta-like protein	LMJF_21_1240
Q4Q6X5	Uncharacterized protein	LMJF_30_3150
Q4QF40	Uncharacterized protein	LMJF_15_1400
E9AC84	Uncharacterized protein	LMJF_02_0090
Q4Q9F9	Methenyltetrahydrofolate cyclohydrolase, EC 3.5.4.9	LMJF_26_0320
Q4Q5N1	Profilin	LMJF_32_0520
Q4QGW5	Putative eukaryotic release factor 3	LMJF_11_1170
Q4QDA3	Putative proteasome regulatory non-ATP-ase subunit	LMJF_19_1120
Q4Q1J6	Putative developmentally regulated GTP-binding protein 1	LMJF_36_2250
E9ADW2	Uncharacterized protein	LMJF_29_1040
Q4QB32	T-complex protein 1 subunit gamma	LMJF_23_1220
Q4QIM7	Uncharacterized protein	LMJF_07_0640
Q4QBH5	CCR4-NOT transcription complex subunit 11	LMJF_23_0020

Q4QIQ9	Putative ATP-dependent DEAD/H RNA helicase	LMJF_07_0340
Q4QHR9	MSP domain-containing protein	LMJF_09_1050
E9AC39	Putative beta eliminating lyase	LMJF_01_0480
A0A0B4ULI4	Phosphopyruvate hydratase, EC 4.2.1.11	
E9ACB1	Putative casein kinase II, alpha chain, EC 2.7.11.1	LMJF_02_0360
Q4Q3U3	Uncharacterized protein	LMJF_33_2440
Q4Q9N7	Uncharacterized protein	LMJF_25_2020
Q4Q5T9	Uncharacterized protein	LMJF_31_3160
Q4Q6V5	Putative 60S ribosomal protein L9	LMJF_30_3340
Q4Q3H3	Putative eukaryotic translation initiation factor 5	LMJF_34_0350
Q4QDX5	Uncharacterized protein	LMJF_18_0700
Q4Q3G0	Putative calcium channel protein	LMJF_34_0480
Q4Q3T1	Putative Unc104-like kinesin	LMJF_33_2560
Q4Q660	Succinyl-diaminopimelate desuccinylase-like protein	LMJF_31_2020
Q4QGW6	WD_REPEATS_REGION domain-containing protein	LMJF_11_1160
O96606	Polyadenylate-binding protein, PABP	PAB1
E9AFX7	Polyadenylate-binding protein, PABP	PABP1 LMJF_35_5040
Q4Q6U8	Guanine nucleotide-binding protein subunit beta-like protein	LMJF_30_3410
E9ADH8	Putative rRNA methyltransferase, EC 2.1.1.- (2'-O-ribose RNA methyltransferase SPB1 homolog)	LMJF_27_1980
Q4Q2S5	RRM domain-containing protein	LMJF_34_2700
Q4Q2J4	RuvB-like helicase, EC 3.6.4.12	LMJF_34_3500
Q4Q5J9	Uncharacterized protein	LMJF_32_0830
O02614	Peptidyl-prolyl cis-trans isomerase, PPlase, EC 5.2.1.8	CYPA LMJF_25_0910
Q4QBW5	Uncharacterized protein	LMJF_22_0300
Q4QAU8	Uncharacterized protein	LMJF_24_0330
Q4Q8Q9	Proteasome subunit beta	LMJF_28_0110
Q4QG66	Uncharacterized protein	LMJF_13_0880
Q4QIV8	Protein kinase domain-containing protein	LMJF_06_1180
Q4QJG3	Protein kinase domain-containing protein	LMJF_05_0390
Q4FX34	Aspartate transaminase, EC 2.6.1.1	asat LMJF_35_0820
Q4Q4D3	Putative 60S ribosomal protein L6	LMJF_33_0720
Q4Q2U1	Uncharacterized protein	LMJF_34_2540
Q9U1D3	Putative adenylate kinase, EC 2.7.4.3	LMJF_04_0960
Q4Q4I6	Heat shock protein 83-1	HSP83-2 HSP83, HSP83-10, HSP83-11, HSP83-12, HSP83-13
Q4QFU6	Uncharacterized protein	LMJF_14_0390
Q4Q0D3	Putative chaperone protein DNAj	LMJF_36_6270
E9AD53	Putative small GTP-binding protein Rab1	LMJF_27_0760

SUPPLEMENT

Q4QIN5	Uncharacterized protein	LMJF_07_0570
Q4QJG7	N(1),N(8)-bis(glutathionyl)spermidine reductase, EC 1.8.1.12 (Trypanothione reductase)	TRYR LMJF_05_0350
Q4QGA9	Alba domain-containing protein	LMJF_13_0450
Q9BJC7	Histone H2B	H2B
E9AD40	Uncharacterized protein	LMJF_27_0630
Q4Q3I7	CS domain-containing protein	LMJF_34_0210
E9AFV6	Uncharacterized protein	LMJF_35_4810
E9ACL5	Uncharacterized protein	LMJF_03_0700
E9AFY5	Uncharacterized protein	LMJF_35_5120
Q4Q6D3	Uncharacterized protein	LMJF_31_1300
Q4Q5E5	Uncharacterized protein	LMJF_32_1370
Q9NF96	Uncharacterized protein	LMJF_04_0990
Q4QB38	Guanine nucleotide-binding protein subunit beta-like protein	CRN12 LMJF_23_1165
E9AFE7	Putative cystathione gamma lyase, EC 4.4.1.1	LMJF_35_3230
Q4Q0M8	Uncharacterized protein	LMJF_36_5340
Q4QIB3	Uncharacterized protein	LMJF_08_0560
E9ADN1	Uncharacterized protein	LMJF_29_0290
Q4Q573	Putative ras-related protein rab-2a	LMJF_32_2030
Q4QAE4	Uncharacterized protein	LMJF_24_1870
Q4QCD2	Methionine--tRNA ligase, EC 6.1.1.10	LMJF_21_0810
E9ACW0	Putative heat shock protein DNAJ	LMJF_27_2400
Q4Q5T1	WD_REPEATS_REGION domain-containing protein	LMJF_32_0050
Q4Q5X2	Uncharacterized protein	LMJF_31_2870
Q4QHR4	Uncharacterized protein	LMJF_09_1110
Q4QH83	Uncharacterized protein	LMJF_10_1290
Q4QHN3	Uncharacterized protein	LMJF_09_1420
Q4QIB4	Translation initiation factor-like protein	LMJF_08_0550
Q4Q055	Putative eukaryotic translation initiation factor 3 subunit 8	LMJF_36_6980
Q4QEI9	Elongation factor 1-alpha	LMJF_17_0080, LMJF_17_0081, LMJF_17_0083, LMJF_17_0084, LMJF_17_0085
Q4QEL2	Putative endoplasmic reticulum oxidoreductin	LMJF_16_1530
Q4QDS7	RING-type domain-containing protein	LMJF_18_1150
Q4Q7F0	Flavoprotein domain-containing protein	LMJF_30_1540
Q4QDX9	Putative 60S ribosomal protein L10a	RPL10a LMJF_18_0620, LMJF_36_3760
Q4Q1T9	Putative Transitional endoplasmic reticulum ATPase	LMJF_36_1370
E9ADG0	Uncharacterized protein	LMJF_27_1820
E9AC63	Uncharacterized protein	LMJF_01_0720

Q4Q9J6	Uncharacterized protein	LMJF_25_2420
Q4QDX2	Citrate synthase	LMJF_18_0670
Q4Q0F4	Putative eukaryotic initiation factor 4a	LMJF_36_6060
Q4Q5X1	Putative aldehyde reductase	LMJF_31_2880
Q4Q7Z6	MsrB domain-containing protein	LMJF_28_2660
E9AE59	Uncharacterized protein	LMJF_29_1980
P50312	Phosphoglycerate kinase, glycosomal, EC 2.7.2.3 (Phosphoglycerate kinase C) (gPGK)	PGKC
Q4QGS1	Putative hydroxyacylglutathione hydrolase, EC 3.1.2.6	LMJF_12_0220
Q4QFP8	Putative small myristoylated protein-3	SMP-3 LMJF_14_0850
Q4QHL3	Putative ribosomal protein l35a	LMJF_10_0070, LMJF_34_2470
Q4Q2K1	Putative cleavage and polyadenylation specificity factor	LMJF_34_3430
E9ADK4	FACT complex subunit	LMJF_29_0020
Q4QFX2	Putative inosine-guanine nucleoside hydrolase	IG-NH LMJF_14_0130
Q4Q0L9	Branchpoint-bridging protein	LMJF_36_5420
Q4Q9M6	Uncharacterized protein	LMJF_25_2120
Q4Q579	Uncharacterized protein	LMJF_32_1975
E9ADW5	Putative ribosomal protein L1a	LMJF_29_1070, LMJF_29_1090
Q4QBC0	Acetyl-coenzyme A synthetase, EC 6.2.1.1	LMJF_23_0540
Q4Q0P8	VHS domain-containing protein	LMJF_36_5140
E9AF44	Putative RNA-binding protein	LMJF_35_2200
Q4Q946	Component of oligomeric Golgi complex 7 (Conserved oligomeric Golgi complex subunit 7)	LMJF_26_1480
Q4QFZ3	Kinesin-like protein	LMJF_13_1610
Q4QC88	Cell division protein kinase 2, EC 2.7.1.-	CRK1 LMJF_21_1080
E9AC43	Putative long-chain-fatty-acid-CoA ligase, EC 6.2.1.3	LMJF_01_0520
Q4Q760	Uncharacterized protein	LMJF_30_2330
Q4QF42	Putative nucleolar RNA binding protein	LMJF_15_1380
Q4Q5T4	Uncharacterized protein	LMJF_32_0020
Q4QF35	Proliferating cell nuclear antigen	LMJF_15_1450
O62591	Probable eukaryotic initiation factor 4A, eIF-4A, EC 3.6.4.13 (ATP-dependent RNA helicase eIF4A)	LmjF.01.0770, LmjF.01.0780
Q4Q1H0	Nuclear pore protein	LMJF_36_2510
Q4Q3L5	Coatomer subunit beta'	LMJF_33_3210
Q4Q821	Vacuolar proton pump subunit B, V-ATPase subunit B (Vacuolar proton pump subunit B)	LMJF_28_2430
Q4QG18	Uncharacterized protein	LMJF_13_1360
Q9U8C0	Histone H2B (Histone H2B variant 2)	H2B LMJF_17_1220
Q4Q9B0	Uncharacterized protein	LMJF_26_0840
Q4QFA8	Protein kinase domain-containing protein	LMJF_15_0770

SUPPLEMENT

Q4Q6Q6	C3H1-type domain-containing protein	LMJF_31_0080
Q4QHI5	Protein transport protein SEC23	LMJF_10_0310
Q4QGH7	Uncharacterized protein	LMJF_12_1120
Q4QIW9	2-deoxy-D-ribose 5-phosphate aldolase, EC 4.1.2.4 (Phosphodeoxyriboaldolase)	LMJF_06_1070
Q4QCL4	Uncharacterized protein	LMJF_21_0030
Q4Q3L7	Small nuclear ribonucleoprotein Sm D2, Sm-D2 (snRNP core protein D2)	LMJF_33_3190
Q4Q198	14-3-3 protein I (14-3-3 protein-like protein)	Lm 14-3-3 I LMJF_36_3210
Q4QBD6	Putative ATP-binding cassette protein subfamily	ABCG5 LMJF_23_0380
Q4QGN8	Uncharacterized protein	LMJF_12_0540
Q4Q970	Heat shock protein 70-related protein	HSP70.4 LMJF_26_1240
Q4Q8J7	Sas10 domain-containing protein	LMJF_28_0720
Q4QI24	Uncharacterized protein	LMJF_09_0105
Q4QBE0	V-type proton ATPase subunit G	LMJF_23_0340
Q4QGE5	Metallo-peptidase, Clan MA(E), family 32	LMJF_13_0090
Q4Q7M5	Putative serine-threonine kinase, EC 2.7.11.1	LMJF_30_0800
Q4QDK6	Putative mitogen-activated protein kinase	LMJF_19_0150
Q4QDJ5	Kinesin-like protein	LMJF_19_0260
Q4Q449	Putative mitogen activated protein kinase	MPK11 LMJF_33_1380
Q4QFY2	Uncharacterized protein	LMJF_14_0030
E9ADB1	Uncharacterized protein	LMJF_27_1300
E9ADX4	Tryparedoxin	TXN1 LMJF_29_1160
Q70GE8	Thiol-dependent reductase 1, EC 1.8.5.1	tdr1 TDR1, LMJF_33_0240
E9ADY5	Putative serine peptidase	LMJF_29_1270
Q4QFG2	Putative 60S ribosomal protein L13a	LMJF_15_0200
Q4Q3B9	Putative 60S ribosomal protein L13a	LMJF_34_0860
Q4Q2Q6	Putative ribosomal protein L3 (Ribosomal protein L3)	LMJF_32_3130, LMJF_34_2870, LMJF_34_2880, LMJF_34_2890, LMJF_34_2900
Q4Q2U5	Protein phosphatase 2C-like protein, EC 3.1.3.16	LMJF_34_2510
Q4Q5R2	Dynein light chain	LMJF_32_0230
Q4Q1S7	Uncharacterized protein	LMJF_36_1490
Q4Q768	Conserved zinc-finger protein	LMJF_30_2250
Q4QF62	60S acidic ribosomal protein P2	LMJF_15_1203, LMJF_15_1207
Q4QGT2	Uncharacterized protein	LMJF_12_0110
Q4Q277	Histone H4	L7845.05 LMJF_02_0020, LMJF_25_2450, LMJF_31_3180, LMJF_35_1310, LMJF_36_0020
Q4Q8I6	Putative RNA binding protein rbp16	LMJF_28_0825

Q4Q1B9	Putative ATP-dependent RNA helicase, EC 3.6.1.-	LMJF_36_3000
Q4QCI6	Uncharacterized protein	LMJF_21_0290
Q4QBG5	Mannose-1-phosphate guanyltransferase, EC 2.7.7.13	GDPMP LMJF_23_0110
Q4QCN8	Phosphatase-like protein	LMJF_20_1640
E9AFP0	Polyadenylate-binding protein, PABP	PABP2 LMJF_35_4130
Q9GRP7	Uncharacterized protein L3377.1L	L3377.1L L7845.04, LMJF_35_1320
Q4Q1B2	Fibrillarin	LMJF_36_3070
Q4Q9Y2	Uncharacterized protein	LMJF_25_1110
E9ADB9	60S acidic ribosomal protein P0	LMJF_27_1380, LMJF_27_1390
Q4QCD1	Uncharacterized protein	LMJF_21_0820
Q4Q557	CSN8_PSD8 EIF3K domain-containing protein	LMJF_32_2180
Q4QFK3	Uncharacterized protein	LMJF_14_1310
Q4QFZ6	Ubiquitin-conjugating enzyme-like protein, EC 6.3.2.19	LMJF_13_1580
Q4Q9N8	Putative 2,4-dihydroxyhept-2-ene-1,7-dioic acid aldolase, EC 4.1.2.-	LMJF_25_2010
Q4QBQ8	Uncharacterized protein	LMJF_22_0890
Q4QBJ1	Putative 40S ribosomal protein L14	LMJF_22_1520, LMJF_22_1560
Q4Q3X5	HIT-type domain-containing protein	LMJF_33_2120
Q4QH17	Putative aminopeptidase, EC 3.4.11.-	LMJF_11_0630
Q4Q2C1	Uncharacterized protein	LMJF_34_4200
Q4QDB1	Phenylalanyl-tRNA synthetase beta subunit, EC 6.1.1.20	LMJF_19_1040
Q4QB63	Uncharacterized protein	LMJF_23_1000
Q4Q756	ADP-ribosylation factor-like protein	LMJF_30_2370
Q4QIY1	Putative cell cycle associated protein MOB1	MOB1 LMJF_06_0960
Q4Q6U6	Uncharacterized protein	LMJF_30_3430
Q4QBY6	Putative heat shock protein DNAJ	LMJF_22_0080
E9ACK3	Uncharacterized protein	LMJF_03_0580
Q4QEM4	Uncharacterized protein	LMJF_16_1420
Q4Q9V1	GTP-binding nuclear protein	LMJF_25_1420
Q95Z84	Spermidine synthase, EC 2.5.1.16	LMJF_04_0580
Q4Q819	DUF676 domain-containing protein	LMJF_28_2445
Q4Q7L5	Adenosine kinase, EC 2.7.1.20	LMJF_30_0880
E9ADY2	TPR_REGION domain-containing protein	LMJF_29_1240
Q4QDU3	UTP--glucose-1-phosphate uridylyltransferase, EC 2.7.7.9	UGP LMJF_18_0990
Q4QFI0	Uncharacterized protein	LMJF_15_0040
Q4QBD8	Putative NADP-dependent alcohol dehydrogenase, EC 1.1.1.1	LMJF_23_0360
Q4Q9A5	Putative 40S ribosomal protein S16 (Ribosomal protein S16)	LMJF_26_0880, LMJF_26_0890

SUPPLEMENT

Q4Q259	Elongation factor 2	EF2-2 EF2-1, LMJF_36_0180, LMJF_36_0190
Q4QDJ1	Putative RNA binding protein	LMJF_19_0300
Q6IMM3	ADP-ribosylation factor 1 (Putative ADP-ribosylation factor)	ARF1 LMJF_31_2280
Q4Q5R0	Protein kinase domain-containing protein	LMJF_32_0250
Q4Q882	Probable methylthioribulose-1-phosphate dehydratase, MTRu-1-P dehydratase, EC 4.2.1.109	LmjF28.1840, LmjF_28_1840
Q4Q598	Uncharacterized protein	LMJF_32_1810
Q4QH70	Seryl-tRNA synthetase, EC 6.1.1.11	LMJF_11_0100
E9AE78	Rab GDP dissociation inhibitor	LMJF_29_2160
Q4Q8L6	40S ribosomal protein S26	LMJF_28_0540
Q4QFP4	Glutathione synthetase, GSH-S, EC 6.3.2.3	LMJF_14_0910
Q4QG06	Putative Ran-binding protein 1	LMJF_13_1480
Q4QJ16	Uncharacterized protein	LMJF_06_0620
Q4QEE0	AAA domain-containing protein	LMJF_17_0540
Q4Q080	Prolyl endopeptidase, EC 3.4.21.-	LMJF_36_6750
Q66NE0	Elongation factor 1B gamma (Elongation factor-1 gamma)	EF1G LMJF_09_0970
P83851	Inosine-uridine preferring nucleoside hydrolase, IU-NH, IU- nucleoside hydrolase, EC 3.2.2.2, EC 3.2.2.3 (Non-specific nucleoside hydrolase)	NSNH
Q4QHA3	LsmAD domain-containing protein	LMJF_10_1110
Q4QCN5	Putative ribosome biogenesis protein	LMJF_20_1670
Q4QEU3	Transaldolase, EC 2.2.1.2	LMJF_16_0760
E9ADN3	TPR_REGION domain-containing protein	LMJF_29_0320
Q4Q9J7	Uncharacterized protein	LMJF_25_2410
Q4Q426	Putative peptidase M20/M25/M40	LMJF_33_1610
Q4Q088	Cytochrome b5 heme-binding domain-containing protein	LMJF_36_6670
Q4Q253	Eukaryotic translation initiation factor 3 subunit L, eIF3L	LMJF_36_0250
Q4Q8H6	Endonuclease/exonuclease/phosphatase-like protein	LMJF_28_0910
Q4QDK5	Putative aminopeptidase	LMJF_19_0160
Q4QC91	Putative 60S ribosomal protein L9	LMJF_21_1050
Q4Q6X0	40S ribosomal protein S26	LMJF_30_3200
E9ADB2	Arginyl-tRNA synthetase, EC 6.1.1.19	LMJF_27_1310
E9AEK1	60S ribosomal protein L30	LMJF_35_0240
Q4QIP1	60S ribosomal protein L7a	LMJF_07_0500, LMJF_07_0510
Q4QCG1	Putative la RNA binding protein	LMJF_21_0540
Q4QHS3	Uncharacterized protein	LMJF_09_1010
Q4Q806	Putative 40S ribosomal protein S17	LMJF_28_2555, LMJF_28_2560
E9ADW9	Uncharacterized protein	LMJF_29_1110
E9ADL3	C2 DOCK-type domain-containing protein	LMJF_29_0110

Q4Q3H8	Guanine nucleotide-binding protein subunit beta-like protein	LMJF_34_0300
Q9BJ48	Uncharacterized protein	
Q4Q6T6	S-adenosylmethionine synthase, EC 2.5.1.6	METK2 METK1, LMJF_30_3500, LMJF_30_3520
Q4QEZ2	Uncharacterized protein	LMJF_16_0280
Q4QHR7	Putative eukaryotic translation initiation factor 2 subunit	LMJF_09_1070
Q4QA19	PPM-type phosphatase domain-containing protein	PP2C LMJF_25_0750
Q4QEJ1	ADP-ribosylation factor-like protein 1	ARL-1 LMJF_17_0070
Q4Q605	Uncharacterized protein	LMJF_31_2560
E9AEJ7	Uncharacterized protein	LMJF_35_0200
Q4Q8P9	Histone H2B	LMJF_28_0210
Q4QBF5	Putative endoribonuclease L-PSP (Pb5)	LMJF_23_0200
Q4QBY9	Uncharacterized protein	LMJF_22_0050
Q4QA21	Eukaryotic translation initiation factor 5A, eIF-5A	EIF5A2 EIF5A1, LMJF_25_0720, LMJF_25_0730
Q4Q5S8	Glycylpeptide N-tetradecanoyltransferase, EC 2.3.1.97	NMT LMJF_32_0080
Q4Q109	Uncharacterized protein	LMJF_36_4060
Q4QJE4	Uncharacterized protein	LMJF_05_0580
Q4Q5U8	Phosphoglycan beta 1,3 galactosyltransferase 5	SCG5 LMJF_31_3090
Q4QEG0	Uncharacterized protein	LMJF_17_0340
Q4Q4E9	Nkap_C domain-containing protein	LMJF_33_0580
Q4Q1D2	40S ribosomal protein S24	S24E-2 S24E-1, LMJF_36_2860, LMJF_36_2870
Q4Q3C1	Elongation factor 1-beta (Elongation factor 1B beta) (Putative translation elongation factor 1-beta)	eEF1B beta 2 eEF1B beta 1, LMJF_34_0820, LMJF_34_0840
Q4QIH4	Putative proteasome regulatory non-ATP-ase subunit	LMJF_07_1120
Q4Q1V1	Putative 40S ribosomal protein S9 (Ribosomal protein S9)	LMJF_36_1250
Q4Q7X6	Malate dehydrogenase, EC 1.1.1.37	cMDH LMJF_28_2860
Q4Q527	Uncharacterized protein	LMJF_32_2480
E9ACW8	Pre-mRNA-processing factor 19, EC 2.3.2.27	LMJF_27_2480
Q4QH87	Uncharacterized protein	LMJF_10_1250
Q4Q4M9	Uncharacterized protein	LMJF_32_3930
E9AER5	Uncharacterized protein	LMJF_35_0900
E9ADX9	Uncharacterized protein	LMJF_29_1210
E9ADE7	Uncharacterized protein	LMJF_27_1680
Q4QAI0	Putative IgE-dependent histamine-releasing factor	LMJF_24_1500, LMJF_24_1510
Q4QCN3	Putative SNAP protein	LMJF_20_1690
Q4QHB3	Nucleoside phosphorylase-like protein, EC 2.4.2.-	LMJF_10_1010
Q4QII4	Peptidyl-prolyl cis-trans isomerase, EC 5.2.1.8	PIN1 LMJF_07_1030
E9AEB9	Putative serine/threonine-protein kinase, EC 2.7.11.1	LMJF_29_2570

SUPPLEMENT

E9AFF2	Putative 60S ribosomal subunit protein L31 (Ribosomal protein L31)	LMJF_35_3280, LMJF_35_3290
Q9U8C2	p21 (p21 antigen protein)	LMJF_35_5290
Q4QGZ7	Uncharacterized protein	LMJF_11_0820
Q4QDS1	Prolyl-tRNA synthetase, EC 6.1.1.15	LMJF_18_1210
Q4QIK0	Splicing factor ptrs1-like protein	LMJF_07_0870
E9ADK9	Putative QA-SNARE protein	LMJF_29_0070
E9AF59	Putative aminopeptidase P	LMJF_35_2350
Q9BJ51	Phosphoglycerate kinase, EC 2.7.2.3	
Q4Q090	Phosphoglycerate mutase (2,3-diphosphoglycerate-independent), EC 5.4.2.12	PGAM LMJF_36_6650
Q4QBH1	Peptidyl-prolyl cis-trans isomerase, PPIase, EC 5.2.1.8	CYP11 LMJF_23_0050
Q25326	Hydrophilic surface protein (Hydrophilic surface protein 1)	haspb
Q4Q9Y6	Uncharacterized protein	LMJF_25_1070
Q4QDL0	Uncharacterized protein	LMJF_19_0110
Q4QFJ8	Inositol-3-phosphate synthase, EC 5.5.1.4	INO1 LMJF_14_1360
E9AEA8	Putative 60S ribosomal protein L13	LMJF_29_2460
Q4QH45	14-3-3 protein II (Putative 14-3-3 protein)	Lm 14-3-3 II LMJF_11_0350
Q4QB44	Stealth_CR2 domain-containing protein	LMJF_23_1120
Q66NE2	Elongation factor 1B alpha (Putative translation elongation factor 1-beta)	LMJF_36_1430
Q4Q5J8	RRM_8 domain-containing protein	LMJF_32_0840
Q4QGA2	Uncharacterized protein	LMJF_13_0520
E9AFS4	CS domain-containing protein	LMJF_35_4470
Q4Q884	Replication protein A subunit	RPA1 LMJF_28_1820
E9AEZ8	Uncharacterized protein	LMJF_35_1760
Q4QFF7	Lysine--tRNA ligase, EC 6.1.1.6 (Lysyl-tRNA synthetase)	LMJF_15_0230
Q4Q8S1	6-phosphogluconolactonase, 6PGL, EC 3.1.1.31	LMJF_26_2700
Q4QJ42	Putative glutamine synthetase, EC 6.3.1.2	LMJF_06_0370
Q4Q8H1	40S ribosomal protein S14	LMJF_28_0960
Q4Q1Y7	Eukaryotic translation initiation factor 6, eIF-6	EIF6 LMJF_36_0890
Q4QIA7	Uncharacterized protein	LMJF_08_0620
Q4Q4Z4	Putative RNA-binding protein	LMJF_32_2810
E9ACP6	Uncharacterized protein	LMJF_04_0123
Q4Q5C3	Mannose-6-phosphate isomerase, EC 5.3.1.8	PMI LMJF_32_1580
Q4Q176	Vacuolar protein sorting-associated protein-like protein	LMJF_36_3420
Q4Q1Y3	Putative 40S ribosomal protein S18 (Ribosomal protein S18)	LMJF_36_0930
E9AEI0	Pyruvate kinase, EC 2.7.1.40	LMJF_35_0030
Q4QH85	Uncharacterized protein	LMJF_10_1270

Q4QCD4	Ras-related protein Rab-21	LMJF_21_0790
Q4FX73	40S ribosomal protein S3a (LmS3a-related protein, LmS3arp)	LmjF.35.0400, LmjF.35.0410, LmjF.35.0420
E9ACA3	Uncharacterized protein	LMJF_02_0280
Q4QBX7	Uncharacterized protein	LMJF_22_0180
E9AFV2	Cyclophilin 40, EC 5.2.1.8	CYP40 LMJF_35_4770
Q4Q6J3	Putative ATP-dependent zinc metalloproteinase, EC 3.4.24.-	LMJF_31_0700
Q4QFI3	Histone H4	LMJF_15_0010
Q4QH01	Putative 40S ribosomal protein S21	LMJF_11_0760, LMJF_11_0780
E9AC79	Putative cytochrome b-domain protein	LMJF_02_0050
Q4Q720	Putative small glutamine-rich tetratricopeptide repeat protein	SGT LMJF_30_2740
Q4Q6F8	Uncharacterized protein	LMJF_31_1050
Q4Q869	Putative ribose 5-phosphate isomerase, EC 5.3.1.6	LMJF_28_1970
Q4Q735	Formyltetrahydrofolate synthetase, EC 6.3.4.3	FTHS LMJF_30_2600
Q4QAZ0	Pyridoxal phosphate homeostasis protein, PLP homeostasis protein	LMJF_23_1480
Q4QC38	Putative RNA helicase	LMJF_21_1552
E9ADT8	Putative high mobility group protein homolog tdp-1	LMJF_29_0850
Q4Q1I4	Uncharacterized protein	LMJF_36_2370
Q4QFT9	CS domain-containing protein	LMJF_14_0450
Q4Q5M5	Uncharacterized protein	LMJF_32_0580
Q4Q288	Serine/threonine-protein kinase TOR, EC 2.7.11.1	TOR2 LMJF_34_4530
E9ADE1	Putative eukaryotic translation initiation factor eIF-4E	EIF4E1 LMJF_27_1620
Q4QBX0	Signal sequence receptor subunit alpha (Translocon-associated protein subunit alpha)	LMJF_22_0260
Q4QJ76	Guanine nucleotide-binding protein subunit beta-like protein	LMJF_06_0030
Q868B1	40S ribosomal protein S5 (40S ribosomal protein S5A) (40S ribosomal protein S5B)	LMJF_11_0960, LMJF_11_0970
Q4Q0F7	Uncharacterized protein	LMJF_36_6030
Q4FWX5	Putative 60S ribosomal protein L2	LMJF_32_3900, LMJF_35_1430, LMJF_35_1440
Q4Q5H5	Putative small nuclear ribonucleoprotein	LMJF_32_1070
Q4Q9Z7	Uncharacterized protein	LMJF_25_0970
Q4Q138	Nascent polypeptide-associated complex subunit beta	LMJF_36_3770
Q4Q9Q5	Uncharacterized protein	LMJF_25_1840
Q4Q2L9	Putative pyruvate/indole-pyruvate carboxylase, EC 4.1.1.74	LMJF_34_3250
Q4Q485	Uncharacterized protein	LMJF_33_1050
E9AFK3	Putative 60S ribosomal protein L23	LMJF_35_3790, LMJF_35_3800
Q4Q843	Putative glycoprotein 96-92	LMJF_28_2210

SUPPLEMENT

Q4Q6R3	5-methyltetrahydropteroyltriglutamate--homocysteine S-methyltransferase, EC 2.1.1.14	LMJF_31_0010
Q4Q6R6	Putative 60S acidic ribosomal protein P2	LIP1 LMJF_30_3720
Q4QD56	Peptidylprolyl isomerase, EC 5.2.1.8	LMJF_19_1530
Q4QHU7	Prolyl endopeptidase, EC 3.4.21.-	OPB LMJF_09_0770
Q4QIC7	Uncharacterized protein	LMJF_08_0420
Q4Q1M7	Phosphomannomutase, EC 5.4.2.8	PMM LMJF_36_1960
Q868G9	Inhibitor of cysteine peptidase	icp LMJF_24_1770
Q4Q600	DNA-directed RNA polymerase subunit, EC 2.7.7.6	RPOIILS LMJF_31_2610
E9AFW9	C3H1-type domain-containing protein	LMJF_35_4950
Q4QF66	Uncharacterized protein	LMJF_15_1180
Q4QDI4	Uncharacterized protein	LMJF_19_0370
Q8I8A4	N-acetylglucosaminylphosphatidylinositol deacetylase, EC 3.5.1.89	GPI12 LMJF_09_0040
Q4QFW6	Thioredoxin-like_fold domain-containing protein	LMJF_14_0190
Q4QCN7	Putative 40S ribosomal protein S11 (Ribosomal protein S11 homolog)	LMJF_20_1650, LMJF_21_1550
E9ADQ2	ADF/Cofilin	LMJF_29_0510
Q4QJ39	Putative 60S ribosomal protein L19	LMJF_06_0410
Q4QJC9	Uncharacterized protein	LMJF_05_0730
Q4QFY6	Pyrroline-5-carboxylate reductase, EC 1.5.1.2	P5CR LMJF_13_1680
Q4QA28	Putative epsin	LMJF_25_0670
Q95Z90	Uncharacterized protein	LMJF_04_0050
Q4Q6F6	Biotin/lipoate protein ligase-like protein, EC 6.3.4.15	LMJF_31_1070
Q4Q2F9	Uncharacterized protein	LMJF_34_3830
Q4QHK7	Uncharacterized protein	LMJF_10_0130
Q4Q1W6	Putative ribosomal protein L24	LMJF_36_1070, LMJF_36_1100
A0A2R4SE78	Glucose-6-phosphate 1-dehydrogenase, EC 1.1.1.49	G6PD
E9ADG2	Uncharacterized protein	LMJF_27_1840
Q4Q3B8	Uncharacterized protein	LMJF_34_0870
E9ACJ7	RRM domain-containing protein	LMJF_03_0520
Q4Q412	Macrophage migration inhibitory factor-like protein	MIF2 LMJF_33_1750
E9AF45	Kinetoplast membrane protein 11 (Kinetoplastid membrane protein-11)	KMP11-1 KMP11-2, LMJF_35_2210, LMJF_35_2220
Q4Q9X1	Uncharacterized protein	LMJF_25_1220
Q4Q2Z5	Uncharacterized protein	LMJF_34_2060
Q4Q5Y2	Uncharacterized protein	LMJF_31_2780
Q4QIL3	Putative 6-phosphofructo-2-kinase/fructose-2,6-biphosphatase	LMJF_07_0760
Q4QE21	Aha1_N domain-containing protein	LMJF_18_0210

Q4Q203	Uncharacterized protein	LMJF_36_0730
Q6S997	Phosphodiesterase, EC 3.1.4.-	PDEB2
Q4Q2K8	Uncharacterized protein	LMJF_34_3360
E9AFR5	Uncharacterized protein	LMJF_35_4380
Q4Q3G4	40S ribosomal protein S25	S25 LMJF_34_0440
E9ADF7	Protein kinase-like protein	LMJF_27_1800
Q4QJ20	Putative 60S ribosomal protein L23a	LMJF_06_0570, LMJF_06_0580
Q4Q7F9	Putative kinesin, EC 3.6.4.4	LMJF_30_1450
Q4Q5K7	Putative RNA binding protein	LMJF_32_0750
Q4Q3M1	Putative 40S ribosomal protein S13	LMJF_19_0390, LMJF_33_3150
E9AEY7	Uncharacterized protein	LMJF_35_1650
Q4QDG7	Methionine aminopeptidase, EC 3.4.11.18	LMJF_19_0550
Q4Q3C4	Uncharacterized protein	LMJF_34_0815
E9ADC5	Uncharacterized protein	LMJF_27_1440
Q4QA79	Cleavage and polyadenylation specificity factor subunit 2 (Cleavage and polyadenylation specificity factor 100 kDa subunit)	LMJF_25_0170
Q4Q7P4	Ribosome biogenesis regulatory protein	LMJF_30_0620
Q4Q931	Putative 40S ribosomal protein S33	S33-1 S33-2, LMJF_26_1630, LMJF_26_1640
Q4QDW3	Putative DNA-directed RNA polymerase II	LMJF_18_0790
Q4QF32	Ribonucleoprotein	LMJF_15_1470
Q4Q9P3	Acyolphosphatase, EC 3.6.1.7	LMJF_25_1960
Q5EEK0	UDP-galactopyranose mutase, EC 5.4.99.9	GLF glf, LMJF_18_0200
Q4QB19	DNA-directed DNA polymerase, EC 2.7.7.7	LMJF_23_1330
O43943	Guanine nucleotide-binding protein subunit beta-like protein	
Q4Q8G4	Putative ribosomal protein S20	LMJF_28_1010, LMJF_28_1030
Q4Q5M1	Uncharacterized protein	LMJF_32_0620
E9AEH2	Ribosomal protein L37	LMJF_33_1955
Q4Q1U1	PARP-type domain-containing protein	LMJF_36_1350
E9AFG1	Uncharacterized protein	LMJF_35_3370
Q4Q439	Uncharacterized protein	LMJF_33_1490
Q4QJE8	Uncharacterized protein	LMJF_05_0540
Q4Q7R0	Putative bystin	LMJF_30_0480
Q4QGW7	Putative 60S ribosomal protein L28	LMJF_11_1110, LMJF_11_1130
Q4QBV0	Putative 40S ribosomal protein S15	LMJF_22_0420, LMJF_22_0460
Q4Q6Y1	Uncharacterized protein	LMJF_30_3090
Q4QCL3	Uncharacterized protein	LMJF_21_0040
Q4Q1C1	Bromo domain-containing protein	LMJF_36_2980

SUPPLEMENT

Q4Q2H9	Putative 60S ribosomal protein L21	LMJF_34_3650
E9AEN3	Conserved SNF-7-like protein	LMJF_35_0580
E9AFK0	Putative 60S ribosomal protein L27A/L29	LMJF_35_3760, LMJF_35_3780
Q4Q9Y7	Uncharacterized protein	LMJF_25_1060
Q4Q1J4	Uncharacterized protein	LMJF_36_2270
Q4Q8T6	Uncharacterized protein	LMJF_26_2550
Q4Q178	60S ribosomal protein L29	LMJF_36_3390, LMJF_36_3400
Q4QA45	Putative RNA-binding protein, UPB2	LMJF_25_0500
Q4Q140	Putative 40S ribosomal protein S27-1	LMJF_36_3750
Q71LW5	Ribosomal protein S2	
Q4QFF3	Putative replication Factor A 28 kDa subunit	LMJF_15_0270
Q4QAA9	Putative 60S ribosomal protein L12	LMJF_24_2210, LMJF_35_2190
Q4Q3K8	Uncharacterized protein	LMJF_34_0010
Q4Q393	Calponin-homology (CH) domain-containing protein	LMJF_34_1120
Q4Q1R6	Uncharacterized protein	LMJF_36_1595
Q4QC92	Putative kinesin, EC 3.6.4.4	LMJF_21_1040
A0A2P0XMV4	Monoglyceride lipase, EC 3.1.1.23	

Supp. Table 11. Proteins that were upregulated (green) or downregulated (red) in amastigotes treated with miltefosine for 24 h.

Entry	Protein names	Gene names
E9AEN3	Conserved SNF-7-like protein	LMJF_35_0580
Q4QHT2	Calmodulin	LMJF_09_0910, LMJF_09_0920, LMJF_09_0930
Q4QBK6	Ca ²⁺ -binding EF-hand protein	LMJF_22_1410
Q4Q0B9	Methylenetetrahydrofolate reductase (NAD(P)H), EC 1.5.1.20	LMJF_36_6390
Q4QI86	Amastin-like protein	LMJF_08_0830
Q4QIS2	Uncharacterized protein	LMJF_07_0220
Q4QH73	GRIP domain-containing protein	LMJF_11_0070
Q4QJI2	Uncharacterized protein	LMJF_05_0210
E9ACM7	Uncharacterized protein	LMJF_03_0820
P12076	Heat shock 70-related protein 1, mitochondrial	HSP70.1
Q4QER3	Stealth_CR3 domain-containing protein	LMJF_16_1050
E9ADF2	Putative dynein heavy chain	LMJF_27_1750
Q4Q847	Uncharacterized protein	LMJF_28_2180
E9AED0	Uncharacterized protein	LMJF_29_2680
Q4Q6D5	Putative ATP-binding cassette protein subfamily C, member 5	ABCC5 LMJF_31_1280
E9AD29	Putative radial spoke protein 3	LMJF_27_0520
Q4Q387	Uncharacterized protein	LMJF_34_1170

Q4Q747	Putative heat shock 70-related protein 1, mitochondrial	LMJF_30_2460
Q4QCM5	Putative N-acyl-L-amino acid amidohydrolase, EC 3.5.1.14	LMJF_20_1560
Q4QH86	Uncharacterized protein	LMJF_10_1260
Q9GU34	Elongation factor 2	EF2-1
Q4Q3I4	CARD domain-containing protein	LMJF_34_0240
E9AEP2	DRIM domain-containing protein	LMJF_35_0670
Q4QDN6	Putative kinesin, EC 3.6.4.4	LMJF_18_1530
Q4QDB7	4-coumarate: coa ligase-like protein, EC 6.2.1.12	LMJF_19_0985
Q4QC65	RF_PROK_I domain-containing protein	LMJF_21_1300
Q4QEI9	Elongation factor 1-alpha	LMJF_17_0080, LMJF_17_0081, LMJF_17_0083, LMJF_17_0084, LMJF_17_0085
Q4Q3K1	Glucose-6-phosphate 1-dehydrogenase, EC 1.1.1.49	G6PD LMJF_34_0080
Q4QJG4	Putative microtubule-associated protein	LMJF_05_0380
Q4Q219	Elongation factor G, mitochondrial, EF-Gmt (Elongation factor G 1, mitochondrial, mEF-G 1) (Elongation factor G1)	MEFG LMJF_36_0570
Q4Q4V5	Putative NADH dehydrogenase subunit NI8M, EC 1.6.5.3	LMJF_32_3170
Q4QDY0	Putative ATP-dependent zinc metallopeptidase	LMJF_18_0610
E9AEN3	Conserved SNF-7-like protein	LMJF_35_0580
Q6IMM3	ADP-ribosylation factor 1 (Putative ADP-ribosylation factor)	ARF1 LMJF_31_2280
Q4QHU7	Prolyl endopeptidase, EC 3.4.21.-	OPB LMJF_09_0770
Q4QC91	Putative 60S ribosomal protein L9	LMJF_21_1050
Q4Q0X2	Putative 60S ribosomal protein L22	LMJF_36_3270, LMJF_36_4420
Q25314	Tubulin beta chain	
Q4QAL9	Actin-interacting protein-like protein	LMJF_24_1130
Q4QIH4	Putative proteasome regulatory non-ATP-ase subunit	LMJF_07_1120
Q4Q8L6	40S ribosomal protein S26	LMJF_28_0540
E9AFK0	Putative 60S ribosomal protein L27A/L29	LMJF_35_3760, LMJF_35_3780
P50312	Phosphoglycerate kinase, glycosomal, EC 2.7.2.3 (Phosphoglycerate kinase C) (gPGK)	PGKC
Q4QDA7	Uncharacterized protein	LMJF_19_1080
Q6YIR7	Quinonoid dihydropteridine reductase QDPR	
Q4QDR6	Uncharacterized protein	LMJF_18_1260
E9AE09	Nodulin-like domain-containing protein	LMJF_29_1500
Q4Q2L9	Putative pyruvate/indole-pyruvate carboxylase, EC 4.1.1.74	LMJF_34_3250

SUPPLEMENT

Q4Q6Y1	Uncharacterized protein	LMJF_30_3090
Q4Q9X4	40S ribosomal protein S25	LMJF_25_1190
K7P582	Cathepsin L-like protease	Cpb

Supp. Table 12. Proteins that were upregulated (green) or downregulated (red) in amastigotes treated with harmonine for 24 h.

Entry	Protein names	Gene names
Q4Q1R6	Uncharacterized protein	LMJF_36_1595
Q4QJ11	Uncharacterized protein	LMJF_06_0670
E9AEN3	Conserved SNF-7-like protein	LMJF_35_0580
Q4QF84	Putative 60S ribosomal protein L6 (Ribosomal protein L6)	LMJF_15_1000
Q4QCL6	Putative ring-box protein 1	LMJF_21_0023
E9ACD7	Gamma-glutamyl phosphate reductase-like protein	LMJF_02_0630
A0A2P0XMV4	Monoglyceride lipase, EC 3.1.1.23	
Q9XZY4	GRAM domain-containing protein	LMJF_04_0240
Q9XZW6	Cysteine proteinase A	cpa
E9AD88	Uncharacterized protein	LMJF_27_1100
Q4Q7Z2	Uncharacterized protein	LMJF_28_2700
Q4QBQ2	Protein kinase domain-containing protein	LMJF_22_0950
Q4QD15	Protein-serine/threonine kinase, EC 2.7.11.-	LMJF_20_0280
Q4QGB4	Sister chromatid cohesion protein	LMJF_13_0400
E9AEL3	Enoyl-CoA hydratase/isomerase family protein, conserved	LMJF_35_0360
Q71LW5	Ribosomal protein S2	
Q4Q3Z5	Putative amastin-like surface protein	LMJF_34_1700, LMJF_34_1760, LMJF_34_1780, LMJF_34_1800, LMJF_34_1820
Q4QGJ3	Uncharacterized protein	LMJF_12_0820
Q4QF88	Sulfhydryl oxidase, EC 1.8.3.2	LMJF_15_0960
Q4QCN5	Putative ribosome biogenesis protein	LMJF_20_1670
Q4Q3F7	Amastin-like protein	LMJF_34_0500
B8YDG1	Leishmanolysin, EC 3.4.24.36	
Q9N2P5	LmRab7 GTP-binding protein (Putative rab7 GTP binding protein)	LmRab7 RAB7, LMJF_18_0890
Q4QDF2	Putative kinesin, EC 3.6.4.4	LMJF_19_0690
Q4Q9Y6	Uncharacterized protein	LMJF_25_1070
Q4Q5G9	Uncharacterized protein	LMJF_32_1130
E9ACG3	Putative ATP-binding cassette protein subfamily F member 1	ABCF1 LMJF_03_0160
Q4QIG6	Putative Qc-SNARE protein	LMJF_08_0030

Q4Q2M1	RNA editing associated helicase 2,putativewith=GeneDB:Tb927.4.1500	REH2 LMJF_34_3230
Q4Q9Y5	RRM domain-containing protein	LMJF_25_1080
Q4Q7S9	Uncharacterized protein	LMJF_30_0300
Q4QJC9	Uncharacterized protein	LMJF_05_0730
Q4QEI9	Elongation factor 1-alpha	LMJF_17_0080, LMJF_17_0081, LMJF_17_0083, LMJF_17_0084, LMJF_17_0085
Q4QER3	Stealth_CR3 domain-containing protein	LMJF_16_1050
E9AC60	Uncharacterized protein	LMJF_01_0690
Q9BHD9	Uncharacterized protein P883.31	P883.31
Q4Q500	SEC7 domain-containing protein	LMJF_32_2750
Q4QFM3	Putative kinesin K39	LMJF_14_1110
Q7KF27	Cytosolic leucyl aminopeptidase, EC 3.4.11.1	lap LAP, LMJF_23_0950
E9AD97	Putative histone H1	LMJF_27_1190, LMJF_27_1240
Q95Z90	Uncharacterized protein	LMJF_04_0050
Q4Q5T4	Uncharacterized protein	LMJF_32_0020
Q4QCI4	Uncharacterized protein	LMJF_21_0310
Q9GU34	Elongation factor 2	EF2-1
E9AFW8	Uncharacterized protein	LMJF_35_4940
E9AFW1	Uncharacterized protein	LMJF_35_4860
Q4Q3Q4	Transcription elongation factor-like protein	LMJF_33_2810
Q4Q0B9	Methylenetetrahydrofolate reductase (NAD(P)H), EC 1.5.1.20	LMJF_36_6390
Q4Q7J6	Succinate dehydrogenase assembly factor 2, mitochondrial, SDH assembly factor 2, SDHAF2	LMJF_30_1070
E9ADF2	Putative dynein heavy chain	LMJF_27_1750
E9ADN1	Uncharacterized protein	LMJF_29_0290
Q4QAZ9	Putative Qb-SNARE protein	LMJF_23_1740
E9AEB9	Putative serine/threonine-protein kinase, EC 2.7.11.1	LMJF_29_2570
Q4Q057	Uncharacterized protein	LMJF_36_6960
Q4FXY8	Elongation factor Ts, mitochondrial, EF-Ts, EF-TsMt	LmjF.29.0720
Q4Q754	Uncharacterized protein	LMJF_30_2390
Q4Q3K1	Glucose-6-phosphate 1-dehydrogenase, EC 1.1.1.49	G6PD LMJF_34_0080
Q4Q8C7	Uncharacterized protein	LMJF_28_1390
Q4Q6Z4	Glyceraldehyde-3-phosphate dehydrogenase, EC 1.2.1.12	LMJF_30_2980
Q4QGN0	Alanine aminotransferase, EC 2.6.1.2	ALAT LMJF_12_0630
E9ADH6	Uncharacterized protein	LMJF_27_1960
Q4Q5P7	Uncharacterized protein	LMJF_32_0380
E9AEH0	Uncharacterized protein	LMJF_33_0765

SUPPLEMENT

E9AFU6	Uncharacterized protein	LMJF_35_4690
E9ACK9	Uncharacterized protein	LMJF_03_0640
E9ACM1	Uncharacterized protein	LMJF_03_0760
Q4QCT5	Uncharacterized protein	LMJF_20_1110
Q4QHC2	Uncharacterized protein	LMJF_10_0920
Q4QC39	Uncharacterized protein	LMJF_21_1560
Q4Q843	Putative glycoprotein 96-92	LMJF_28_2210
E9ADF0	Uncharacterized protein	LMJF_27_1730
Q4Q3E9	Uncharacterized protein	LMJF_34_0580
Q4QAD2	Uncharacterized protein	LMJF_24_1980
Q4Q0D2	Glucose transporter, Iugt3	LMJF_36_6280
Q4QIH5	Uncharacterized protein	LMJF_07_1110
Q4QI83	Uncharacterized protein	LMJF_08_0860
Q4Q205	Uncharacterized protein	LMJF_36_0710
Q4Q450	Uncharacterized protein	LMJF_33_1370
E9ADG8	Uncharacterized protein	LMJF_27_1895
Q4QDN6	Putative kinesin, EC 3.6.4.4	LMJF_18_1530
E9AFF5	LRRcap domain-containing protein	LMJF_35_3310
Q4Q0P8	VHS domain-containing protein	LMJF_36_5140
Q4Q9Q7	Uncharacterized protein	LMJF_25_1820
E9ACA3	Uncharacterized protein	LMJF_02_0280
Q4Q9X1	Uncharacterized protein	LMJF_25_1220
Q4Q327	Putative amastin-like surface protein	LMJF_34_1560, LMJF_34_1740, LMJF_34_1900
Q4QFI5	Putative glutathione-S-transferase/glutaredoxin	LMJF_14_1480
E9AFR1	Uncharacterized protein	LMJF_35_4340
Q9BJ48	Uncharacterized protein	
E9AC37	Uncharacterized protein	LMJF_01_0460
E9ACL5	Uncharacterized protein	LMJF_03_0700
Q4Q0Y0	Uncharacterized protein	LMJF_36_4340
Q4QIA5	Uncharacterized protein	LMJF_08_0640
E9AD29	Putative radial spoke protein 3	LMJF_27_0520
Q4Q6F8	Uncharacterized protein	LMJF_31_1050
E9AFK1	Uncharacterized protein	LMJF_35_3770
E9ABZ5	Uncharacterized protein	LMJF_01_0060
E9AC84	Uncharacterized protein	LMJF_02_0090
E9AEJ6	FCP1 homology domain-containing protein	LMJF_35_0190
Q4Q8F4	Uncharacterized protein	LMJF_28_1120
Q4Q6C5	Uncharacterized protein	LMJF_31_1380

E9AEP2	DRIM domain-containing protein	LMJF_35_0670
Q4QIR6	Putative ubiquitin-protein ligase-like, EC 6.3.2.19	LMJF_07_0280
Q4QEG0	Uncharacterized protein	LMJF_17_0340
Q4QJ32	ATP-NAD kinase-like protein, EC 2.7.1.23	LMJF_06_0460
Q4Q2R2	Regulatory subunit of protein kinase a-like protein	LMJF_34_2820
Q4QFZ5	Tcp10_C domain-containing protein	LMJF_13_1590
E9AE81	Uncharacterized protein	LMJF_29_2190
Q4QII7	RNA binding protein-like protein	LMJF_07_1000
Q4Q0H5	Uncharacterized protein	LMJF_36_5850
E9ADU9	Letm1 RBD domain-containing protein	LMJF_29_0920
Q4QIM8	Calcium-transporting ATPase, EC 7.2.2.10	LMJF_07_0630
Q4QDA9	Uncharacterized protein	LMJF_19_1060
E9ADA3	Guanine nucleotide-binding protein subunit beta-like protein	LMJF_27_1250
E9AET6	Dolichyl-diphosphooligosaccharide--protein glycotransferase, EC 2.4.99.18	LMJF_35_1130
Q4QFP2	Putative immunodominant antigen	LMJF_14_0930
Q4Q2H7	H(+)-transporting two-sector ATPase, EC 7.1.2.2	LMJF_34_3670
Q4QDV7	Uncharacterized protein	LMJF_18_0850
Q4Q5T1	WD_REPEATS_REGION domain-containing protein	LMJF_32_0050
Q4Q1C5	Non-specific serine/threonine protein kinase, EC 2.7.11.1	LMJF_36_2940
O97193	Fructose-bisphosphatase, EC 3.1.3.11	FBP LMJF_04_1160
E9AEI6	Uncharacterized protein	LMJF_35_0090
Q4QED4	Putative P-type ATPase	LMJF_17_0600
Q4QAI0	Putative IgE-dependent histamine-releasing factor	LMJF_24_1500, LMJF_24_1510
Q4QJ96	Putative ATPase	LMJF_05_1060
Q4QFN8	Uncharacterized protein	LMJF_14_0970
Q4QIJ3	DUF3437 domain-containing protein	LMJF_07_0940
Q4Q5X2	Uncharacterized protein	LMJF_31_2870
E9ADW5	Putative ribosomal protein L1a	LMJF_29_1070, LMJF_29_1090
Q4Q1Y3	Putative 40S ribosomal protein S18 (Ribosomal protein S18)	LMJF_36_0930
Q4QJ42	Putative glutamine synthetase, EC 6.3.1.2	LMJF_06_0370
Q4QHA6	Putative eukaryotic translation initiation factor 4 gamma	LMJF_10_1080
Q4Q660	Succinyl-diaminopimelate desuccinylase-like protein	LMJF_31_2020
Q4Q3M1	Putative 40S ribosomal protein S13	LMJF_19_0390, LMJF_33_3150
P90627	Cathepsin B-like protease	
Q4QFB6	Uncharacterized protein	LMJF_15_0690
E9AE98	Aspartyl putative aminopeptidase, EC 3.4.11.-	LMJF_29_2360
Q4QD34	Phosphoglycerate kinase, EC 2.7.2.3	PGKC LMJF_20_0100

SUPPLEMENT

Q4Q9T0	Uncharacterized protein	LMJF_25_1610
Q4QCM4	Putative N-acyl-L-amino acid amidohydrolase, EC 3.5.1.14	LMJF_20_1570
Q4QGD2	Putative small Rab GTP binding protein	LMJF_13_0220
E9AEW8	Uncharacterized protein	LMJF_35_1450
O02614	Peptidyl-prolyl cis-trans isomerase, PPlase, EC 5.2.1.8	CYPA LMJF_25_0910
E9AE78	Rab GDP dissociation inhibitor	LMJF_29_2160
Q95Z84	Spermidine synthase, EC 2.5.1.16	LMJF_04_0580
Q4Q884	Replication protein A subunit	RPA1 LMJF_28_1820
Q4QAY0	Uncharacterized protein	LMJF_23_1580
Q4QBU8	Uncharacterized protein	LMJF_22_0480
Q4Q510	SpoU_methylase domain-containing protein	LMJF_32_2650
E9AC43	Putative long-chain-fatty-acid-CoA ligase, EC 6.2.1.3	LMJF_01_0520
E9ADB9	60S acidic ribosomal protein P0	LMJF_27_1380, LMJF_27_1390
Q4Q666	Tryparedoxin-like protein	LMJF_31_1960
Q4QDU3	UTP--glucose-1-phosphate uridylyltransferase, EC 2.7.7.9	UGP LMJF_18_0990
Q4QEX2	Putative fucose kinase, EC 2.7.1.52	LMJF_16_0480
Q4Q561	Uncharacterized protein	LMJF_32_2150
Q4Q190	Uncharacterized protein	LMJF_36_3280
Q4QC89	Putative 40S ribosomal protein S23	LMJF_21_1060, LMJF_21_1070
E9AD59	Uncharacterized protein	LMJF_27_0820
Q4Q198	14-3-3 protein I (14-3-3 protein-like protein)	Lm 14-3-3 I LMJF_36_3210
Q4QGN1	Uncharacterized protein	LMJF_12_0620
Q4QH88	Uncharacterized protein	LMJF_10_1240
E9ACV1	Obg-like ATPase 1	LMJF_27_2330
Q4Q4D3	Putative 60S ribosomal protein L6	LMJF_33_0720
Q4Q7S8	Uncharacterized protein	LMJF_30_0310
Q4Q2U9	Uncharacterized protein	LMJF_34_2480
Q4QC91	Putative 60S ribosomal protein L9	LMJF_21_1050
Q4Q6X0	40S ribosomal protein S26	LMJF_30_3200
Q4QH70	Seryl-tRNA synthetase, EC 6.1.1.11	LMJF_11_0100
Q4Q2E4	AP-1 complex subunit gamma	LMJF_34_3970
Q4QA19	PPM-type phosphatase domain-containing protein	PP2C LMJF_25_0750
Q4Q5P6	Putative 26S proteasome regulatory subunit	LMJF_32_0390
O43943	Guanine nucleotide-binding protein subunit beta-like protein	
Q4QHR7	Putative eukaryotic translation initiation factor 2 subunit	LMJF_09_1070
Q4Q127	Eukaryotic translation initiation factor 3 subunit I, eIF3i	LMJF_36_3880
Q4Q756	ADP-ribosylation factor-like protein	LMJF_30_2370
Q4QGX0	Putative lanosterol 14-alpha-demethylase, EC 1.14.13.70	LMJF_11_1100

Q4QDA7	Uncharacterized protein	LMJF_19_1080
Q4QDL5	40S ribosomal protein S2	LMJF_19_0060
Q4FWX5	Putative 60S ribosomal protein L2	LMJF_32_3900, LMJF_35_1430, LMJF_35_1440
P50312	Phosphoglycerate kinase, glycosomal, EC 2.7.2.3 (Phosphoglycerate kinase C) (gPGK)	PGKC
E9AD67	Uncharacterized protein	LMJF_27_0900
Q4Q735	Formyltetrahydrofolate synthetase, EC 6.3.4.3	FTHS LMJF_30_2600
O96427	Glycosomal glyceraldehyde-3-phosphate dehydrogenase, EC 1.2.1.12	GAPDH
E9ADG0	Uncharacterized protein	LMJF_27_1820
Q4QF35	Proliferating cell nuclear antigen	LMJF_15_1450
Q4Q6N4	Kinesin-like protein	LMJF_31_0290
Q4Q5S8	Glycylpeptide N-tetradecanoyltransferase, EC 2.3.1.97	NMT LMJF_32_0080
Q4Q6N9	Putative ATP-dependent RNA helicase	LMJF_31_0250
E9AEU8	Thioredoxin-like protein	LMJF_35_1250
Q4QH45	14-3-3 protein II (Putative 14-3-3 protein)	Lm 14-3-3 II LMJF_11_0350
Q4Q3L7	Small nuclear ribonucleoprotein Sm D2, Sm-D2 (snRNP core protein D2)	LMJF_33_3190
Q4Q7Z6	MsrB domain-containing protein	LMJF_28_2660
Q4QFK3	Uncharacterized protein	LMJF_14_1310
Q9U1E5	Putative ubiquitin carboxy-terminal hydrolase (Putative ubiquitin hydrolase)	L1648.03 LMJF_32_2910
Q4QIC5	Uncharacterized protein	LMJF_08_0440
Q4Q1D2	40S ribosomal protein S24	S24E-2 S24E-1, LMJF_36_2860, LMJF_36_2870
E9AEK1	60S ribosomal protein L30	LMJF_35_0240
Q6YIR7	Quinonoid dihydropteridine reductase QDPR	
Q4Q573	Putative ras-related protein rab-2a	LMJF_32_2030
E9ACE8	Putative dipeptylcarboxypeptidase (Putative peptidyl dipeptidase)	DCP LMJF_02_0740, LMJF_27_2660
Q4Q5H5	Putative small nuclear ribonucleoprotein	LMJF_32_1070
Q4Q3E2	26S proteasome regulatory subunit RPN11	LMJF_34_0650
A0A2R4SE78	Glucose-6-phosphate 1-dehydrogenase, EC 1.1.1.49	G6PD
Q4Q5K7	Putative RNA binding protein	LMJF_32_0750
Q4Q0X2	Putative 60S ribosomal protein L22	LMJF_36_3270, LMJF_36_4420
Q4QAT9	Ubiquitin carboxyl-terminal hydrolase, EC 3.4.19.12	LMJF_24_0420
Q4Q1P8	Putative aldehyde dehydrogenase, EC 1.2.1.3	LMJF_36_1760
Q4Q9N8	Putative 2,4-dihydroxyhept-2-ene-1,7-dioic acid aldolase, EC 4.1.2.-	LMJF_25_2010

SUPPLEMENT

Q4Q9A5	Putative 40S ribosomal protein S16 (Ribosomal protein S16)	LMJF_26_0880, LMJF_26_0890
Q4Q1S5	Uncharacterized protein	LMJF_36_1510
Q6Y9S1	Phosphogluconate dehydrogenase (NADP(+)-dependent, decarboxylating), EC 1.1.1.44	
Q4Q8L6	40S ribosomal protein S26	LMJF_28_0540
Q4Q0Q0	40S ribosomal protein SA	LmjF36.5010, LmjF_36_5010
		LmjF36.5120, LmjF_36_5120
Q4Q426	Putative peptidase M20/M25/M40	LMJF_33_1610
Q4QBQ1	Putative kinesin, EC 3.6.4.4	LMJF_22_0960
E9AFK0	Putative 60S ribosomal protein L27A/L29	LMJF_35_3760, LMJF_35_3780
Q4QCD4	Ras-related protein Rab-21	LMJF_21_0790
Q4Q2H9	Putative 60S ribosomal protein L21	LMJF_34_3650
Q4Q906	Uncharacterized protein	LMJF_26_1860
Q4Q3B2	Uncharacterized protein	LMJF_34_0930
Q4Q8Y0	Uncharacterized protein	LMJF_26_2120
Q4QHL6	Uncharacterized protein	LMJF_10_0040
Q4Q216	60S ribosomal protein L40 (Ubiquitin-60S ribosomal protein L40)	LMJF_36_0600
E9ABZ2	Kinesin-like protein	LMJF_01_0030
Q4QAF2	RRM domain-containing protein	LMJF_24_1790
Q4QB19	DNA-directed DNA polymerase, EC 2.7.7.7	LMJF_23_1330
P07382	Bifunctional dihydrofolate reductase-thymidylate synthase, DHFR-TS [Includes: Dihydrofolate reductase, EC 1.5.1.3; Thymidylate synthase, EC 2.1.1.45]	LmjF06.0860, LmjF_06_0860
Q4Q374	Uncharacterized protein	LMJF_34_1280
Q9NJT8	Protein-serine/threonine kinase, EC 2.7.11.-	
R9VXJ6	Thiol-specific antioxidant	TSA
Q4Q6E9	Putative monoglyceride lipase, EC 3.1.1.23	LMJF_31_1140
Q4QD68	Cysteine peptidase A (CPA)	CPA LMJF_19_1420
K7PNP9	Cysteine protease	cpb
Q4QGK5	Uncharacterized protein	LMJF_12_0950

Supp. Table 13. Proteins that were upregulated (green) or downregulated (red) in amastigotes treated with compound 10 for 6 h.

Entry	Protein names	Gene names
P12076	Heat shock 70-related protein 1, mitochondrial	HSP70.1
Q9GU34	Elongation factor 2	EF2-1
Q4Q325	Putative amastin-like surface protein	LMJF_34_1700, LMJF_34_1760, LMJF_34_1780, LMJF_34_1800, LMJF_34_1820

Q4Q2M1	RNA editing associated helicase 2,putativewith=GeneDB:Tb927.4.1500	REH2 LMJF_34_3230
Q4Q3F7	Amastin-like protein	LMJF_34_0500
E9ADF2	Putative dynein heavy chain	LMJF_27_1750
Q4QER3	Stealth_CR3 domain-containing protein	LMJF_16_1050
E9AD29	Putative radial spoke protein 3	LMJF_27_0520
Q4Q131	Diadenosine tetraphosphate synthetase, EC 6.1.1.14	LMJF_36_3840
Q25306	Guanine nucleotide-binding protein subunit beta-like protein (Antigen LACK)	
Q4Q0D2	Glucose transporter, Igmt3	LMJF_36_6280
Q4QDW0	Uncharacterized protein	LMJF_18_0820
E9AD28	Putative calpain-like cysteine peptidase	LMJF_27_0510
Q4QIR6	Putative ubiquitin-protein ligase-like, EC 6.3.2.19	LMJF_07_0280
K7PN53	Cysteine protease	cpb
Q868B1	40S ribosomal protein S5 (40S ribosomal protein S5A) (40S ribosomal protein S5B)	LMJF_11_0960, LMJF_11_0970
P50312	Phosphoglycerate kinase, glycosomal, EC 2.7.2.3 (Phosphoglycerate kinase C) (gPGK)	PGKC
E9AEK1	60S ribosomal protein L30	LMJF_35_0240
Q4Q1Y3	Putative 40S ribosomal protein S18 (Ribosomal protein S18)	LMJF_36_0930
Q4QC91	Putative 60S ribosomal protein L9	LMJF_21_1050
Q4Q138	Nascent polypeptide-associated complex subunit beta	LMJF_36_3770
Q4Q6T6	S-adenosylmethionine synthase, EC 2.5.1.6	METK2 METK1, LMJF_30_3500, LMJF_30_3520
E9AFK0	Putative 60S ribosomal protein L27A/L29	LMJF_35_3760, LMJF_35_3780
Q4Q3G4	40S ribosomal protein S25	S25 LMJF_34_0440
Q4Q3M1	Putative 40S ribosomal protein S13	LMJF_19_0390, LMJF_33_3150
E9ADI0	GMP_PDE_delta domain-containing protein	LMJF_27_2000
Q4QDR6	Uncharacterized protein	LMJF_18_1260
Q4Q5K7	Putative RNA binding protein	LMJF_32_0750
Q6YIR7	Quinonoid dihydropteridine reductase QDPR	
Q4Q8L6	40S ribosomal protein S26	LMJF_28_0540
E9AC43	Putative long-chain-fatty-acid-CoA ligase, EC 6.2.1.3	LMJF_01_0520
E9AEY7	Uncharacterized protein	LMJF_35_1650
Q4Q747	Putative heat shock 70-related protein 1, mitochondrial	LMJF_30_2460
Q6Y9S1	Phosphogluconate dehydrogenase (NADP(+)- dependent, decarboxylating), EC 1.1.1.44	

Supp. Table 14. Proteins that were upregulated (green) or downregulated (red) in amastigotes treated with compound 1o for 24 h.

Entry	Protein names	Gene names
Q4Q2Y5	Protein kinase domain-containing protein	LMJF_34_2150
Q4QEI9	Elongation factor 1-alpha	LMJF_17_0080, LMJF_17_0081, LMJF_17_0083, LMJF_17_0084, LMJF_17_0085
Q4Q325	Putative amastin-like surface protein	LMJF_34_1700, LMJF_34_1760, LMJF_34_1780, LMJF_34_1800, LMJF_34_1820
Q4QD15	Protein-serine/threonine kinase, EC 2.7.11.-	LMJF_20_0280
Q4QCG2	Uncharacterized protein	LMJF_21_0530
Q4QIJ4	Uncharacterized protein	LMJF_07_0930
Q4QEV9	Putative histone H3	LMJF_16_0600
E9AD01	Kinetoplast-associated protein-like protein	LMJF_27_0240
Q4QE94	Uncharacterized protein	LMJF_17_0960
Q4Q5Z0	Phosphatidylinositol-4-phosphate 5-kinase-like protein	LMJF_31_2710
E9ADF2	Putative dynein heavy chain	LMJF_27_1750
Q4QCL6	Putative ring-box protein 1	LMJF_21_0023
Q4Q3F7	Amastin-like protein	LMJF_34_0500
Q4QHV2	Putative cleavage and polyadenylation specificity factor 30 kDa subunit	LMJF_09_0720
Q4QIS2	Uncharacterized protein	LMJF_07_0220
E9ADH5	Uncharacterized protein	LMJF_27_1950
A0A2P0XMV4	Monoglyceride lipase, EC 3.1.1.23	
Q4Q0B9	Methylenetetrahydrofolate reductase (NAD(P)H), EC 1.5.1.20	LMJF_36_6390
Q4QF88	Sulfhydryl oxidase, EC 1.8.3.2	LMJF_15_0960
Q4Q2M1	RNA editing associated helicase 2, putative with=GeneDB:Tb927.4.1500	REH2 LMJF_34_3230
E9ACG3	Putative ATP-binding cassette protein subfamily F member 1	ABCF1 LMJF_03_0160
Q4Q197	Uncharacterized protein	LMJF_36_3220
Q4QER3	Stealth_CR3 domain-containing protein	LMJF_16_1050
Q4Q695	Uncharacterized protein	LMJF_31_1670
Q4Q4E0	Uncharacterized protein	LMJF_33_0650
Q4QAZ9	Putative Qb-SNARE protein	LMJF_23_1740
Q4QI86	Amastin-like protein	LMJF_08_0830
Q4Q5H6	Guanine nucleotide-binding protein subunit beta-like protein	LMJF_32_1060
Q4QHH8	Putative folate/biopterin transporter	LMJF_10_0390
Q4QGB4	Sister chromatid cohesion protein	LMJF_13_0400
Q4QDF2	Putative kinesin, EC 3.6.4.4	LMJF_19_0690

Q4Q747	Putative heat shock 70-related protein 1, mitochondrial	LMJF_30_2460
Q4QH24	Putative transcription modulator/accessory protein	LMJF_11_0560
Q4QJ83	Uncharacterized protein	LMJF_05_1190
Q4QCS9	Putative calpain-like cysteine peptidase, EC 3.4.22.-, EC 3.4.22.33	LMJF_20_1180
Q4QC71	Putative adenylate kinase, EC 2.7.4.3	LMJF_21_1250
Q4Q1Z8	Calpain catalytic domain-containing protein	LMJF_36_0780
Q4QEN5	Cytochrome c (Putative cytochrome c)	LMJF_16_1310, LMJF_16_1320
Q4QFM3	Putative kinesin K39	LMJF_14_1110
Q4Q0D2	Glucose transporter, lmg13	LMJF_36_6280
E9AD29	Putative radial spoke protein 3	LMJF_27_0520
Q4Q0Z1	Uncharacterized protein	LMJF_36_4230
Q9U0W1	Acetyl-coenzyme A synthetase, EC 6.2.1.1	L7836.01 LMJF_23_0710
Q4Q7J2	Putative RNA-binding protein	LMJF_30_1110
Q4QGJ3	Uncharacterized protein	LMJF_12_0820
Q4QGN0	Alanine aminotransferase, EC 2.6.1.2	ALAT LMJF_12_0630
Q4QAV5	Uncharacterized protein	LMJF_24_0260
E9AFQ2	Ubiquinone biosynthesis O-methyltransferase, mitochondrial (3-demethylubiquinol 3-O-methyltransferase, EC 2.1.1.64) (Polyprenyldihydroxybenzoate methyltransferase, EC 2.1.1.114)	LMJF_35_4250
Q4Q5G9	Uncharacterized protein	LMJF_32_1130
Q4QIG6	Putative Qc-SNARE protein	LMJF_08_0030
Q4QHP3	Putative paraflagellar rod component	LMJF_09_1320
E9AED0	Uncharacterized protein	LMJF_29_2680
Q4Q166	Uncharacterized protein	LMJF_36_3520
E9AES2	Putative aldose 1-epimerase, EC 5.1.3.3	LMJF_35_0970
Q4QGC8	Putative N-acetyltransferase subunit ARD1	LMJF_13_0260
Q4Q6R7	Putative CPSF-domain protein	LMJF_30_3710
Q7KF27	Cytosolic leucyl aminopeptidase, EC 3.4.11.1	lap LAP, LMJF_23_0950
Q4QC39	Uncharacterized protein	LMJF_21_1560
Q4Q615	Putative lipase, EC 3.1.1.3	LMJF_31_2460
Q4QEQ4	Tyrosyl or methionyl-tRNA synthetase-like protein, EC 6.1.1.-	LMJF_16_1130
E9ACK6	Kinase-like protein	LMJF_03_0610
Q4QC37	Uncharacterized protein	LMJF_21_1555
Q9N853	Uncharacterized protein	LMJF_04_0140, LMJF_04_0150, LMJF_04_0160
Q4QBP8	Uncharacterized protein	LMJF_22_0990
Q4QD68	Cysteine peptidase A (CPA)	CPA LMJF_19_1420
Q4Q396	Dihydroxyacetonephosphate acyltransferase, EC 2.3.1.42	DAT LMJF_34_1090

SUPPLEMENT

E9ADF0	Uncharacterized protein	LMJF_27_1730
Q4Q6D5	Putative ATP-binding cassette protein subfamily C, member 5	ABCC5 LMJF_31_1280
Q4QDH0	Uncharacterized protein	LMJF_19_0510
E9AE36	Putative paraflagellar rod protein 1D	LMJF_29_1750
Q25312	DNA-directed RNA polymerase subunit, EC 2.7.7.6	RPOIILS
E9ADX5	EF-hand domain-containing protein	LMJF_29_1170
Q4Q9S9	Uncharacterized protein	LMJF_25_1620
B8YDG1	Leishmanolysin, EC 3.4.24.36	
Q4QHC2	Uncharacterized protein	LMJF_10_0920
Q4Q3Q5	Uncharacterized protein	LMJF_33_2800
E9AFK1	Uncharacterized protein	LMJF_35_3770
Q4QDN6	Putative kinesin, EC 3.6.4.4	LMJF_18_1530
E9ADH2	Uncharacterized protein	LMJF_27_1930
Q4Q1Q2	Uncharacterized protein	LMJF_36_1720
Q5SDH5	Putative calpain-like cysteine peptidase (Small myristoylated protein 1)	SMP-1 LMJF_20_1310
Q4Q793	Uncharacterized protein	LMJF_30_2010
Q4Q314	CARD domain-containing protein	LMJF_34_0240
Q4Q327	Putative amastin-like surface protein	LMJF_34_1560, LMJF_34_1740, LMJF_34_1900
Q4QDG9	Uncharacterized protein	LMJF_19_0520
Q4Q6Z3	Uncharacterized protein	LMJF_30_2990
Q4QJJ9	Putative paraflagellar rod component par4	LMJF_05_0040
K7PN53	Cysteine protease	cpb
Q4QFL2	Uncharacterized protein	LMJF_14_1220
Q4QF65	Uncharacterized protein	LMJF_15_1190
E9ACP2	Uncharacterized protein	LMJF_03_0970
Q4QGR1	Myotubularin phosphatase domain-containing protein	LMJF_12_0320
Q4QAW6	Glycosomal membrane like protein	LMJF_24_0150
Q4Q2Z8	Uncharacterized protein	LMJF_34_2030
Q9U1E6	Putative outer dynein arm docking complex (Uncharacterized protein L1648.02)	L1648.02 DC2, LMJF_32_2900
Q4QEW8	Uncharacterized protein	LMJF_16_0520
Q4Q0T5	Uncharacterized protein	LMJF_36_4780
Q4QIW4	Uncharacterized protein	LMJF_06_1120
Q4QE77	WW domain-containing protein	LMJF_17_1140
Q4QFK1	Uncharacterized protein	LMJF_14_1330
E9ACN8	Amidohydro_3 domain-containing protein	LMJF_03_0930
Q4Q963	Uncharacterized protein	LMJF_26_1310

Q4QEK4	Prohibitin	LMJF_16_1610
Q4QCS8	Putative calpain-like cysteine peptidase, EC 3.4.22.-, EC 3.4.22.33	LMJF_20_1185
Q4QCI4	Uncharacterized protein	LMJF_21_0310
Q4Q242	ER membrane protein complex subunit 3	LMJF_36_0360
Q4Q5Q0	Uncharacterized protein	LMJF_32_0350
Q4Q0L5	DAO domain-containing protein	LMJF_36_5460
Q95Z93	Calcium-transporting ATPase, EC 7.2.2.10	LMJF_04_0010
Q4Q847	Uncharacterized protein	LMJF_28_2180
Q4QDQ9	Uncharacterized protein	LMJF_18_1300
E9AD42	Uncharacterized protein	LMJF_27_0650
E9AFW1	Uncharacterized protein	LMJF_35_4860
E9ACD8	Uncharacterized protein	LMJF_02_0640
E9ACCO	Uncharacterized protein	LMJF_02_0460
Q4QDK0	ADP/ATP translocase (ADP,ATP carrier protein)	ANC2 ANC1, LMJF_19_0200, LMJF_19_0210
P39095	60S ribosomal protein L30	RPL30
Q4QCW2	Cytochrome c oxidase assembly factor-like protein, EC 1.9.3.1	LMJF_20_0840
Q4Q2E8	Non-specific serine/threonine protein kinase, EC 2.7.11.1	TOR3 LMJF_34_3940
Q4QDR6	Uncharacterized protein	LMJF_18_1260
E9AEX6	Putative reiske iron-sulfur protein, EC 1.10.2.2	LMJF_35_1540
E9ACM7	Uncharacterized protein	LMJF_03_0820
Q4Q3R8	Uncharacterized protein	LMJF_33_2680
Q4Q353	Uncharacterized protein	LMJF_34_1490
Q4QGD8	Uncharacterized protein	LMJF_13_0160
E9ACC9	Uncharacterized protein	LMJF_02_0550
Q4QEM2	Paraflagellar rod protein 2C	LMJF_16_1425, LMJF_16_1427, LMJF_16_1430
Q4Q801	Uncharacterized protein	LMJF_28_2610
E9ADG8	Uncharacterized protein	LMJF_27_1895
Q4Q8F5	Guanine nucleotide-binding protein subunit beta-like protein	LMJF_28_1110
Q4Q0W1	Putative ABC1 protein	LMJF_36_4530
Q4QBF3	Putative ATP-binding cassette protein subfamily C,member 2	ABCC2 LMJF_23_0220
E9AFR9	Putative mitochondrial phosphate transporter	LMJF_35_4420
Q4QID5	Uncharacterized protein	LMJF_08_0340
Q4Q205	Uncharacterized protein	LMJF_36_0710
E9AFU6	Uncharacterized protein	LMJF_35_4690
Q4Q7L0	DUF4139 domain-containing protein	LMJF_30_0930
Q4Q8N2	Sacchrp_dh_NADP domain-containing protein	LMJF_28_0380

SUPPLEMENT

Q4Q4P2	Uncharacterized protein	LMJF_32_3800
Q4Q666	Tryparedoxin-like protein	LMJF_31_1960
Q4QJ94	Uncharacterized protein	LMJF_05_1080
Q4QGN3	Uncharacterized protein	LMJF_12_0600
Q4Q0W2	Uncharacterized protein	LMJF_36_4520
E9ACD7	Gamma-glutamyl phosphate reductase-like protein	LMJF_02_0630
E9AFU0	J domain-containing protein	LMJF_35_4630
Q4Q9Y0	Putative cytochrome c oxidase VII, EC 1.9.3.1	LMJF_25_1130
Q4QGA0	Uncharacterized protein	LMJF_13_0540
Q4Q1S4	Putative nima-related protein kinase, EC 2.7.11.1	LMJF_36_1520
Q4Q8K9	Putative dynein heavy chain	LMJF_28_0610
Q4Q830	Uncharacterized protein	LMJF_28_2350
Q4QIK9	Flavoprotein subunit-like protein	LMJF_07_0800
E9ACL5	Uncharacterized protein	LMJF_03_0700
Q9U0T9	Putative calpain-like cysteine peptidase, EC 3.4.22.-	LMJF_04_0450
Q4QJF3	Uncharacterized protein	LMJF_05_0490
Q4QDW0	Uncharacterized protein	LMJF_18_0820
Q4QER8	Stealth_CR3 domain-containing protein	LMJF_16_1010
Q4QCI1	Metallo-peptidase, Clan ME, Family M16	LMJF_21_0340
E9AEZ7	Uncharacterized protein	LMJF_35_1755
Q9GU34	Elongation factor 2	EF2-1
Q4QGR8	Cysteinyl-tRNA synthetase, EC 6.1.1.16	LMJF_12_0250
Q4QIT8	Putative cytochrome c1, heme protein, mitochondrial, EC 1.10.2.2	LMJF_07_0060
Q4QB10	Fer2_3 domain-containing protein	LMJF_23_1410
Q4Q7B3	Uncharacterized protein	LMJF_30_1810
Q4QID2	Uncharacterized protein	LMJF_08_0370
Q4Q5U3	Methylcrotonoyl-coa carboxylase biotinylated subunitprotein-like protein, EC 6.4.1.4	LMJF_31_3130
Q4Q131	Diadenosine tetraphosphate synthetase, EC 6.1.1.14	LMJF_36_3840
Q4Q8C7	Uncharacterized protein	LMJF_28_1390
Q4Q0W8	Uncharacterized protein	LMJF_36_4460
Q4Q3E6	Putative enoyl-[acyl-carrier-protein] reductase	LMJF_34_0610
E9AFR1	Uncharacterized protein	LMJF_35_4340
E9AFQ7	Uncharacterized protein	LMJF_35_4300
E9AFJ4	Glycosomal membrane protein	LMJF_35_3700
Q4QEH6	ER membrane protein complex subunit 2	LMJF_17_0120
Q4Q595	Putative rab11B GTPase	LMJF_32_1840
Q4QIW5	Uncharacterized protein	LMJF_06_1110

E9AD88	Uncharacterized protein	LMJF_27_1100
E9AEZ5	Ubiquitinyl hydrolase 1, EC 3.4.19.12	LMJF_35_1740
Q4QIR6	Putative ubiquitin-protein ligase-like, EC 6.3.2.19	LMJF_07_0280
E9AD84	Cysteine desulfurase, EC 2.8.1.7	LMJF_27_1060
Q4QJ98	Stomatin-like protein	LMJF_05_1040
E9AEW1	Metallo-peptidase, Clan ME, Family M16, EC 1.10.2.2	LMJF_35_1380
K7P5C3	Cathepsin L-like protease	Cpb
E9AFL1	Putative nucleoside diphosphate kinase, EC 2.7.4.6	LMJF_35_3870
Q4QIE9	Inositol phosphosphingolipid phospholipase C-Like	ISCL LMJF_08_0200
Q4QFZ4	Uncharacterized protein	LMJF_13_1600
E9AD28	Putative calpain-like cysteine peptidase	LMJF_27_0510
Q4QCF1	Putative phosphoglucomutase, EC 5.4.2.2	LMJF_21_0640
Q4Q1I3	Methyltransferase, EC 2.1.1.-	LMJF_36_2380
Q4Q137	Uncharacterized protein	LMJF_36_3780
Q4Q9V6	Uncharacterized protein	LMJF_25_1370
Q4QD20	Uncharacterized protein	LMJF_20_0240
Q4QAB4	GP-PDE domain-containing protein	LMJF_24_2160
Q4QJ13	Putative lanosterol synthase, EC 5.4.99.8	LMJF_06_0650
Q4VT70	Phosphotransferase, EC 2.7.1.-	HK LMJF_21_0240
Q4QG67	Metallo-peptidase, Clan ME, Family M16, EC 3.4.24.6, EC 3.4.24.64	LMJF_13_0870
Q4Q8M1	Putative propionyl-coa carboxylase beta chain, EC 6.4.1.3	LMJF_28_0490
Q4Q8Z2	Uncharacterized protein	LMJF_26_2000
O43994	Leishmanolysin, EC 3.4.24.36	gp63-6
Q4QFH9	NADH-cytochrome b5 reductase, EC 1.6.2.2	LMJF_15_0050
Q4Q2C8	ER membrane protein complex subunit 1	LMJF_34_4130
Q4Q079	Uncharacterized protein	LMJF_36_6760
Q4QE34	3Beta_HSD domain-containing protein	LMJF_18_0080
Q4QH77	Uncharacterized protein	LMJF_11_0030
Q4QDJ8	Uncharacterized protein	LMJF_19_0230
E9ADU9	Letm1 RBD domain-containing protein	LMJF_29_0920
Q4Q2W6	Asparagine--tRNA ligase, EC 6.1.1.22	LMJF_34_2340
Q4QCE9	Cytosolic Fe-S cluster assembly factor NUBP1 homolog	LMJF_21_0660
E9AFH5	Structural maintenance of chromosomes protein	LMJF_35_3510
Q4Q8P6	Glycerol-3-phosphate dehydrogenase, EC 1.1.5.3	LMJF_28_0240
Q4QGV7	Putative ATP-binding cassette protein subfamily A, member4	ABCA4 LMJF_11_1250
Q4QJA4	NADH dehydrogenase [ubiquinone] flavoprotein 1, mitochondrial, EC 7.1.1.2	LMJF_05_0980
Q4QG07	Uncharacterized protein	LMJF_13_1470

SUPPLEMENT

E9AFU8	Uncharacterized protein	LMJF_35_4710
Q4Q699	Putative 3-ketoacyl-CoA thiolase-like protein, EC 2.3.1.16	LMJF_31_1630
Q4Q159	Uncharacterized protein	LMJF_08_1100
Q4Q057	Uncharacterized protein	LMJF_36_6960
Q5QQ43	Isopentenyl-pyrophosphate isomerase (Putative isomerase, EC 5.3.3.2)	idi1 LMJF_35_5330
E9AEB3	ATP-dependent 6-phosphofructokinase, ATP-PFK, Phosphofructokinase, EC 2.7.1.11 (Phosphohexokinase)	pfk LMJF_29_2510
Q4QDN8	Plasma membrane ATPase, EC 7.1.2.1	H1A-1 LMJF_18_1510
Q4Q214	Uncharacterized protein	LMJF_36_0620
Q4Q8F4	Uncharacterized protein	LMJF_28_1120
E9AF02	Trypanin-like protein	LMJF_35_1810
Q4QCM5	Putative N-acyl-L-amino acid amidohydrolase, EC 3.5.1.14	LMJF_20_1560
O97200	Uncharacterized protein	LMJF_04_0550
Q4QGX0	Putative lanosterol 14-alpha-demethylase, EC 1.14.13.70	LMJF_11_1100
Q4Q483	Uncharacterized protein	LMJF_33_1070
Q4QGM6	Cytochrome c oxidase subunit IV, EC 1.9.3.1	LMJF_12_0670
Q4Q1U2	Putative N-acetyltransferase subunit Nat1	LMJF_36_1340
Q4QJ88	V-type proton ATPase subunit	LMJF_05_1140
Q4Q0P9	Uncharacterized protein	LMJF_36_5130
Q4Q6F8	Uncharacterized protein	LMJF_31_1050
Q4Q1B2	Fibrillarin	LMJF_36_3070
E9ADY2	TPR_REGION domain-containing protein	LMJF_29_1240
Q4QFP2	Putative immunodominant antigen	LMJF_14_0930
Q4QCD1	Uncharacterized protein	LMJF_21_0820
Q4Q271	Stress-inducible protein STI1 homolog	LMJF_36_0070
Q4QGW5	Putative eukaryotic release factor 3	LMJF_11_1170
Q4QFA8	Protein kinase domain-containing protein	LMJF_15_0770
Q4QBW5	Uncharacterized protein	LMJF_22_0300
Q4QFJ8	Inositol-3-phosphate synthase, EC 5.5.1.4	INO1 LMJF_14_1360
Q4Q182	Bromo domain-containing protein	LMJF_36_3360
Q4QAE5	Uncharacterized protein	LMJF_24_1860
Q4QGR4	Uncharacterized protein	LMJF_12_0290
Q4QCG8	Vacuolar protein sorting-associated protein 35	LMJF_21_0470
Q4QFY6	Pyrroline-5-carboxylate reductase, EC 1.5.1.2	P5CR LMJF_13_1680
Q4QC67	Putative R-SNARE protein	LMJF_21_1290
Q4Q745	Putative heat shock 70-related protein 1, mitochondrial	LMJF_30_2470, LMJF_30_2480
Q4Q1M7	Phosphomannomutase, EC 5.4.2.8	PMM LMJF_36_1960
E9AD58	Glutaredoxin-like protein	LMJF_27_0810

Q4Q3E9	Uncharacterized protein	LMJF_34_0580
Q4QFP4	Glutathione synthetase, GSH-S, EC 6.3.2.3	LMJF_14_0910
Q4QBK1	I/6 autoantigen-like protein	LMJF_22_1460
Q4Q5R2	Dynein light chain	LMJF_32_0230
Q25326	Hydrophilic surface protein (Hydrophilic surface protein 1)	haspb
Q4Q521	HD domain-containing protein	LMJF_32_2540
Q4QH87	Uncharacterized protein	LMJF_10_1250
Q4Q740	Putative heat shock 70-related protein 1,mitochondrial	LMJF_30_2550
Q4QFU6	Uncharacterized protein	LMJF_14_0390
Q4Q080	Prolyl endopeptidase, EC 3.4.21.-	LMJF_36_6750
Q4Q2C1	Uncharacterized protein	LMJF_34_4200
E9ACH3	Uncharacterized protein	LMJF_03_0260
E9ADT8	Putative high mobility group protein homolog tdp-1	LMJF_29_0850
Q4Q6X0	40S ribosomal protein S26	LMJF_30_3200
Q4QGE5	Metallo-peptidase, Clan MA(E), family 32	LMJF_13_0090
Q4Q760	Uncharacterized protein	LMJF_30_2330
Q4QCN8	Phosphatase-like protein	LMJF_20_1640
Q4QIB3	Uncharacterized protein	LMJF_08_0560
Q4QHR7	Putative eukaryotic translation initiation factor 2 subunit	LMJF_09_1070
Q4QHS3	Uncharacterized protein	LMJF_09_1010
A0A2R4SDX9	Heat shock protein 70	hsp70
Q4QC91	Putative 60S ribosomal protein L9	LMJF_21_1050
Q4Q127	Eukaryotic translation initiation factor 3 subunit I, eIF3i	LMJF_36_3880
Q4QA28	Putative epsin	LMJF_25_0670
Q4Q2T8	Uncharacterized protein	LMJF_34_2570
Q4Q8H1	40S ribosomal protein S14	LMJF_28_0960
Q4Q5N1	Profilin	LMJF_32_0520
Q4Q5S8	Glycylpeptide N-tetradecanoyltransferase, EC 2.3.1.97	NMT LMJF_32_0080
Q4QB24	Uncharacterized protein	LMJF_23_1280
Q4Q882	Probable methylthioribulose-1-phosphate dehydratase, MTRu-1-P dehydratase, EC 4.2.1.109	LmjF28.1840, LmjF_28_1840
Q4QIC7	Uncharacterized protein	LMJF_08_0420
Q4QG86	Peptidase_M24 domain-containing protein	LMJF_13_0680
Q4QIP1	60S ribosomal protein L7a	LMJF_07_0500, LMJF_07_0510
Q4QGW1	Putative S-phase kinase-associated protein	LMJF_11_1210
Q4Q1Y3	Putative 40S ribosomal protein S18 (Ribosomal protein S18)	LMJF_36_0930
Q4Q869	Putative ribose 5-phosphate isomerase, EC 5.3.1.6	LMJF_28_1970
Q4QCE8	Metallo-beta-lactamase family-like protein	LMJF_21_0670
Q4QBL5	Uncharacterized protein	LMJF_22_1320

SUPPLEMENT

Q4QIV8	Protein kinase domain-containing protein	LMJF_06_1180
Q4QAC5	Putative 60S ribosomal protein L26	LMJF_24_2050, LMJF_35_1670
E9ADB1	Uncharacterized protein	LMJF_27_1300
Q4Q5X2	Uncharacterized protein	LMJF_31_2870
Q4QII4	Peptidyl-prolyl cis-trans isomerase, EC 5.2.1.8	PIN1 LMJF_07_1030
Q4QB63	Uncharacterized protein	LMJF_23_1000
Q4Q0L9	Branchpoint-bridging protein	LMJF_36_5420
Q4Q6T6	S-adenosylmethionine synthase, EC 2.5.1.6	METK2 METK1, LMJF_30_3500, LMJF_30_3520
E9AC39	Putative beta eliminating lyase	LMJF_01_0480
Q4Q5E5	Uncharacterized protein	LMJF_32_1370
Q4QJA6	Dipeptidyl peptidase 3, EC 3.4.14.4 (Dipeptidyl aminopeptidase III) (Dipeptidyl peptidase III)	LMJF_05_0960
P12076	Heat shock 70-related protein 1, mitochondrial	HSP70.1
Q4QFM9	Putative dynein heavy chain	LMJF_14_1060
Q4Q7R4	RRF domain-containing protein	LMJF_30_0440
Q4QC88	Cell division protein kinase 2, EC 2.7.1.-	CRK1 LMJF_21_1080
Q4QFL3	FCP1 homology domain-containing protein	LMJF_14_1210
Q95Z90	Uncharacterized protein	LMJF_04_0050
Q4QC38	Putative RNA helicase	LMJF_21_1552
E9ADK4	FACT complex subunit	LMJF_29_0020
Q868B1	40S ribosomal protein S5 (40S ribosomal protein S5A) (40S ribosomal protein S5B)	LMJF_11_0960, LMJF_11_0970
Q4QJ76	Guanine nucleotide-binding protein subunit beta-like protein	LMJF_06_0030
Q4Q9Y6	Uncharacterized protein	LMJF_25_1070
E9ACA3	Uncharacterized protein	LMJF_02_0280
Q4Q735	Formyltetrahydrofolate synthetase, EC 6.3.4.3	FTHS LMJF_30_2600
Q4QA19	PPM-type phosphatase domain-containing protein	PP2C LMJF_25_0750
Q4QJ39	Putative 60S ribosomal protein L19	LMJF_06_0410
Q4QDJ5	Kinesin-like protein	LMJF_19_0260
Q4QFT9	CS domain-containing protein	LMJF_14_0450
Q4QEJ3	Uncharacterized protein	LMJF_17_0050
Q4QHU7	Prolyl endopeptidase, EC 3.4.21.-	OPB LMJF_09_0770
Q4Q3M1	Putative 40S ribosomal protein S13	LMJF_19_0390, LMJF_33_3150
E9ADQ2	ADF/Cofilin	LMJF_29_0510
Q4Q7R2	Aspartyl-tRNA synthetase, EC 6.1.1.12	LMJF_30_0460
Q4QBN6	Putative dynein heavy chain, cytosolic	LMJF_22_1110
Q4Q1I4	Uncharacterized protein	LMJF_36_2370
Q4Q690	CULLIN_2 domain-containing protein	LMJF_31_1720

Q4QE92	Uncharacterized protein	LMJF_17_0990
Q4Q884	Replication protein A subunit	RPA1 LMJF_28_1820
Q4Q1V1	Putative 40S ribosomal protein S9 (Ribosomal protein S9)	LMJF_36_1250
Q4QGH7	Uncharacterized protein	LMJF_12_1120
Q4QBI7	Putative ser/thr protein phosphatase	LMJF_22_1600
E9AFK3	Putative 60S ribosomal protein L23	LMJF_35_3790, LMJF_35_3800
Q4QCC5	Methionine aminopeptidase 2, MAP 2, MetAP 2, EC 3.4.11.18 (Peptidase M)	LMJF_21_0840
Q4QBY9	Uncharacterized protein	LMJF_22_0050
Q4Q8S7	Uncharacterized protein	LMJF_26_2640
Q4Q3G4	40S ribosomal protein S25	S25 LMJF_34_0440
Q4Q9Y2	Uncharacterized protein	LMJF_25_1110
Q4Q109	Uncharacterized protein	LMJF_36_4060
Q4QAT9	Ubiquitin carboxyl-terminal hydrolase, EC 3.4.19.12	LMJF_24_0420
Q4QE19	Putative 60S ribosomal protein L7	LMJF_18_0230
Q4QIN5	Uncharacterized protein	LMJF_07_0570
Q4QBC0	Acetyl-coenzyme A synthetase, EC 6.2.1.1	LMJF_23_0540
E9AEQ8	FAD:protein FMN transferase, EC 2.7.1.180 (Flavin transferase)	LMJF_35_0830
E9ADW9	Uncharacterized protein	LMJF_29_1110
Q4Q0F4	Putative eukaryotic initiation factor 4a	LMJF_36_6060
E9AC95	Phosphoglycan beta 1,3 galactosyltransferase	SCGR3 LMJF_02_0200
Q4QH45	14-3-3 protein II (Putative 14-3-3 protein)	Lm 14-3-3 II LMJF_11_0350
Q4QBD6	Putative ATP-binding cassette protein subfamily	ABCG5 LMJF_23_0380
Q4QHA3	LsmAD domain-containing protein	LMJF_10_1110
Q4Q2K1	Putative cleavage and polyadenylation specificity factor	LMJF_34_3430
E9ACP6	Uncharacterized protein	LMJF_04_0123
Q4QJ42	Putative glutamine synthetase, EC 6.3.1.2	LMJF_06_0370
Q4QB38	Guanine nucleotide-binding protein subunit beta-like protein	CRN12 LMJF_23_1165
Q4QAI0	Putative IgE-dependent histamine-releasing factor	LMJF_24_1500, LMJF_24_1510
Q4QD18	Midasin	LMJF_20_0260
E9ADE1	Putative eukaryotic translation initiation factor eIF-4E	EIF4E1 LMJF_27_1620
Q4QDI1	Putative Qc-SNARE protein	LMJF_19_0400
Q4Q573	Putative ras-related protein rab-2a	LMJF_32_2030
E9ACE8	Putative dipeptylcarboxypeptidase (Putative peptidyl dipeptidase)	DCP LMJF_02_0740, LMJF_27_2660
Q4Q710	Uncharacterized protein	LMJF_30_2830
Q4QH84	Uncharacterized protein	LMJF_10_1280
Q4Q9I9	Methylmalonyl-coa epimerase-like protein, EC 5.1.99.1	LMJF_26_0020

SUPPLEMENT

Q4QH01	Putative 40S ribosomal protein S21	LMJF_11_0760, LMJF_11_0780
Q4QJC2	MYND zinc finger (ZnF) domain-like protein	LMJF_05_0800
Q4Q9B0	Uncharacterized protein	LMJF_26_0840
Q6YIR7	Quinonoid dihydropteridine reductase QDPR	
P12077	Heat shock 70-related protein 4	HSP70.4
Q4QDL0	Uncharacterized protein	LMJF_19_0110
Q4QBX7	Uncharacterized protein	LMJF_22_0180
Q4QIH4	Putative proteasome regulatory non-ATP-ase subunit	LMJF_07_1120
Q4QAU8	Uncharacterized protein	LMJF_24_0330
Q4QBH1	Peptidyl-prolyl cis-trans isomerase, PPIase, EC 5.2.1.8	CYP11 LMJF_23_0050
Q4FWX5	Putative 60S ribosomal protein L2	LMJF_32_3900, LMJF_35_1430, LMJF_35_1440
Q4Q605	Uncharacterized protein	LMJF_31_2560
Q4QCD4	Ras-related protein Rab-21	LMJF_21_0790
Q4QFF7	Lysine--tRNA ligase, EC 6.1.1.6 (Lysyl-tRNA synthetase)	LMJF_15_0230
Q4QEM4	Uncharacterized protein	LMJF_16_1420
Q4Q5J8	RRM_8 domain-containing protein	LMJF_32_0840
Q4Q1U1	PARP-type domain-containing protein	LMJF_36_1350
P50312	Phosphoglycerate kinase, glycosomal, EC 2.7.2.3 (Phosphoglycerate kinase C) (gPGK)	PGKC
Q6S997	Phosphodiesterase, EC 3.1.4.-	PDEB2
Q4QFW6	Thioredoxin-like_fold domain-containing protein	LMJF_14_0190
Q4Q138	Nascent polypeptide-associated complex subunit beta	LMJF_36_3770
Q4QAS3	Npa1 domain-containing protein	LMJF_24_0600
Q4QCY4	CTP synthase, EC 6.3.4.2 (UTP--ammonia ligase)	LMJF_20_0560
E9AC63	Uncharacterized protein	LMJF_01_0720
A0A2R4SE78	Glucose-6-phosphate 1-dehydrogenase, EC 1.1.1.49	G6PD
Q4Q0E2	Uncharacterized protein	LMJF_36_6180
Q4Q426	Putative peptidase M20/M25/M40	LMJF_33_1610
Q4QBY6	Putative heat shock protein DNAJ	LMJF_22_0080
Q4QFL6	Poly(A) polymerase, EC 2.7.7.19	LMJF_14_1180
Q4QES2	Uncharacterized protein	LMJF_16_0980
Q4QHN3	Uncharacterized protein	LMJF_09_1420
E9ADI0	GMP_PDE_delta domain-containing protein	LMJF_27_2000
E9ACW8	Pre-mRNA-processing factor 19, EC 2.3.2.27	LMJF_27_2480
Q4QEZ2	Uncharacterized protein	LMJF_16_0280
Q4Q720	Putative small glutamine-rich tetratricopeptide repeat protein	SGT LMJF_30_2740
Q4QAZ0	Pyridoxal phosphate homeostasis protein, PLP homeostasis protein	LMJF_23_1480

Q4Q3L1	Uncharacterized protein	LMJF_33_3250
Q4Q9U9	Exonuclease domain-containing protein	LMJF_25_1440
Q4QCH2	NTF2 domain-containing protein	LMJF_21_0430
Q4Q9Q5	Uncharacterized protein	LMJF_25_1840
Q4Q6R6	Putative 60S acidic ribosomal protein P2	LIP1 LMJF_30_3720
Q4QEI8	Elongation factor 1-alpha	LMJF_17_0082
E9AEK1	60S ribosomal protein L30	LMJF_35_0240
Q4QA79	Cleavage and polyadenylation specificity factor subunit 2 (Cleavage and polyadenylation specificity factor 100 kDa subunit)	LMJF_25_0170
Q4QIA7	Uncharacterized protein	LMJF_08_0620
Q4Q5H5	Putative small nuclear ribonucleoprotein	LMJF_32_1070
Q4QF35	Proliferating cell nuclear antigen	LMJF_15_1450
O43943	Guanine nucleotide-binding protein subunit beta-like protein	
Q4QBS1	Uncharacterized protein	LMJF_22_0760
Q4Q870	Elongation factor G2-like protein	LMJF_28_1960
E9AFH3	Uncharacterized protein	LMJF_35_3490
E9AEL3	Enoyl-CoA hydratase/isomerase family protein, conserved	LMJF_35_0360
Q4QJ20	Putative 60S ribosomal protein L23a	LMJF_06_0570, LMJF_06_0580
Q4Q088	Cytochrome b5 heme-binding domain-containing protein	LMJF_36_6670
Q4Q6D3	Uncharacterized protein	LMJF_31_1300
Q4Q216	60S ribosomal protein L40 (Ubiquitin-60S ribosomal protein L40)	LMJF_36_0600
Q4QIE0	Superoxide dismutase, EC 1.15.1.1	FESODA LMJF_08_0290
Q4Q931	Putative 40S ribosomal protein S33	S33-1 S33-2, LMJF_26_1630, LMJF_26_1640
Q4Q0H6	Putative kinetoplast-associated protein	LMJF_36_5845
E9ADG2	Uncharacterized protein	LMJF_27_1840
Q4Q4T1	Dopey_N domain-containing protein	LMJF_32_3410
Q4Q2L9	Putative pyruvate/indole-pyruvate carboxylase, EC 4.1.1.74	LMJF_34_3250
Q4QDJ1	Putative RNA binding protein	LMJF_19_0300
E9AC43	Putative long-chain-fatty-acid-CoA ligase, EC 6.2.1.3	LMJF_01_0520
Q4Q7R0	Putative bystin	LMJF_30_0480
E9AFK0	Putative 60S ribosomal protein L27A/L29	LMJF_35_3760, LMJF_35_3780
Q4Q439	Uncharacterized protein	LMJF_33_1490
Q6Y9S1	Phosphogluconate dehydrogenase (NADP(+)-dependent, decarboxylating)	
E9AE96	Uncharacterized protein	LMJF_29_2340
Q4Q6Y1	Uncharacterized protein	LMJF_30_3090
Q4Q7V4	MATH domain-containing protein	LMJF_30_0050

SUPPLEMENT

Q4QGT2	Uncharacterized protein	LMJF_12_0110
Q4QCL3	Uncharacterized protein	LMJF_21_0040
Q4Q170	Small acidic protein	LMJF_36_3480
Q4Q4F0	Uncharacterized protein	LMJF_33_0570
E9AEY7	Uncharacterized protein	LMJF_35_1650
Q4QFW7	Putative carboxypeptidase	LMJF_14_0180
Q4Q9P3	Acylphosphatase	LMJF_25_1960
Q4Q9X4	40S ribosomal protein S25	LMJF_25_1190
K7PNP9	Cysteine protease	cpb
Q4QGK5	Uncharacterized protein	LMJF_12_0950
Q4QF84	Putative 60S ribosomal protein L6	LMJF_15_1000
K7P582	Cathepsin L-like protease	Cpb